THE UNIVERSITY OF ASTON IN BIRMINGHAM

"The temperature and field dependence of thermionic and photoelectric currents"

Thesis submitted for the degree of

Doctor of Philosophy

by

Robert Keith Fitch,

Physics Department

September 1968

Acknowledgments

My thanks are due to Dr. C.S. Bull for his supervision of this work and for his continual encouragement and invaluable help. My thanks are also due to Professor S.E. Hunt and Mr. H. Orwin for their help and in particular for them making it possible, at critical points, to start and continue with this work.

My thanks are finally due to many other members of the academic and technical staff in the Physics Department.

Synopsis

The object of the work described in this thesis has been to investigate some aspects of thermionic and photoelectric emission from an overall point of view rather than in one particular and narrow section of the subject. With this in mind it was considered necessary that a reasonable fraction of this thesis should be devoted to a fairly critical review of the relevant published literature. Chapter (1) is concerned with the interpretation of thermionic measurements, whereas Chapter (3) deals with the existing and new theories of the work function and its temperature dependence. Also included in this Chapter is a review of some of the most important and reliable measurements that have been reported on the variation of work function with temperature.

Chapter (2) gives the results of thermionic emission measurements on oxide coated cathodes. The total emission has been estimated from a detailed study of valve characteristics and this method has been successfully applied to find the relationship between the total emission and the space charge limited current. In Chapter (6) these results have been used to examine the influence of small changes in applied field on the thermionic currents.

Chapters (4) and (5) are concerned with photoelectric emission from clean metals and oxide cathodes, from just above room temperature to nearly liquid helium temperature. The results of this work have shown that it appears to be necessary to consider

the work function in two parts. Firstly there is a bulk effect which is not critically dependent upon the temperature or applied field. On the other hand a photoelectric emission has been observed in the long wavelength tail which is both temperature and field dependent. An attempt has been made to explain these results in terms of the new theoretical ideas of the work function recently put forward by Dr. C.S. Bull, in this department. The experimental results do appear to support some of his conclusions, although it has been found necessary to modify his proposed model of the work function.

Index

Chapter 1.

Interpretation of thermionic measurements

1.1 Introduction

Although the subjects of thermionic and photo electric emission have been studied extensively for more than half a century, there is still a considerable research effort, in industrial and academic institutions, in both of these fields. There are a number of reasons for this besides the obvious need for improved devices. Recent work has shown that earlier experimental work was not always satisfactory on account of the unreliable experimental conditions. However even when these conditions have been improved it is often the case that interpretation of experimental results can be mistaken. It is for this reason that a critical review of some of the important work in thermionic emission is given in this chapter.

1.2 Thermionic emission

It is usually understood that the saturated current density, i_s, from a pure metal surface when heated to $T^{\circ}K$, is given by the Richardson - Dushmann equation;

$$i_s = A\,(1-r)\,T^2 \exp\left(-\,e\phi/kT\right) \quad \ldots\ldots\ldots \quad (1)$$

where A has a theoretical value = $\frac{4\pi mek^2}{h^3}$

$$= 120 \text{ amp cm}^{-2} \text{ T}^{-2}$$

ϕ = total work function

and r = mean reflection coefficient for electrons at the surface.

For convenience in experimental work, equation (1) is frequently written in the form,

$$i_s = A^* T^2 \exp(-e\phi/kT) \ldots\ldots\ldots \quad (2)$$

A "Richardson plot" of $\ln(i_s/T^2)$ against $\frac{1}{T}$ should produce a straight line whose slope gives the value of the work function and whose intercept on the current axis given A^*. The work function, ϕ_R, determined from the slope can be expressed as,

$$\phi_R = -\frac{k}{e} \cdot \frac{d(\ln i_s/T^2)}{d(\frac{1}{T})}$$

Assuming A is independent of temperature, then from equation (1),

$$\phi_R = \phi - T\left(\frac{d\phi}{dT}\right) - \frac{T^2}{1-r} \cdot \frac{k}{e}\left(\frac{dr}{dT}\right) \ldots \quad (3)$$

For clean metals $\left(\frac{dr}{dT}\right)$ is small and therefore a linear Richardson plot implies that either $\left(\frac{d\phi}{dT}\right)$ is constant or zero. On the other hand a non-linear Richardson plot can imply a non linear dependence of ϕ, A or r on T. Generally it

is therefore accepted that the value of ϕ_R from a linear Richardson plot is the work function at $0^{\circ}K$. However equation (3) expresses no real way in which ϕ varies with T, and ignores negative powers of T. If we represent ϕ as a complete power series in T in the form,

$$\phi = \phi(o) + \alpha T + \beta T^2 + ... + aT^{-1} + bT^{-2} + ...$$

then

$$\frac{d\phi}{dT} = \alpha + 2\beta T + ... - aT^{-2} - 2bT^{-3} ....$$

and,

$$i_s = A^* T^2 \left\{ e^{\frac{-e\phi(o)}{kT}} \cdot e^{\frac{-e\alpha}{k}} \cdot e^{\frac{-e\beta T}{k}} \cdot .... \right.$$

$$\left. .... e^{\frac{-ea}{kT^2}} \cdot e^{\frac{-eb}{kT^3}} .... \right\}$$

Again assuming A^* is constant,

$$\phi_R = \frac{-e}{k} \left(\phi(o) - \beta T^2 - 2\gamma T^3 ..... \right.$$

$$\left. ..... + \frac{2a}{T} + \frac{3b}{T^2} + ... \right)$$

Experimentally there is little or no evidence at high temperatures that β, γ etc. exist. However the coefficients a, b etc. are only significant at low temperatures when normal thermionic emission measurements are not possible. Thus interpretation of a Richardson line is difficult even on this basis and is clearly worse if account is taken of the possible variations of A and r with temperature. Similar difficulties

obviously arise in determining A from the Richardson line.

For an excess semi-conductor i_s is approximately given by the Fowler equation,

$$i_s = B\,(1 - r)\; n_o^{1/2}\; T^{5/4}\; \exp\left\{-\frac{X + \frac{\Delta E}{2}}{kT}\right\} \quad \ldots\ldots (4)$$

where,

B = constant

n_o = impurity donor density

X = depth of bottom of conduction band from the vacuum level

and

ΔE = Energy gap between donor centres and bottom of the conduction band.

In practice T^2 is frequently used instead of $T^{5/4}$ because the slope of the Richardson line is very insensitive to the power of T , and the total work function ϕ is given by,

$$\phi = X + \frac{E}{2}$$

Nottingham[1] remarks that statements which are made that emission measurements are not capable of deciding correct power of T, confuse the issue since choice of power of T depends upon use to which it is to be put. Consequently he says that the most useful result is,

$$i = a \exp\left(-\frac{e\Phi}{kT}\right)$$

where Φ = Work factor = $\phi_R + 2V_T$

a = thermionic constant determined by experiment

and $V_T = \frac{kT}{e}$

On the other hand Hensley[2], in discussing thermionic emission from non-metallic cathodes, defines work function in three ways. Namely, "true work function", which is the difference between Fermi energy and surface potential, "effective work function" determined by substitution of T and i_s into equation (1) using A = 120 and r = 0, and the "Richardson work function", which is obtained from the slope of the Richardson line. He claims that the last method is of little value and that the same information can be obtained from the "effective work function" much more easily from a single pair of observations of i_s and T. He suggests this despite the fact that values of A differ from 120 by several orders of magnitude for composite emitters. His view is therefore an apparent acceptance of the inability to solve the emission problem in any other way.

In the shape of the current-voltage curves for a diode, when an emission current is being drawn under normal conditions, three reasonably well defined regions may be distinguished. These are shown in figure (1) and are the retarding region, the space charge limited region and the emission in accelerating fields.

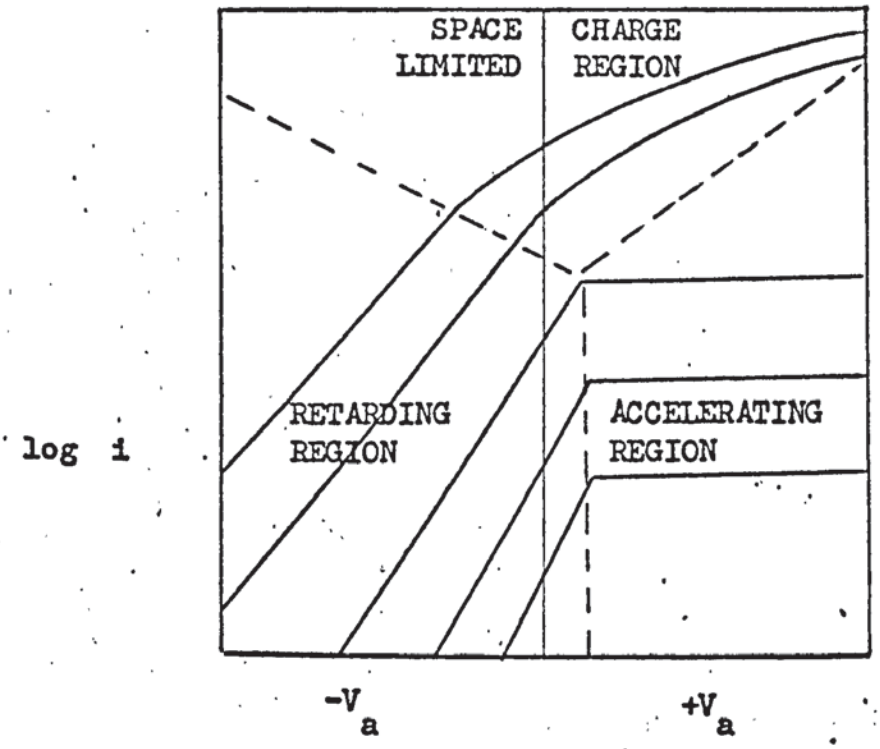

Figure 1

1.3 Emission in retarding fields

In this region only electrons which have energies greater than the barrier imposed between anode and cathode by the retarding voltage will reach the anode. This barrier includes the contact potential difference, V_c, between the anode and cathode. The retarding field current, i_r, is given by,

$$i_r = i_s \exp\left(\frac{eV_E}{kT}\right) \quad \ldots\ldots\ldots \quad (5)$$

where V_E = effective anode voltage = $-V_a + \phi_c - \phi_a$

V_a = applied anode voltage

ϕ_c = cathode work function

ϕ_a = anode work function

and $V_c = \phi_a - \phi_c$.

This enables the cathode temperature to be determined from the slope of the graph of ln i_r against V_a, if V_c is assumed constant.

Substitution of V_E and i_s in equation (5) gives,

$$i_r = A^* T^2 \exp\left(\frac{-e\phi_c}{kT}\right) \exp\left\{\frac{e}{kT}\left(-V_a + \phi_c - \phi_a\right)\right\}$$

or

$$i_r = A^* T^2 \exp\left\{-\frac{e(V_a + \phi_a)}{kT}\right\} \quad \ldots\ldots \quad (6)$$

It is seen from equation (6) that i_r depends only on T, V_a and ϕ_a and is independent of ϕ_c. Thus a plot of ln $\left(\frac{i_r}{T^2}\right)$ against $\frac{1}{T}$ for a fixed value of $-V_a$ should produce a straight line whose gradient yields the value of ϕ_a. This analysis of the retarding current to measure the anode work function was first used by Sano[3] and has since been used with some success by several other workers - eg. Shelton[4], Kisliuk[5] and Laue and Dyer[6].

However at least two criticisms can be made of this method. Firstly it is even more difficult in interpretation than the conventional Richardson technique, with regard to the value of ϕ_a and temperature. Secondly, the assumption must be made that ϕ_a is independent of the applied field and hence the selected value of V_a, and this is known to be not true particularly with complex surfaces even at very low applied fields.

1.4 Space charge limited emission

For low anode volts the electrons form a negative space charge in front of the cathode, which causes an increase in the

potential barrier corresponding to the work function. This space charge limits the current which is, in the main, a function of the geometry of the anode-cathode assembly. However at sufficiently low temperatures the space charge is negligible and there should be an abrupt change from the retarding to the accelerating regions.

The anode current, i_a, for a planar diode of spacing, d, under space charge limited conditions is given by Child's law,

$$i_a = \text{constant} \times \frac{V_a^{3/2}}{d^2}$$

This is only an approximate result since it neglects the Maxwellian distribution of initial velocities of the electrons. The main effect of this is to produce a region of minimum potential, V_m, between the anode and cathode at a distance say, x_m, from the cathode. The potential will subsequently increase, for increasing values of x, until V_a is reached at x = d. Thus any electrons with sufficient energy to penetrate beyond x_m will ultimately reach the anode.

For this more realistic case we can use the Child-Langmuir equation,

$$i_a = \text{constant} \frac{(Va - Vm)^{3/2}}{(d - x_m)^2} \left\{ 1 + \text{constant} \left\{ \frac{T}{Va - Vm} \right\}^{\frac{1}{2}} \right\} \quad (7)$$

although it may be more exact to use the effective voltage, which takes into account the contact potential, instead of V_a.

For more practical types of diodes, which are frequently of coaxial cylinder design, Langmuir has derived a more complex

expression, involving a function of the ratio of the cylinder radii. When account is also taken of the thermal velocities, this becomes still more complex since allowance should be made for the tangential as well as the radial components of velocity. Reasonable agreement between calculated and measured results have been obtained for example by Ferris[7], but Boot and Randall[8] found numerous deviations at high voltages. Hensley[2] says the equations are mainly useful in estimating the limits of current which can be judged free of space charge at a given voltage.

Hermann and Wagener[9] and Nottingham[1] state that the space charge limited current will not be influenced by the cathode work function. This argument claims that as the cathode work function decreases and more electrons leave the cathode, these electrons increase the space charge by an amount which compensates for the decrease in work function.

Thus the total potential barrier remains unchanged and only the position of V_m is modified. This view has been partly supported by both the work of Gysae and Wagnener[10] and Crowell [11]. However these experiments do not show that the space charge current is independent of the total emission, because it will be seen later that there is no good correlation between cathode work function and total emission.

Bull [12] critices the approach of Langmuir in that the laws are only approximate and do not attempt to separate the space charge effects from the total emission effects. In fact equation (7) is not usable when V_a is nearly equal to the height of the potential

barrier and therefore cannot be extended into the retarding region. Any form of Child's equation breaks down entirely when V or $(V_a - V_m)$ approaches $\frac{kT}{e}$ or smaller values. Furthermore Bull states that the limitation of Langmuir's method is that he takes V_m to be a definite potential in which two independent regions are separated by a field free space.

In a different approach to the problem of the space charge limited current, Bull[13] expresses the properties of a diode in terms of 30 partial differential coefficients of five interdependent variables. These variables are the total emission, i_s, the anode current, i, the anode voltage, V_a, the value of the potential minimum, V_m, and the distance, x, between anode and cathode. Only three of the variables are independent and one relationship between these variables is the Maxwell-Boltzmann relation.

$$i = i_s \exp (eV_m/kT)$$

Because of the unknown temperature dependence of the constants A* and ϕ_c, Bull found it desirable to omit reference to the cathode temperature as an independent variable. This is because the total emission is always a rapidly varying function of temperature, whereas the emission velocities, which influence the space charges, vary only as the square root of the temperature.

Nottingham[1] has also derived a set of similar partial differential coefficients but whilst his five variables include x, i_s and V_a, the other two are the cathode temperature and the contact

potential difference, including its temperature dependence. This appears to be a more impractical situation and in his derivations he refers to the untenable idea of unlimited emission. This would require a potential barrier of unlimited depth to keep the current in the space charge to a low value.

One of the coefficients given by Bull $\left(\frac{\partial i}{\partial i_s}\right)_{v,x}$ relates the total emission with anode current. This relationship appears to be in contradiction to the earlier discussion of experimental work, but Bull[14] made an estimate of this to be about 10^{-3}. Figure (2) shows how Bull represents the relation between i_s and i for constant V and x.

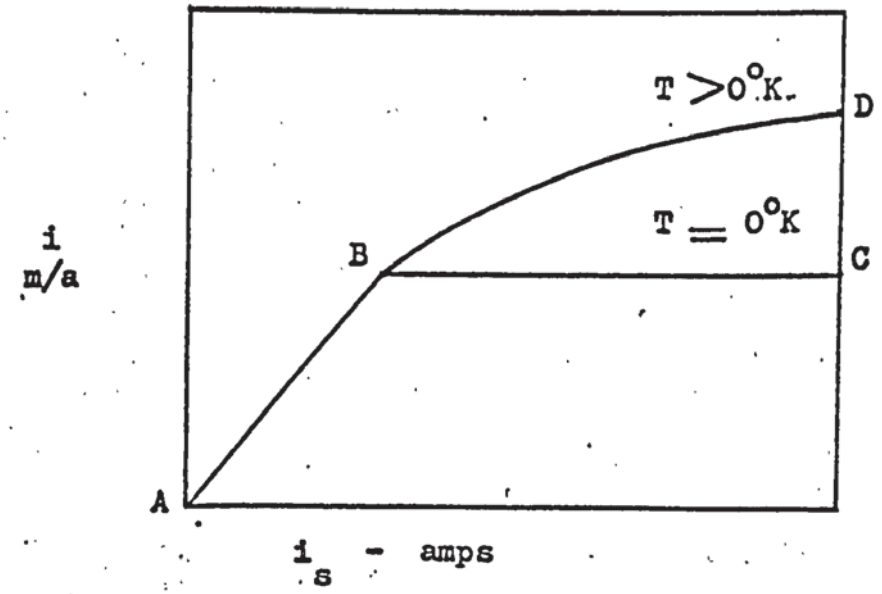

Figure 2

The line ABC represents that given by Child's law in which emission velocities are neglected, and BC represents the region in which i is independent of i_s. In a real case, T> 0°K, the curve follows the line AB for low values of i_s, and BD for higher i_s.

The line BD has slope $\left(\frac{\partial i}{\partial i_s}\right)_{v,x}$, and this slope varies from zero upwards in the space charge limited region with variation in T or i_s. It is therefore a differential coefficient having a wide range of variation with temperature, even though its normal value is small. In contrast the anode current depends very little on temperature when there is space charge. It will be shown in chapter 2 that this idea has been supported by experimental measurements on total emission and space charge limited current.

1.5 Emission in accelerating fields

For higher anode voltages, the potential barrier due to the space charge disappears and the current saturates. The potential energy, V, of an electron at a distance x normally from the surface of a metal is given by

$$V = \frac{-e^2}{4x} - eEx$$

where the first term results from the mirror image force and the second from the applied field, E. V has a maximum at the position,

$$x_o = \frac{1}{2}\left(\frac{e}{E}\right)^{1/2}$$

where the potential energy is less than the zero field height by the amount,

$$-V(x_o) = (e^3 E)^{1/2}$$

This lowering of the surface barrier gives rise to the Schottky effect[15]. Now the effective value of the work function,

$$\phi_1 = \phi - (e^3 E)^{1/2}$$

so that the saturated current is,

$$i_s = A^* \quad T^2 \exp \quad \left\{ \frac{-e\left[\phi - (e^3 E)^{1/2} \right]}{kT} \right\}$$

A plot of ln i against $E^{1/2}$, known as a Schottky plot, should produce a straight line from which extrapolation gives the zero field emission. With clean metals there has been reasonable agreement with experimental results, and this supports the mirror image model. However Schottky recognised that it is not valid for small distances from the surface because as x approaches zero the work done to remove an electron would be infinite. He suggested that below some critical distance from the surface the potential energy in that region would be a linear function of x. An alternative point of view is just to ignore this difficulty, as no experiments have yet been devised which yield quantitative analysis of the forces at these small distances from the surface. It is necessary to assume, in any case, that the force is zero at the surface.

As the field increases a further complexity arises due to the change in both the shape and position of the barrier. It is thought that this produces a reflection for low energy electrons which is in series with the stationary reflector presented by the metals surface field. This is supposed to produce an electron-wave interference effect and hence a periodic deviation from the Schottky effect. This has been observed experimentally by Hass and Coomes[16] but the effect is very small, with deviations from the Schottky line of less than 0.3%. It is possible that this small difference is only about

the same order of accuracy as the experimental observations.

For a semiconducting surface the image field will be weaker but if the effective dielectric constant is fairly large the image force will be almost as great as a metal. However Padovani[17], using a semiconductor surface of Au Ga As, found that, in order to explain the observed behaviour in terms of image force theory, it was necessary to choose a static dielectric constant and an image force dielectric constant which was dependent on temperature and carrier concentration. Considering the difficulties already discussed with metals it is not surprising that these extra complications in the assumptions used should be necessary to fit experimental results to theory.

The effect of a patchy work function also introduces a further problem and has been discussed by Herring and Nicols[18]. They show that if the applied field is either smaller or larger than the patch field, then the Schottky plots will be linear, and with the same slope as that of a uniform surface. That is with weak fields the emission is composed mainly from the low work function patches, whereas at high fields the emission is due to the sum of the currents from high and low work function areas. The weak field case has been supported experimentally by Venema et al[19], who used a scanning technique to show that a large fraction of the emission came from the small work function areas.

However when the applied field is the same order as the patch field, the Schottky plots will be non-linear and its average slope will be considerably greater than for a uniform

surface. This is often referred to as the anomalous Schottky effect. Thus it should be possible to get some information about the patch nature of the surface.

With semiconducting surfaces the effect of patches is even more complex as it cannot be assumed that the electro chemical potential of the electron inside the conductor is the same under all points of the emitting surface. Neither can it be assumed that the chemical potential is unaffected by the field.

In the case of practical thermionic emitters, such as oxide cathodes, it is frequently the case that the zero field emission is required from measurements in which only a very small accelerating voltage has been applied. In this case it is clearly impossible even to attempt to apply a Schottky correction because the effective voltage is not known accurately, since the contact potential difference is also not known exactly.

Many workers have reported serious deviations from the Schottky theory for composite emitters. This has been attributed to such effects as patchiness of the surface and actual surface roughness, which could yield high fields even at low voltages. These remarks are partly supported by Hung[20] and Shibata[21] with oxide cathodes and Hass and Thomas[22] with commercial matrix cathodes. In addition Shibata concluded that the deviation was partly caused by an avalanche effect due to secondary emission in the cores of the matrix.

These difficulties are summarised by Hensley[2] who says

that attempts to obtain the value of the emission at zero applied field for non metallic cathodes, using Schottky plots, are seldom meaningful and represent a needless expenditure of effort. This is in agreement with Beck[23] who says that the simplest plot of ln i against V curves with extrapolation back to V = 0 is the best empirical approach.

When the field is very high, of the order of 10^7 v/cm, the potential barrier in front of the cathode becomes so narrow, of the order of a few atomic diameters, that electrons can tunnel through the barrier to give cold field emission. Attempts have been made by Good [24] and Christov [25] to produce a complete analytical theory of electron emission from metals. This is developed on the basis of a general integral expression for the total transmission probability of an incident electron on the potential barrier at the metal surface. The integral is expressed as a sum of three conveniently defined integrals which give the current density in the ranges of conditions pertaining to the Schottky effect, the field effect and intermediate conditions. This has proved only to be partly successful, and also does not appear to clarify the situation greatly.

1.6 Departures from the ideal current-voltage characteristics

It is well known that the transition from the retarding field to the saturated emission, is not as sharp as might be expected by equation (5), if only the Maxwell-Boltzmann distribution of electron velocities applied and were effective. Curvature of the "knee" can arise on account of several factors. Thoseusually

considered are the field dependent reflection of electrons, non-uniform work functions, tube geometry and space charge.

The reflection of electrons will cause a deviation of the thermally emitted electrons from a Maxwellian distribution. For clean uniform metals the value of r will be small, but if the surface is covered with a foreign element r may be larger. However these effects are difficult to study experimentally due to the non uniform surface. The effect of such patches can be simulated by a velocity dependent reflection coefficient.[26] Nottingham has shown that the velocity distribution for polycrystalline surfaces is non-Maxwellian for energies less than 0.5eV. Sometimes it is also necessary to consider the effect of reflection in the collector patch field. Fortunately in the case of a cylindrical system, this can be largely neglected as there will be a good chance of the reflected electron missing the emitter and reaching the collector on the other side of the collector if it is reflected on one side.

From this discussion it is clear that with a complex emitter, curvature of the knee should be expected - and is found, eg. Hung[20]. Nevertheless it is of interest to consider some of the recent work on clean uniform emitters to show that even in this case the situation does not appear to be fully understood.

Hutson[27] used a 180° velocity analyser to measure the electron energy distribution for various crystal faces of tungsten. He showed that they were not Maxwellian and claimed that this was due to a reflection coefficient as given by Nottingham[1],

$r = \exp -\left(\frac{V}{0.191}\right)$, where V volts is the energy of the electron in excess of that needed to escape. For example this gives 37% loss at 0.191 V, and would produce a departure from the ideal characteristic. This method was rather complicated and the fitting of experimental points to expected distributions was not very accurate due to instrumental limitations.

Shelton [4] criticised the conventional retarding potential experiment which he states prevents exact determination of the energy distributions. He performed experiments under very carefully controlled conditions at 10^{-10} torr, using a three element retarding potential method on the (211) face of tantalum. The thermally emitted electrons were accelerated to an intermediate electrode in an axial magnetic field. This reduced the space charge and defined the small emitting area accurately. The electrons passing through the aperture were recorded on a third electrode of tantalum and the collector current was measured as a function of the retarding potential. Assuming the collector temperature was constant he was then able to measure the anode work function by the Sano [3] method. Furthermore conventional Richardson plots gave the emitter work function, assumed to be at $0^{\circ}K$, so that he was able to measure the temperature variation of ϕ. This was found to be -0.17×10^{-4} $eV/^{\circ}K$ for ϕ_{211} for tantalum as 4.35eV.

The retarding characteristics showed the curve at the knee to extend over only about 20mV. This seemed to indicate only a slowly varying value of r, which confirmed the ideal Maxwellian

distribution, and therefore disputing the expression given by Nottingham.

These experiments appear convincing but can be criticised on two grounds. Firstly the use of a third electrode, magnetic field and small aperture, complicates the situation to an unknown extent due to the electron optics of the device. Secondly it is likely that with the large accelerating voltage on the aperture, the retarding field from the collector has little effect at the emitter surface and only acts on the electrons which have already been emitted under the influence of the accelerating field. This point of view seems to be supported by the complete flatness of the saturated region in Shelton's curves. Despite this a number of other workers have applied Shelton's technique.

Kisliuk[5] investigated the reflection of slow electrons from tungsten using a modification of Shelton's method. In this case the accelerator divided two pumped systems so that gas could be admitted to the collector only, in order to study the effects of adsorption of gas on the collector. He was unable to get the sharp knee like Shelton although the curvature was less than predicted by Nottingham. Furthermore electron microscopic examinations did not reveal any patchiness on the surface.

Kisliuk points out that in this method the total collected current is the current arriving at the collector minus the reflected current and the secondary electron current. The number in each case is about equal at 10v but for higher energies the number of secondaries is greater. He confirmed this experimentally for various

crystal faces and attributed dips in the curves as due to diffraction effects in which reflections occur from different crystal planes. Shelton did not get this effect with tantalum. Kisluik concluded that, from experiments on gas adsorption, Shelton's result could be explained if there was a monolayer of impurity on the tantalum. This is despite the rigorous treatment of the tantalum specimens.

Love and Dyer[6] and Love and Wilson[28] used Sheltons method for the (311) plane of tungsten and their results show considerable curvature of the knee, but they make no reference to it.

Hass and Thomas[22] used an electron probe method to scan the surface of a commercial matrix cathode and obtained considerable curvature of the knee. They claimed that this was not due to energy distribution of the electron beam, or due to patches because of the slow variation of work function near the spot under investigation. They showed that this was more likely due to a resistive layer present at the surface. This was shown from the slope of the voltage departure against current curves for several micro regions.

Heil and Holloway[29], using a direct beam method, measured the zero energy reflection coefficient of freshly evaporated silver. They found r rose from 7% at zero energy to 39% above zero energy. They criticised Shelton's method as the decrease of the reflection coeffficient could be due to the re-collection of the reflected portion of the beam between aperture and collector. Shelton's method would thus give an average reflection coefficient and not a zero energy value. Furthermore they conclude that the

simple wave mechanical calculation of reflection at a potential step cannot be realised in practice as the theory neglects electron scattering during entry into the material. In a theoretical paper, Heil[30], shows the surprising result that reflection is independent of patch composition, size and distribution.

Recently Abey[31] applied Shelton's method to the (100) face of tungsten-rhenium alloy, using vac-ion pumps. He also found a curvature of the knee which was a function of the retarding voltage. He then attempted to explain this using a reflection coefficient of the form $\alpha \exp\left(\frac{-p^2}{2mw}\right)$ for the emitted and collected electrons, where α and w are constants and p is the normal component of momentum outside the surface. This then modified the usual equations for retarding current, saturated current and emitter temperature. Despite this further complexity the functions were insensitive to changes in α and he admitted that it was not possible to say whether the curvature was due to a reflection of this form. The loss of current was real and it was also produced with a (100) tungsten specimen. It is particularly interesting to note that he says that it did not depend upon the accelerating voltage provided it was greater than 100v. This remark seems to support the criticism made earlier of the Shelton technique, that the small retarding field will have little effect at the emitter surface with large accelerating voltages on the aperture.

In conclusion of this section it can be assumed that the curvature of the knee is, at least, partly dependent on such things as patchiness, reflection and space charge. However the

work described on clean surfaces has shown that the situation is at present not fully understood. It has also been shown that interpretation of these experiments is difficult and can be mistaken. This will be referred to again in Chapter (6).

1.7 Measurement of total emission and cathode evaluation.

The earlier discussion has shown that it is difficult to measure the zero field emission at normal operating temperatures. This is particularly the case with low work function cathodes because the space charge limitation starts at relatively low temperatures. If the applied field is sufficient to remove the space charge, then other serious effects may be introduced. These include such phenomena as the joule heating of the cathode coating by the emission current passing through it, and gas evolution from the electrodes which may poison the cathode. It is therefore the purpose of this section to discuss methods which have been used to measure the total emission as a means of evaluating the emissive properties of the cathode, particularly the oxide cathode.

1.7.1 Retarding fields

Hinsh[32] and Roethe[33] have used the retarding field characteristic to measure the contact potential difference (C.P.D.) at sufficiently low temperatures so that there is no appreciable space charge limitation. Then by extrapolating the retarding field characteristic at normal temperature until it meets the C.P.D. value determined for the lower temperature, this gives an estimate of the total emission at the higher temperature. However its serious limitation is that it takes no account of the variation

of C.P.D. with temperature.

1.7.2 Noise test

A comparison of valves can be made using a noise test - eg. Almer et al[34]. The noise for the valve with nominal fixed anode current and voltage, and with the cathode at reduced temperature, is compared with the noise of a directly heated saturated diode. The current in the noise diode is adjusted so that its noise equals that of the valve under test. The diode current, i_d, is then an inverse measure of the quality of the valve, ie. for high i_d the worse the emission of the valve under test. Consequently this method is useful for comparitive purpose but does not give absolute emission values.

1.7.3 Underheating method

In one method, (McCormack[35]), the cathode is judged in terms of the lowest temperature at which the space charge region commences. For the poorer cathodes this occurs at the higher temperature. More recently Dominquez et al[36] modified this for the 'dip testing method'. The anode current is recorded as a function of time after switching off the cathode heater and then switching it back on again. The characteristic dip in the curve gives information about the cathode - ie. with the less active cathode the current falls off more rapidly. This is a relatively crude method and its only real merit is that it is independent of tube geometry.

1.7.4 Low temperature technique

Metson[37] and his colleagues, eg. Lawson[38] used a low

temperature technique in which the space charge and power dissipation in the valve is negligible. They convert the low temperature emission to the normal temperature by a factor which from 700 to 1050°K is of the order of 1000. This method must have its limitations because it takes no account of the variation of A* and ϕ with temperature and from valve to valve.

Holmes [39] realised some of these limitations and used a less approximate but still fairly simple method. For a given value he plotted characteristics of ln i against $\frac{1}{T}$ for different anode voltages in the range 3.0 to 5.0v. Each curve showed a point from which it departed from its linearity. This point is assumed to be the zero field emission after the removal of the space charge. Over a limited temperature range these points lay on a straight line and by extrapolating this to normal temperature, the total emission was obtained. The extent of the extrapolation seems questionable as it could not be linear over a large temperature range. Holmes found no clear correlation between cathode work function and the total emission. This is not surprising because no account was taken of A*. In certain instances the values differed by as much as 50% from the pulsed emission values described in the next section.

1.7.5 Pulsed measurements

This is almost certainly the most commonly used technique. In certain cases (eg. Yazawa [40]) the short duration of the pulse is determined and controlled by the application of a condenser discharge through the tube. It is more customary to use pulses of about 1 μ sec at various high voltages so that the results can

be extrapolated to zero field. Sproul [40] and Coomes [42] first used this technique and reported emissions as high as 100 amp/cm^2 for an oxide cathode at 1075°K. However no good agreement has been found between pulsed and D.C. methods. In general a good pulsed emitter is usually a good D.C. emitter, but the reverse is not always true. Even for these short durations the heating of the cathode cannot be ignored and may be as much as 50°c. (Moyzhes et al[73]). Recently Beck and Maloney[43] described a method to measure this temperature rise, so that it is possible to correct for this. However if the resultant effect of the cooling of the cathode, due to the emission and the Joule heating, is the same order as the input heater power, the temperature of the cathode becomes unstable. This accumulative process may destroy the cathode.

In many instances a decay of the emission is followed by the application of the pulse, but the rate of the decay appears to be independent of the pulse duration or repetition frequency. In the case of the oxide cathode this has been explained as being due to the flow of barium ions towards the cathode core under the influence of the high field. However this decay will almost certainly be influenced by the base metal, anode material and barrier layer at the core-coating interfaoe (Eisenstein[44], Wright[45]). Therefore it can be seen that pulsed emission measurements on complex cathodes still remain problematical.

Finally Nottingham[1] reviewed the problem of cathode evaluation in some detail. He argues that Schottky plots with pulse or D.C. methods are not meaningful with these cathodes and

the retarding field methods suffer because of the nature of the surfaces and the difficulty of measuring the extremely low currents. It will be shown later that the last remark is not very relevant. On the other hand methods involving underheating, noise or deviations from the space charge laws are only approximate.

Nottingham attempts to idealise the problem in terms of tube geometry, uniformity of emission, temperature determination and uniformity of collector work function. He utilises the idea of unlimited emission and variation of C.P.D. with temperature to produce a set of master curves. Hence by combining measurements at low temperatures in the retarding region with those at high temperature in accelerating region, these can be made to fit the master curves. The final analysis involves the application of the Richardson and Fowler equations. This also requires computation of the variation of C.P.D. with temperature, assuming an average value of the anode work function. That is, he neglects the variation of ϕ_a with temperature.

The results of this analysis show some agreement between theory and experiment, but it is obvious that the method is exceedingly complex and not necessarily exact. It does not succeed in sorting out space charge effects from total emission effects and leaves some questions unanswered.

In the next chapter results will be presented of work which was undertaken in an attempt to measure the total emission without removing the space charge. The success of this will then be illustrated by some applications of this technique in practical problems in thermionic emission.

Chapter 2

Measurements of total emission and space charge limited current

2.1 Measurement of total emission.

It has been shown in the preceeding chapter that one difficult experimental problem in thermionic emission studies is the determination of the value of the total emission when the applied field is zero. This measure of the emission is not only a widely accepted and convenient definition of the total emission itself, but is frequently required for the study of the noise of the device.

Some criticisms have already been made of the existing techniques. The most frequently used pulse technique, obviously raises many questions with oxide cathodes due to the very complex - and still not fully understood - nature of the emission mechanism. It was therefore decided to make a detailed study of diode characteristics over a large range of currents to see if it was possible to extend the method described earlier in section 1.7.1.

The diodes used in the first part of the investigation were EA50's and in the second part EB91's. These valves are almost identical in structure except that the EB91 is a double diode. The circuit of the apparatus used, is shown in figure (3). The diode was mounted in its P.T.F.E. valve holder in a light tight box to

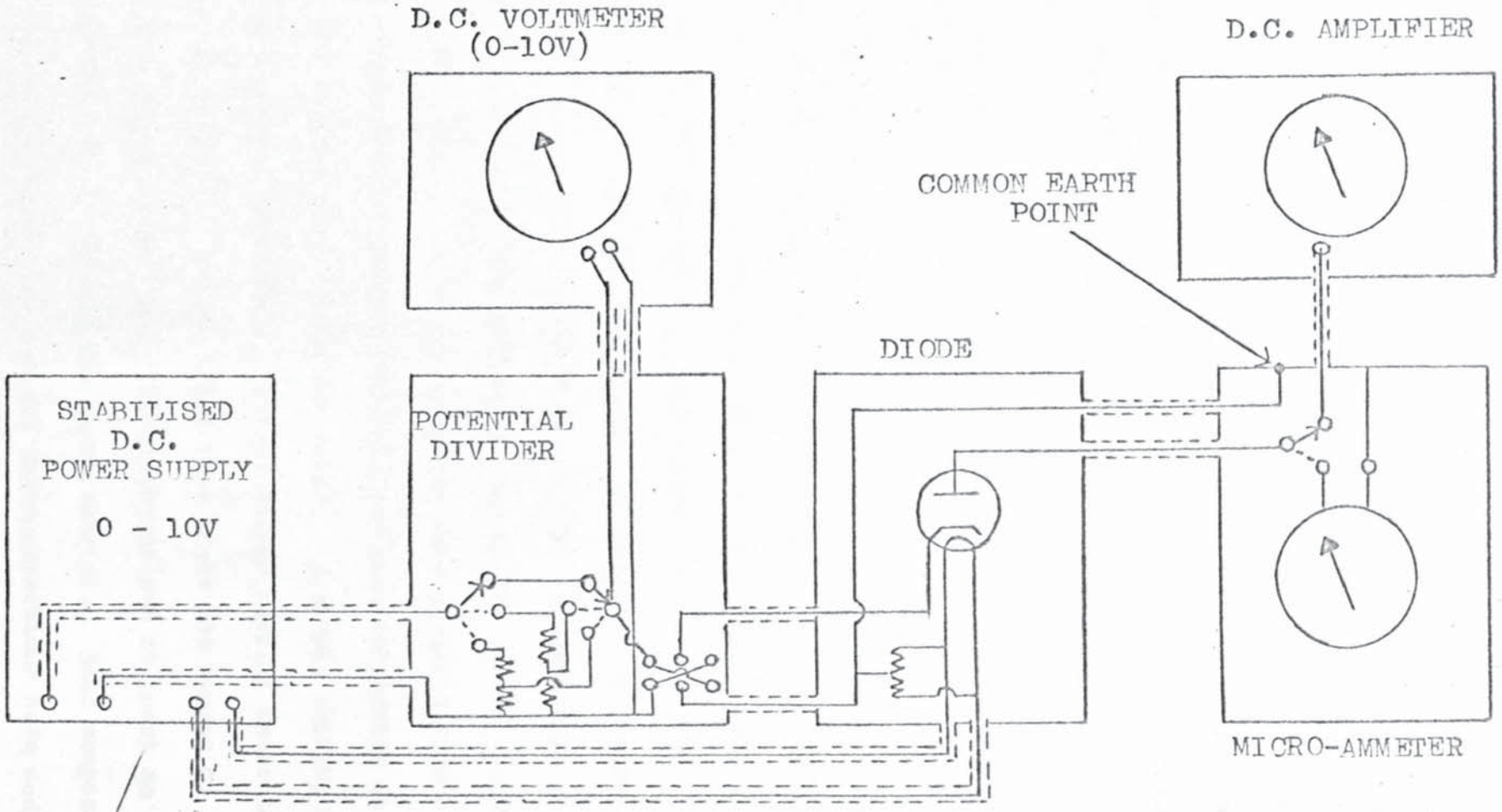

CIRCUIT FOR TOTAL EMISSION MEASUREMENTS

FIGURE 3

avoid errors due to photo-emission caused by ambient light, when the very low thermionic currents were being measured. The box also provided adequate electrostatic screening. A Solatron stabilised D.C. power supply unit provided the variable anode voltage via a low resistance potential divider. This was monitored on a D.C. voltmeter and was variable in 0.025v steps in the range -2.0 to +2.5v. Another similar power supply unit provided stabilised heating for the diode heater. Both D.C. outputs were isolated from earth potential. The anode current could be measured in the range 2×10^{-14} amp to 100 m/a. In the lower range, 2×10^{-14} to 10^{-6} amp, measurement was by means of an AVO D.C. amplifier, which had switched input resistors from 10^{7} to $10^{13} \Omega$. On the lowest current range the time constant was about 30 secs, and proper allowance had to be made for this when taking readings. The voltage necessary to produce full scale deflection on the ranges graduated 0 to 10 and 0 to 3, was 30mV and 24mV respectively. Due allowance was made for the potential drop in the current meter when taking readings. The higher currents were measured with a Cambridge unipivot micro-ammeter and this was also calibrated to allow for the voltage drop across the meter. A simple switch, made with polystyrene insulation, enabled either current meter to be used in the circuit. It was found that where the ranges of the meter overlapped at 10^{-6} amp, the agreement was at least as good as the accuracy of reading the micro ammeter. Each component was enclosed in a screened box and all interconnections were made with non-microphonic low noise coaxial cable. Only one common

earth point, made at the screen of the D.C. amplifier, was used to avoid any possibility of 'earth loops' being set up. Very good reproducibility was obtained with this circuit arrangement. Leakage currents were at least less than the lower limit of sensitivity of the amplifier - ie. $\sim 1 \times 10^{-14}$ amp.

Before any measurements were made each diode was operated for several hours at normal working temperatures ($V_f = 6.3v$) and with 2.5v on the anode. Actual measurements were always taken starting at the highest temperature before gradually lowering the temperature at the required intervals. Operation in this manner contributed to the very good reproducibility mentioned above. Suggestions for the reason for this have been made by Metson et al[46] and Nottingham[1], who consider that the donor concentrations are "frozen in" as the temperature is reduced and so remain stable during the time of the experiment. The reproducibility was so good that agreement between experimental points was obtained even after a time interval of several months, provided the temperatures were reduced during an experiment as described above.

The characteristics of six diodes are shown in figures 4a to 4f and are plotted as log i against Va. The current varies over 13 or 14 orders of magnitude. The figures clearly show the retarding, accelerating and space charge regions for various filament voltages. In the figures reproduced here, characteristics for all the filament voltages, eg. 5.7, 5.2, 4.0 and 3.0, which were used, are not shown. These have been omitted for clarity because the figures have been reduced from their original size of

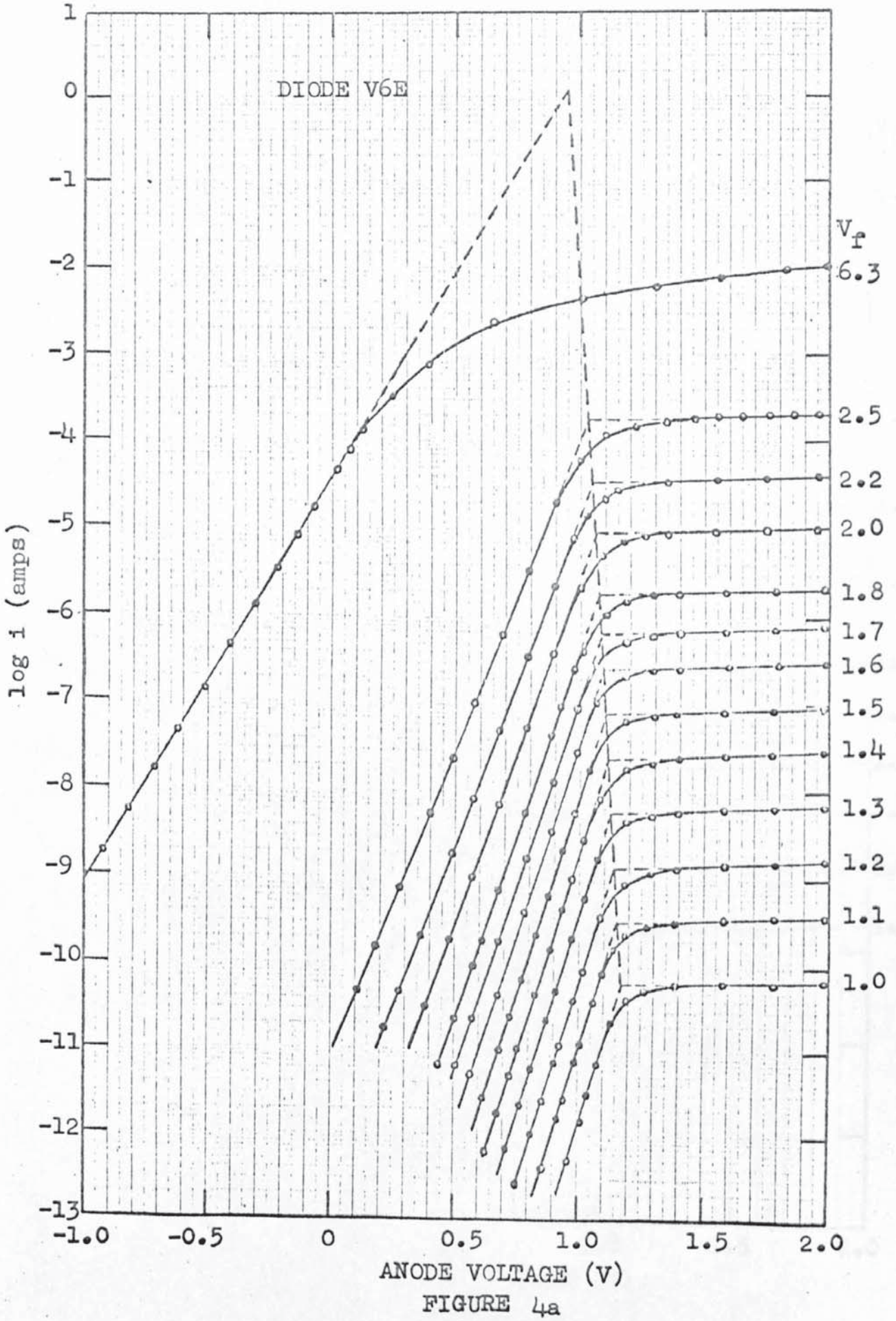
DIODE V6E
log i (amps)
1
0
-1
-2
-3
-4
-5
-6
-7
-8
-9
-10
-11
-12
-13
-1.0
-0.5
0
0.5
1.0
1.5
2.0
ANODE VOLTAGE (V)
V_f
6.3
2.5
2.2
2.0
1.8
1.7
1.6
1.5
1.4
1.3
1.2
1.1
1.0

FIGURE 4a

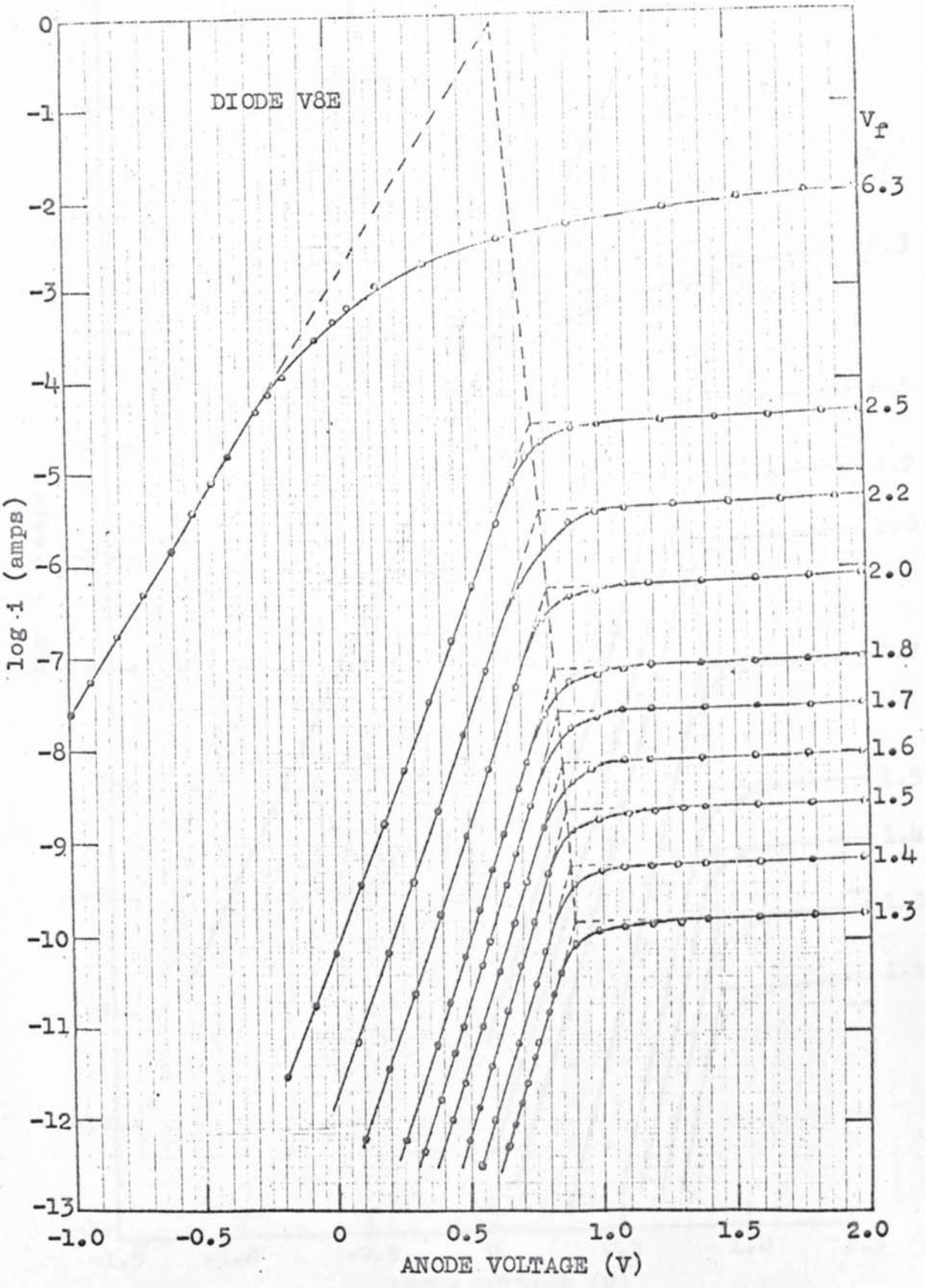
DIODE V8E
V_f
6.3
2.5
2.2
2.0
1.8
1.7
1.6
1.5
1.4
1.3
log i (amps)
0
-1
-2
-3
-4
-5
-6
-7
-8
-9
-10
-11
-12
-13
-1.0
-0.5
0
0.5
1.0
1.5
2.0
ANODE VOLTAGE (V)

FIGURE 4b

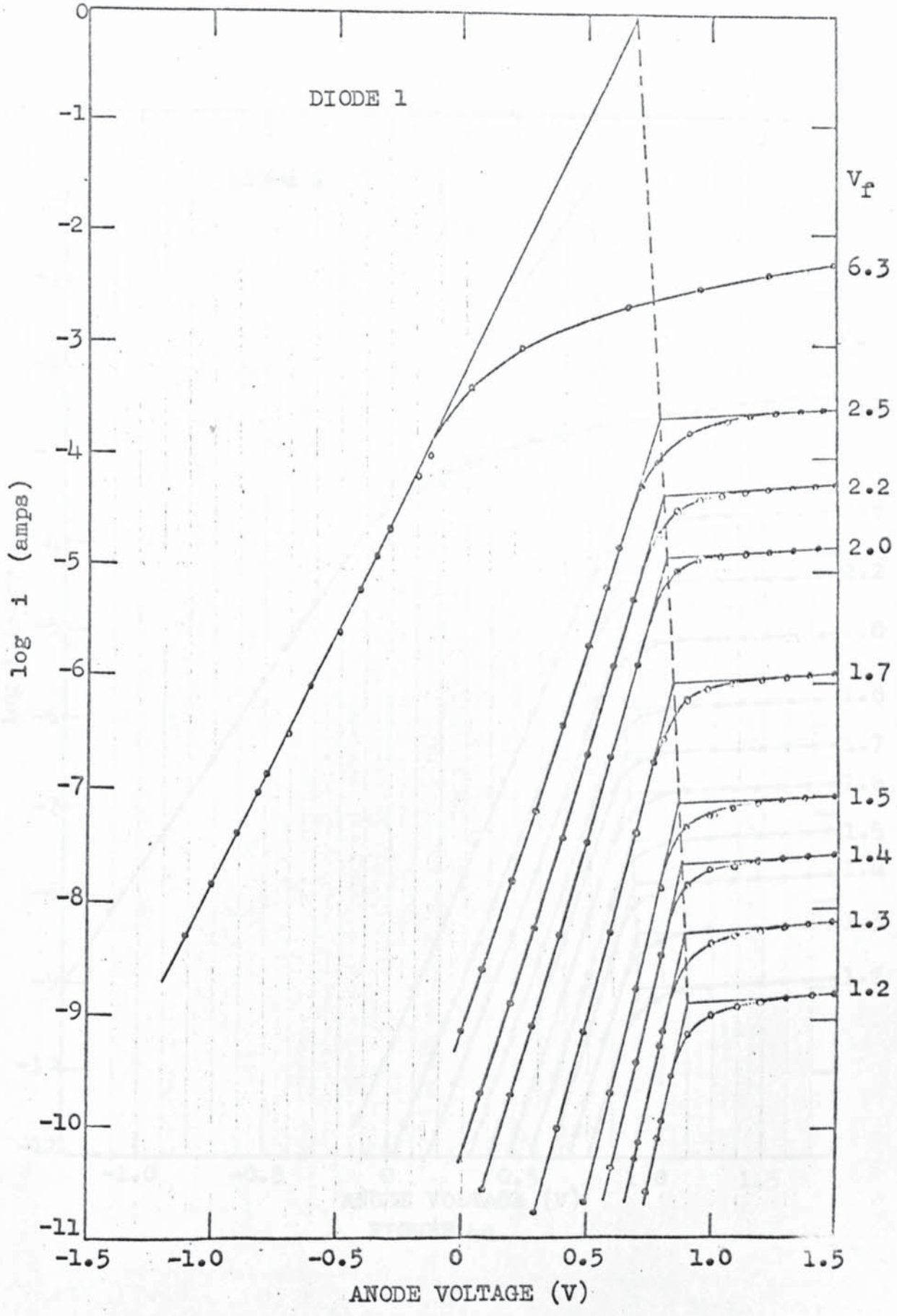
DIODE 1
log i (amps)
0
-1
-2
-3
-4
-5
-6
-7
-8
-9
-10
-11
-1.5
-1.0
-0.5
0
0.5
1.0
1.5
ANODE VOLTAGE (V)
V_f
6.3
2.5
2.2
2.0
1.7
1.5
1.4
1.3
1.2

FIGURE 4c

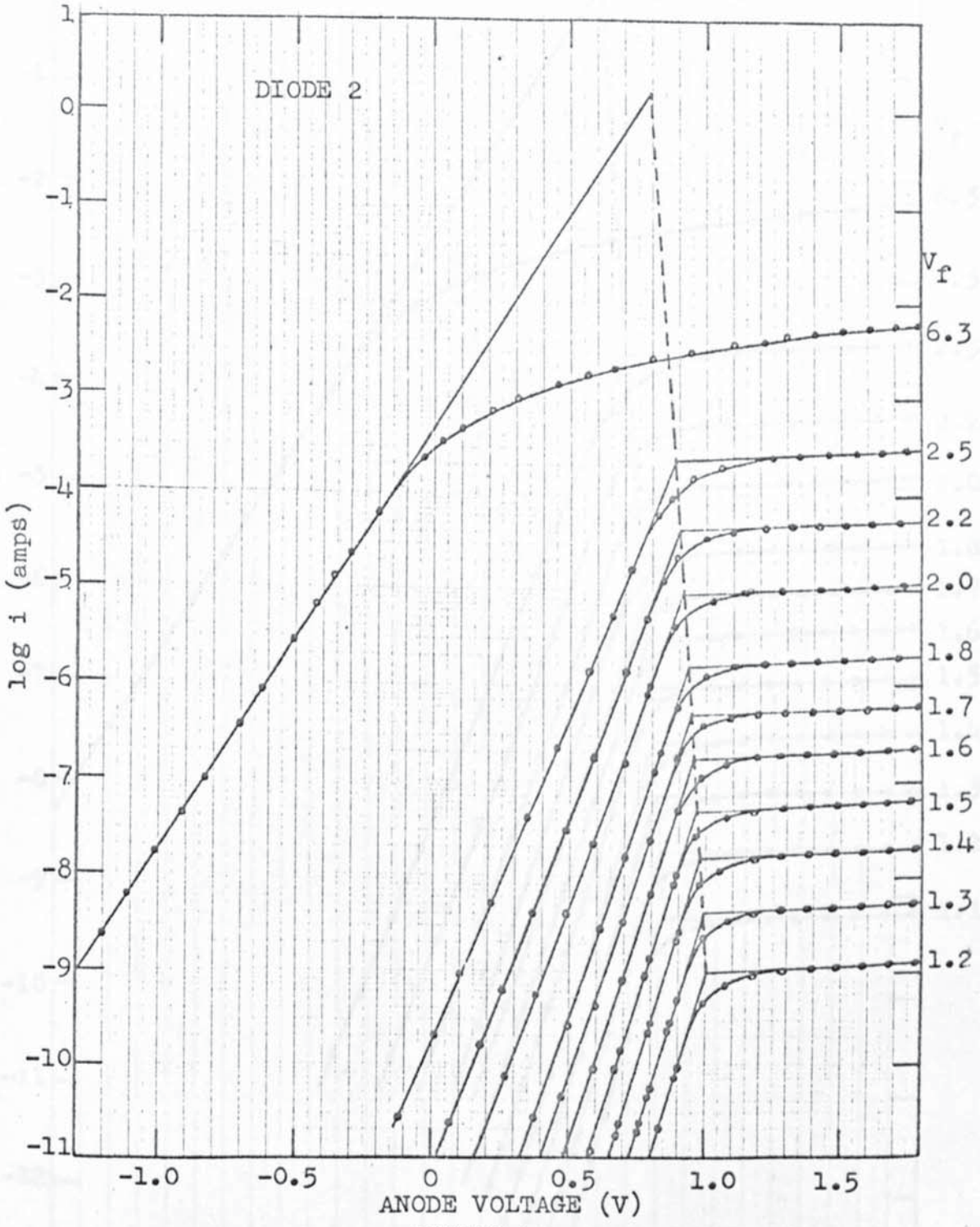
DIODE 2
log i (amps)
1
0
-1
-2
-3
-4
-5
-6
-7
-8
-9
-10
-11
-1.0
-0.5
0
0.5
1.0
1.5
ANODE VOLTAGE (V)
V_f
6.3
2.5
2.2
2.0
1.8
1.7
1.6
1.5
1.4
1.3
1.2

FIGURE 4d

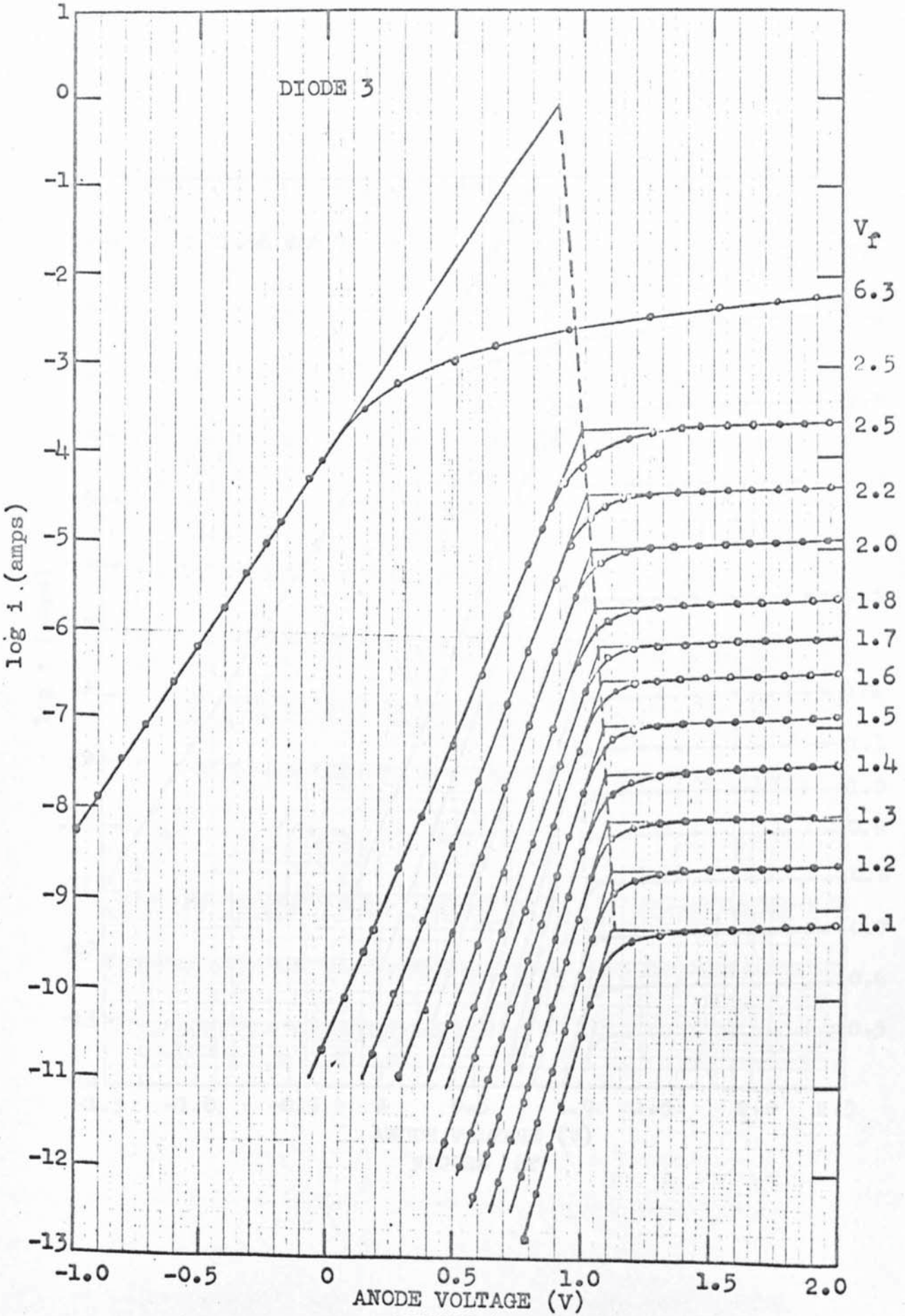
DIODE 3
log i (amps)
1
0
-1
-2
-3
-4
-5
-6
-7
-8
-9
-10
-11
-12
-13
-1.0
-0.5
0
0.5
1.0
1.5
2.0
ANODE VOLTAGE (V)
V_f
6.3
2.5
2.5
2.2
2.0
1.8
1.7
1.6
1.5
1.4
1.3
1.2
1.1

FIGURE 4e

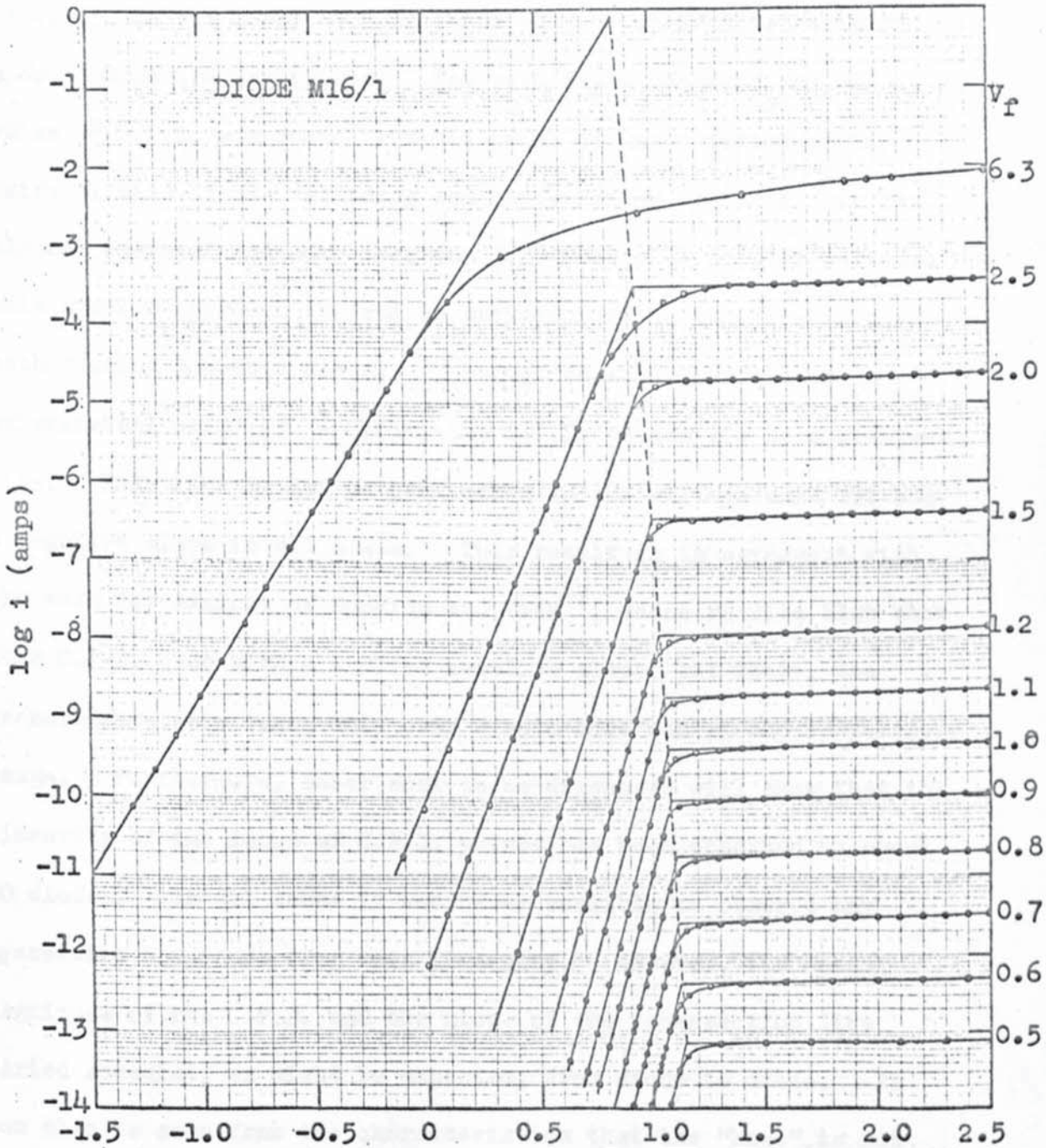
DIODE M16/1
V_f
6.3
2.5
2.0
1.5
1.2
1.1
1.0
0.9
0.8
0.7
0.6
0.5
log i (amps)
0
-1
-2
-3
-4
-5
-6
-7
-8
-9
-10
-11
-12
-13
-14
-1.5
-1.0
-0.5
0
0.5
1.0
1.5
2.0
2.5
ANODE VOLTAGE (V)

FIGURE 4f

20" x 16".

One main point of interest is to be found in the values of C.P.D. at the lower cathode temperatures, where the effects of space charge are negligible. The zero field emission and the value of C.P.D. was found from the point of intersection of the extrapolation of the retarding and accelerating regions. It has already been pointed out, (section 1.5) that with complex cathodes this simpler approach is just as satisfactory as the more involved method using Schottky plots. The figures show that within an experimental error of $\pm$ 0.01v, the C.P.D. points lie on a straight line. This line is not perpendicular to the voltage axis but has a negative slope in all cases. This result is in agreement with the work for example of Hopkins and Vick[47], whose results also show this C.P.D. line with a similar negative slope, but there, the measurements were taken only over a much more restricted temperature range. Furthermore, later work to be discussed will show that the linearity of the locus of C.P.D. points has been observed on about 30 diodes. In all cases it was never possible to observe any systematic departure from this linearity. However, the actual magnitude of the C.P.D. and the slope of the intersection line varied somewhat, as might be expected, from diode to diode. It can also be seen from the characteristics that the "knee" is not sharply defined even at the lowest temperatures. The present theories attempting to explain this phenomena have already been discussed in chapter 1. However no additional comment will be made at this stage, but instead has been allocated a small section

in chapter (6).

A further consideration must now be made on account of the cylindrical geometry of the diodes. Nottingham[1] has calculated the effect on the characteristics of the cylindrical rather than the planar geometry of the electrodes. This is illustrated in 5a in which log i against V characteristics are given for various ratios, $\frac{1}{a}$, of the anode to cathode radii. It is seen that as $\frac{1}{a}$ increases from unity in the plane parallel configuration, to infinity, the retarding regions of the characteristics are displaced to the more negative anode voltages when the currents are small. In addition the retarding plots show a small curvature as the saturated current is reached. For the EA50 diodes $\frac{1}{a}$ is about 1.4 so that it is nearly equivalent to the plane parallel case. Therefore provided measurements are taken far enough in the retarding region the slope of the retarding characteristic is indistinguishable from the Boltzmann line for plane parallel geometry.

The magnitude of the displacement of the characteristics is also a function of the temperature. For a value of $\frac{1}{a} = 1.5$, Nottingham gives this as 0.4 $\frac{kT}{e}$. C.P.D. points will therefore be in error by about 0.04V at 1100°K and about 0.02V at 550°K. The shift of these characteristics is illustrated in figure 5b for three temperatures, $T_1 \gtrsim T_2 > T_3$.

If it is assumed that the C.P.D. line CB, obtained experimentally, continues to behave in this manner towards the higher temperatures, then where the extrapolations of CB and XY meet at A this gives an estimate of the total emission for zero

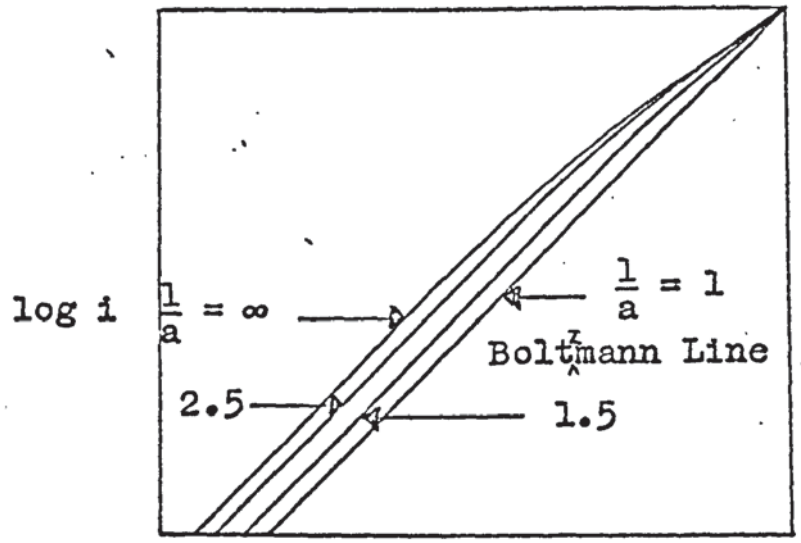

(a)

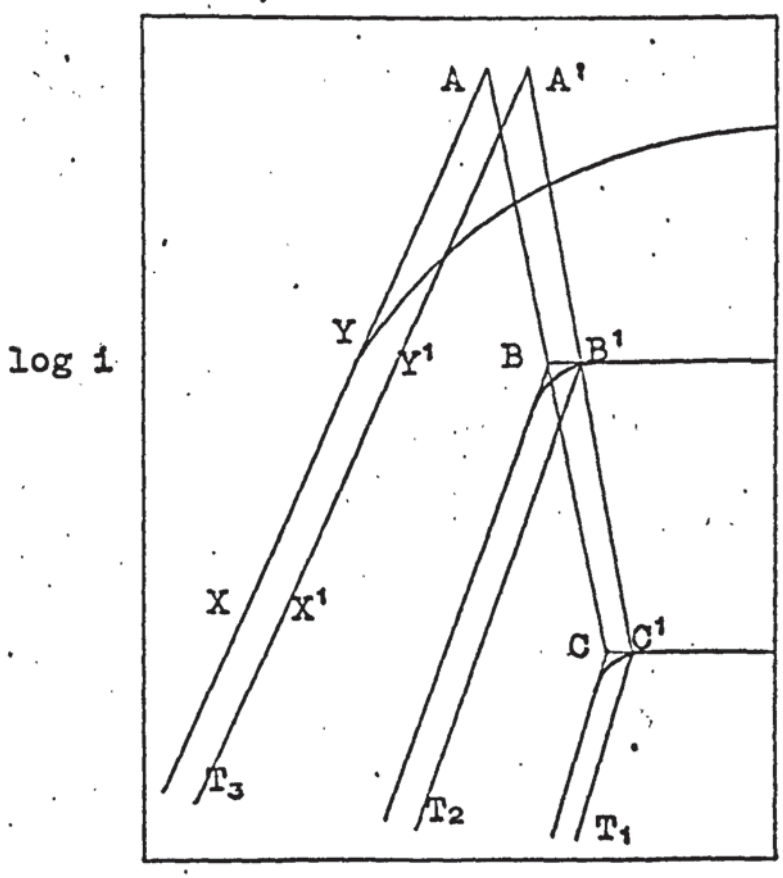

(b)

FIGURE 5

field, at normal operating temperature. It can be seen from the figure that extrapolation of C'B' and X'Y' to A', using the conversion to the plane parallel case, gives almost exactly the same value of total emission. The Nottingham corrections are not therefore significant in this respect and are not illustrated in the diagrams showing experimental results.

Using this method for the diodes shown in figures 4a to 4f, this gave values of total emission from 0.8 to 1.8 amps for a cathode area of $0.28cm^2$. These values are in reasonable agreement with results obtained by other methods, and published elsewhere, but on the average are lower than obtained with pulsed techniques. However they do not involve effects of high electric fields which pulse techniques produce, which were discussed in section 1.7.5.

The validity of the extrapolation to points such as A now comes into question. From these measurements calculations have been made which support this method in the following way. The cathode temperatures were calculated from the slope of the retarding plots using equation (5). A typical curve of cathode temperature against filament voltage is shown in figure (6) for diode V6E. The shape of this curve is similar to those shown by Metson[37] and Nagy[48]. Criticisms of this method for determination of cathode temperature have been made - eg. Nergaard[49] - but Nottingham[50] states that when the method is applied carefully it is one of the best methods. In some cases measurements were taken down to cathode temperatures as low as about $130^{\circ}c$, but below this the anode current was indistinguishable from leakage currents.

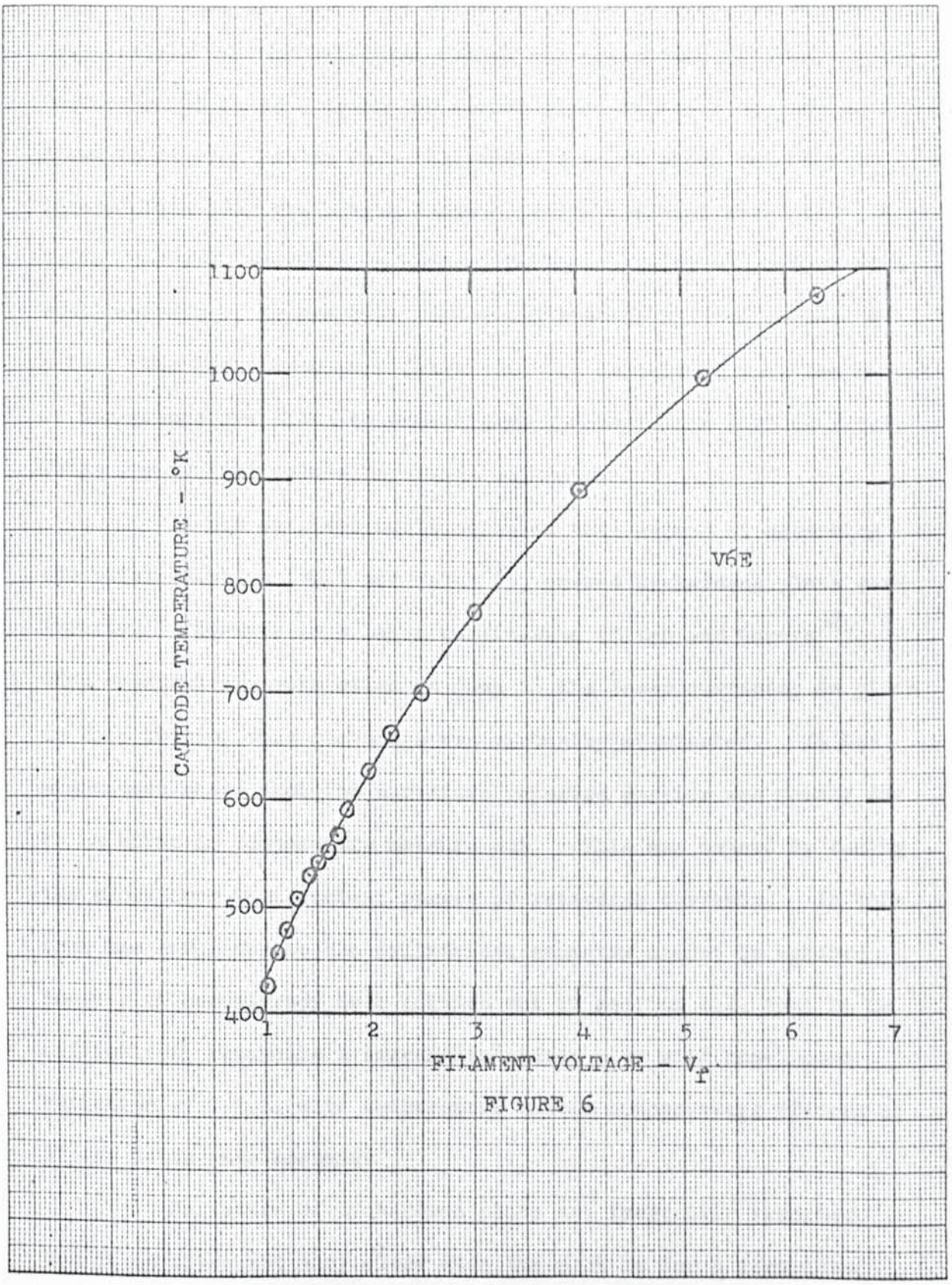
1100
1000
900
800
700
600
500
400
CATHODE TEMPERATURE - °K
1
2
3
4
5
6
7
FILAMENT VOLTAGE — V_f
VBE

FIGURE 6

Using the values of saturated emission measured at low temperatures and the estimated values at higher temperatures, Richardson plots were drawn for diodes given in 4a to 4e, and are shown in figures 7a to 7e. All these figures shown sensibly linear plots over the entire range of total emission currents. It is, however, possible to notice, but not specify the amount of a small curvature, in one case convex and another concave to the $\frac{1}{T}$ axis. The Richardson work functions, ϕ_R, calculated from the slopes of the graphs are shown on each figure and vary from 1.23 to 1.5eV. These are typical values for oxide cathodes.

In the earliest publication of this method of measuring the total emission (Bull and Fitch[51]), curved Richardson plots were reported. However in a later publication (Fitch and Coutts[52]), when measurements were extended down to the lower currents, as given in this thesis, this curvature was virtually eliminated. It has since been shown that the curvature reported earlier was mainly due to an error in temperature measurement. This was caused by taking the slope over insufficient ranges of retarding currents. In this case the error due to the cylindrical geometry cannot be ignored. However it has already been pointed out in section 1.2, that it is difficult to reconcile a linear Richardson plot with non-linear variation of C.P.D. with temperature unless compensating effects of A* are taken into account.

Curvature of Richardson plots are frequently reported, but it is often not very clear when the plot is for a restricted range of currents - eg. Higginson[53] and Hopkins and Vick[47]. More

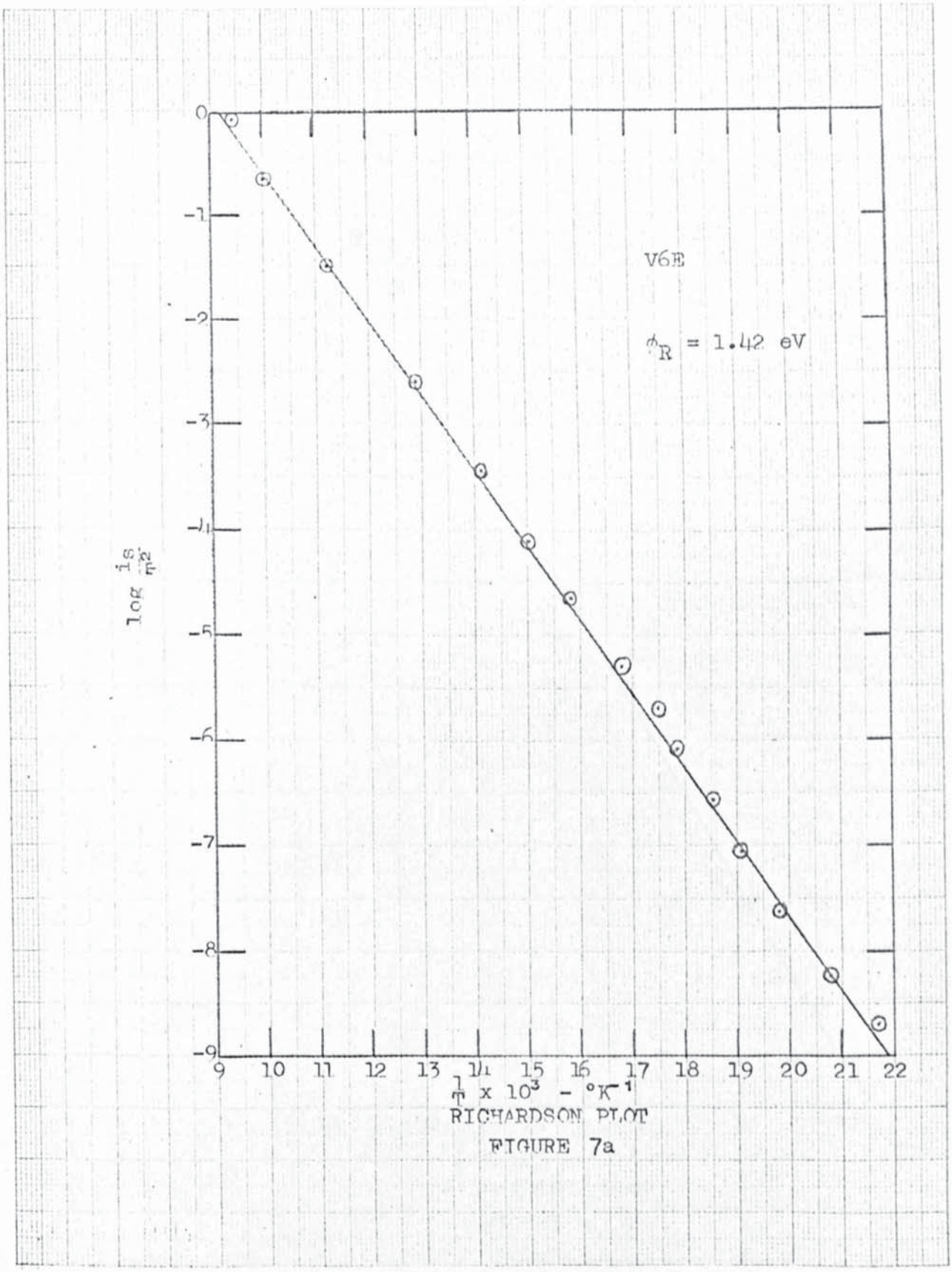

RICHARDSON PLOT

FIGURE 7a

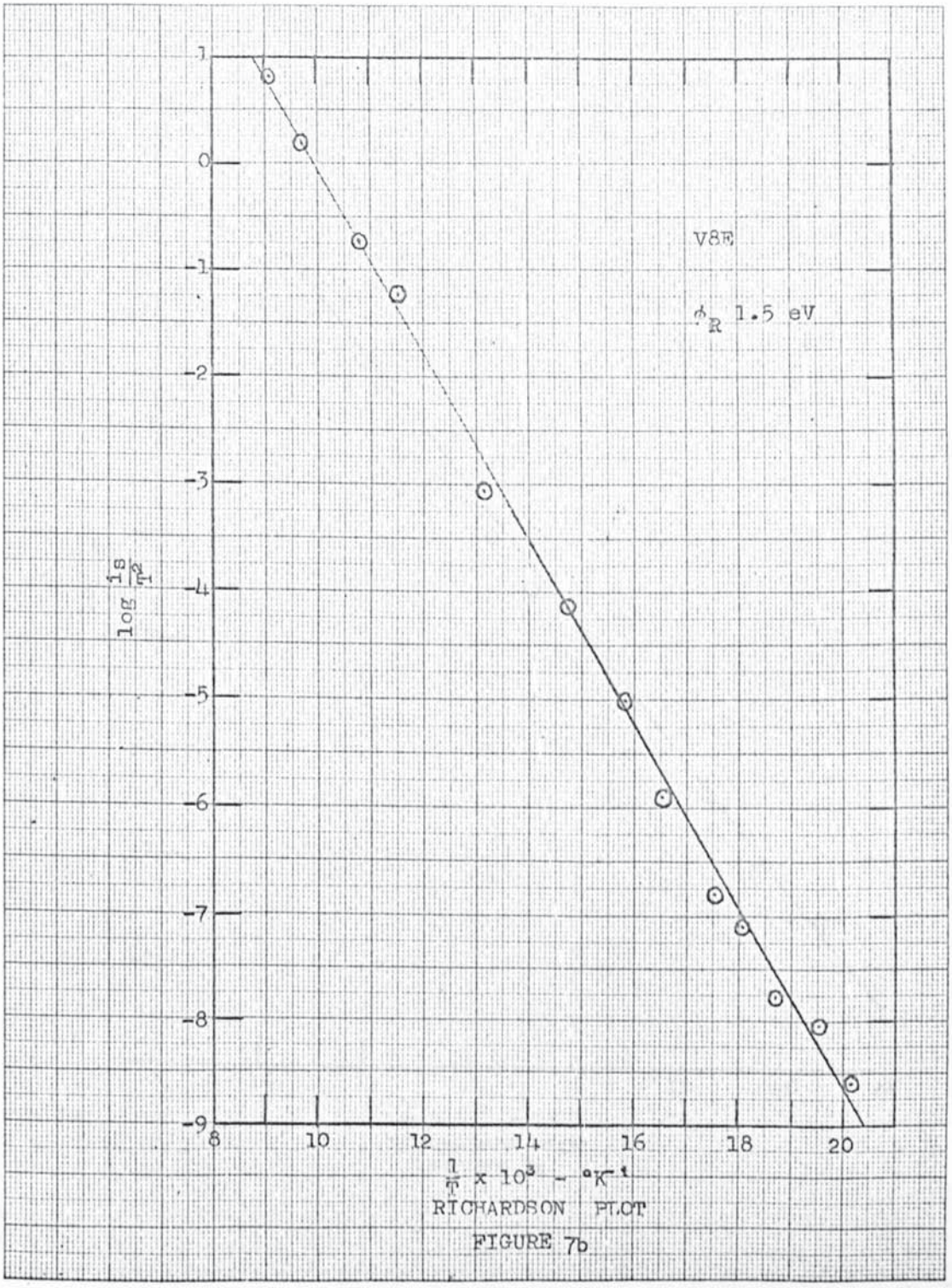

RICHARDSON PLOT

FIGURE 7b

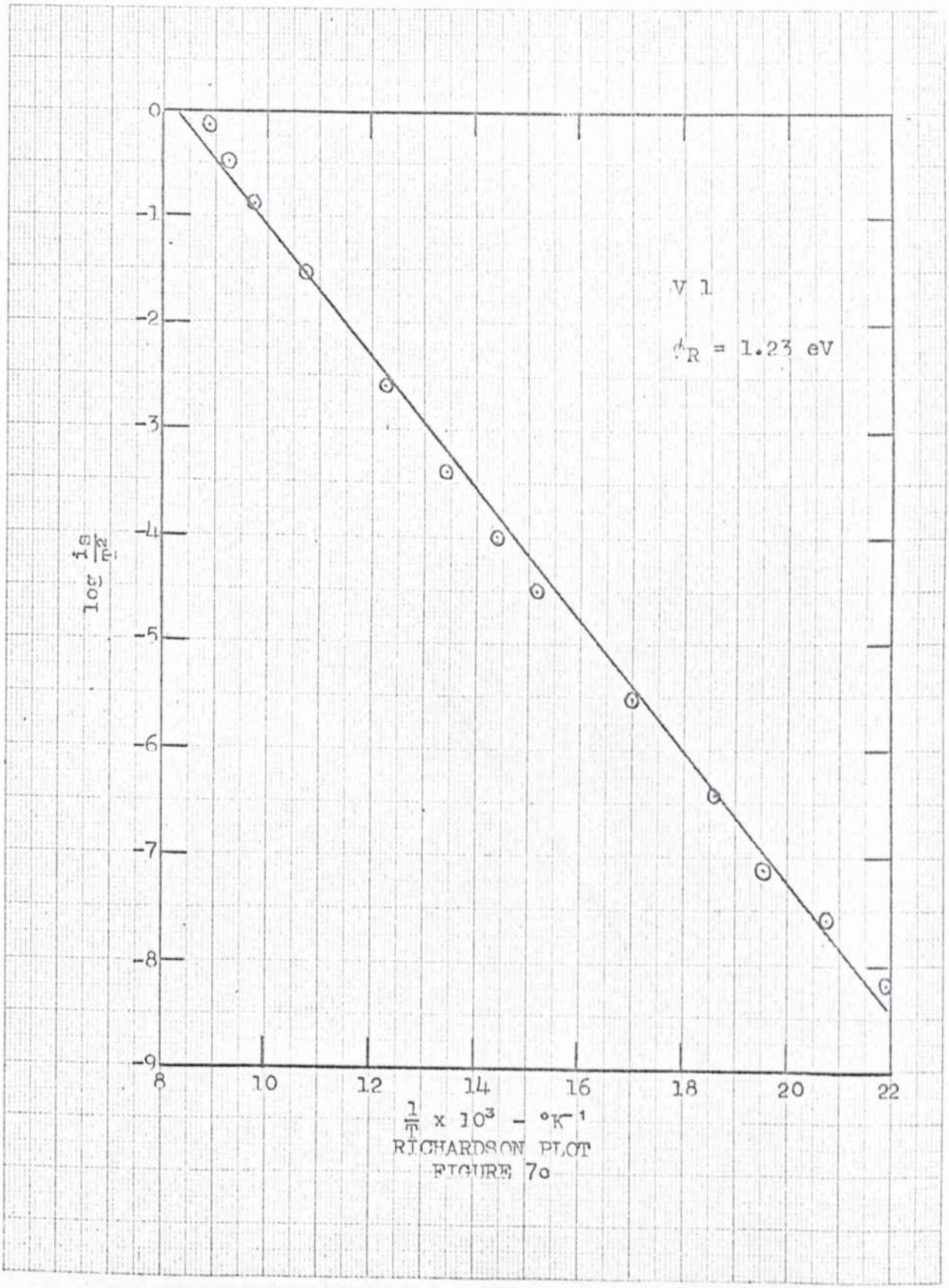

RICHARDSON PLOT
FIGURE 7o

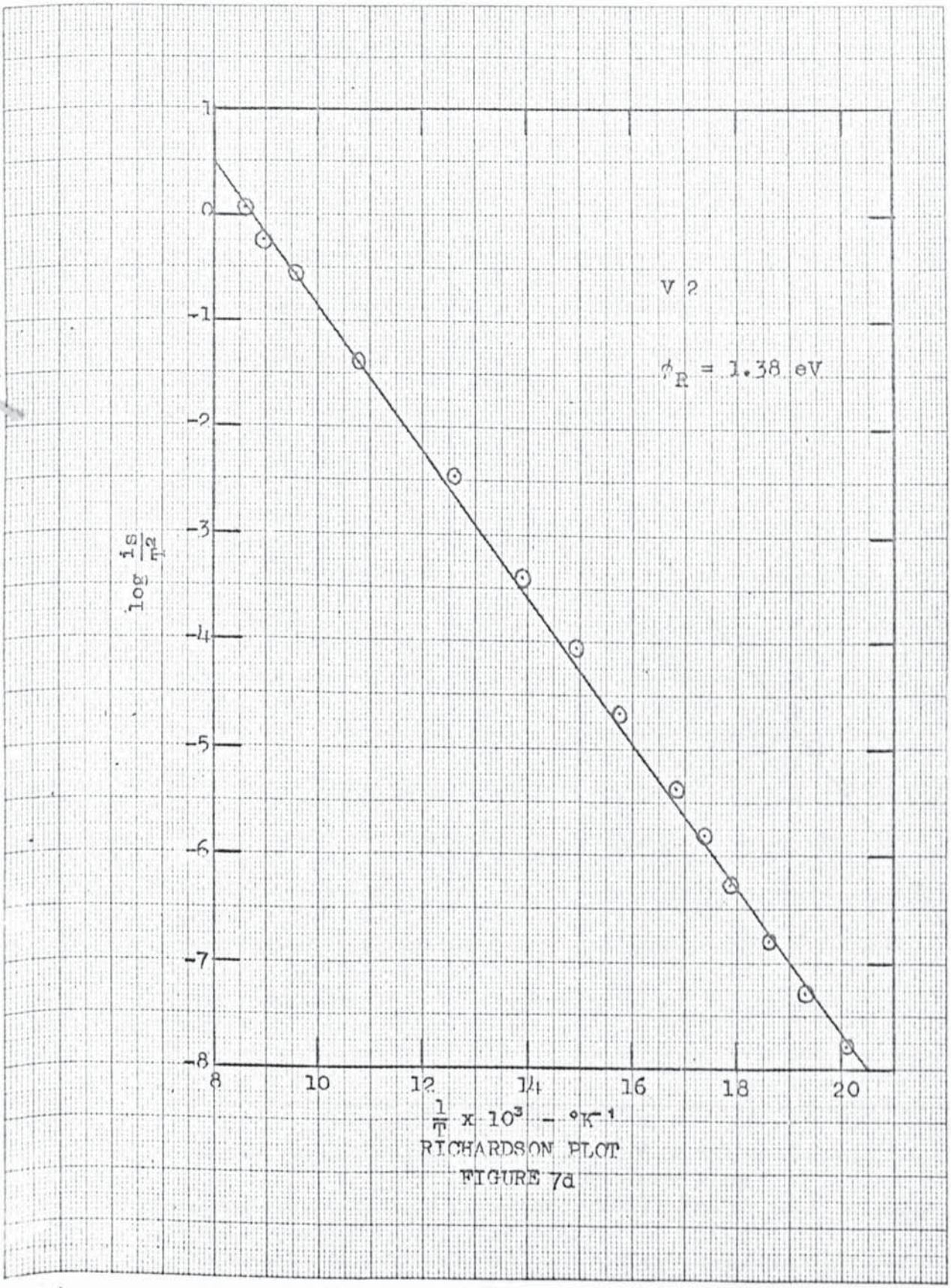

RICHARDSON PLOT

FIGURE 7a

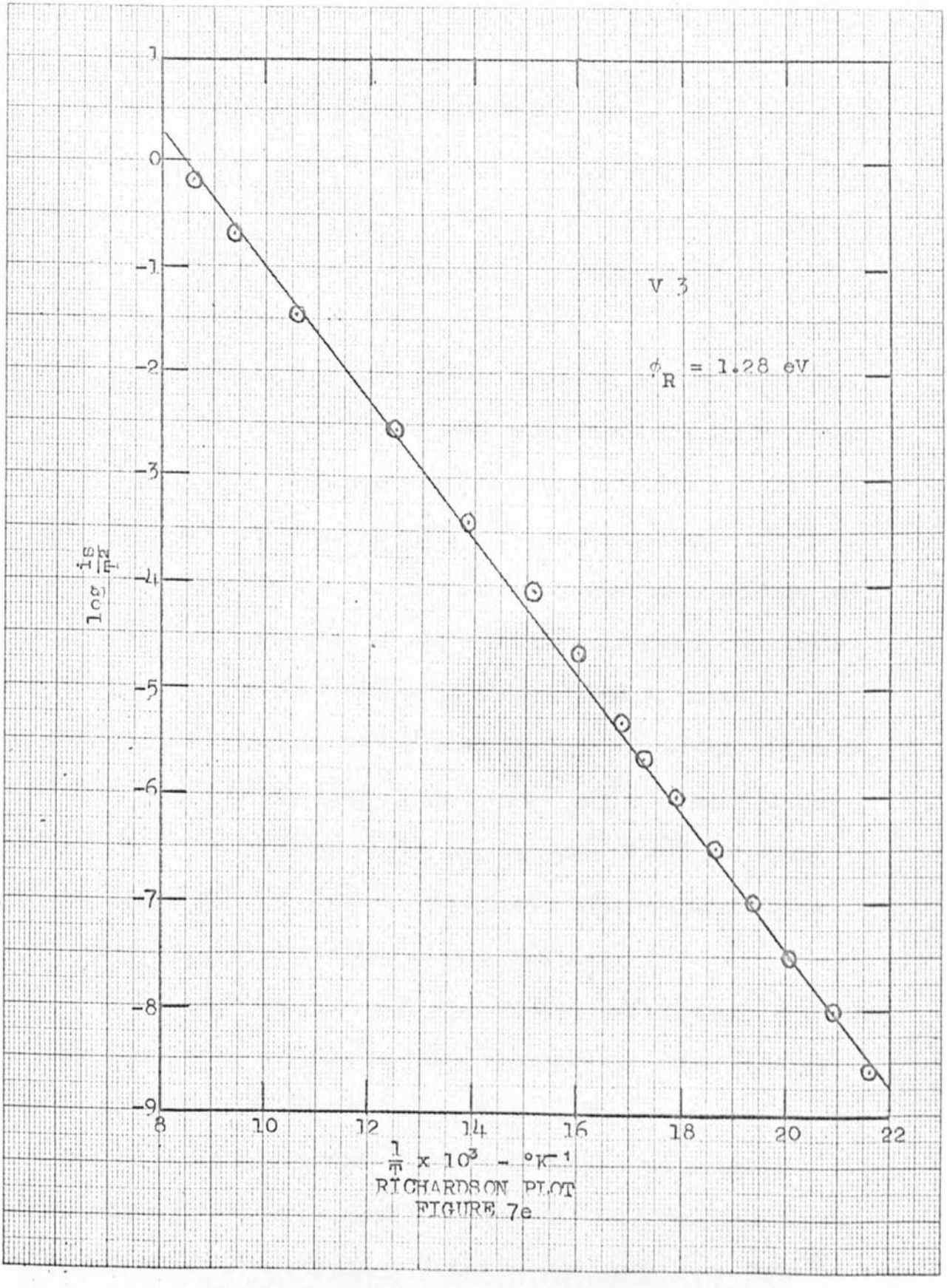

RICHARDSON PLOT
FIGURE 7e

recently Dewberry[54] reported considerable curvature of Richardson plots for oxide cathodes in the upper range of normal operating temperatures, 850 - 1100°K. He attributed this as being most likely due to the increase of the surface work function due to the adsorption of an electro-negative layer of unspecified substance. He makes no comment on the fact that a normal D.C. method for emission measurements was used at all temperatures. It has already been pointed out in section 1.7 that this is known to be unsatisfactory.

The variation of C.P.D. with temperature for diode V6E is shown in figure (8). The magnitude of this variation - $\sim 10^{-4}$ eV/°K - is similar to that reported by Arizumi[55] and Hopkins and Vick[47]. However exact comparison is not justified because anode surface and temperature effects may well be different in each case. Recently Krasin'Kova et al[56] used a retarding field method to obtain temperature variations of cathode work function for mixed oxides and found them to lie in the range 5 to 8 x 10^{-4} eV/°K. However they used the very dubious value of A = 120 amp. cm^{-2} $T°K^{-2}$ for oxide cathodes, together with Schottky plots under pulsed conditions to infer the temperature variation of work function.

With diode V6E a "Sano" plot of $\log i_r/T^2$ against $\frac{1}{T}$, with currents taken at Va = 0.9v, is shown in figure 9. The slope of this graph yields a value for ϕ_a = 2.68 eV. This low value for the Nickel anode could be expected since it is known that an anode becomes contaminated with evaporated materials from an oxide cathode during the activation process. Hopkins[57] and Hopkins and Ross[58]

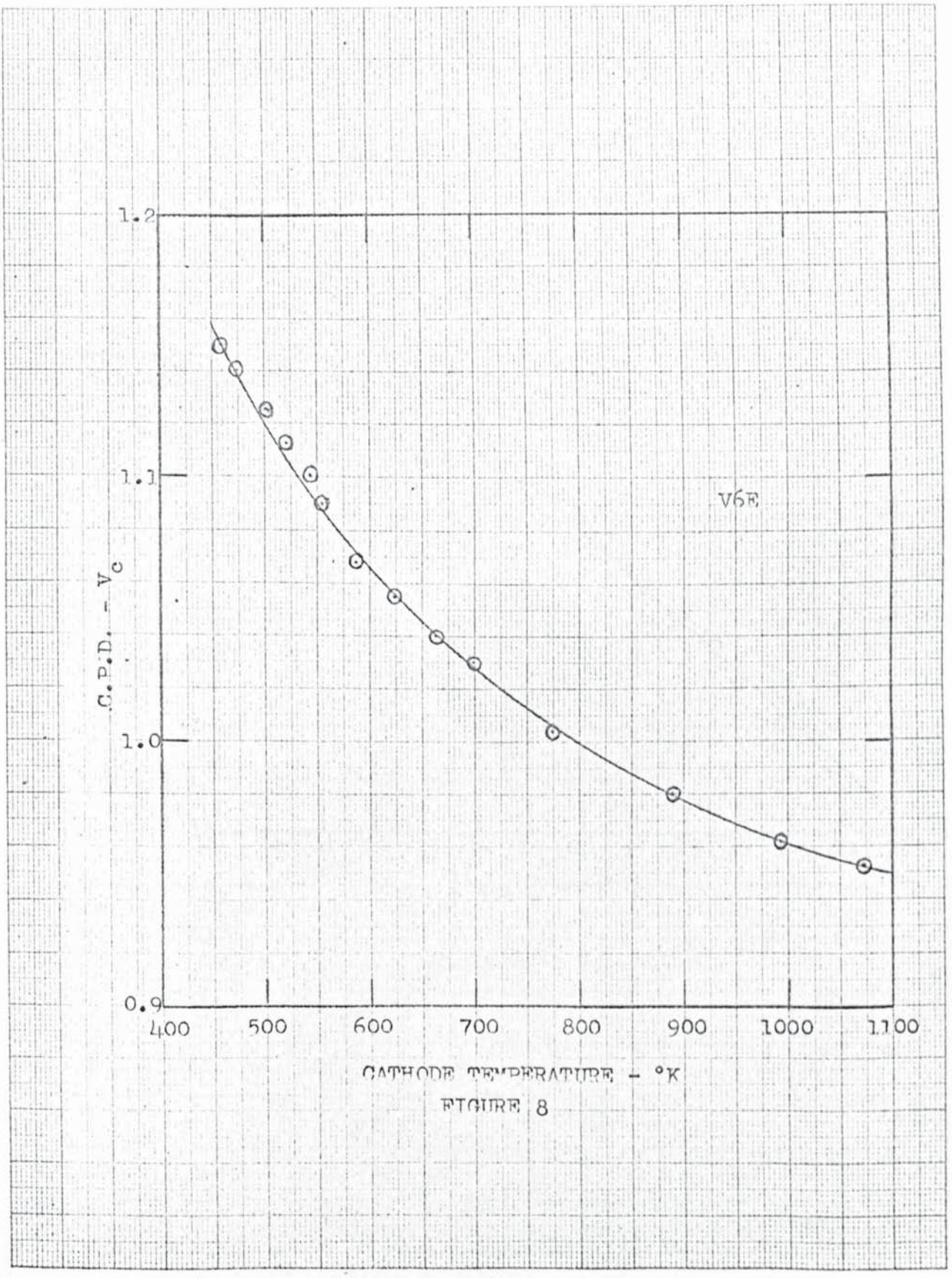
1.2
1.1
1.0
0.9
C.P.D. - V_c
V6E
400
500
600
700
800
900
1000
1100
CATHODE TEMPERATURE - °K

FIGURE 8

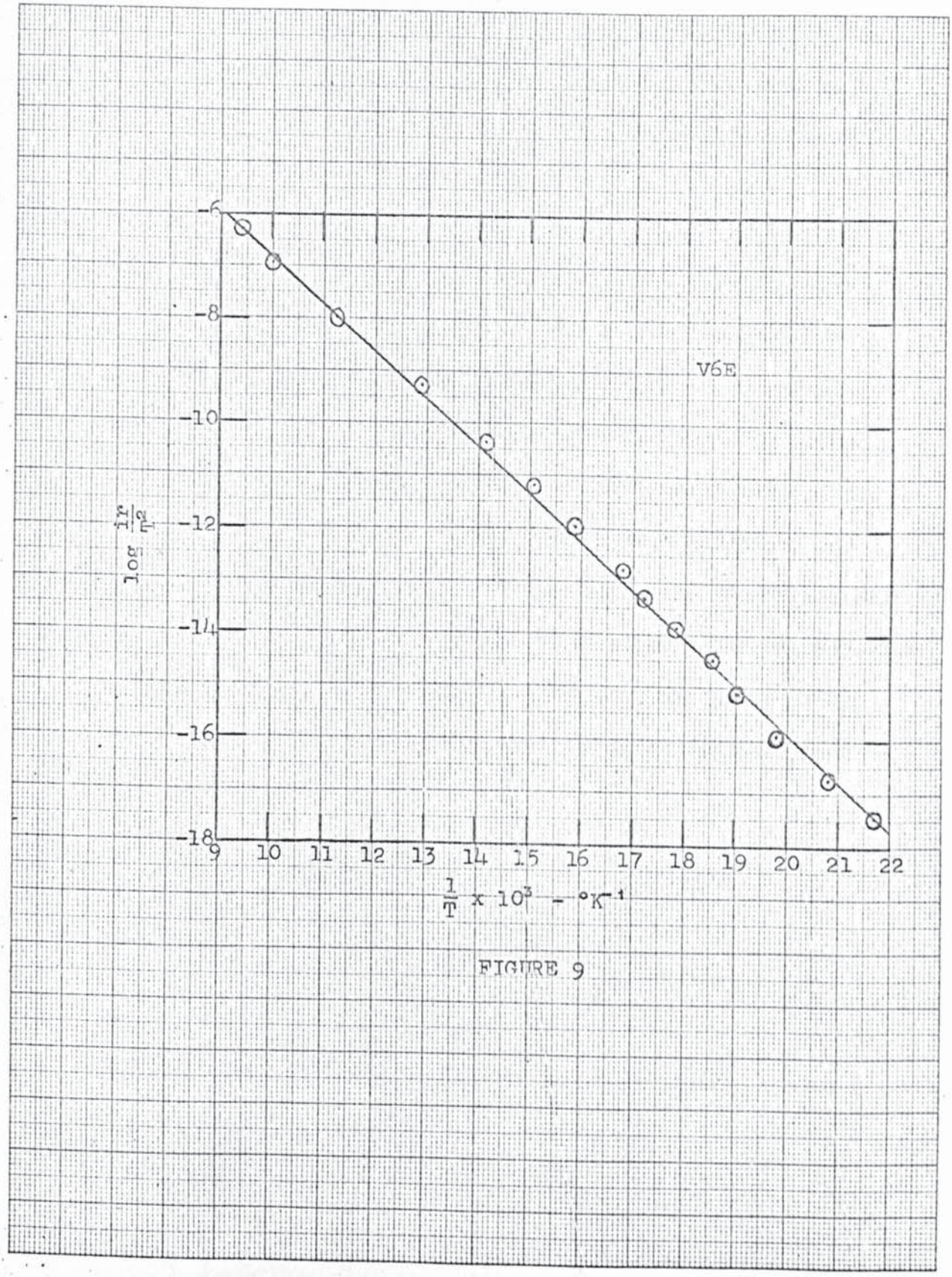
V6E
-6
-8
-10
-12
-14
-16
-18
9
10
11
12
13
14
15
16
17
18
19
20
21
22
log a/a'
1/T x 10³ - °K⁻¹

FIGURE 9

have shown that evaporated materials from the cathode reduce the anode work function during the early breakdown of the carbonates, but subsequently during activation, oxygen released from the cathode produces a small increase in anode work function.

With the Richardson work function of 1.42eV and the anode work function of 2.68eV, this gives the C.P.D. as 1.24 V. This agrees reasonably well with the value of C.P.D. = 1.17 V at the lowest temperature in figure 4a. Better agreement cannot be expected since the "Sano" method can only be of great value when the anode is kept at constant temperature. In addition there still remains the difficulty of interpretation of the Richardson work function, and presumably also for the anode work function using the "Sano" method.

Further evidence can be produced to support the extrapolation used in the total emission method, by calculating the space charge smoothing factor from the characteristics, using expressions derived by Bull[13].

One such equation is,

$$\left(\frac{\partial i}{\partial i_s}\right)_{v,x} = \frac{x\, g_x}{2 i_s} + \frac{i}{i_s}, \text{ where } g_x = \left(\frac{\partial i}{\partial x}\right)_{V,i_s}$$

from which by putting $\xi = \frac{x g_x}{2i}$, we get

$$\left(\frac{\partial i}{\partial i_s}\right)_{V,x} = \frac{i}{i_s}(1 + \xi) \quad \ldots\ldots \quad (8)$$

The factor $(1 + \xi)$ is found to be a theoretical estimate

of the space charge smoothing factor.

In addition Bull[13] shows that,

$$\left(\frac{\partial V}{\partial V_m}\right)_{i,x} = \frac{1}{g_m}\left(\frac{ei}{kT} + \frac{xg_x}{2}\cdot\frac{e}{kT}\right)$$

where $g_m = \left(\frac{\partial i}{\partial V}\right)_{i_s,x}$

$$\therefore \quad \left(\frac{\partial V}{\partial V_m}\right)_{i,x} = \frac{1}{g_m}(1+\xi)\frac{ei}{kT} \quad \ldots\ldots (9)$$

Therefore if two characteristics curves are drawn for which there is a small difference of i_s, say δi_s, brought about by a negligible change in T, equations 8 and 9 give alternative methods of calculating $(1+\xi)$. In using the curves, it is more accurate to measure i_s, δi_s and δV_m from a graph of log i against V, and i, δi and g_m from a graph of i against V. A curve showing the variation of log $(1+\xi)$ with anode current is shown in figure 10. This curve is in good agreement with a similar one found by Richards[59] and other workers in this laboratory. The two sets of experimental points marked Δ and Θ lie very close together. In equation 8 we require not only a ratio $\left(\frac{\delta i}{\delta i_s}\right)$ but also the ratio $\frac{i}{i_s}$. These can be obtained only by the extrapolation of curves as described above. Differences in temperature for the two cases give $\frac{\delta i_r}{i_r}$, in the retarding region, a value slowly decreasing with increasing current and the value would not be equal to $\frac{\delta i_s}{i_s}$. Consequently the use of equation 8 is somewhat sensitive to δi_s and i_s. Equation

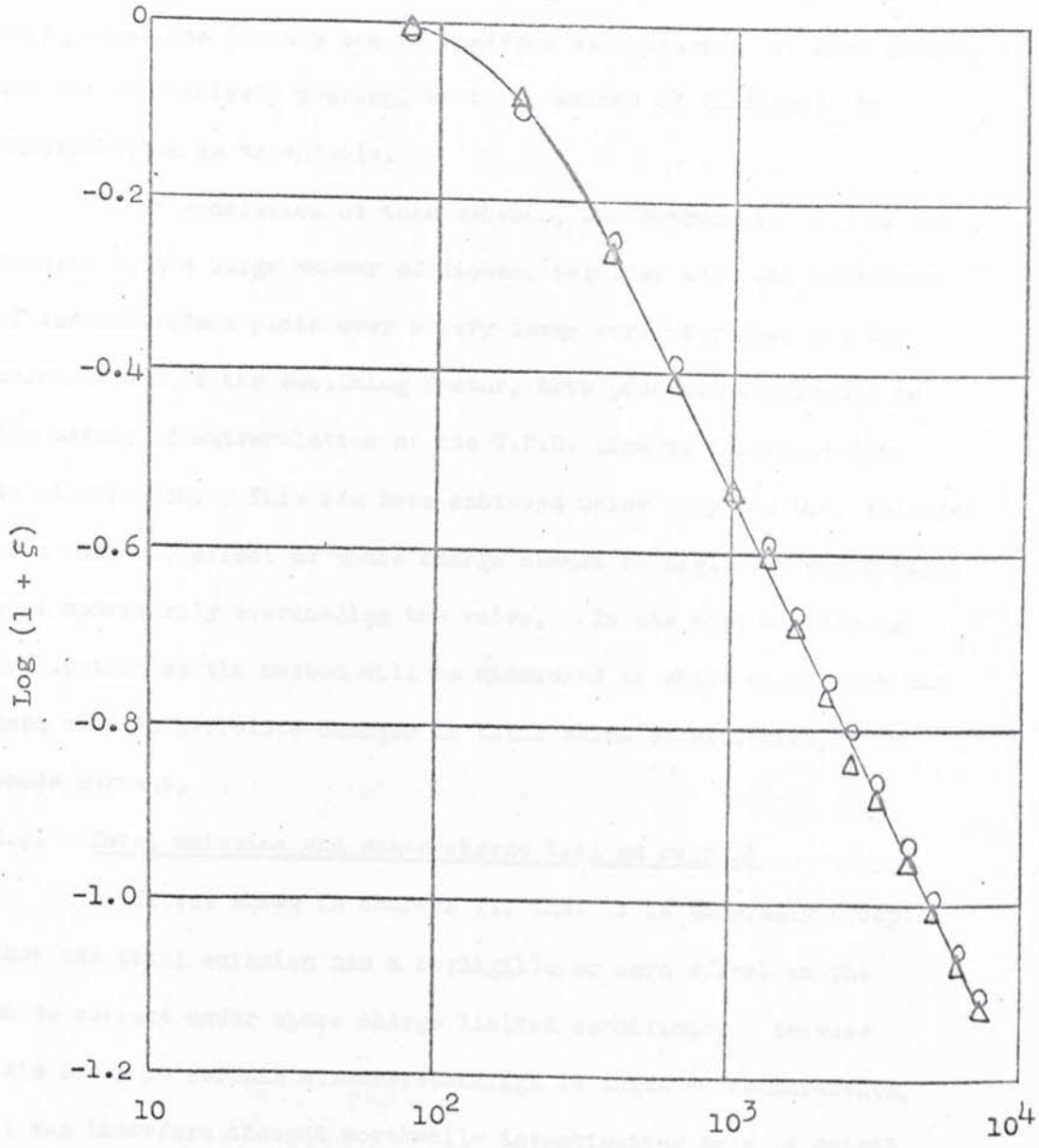

FIGURE 10

9 on the other hand requires no extrapolation, since i_s and δi_s are not required. Consequently the agreement between the results using equations 8 and 9 can be regarded as supporting to some extent, but not exhaustively proving, that the method of finding i_s by extrapolation is acceptable.

In conclusion of this section, the reproducibility of the results with a large number of diodes, together with the behaviour of the Richardson plots over a very large current range, and the calculations of the smoothing factor, have produced confidence in the method of extrapolation of the C.P.D. line to determine the total emission. This has been achieved using very low D.C. voltages even when the effect of space charge cannot be neglected and without even momentarily overloading the valve. In the next section an application of the method will be discussed in which an attempt has been made to correlate changes in total emission with changes in anode current.

2.2. Total emission and space charge limited current

It was shown in chapter (1) that it is generally accepted that the total emission has a negligible or zero effect on the anode current under space charge limited conditions. Because this leads to certain misunderstandings in emission measurements, it was therefore thought worthwhile investigating this in detail by applying the method described in 2.1. These measurements (Fitch and Coutts)[60] were made on a particular batch of EB91's, kindly supplied for these tests by Mullards Ltd. They are double diodes so that, during measurements on each diode, both cathodes

were maintained at earth potential and the shield and anode of the other diode were kept at a small negative potential with respect to the cathodes. This avoided any spurious currents arising from the diode not in use. Measurements were made on 27 diodes, but the results from three were rejected because two had very high conductances which could be explained as being due to small clearances and the other gave a cathode temperature outside the range considered, on account of a suspected damaged heater.

Characteristics of four of the diodes are shown in figures 11a to 11d. These were selected because they illustrate diodes of different total emission, C.P.D. and variation of C.P.D. with temperature. The remaining 20 characteristics are shown in appendix 1a to 1t. These diagrams are reduced in size and do not include the actual experimental points. The extrapolations were made from C.P.D. points using the largest range of currents possible. That is, at the high end they were limited by the onset of space charge and the lower limits by leakage currents and sensitivity of the amplifier. As in the previous case the diodes were cylindrical and corrections were made, but are not shown, using the Nottingham[1] method, for the value of $a^{-1} = 1.3$. The cathode temperatures were measured from the slope of the retarding potential lines. For $V_f = 6.3v$, they were found to have a mean value of $1100^{\circ}K$ with a root mean square deviation of $13^{\circ}K$. The space charge limited current for this temperature was taken at an effective voltage of 1.5v. That is the anode current was measured at 1.5v, that is to say, the anode current was taken at 1.5v above the C.P.D. point at

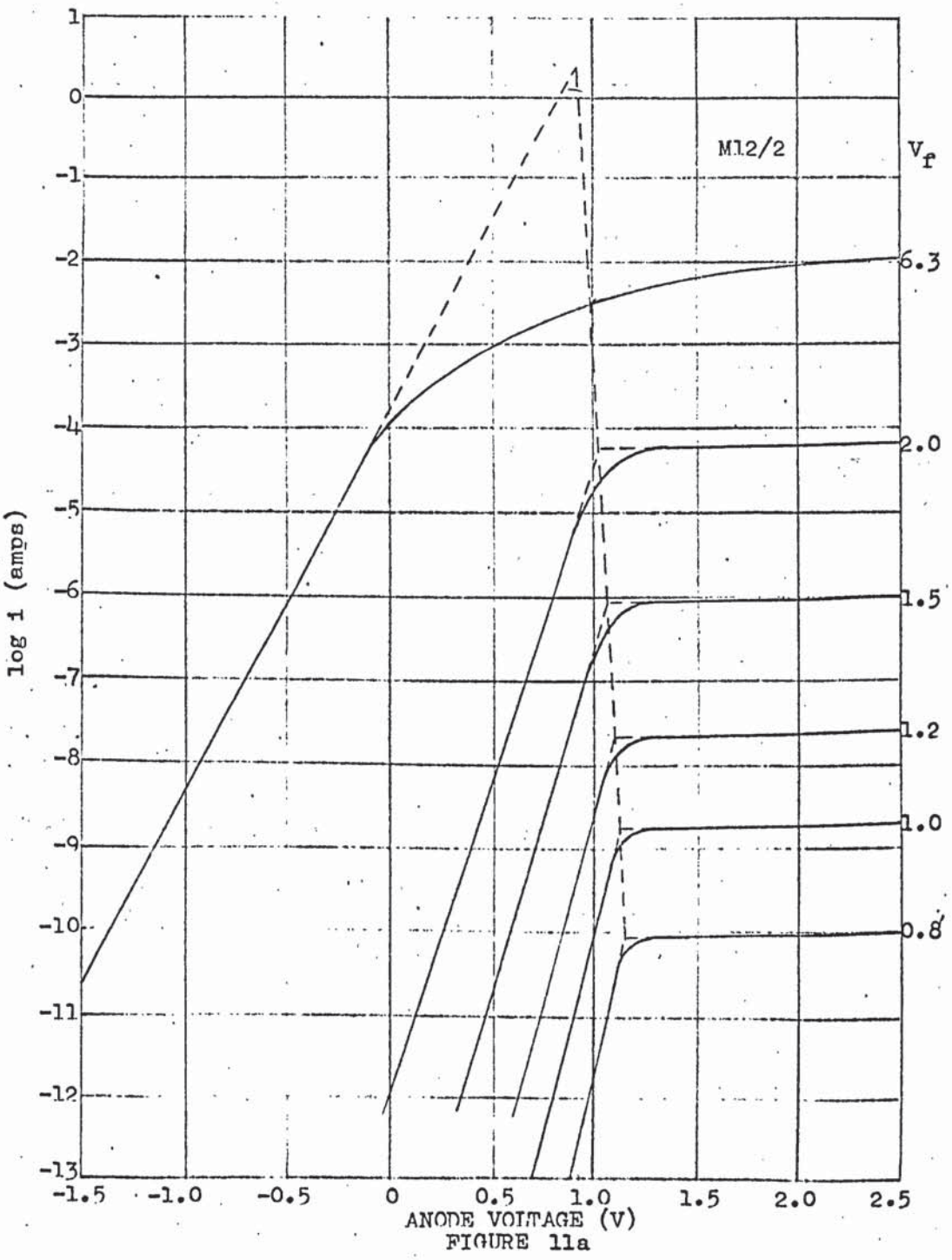
M12/2
V_f
6.3
2.0
1.5
1.2
1.0
0.8
log i (amps)
1
0
-1
-2
-3
-4
-5
-6
-7
-8
-9
-10
-11
-12
-13
-1.5
-1.0
-0.5
0
0.5
1.0
1.5
2.0
2.5
ANODE VOLTAGE (V)

FIGURE 11a

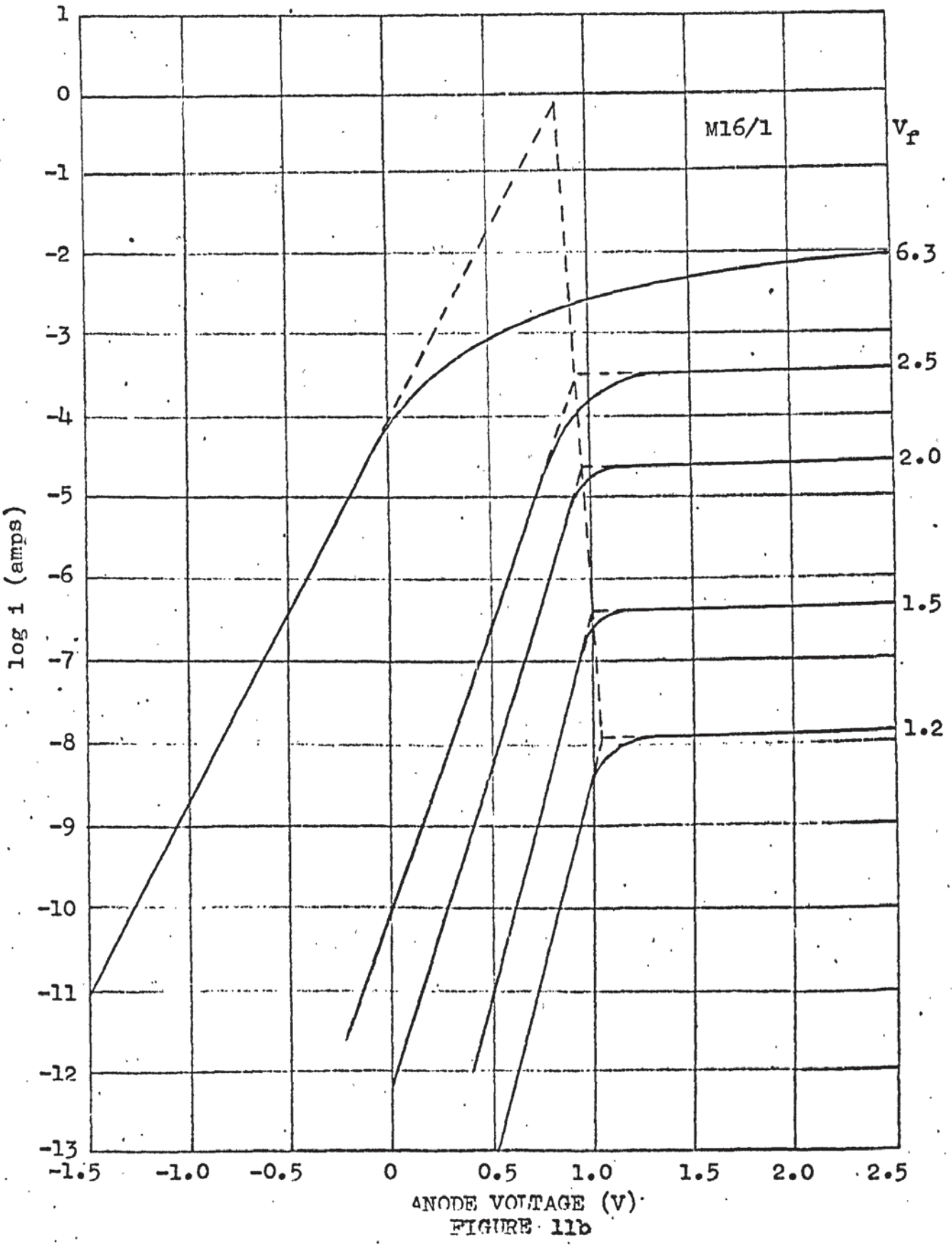
M16/1
V_f
6.3
2.5
2.0
1.5
1.2
log i (amps)
1
0
-1
-2
-3
-4
-5
-6
-7
-8
-9
-10
-11
-12
-13
-1.5
-1.0
-0.5
0
0.5
1.0
1.5
2.0
2.5
ANODE VOLTAGE (V)

FIGURE 11b

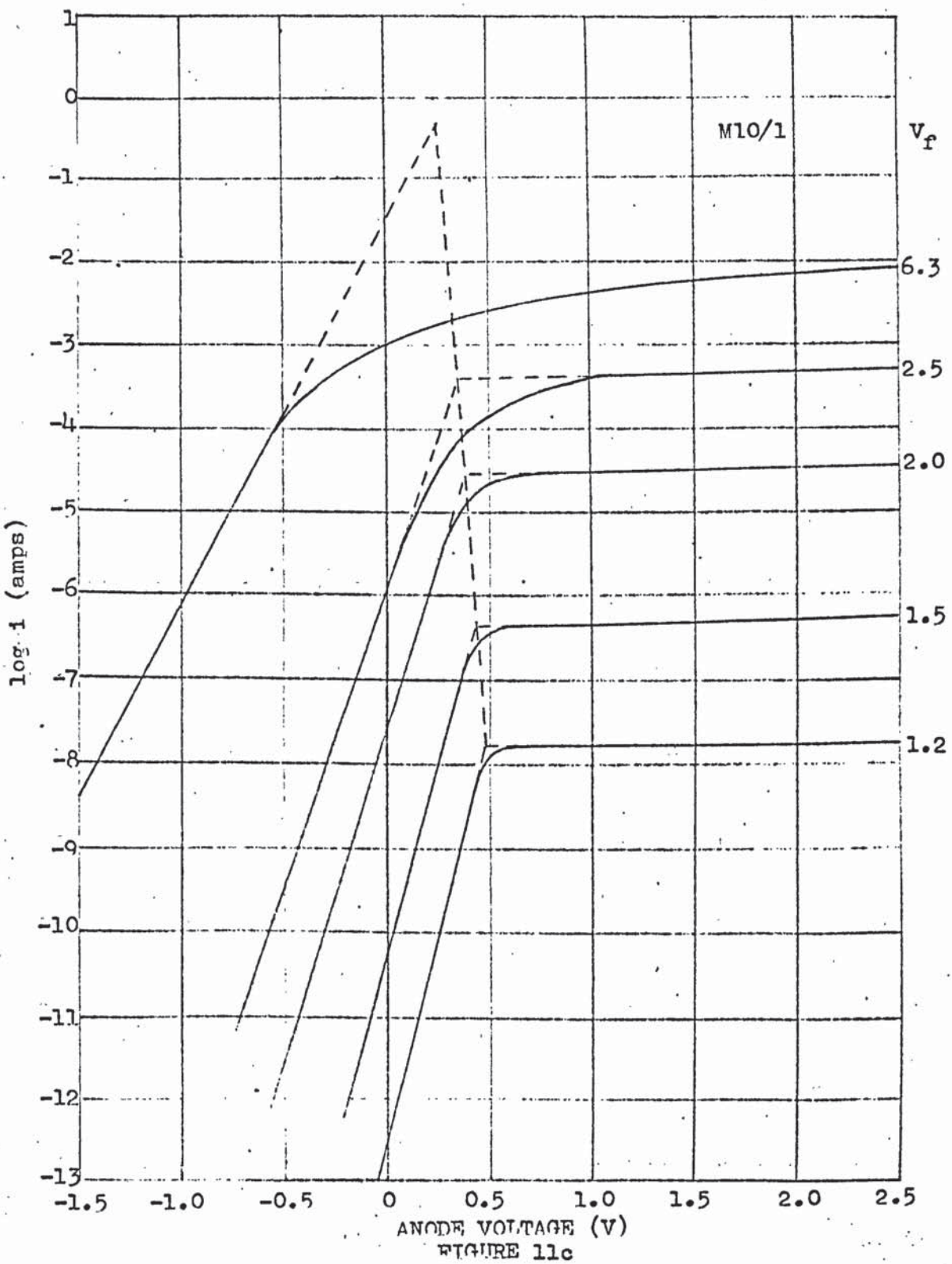
M10/1
V_f
6.3
2.5
2.0
1.5
1.2
log i (amps)
1
0
-1
-2
-3
-4
-5
-6
-7
-8
-9
-10
-11
-12
-13
-1.5
-1.0
-0.5
0
0.5
1.0
1.5
2.0
2.5
ANODE VOLTAGE (V)

FIGURE 11c

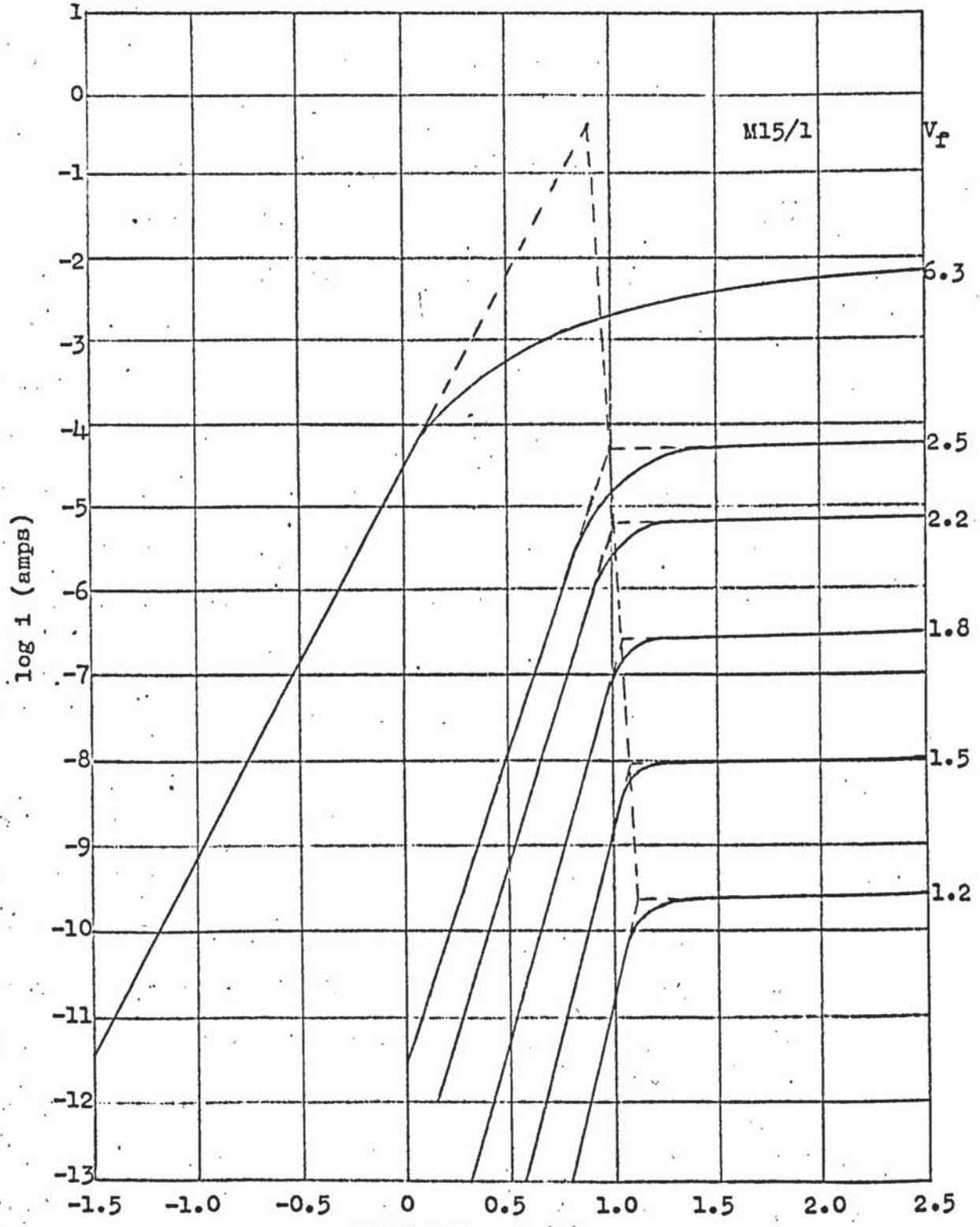
M15/1
V_f
6.3
2.5
2.2
1.8
1.5
1.2
log i (amps)
1
0
-1
-2
-3
-4
-5
-6
-7
-8
-9
-10
-11
-12
-13
-1.5
-1.0
-0.5
0
0.5
1.0
1.5
2.0
2.5
ANODE VOLTAGE (V)

FIGURE 11d

6.3v. These results are tabulated in Table (1) page 40 and are grouped into three distinct temperature ranges - namely 1075 - 1090°K, 1091 - 1105°K and 1106 - 1120°K.

The total emission plotted as a function of the anode current is shown in figure 12 and illustrates that i_a depends upon i_s. The spread of the results is to be expected. The accuracy of the total emission values is limited and small variations in the cathode area and cathode to anode ratio must occur. The temperature grouping, however, shows that there is no correlation between emission and cathode temperature, ie. the high emission values are not associated with high temperature values. The average slope of a curve drawn through the points on figure 12 gives a value of $\left(\frac{\delta i}{\delta i_s}\right)$ of about 2×10^{-3}. This is comparable with the rough estimate of about 10^{-3} given by Bull[14].

Furthermore the anode current given by Child's law, for the spacing of 0.15 cm and anode voltage of 1.5v, is 5.4 m/a for the cathode area of $0.28 cm^2$. The lowest value of i_a on the figure is about 6.5 m/a. It is expected this observed value should be somewhat larger because the value of 5.4 m/a is obtained by neglecting the thermal emission velocities.

An attempt was made to measure the value of $\left(\frac{\delta i}{\delta i_s}\right)$ for three different cathode temperatures, corresponding to V_f = 7.0, 6.3 and 5.5v. The value of $\left(\frac{\delta i}{\delta i_s}\right)$ as predicted by Bull, should be larger for higher temperatures. The results found are illustrated in figure 13 for four diodes operating at three temperatures. The figure shows that $\left(\frac{\delta i}{\delta i_s}\right)$ decreases as the temperature increases,

DIODE NUMBER	TOTAL EMISSION-i_s amps	ANODE CURRENT-i m/a	CATHODE TEMPERATURE °K	CATHODE WORK FUNCTION - eV	A amp/cm² °K²	
M15/2	1.2	9.6	1110	1.39	3.5	H
M11/2	1.35	9.4	1113	1.275	2.5	
M12/2	2.2	10.3	1117	1.23	1.85	
M 8/2	1.4	9.7	1118	1.41	12.0	
P 1/2	0.50	6.7	1118	1.275	0.89	
P 1/1	1.55	8.9	1120	1.24	1.34	
P 2/1	2.05	9.9	1120	1.20	1.13	
P 2/2	1.40	8.8	1120	1.24	1.42	
M14/2	1.95	9.9	1105	1.265	3.2	N
M17/2	1.15	9.3	1093	1.34	3.95	
M 9/2	1.45	9.0	1095	1.235	1.58	
M10/2	1.50	9.1	1095	1.355	12.6	
M 6/2	1.8	10.3	1105	1.35	5.6	
M 4/2	2.6	10.8	1095	1.34	11.3	
M16/1	0.85	8.4	1105	1.285	1.58	
M10/1	0.45	6.8	1099	1.22	0.42	
M 6/1	0.96	8.8	1097	1.35	3.2	
M 7/1	0.95	9.2	1103	1.365	6.0	
M15/1	0.45	7.8	1095	1.28	1.05	
M19/2	0.80	7.7	1080	1.33	1.75	L
M20/2	0.15	7.2	1076	1.75	62.0	
M 5/1	1.1	8.2	1078	1.295	2.8	
M 4/1	1.45	9.8	1088	1.28	3.5	
M20/1	0.35	7.3	1076	1.45	4.95	

TABLE 1.

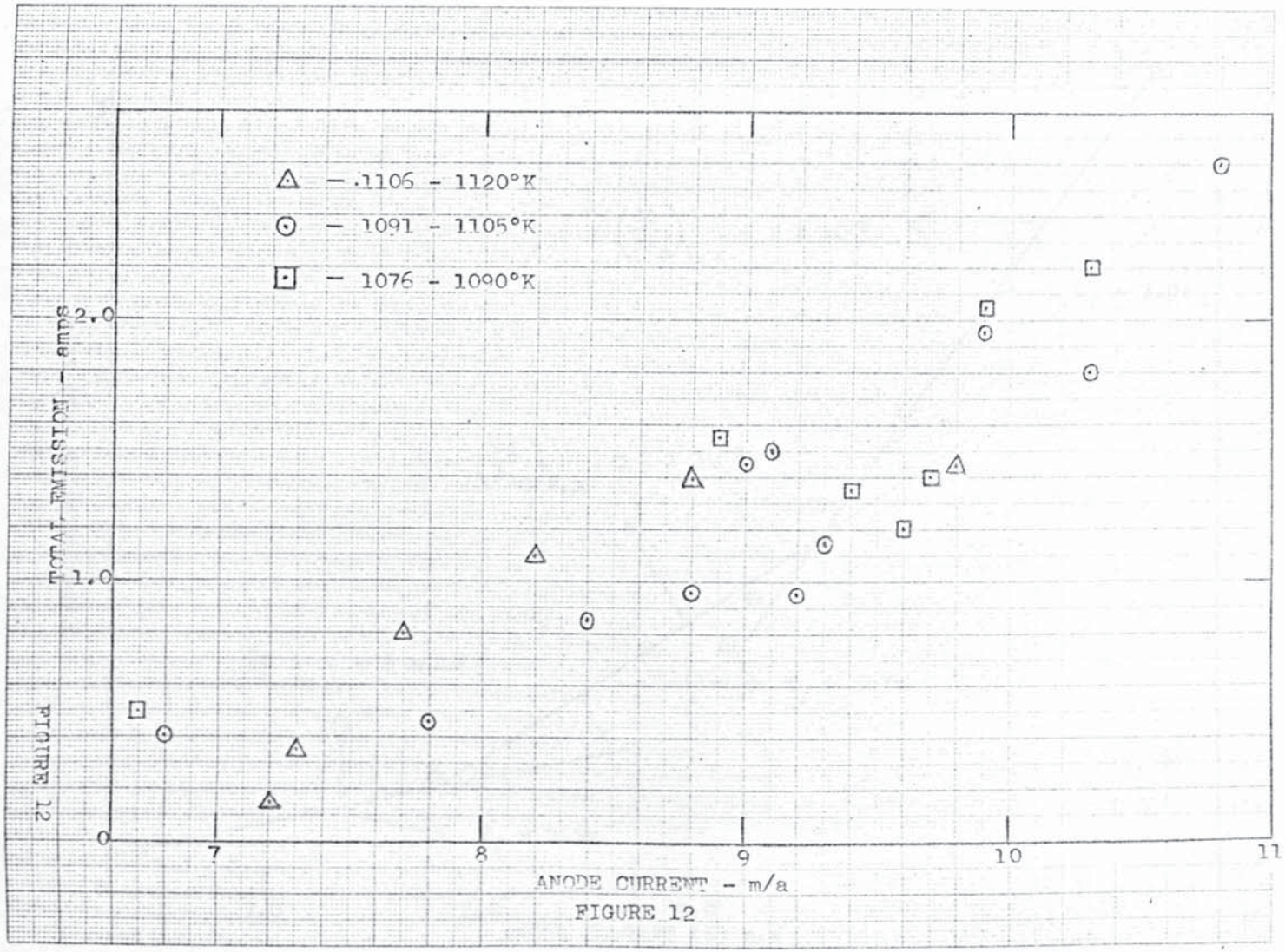

FIGURE 12

FIGURE 12

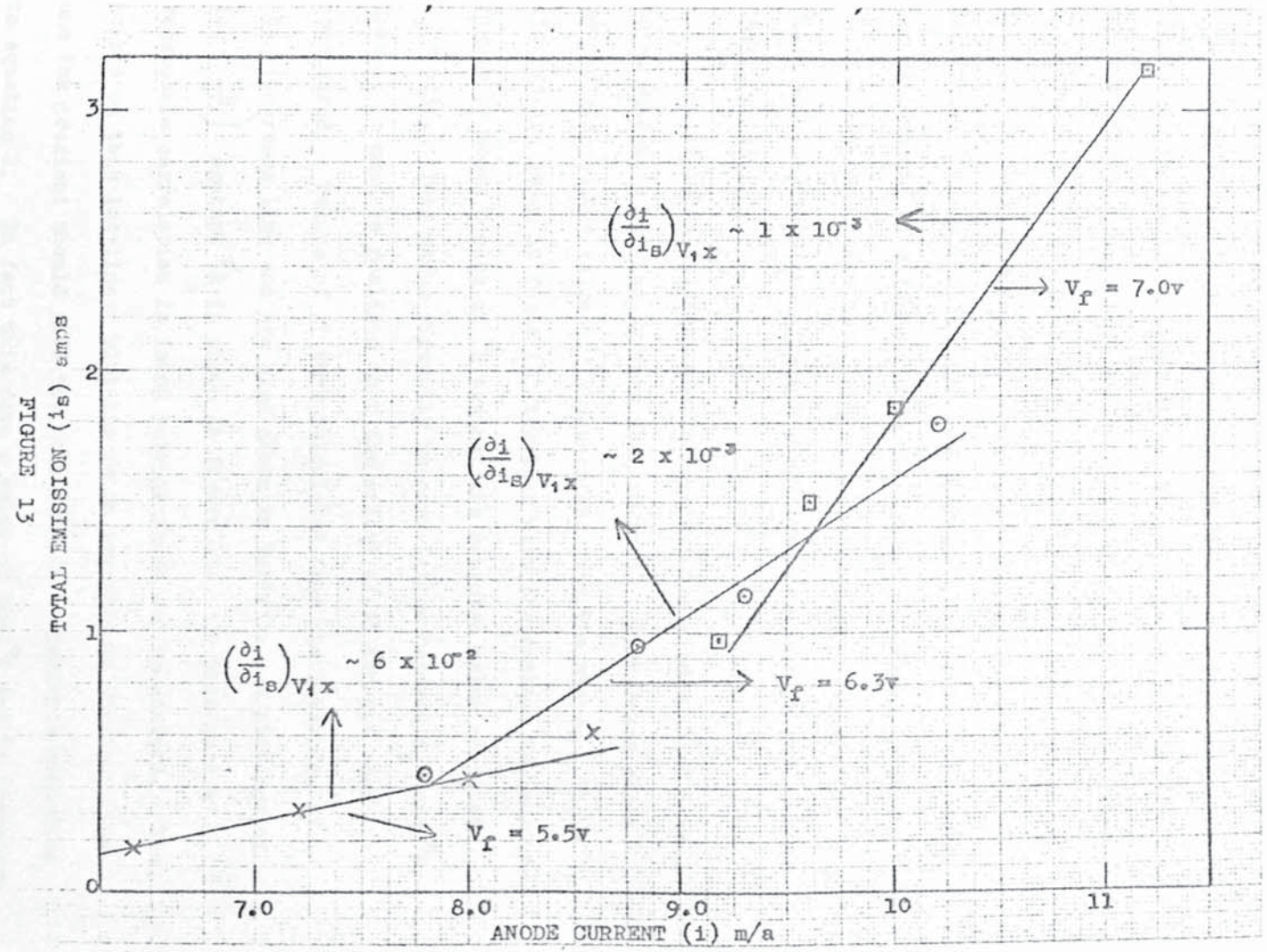
FIGURE 13
TOTAL EMISSION (i_s) amps
3
2
1
0
7.0
8.0
9.0
10
11
ANODE CURRENT (i) m/a
$\left(\frac{\partial i}{\partial i_s}\right)_{V_1 x}$ ~ 1 x 10^{-3}
V_f = 7.0v
$\left(\frac{\partial i}{\partial i_s}\right)_{V_1 x}$ ~ 2 x 10^{-3}
$\left(\frac{\partial i}{\partial i_s}\right)_{V_1 x}$ ~ 6 x 10^{-2}
V_f = 6.3v
V_f = 5.5v
FIGURE 13

which is apparently in disagreement with Bull. However perhaps this result should have been anticipated because Bull's prediction really only holds for a fixed value of i_s. Clearly the three different temperatures give values of i_s and i_a which constitute different regions of the curved characteristics illustrated in figure 2. Thus an alternative way of measuring this would be required. This would be much more difficult and would involve the use of cathodes of different work functions in the same geometry, so that the same value of i_s could be obtained by operating at different temperatures. This has not been possible in the present investigation.

It is of interest now to consider the diodes which have total emissions varying by more than 10 to 1. Richardson plots were drawn and the value of ϕ_R determined from the slope. These figures are shown in Table (1) together with the cathode temperatures. Figure 14 shows a plot of ϕ_R against the measured value of i_s at $V_f = 6.3v$. This shows virtually no correlation between i_s and ϕ_R. However it must be realised that the effect of A* has not been considered. Values of A* were calculated from the intercept of the Richardson line and are also shown in Table 1. A plot now of $\log\left(\frac{i_s}{A^*}\right)$ against ϕ_R is shown in figure 15. In this case a reasonable correlation is found between these two parameters. The points on this log-linear plot lie on an approximate straight line and the gradient should give the mean cathode temperature according to equation 2. In fact this gave a value of 1050°K and is therefore in reasonable agreement with the individual cathode temperatures.

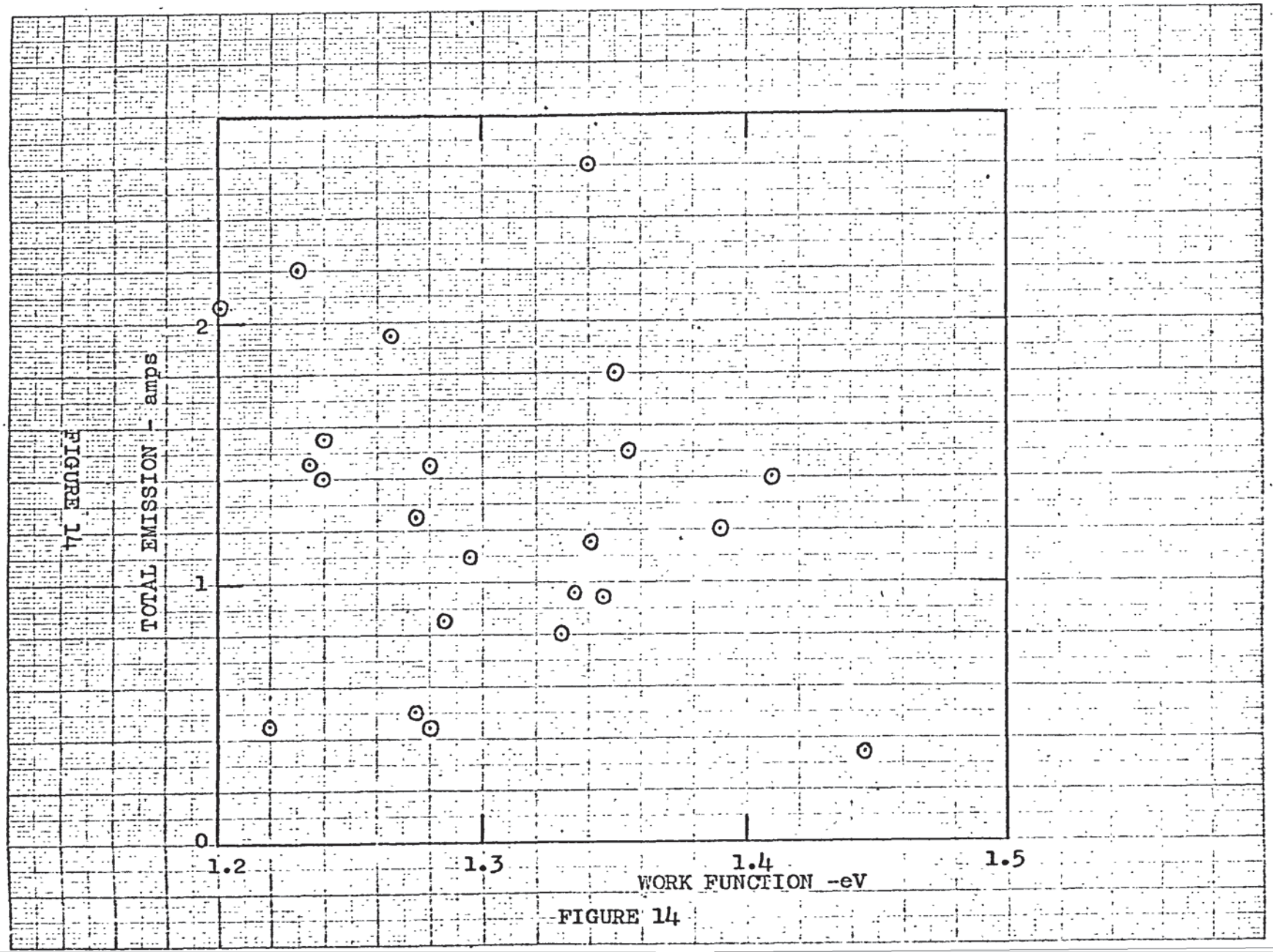

FIGURE 14

FIGURE 14

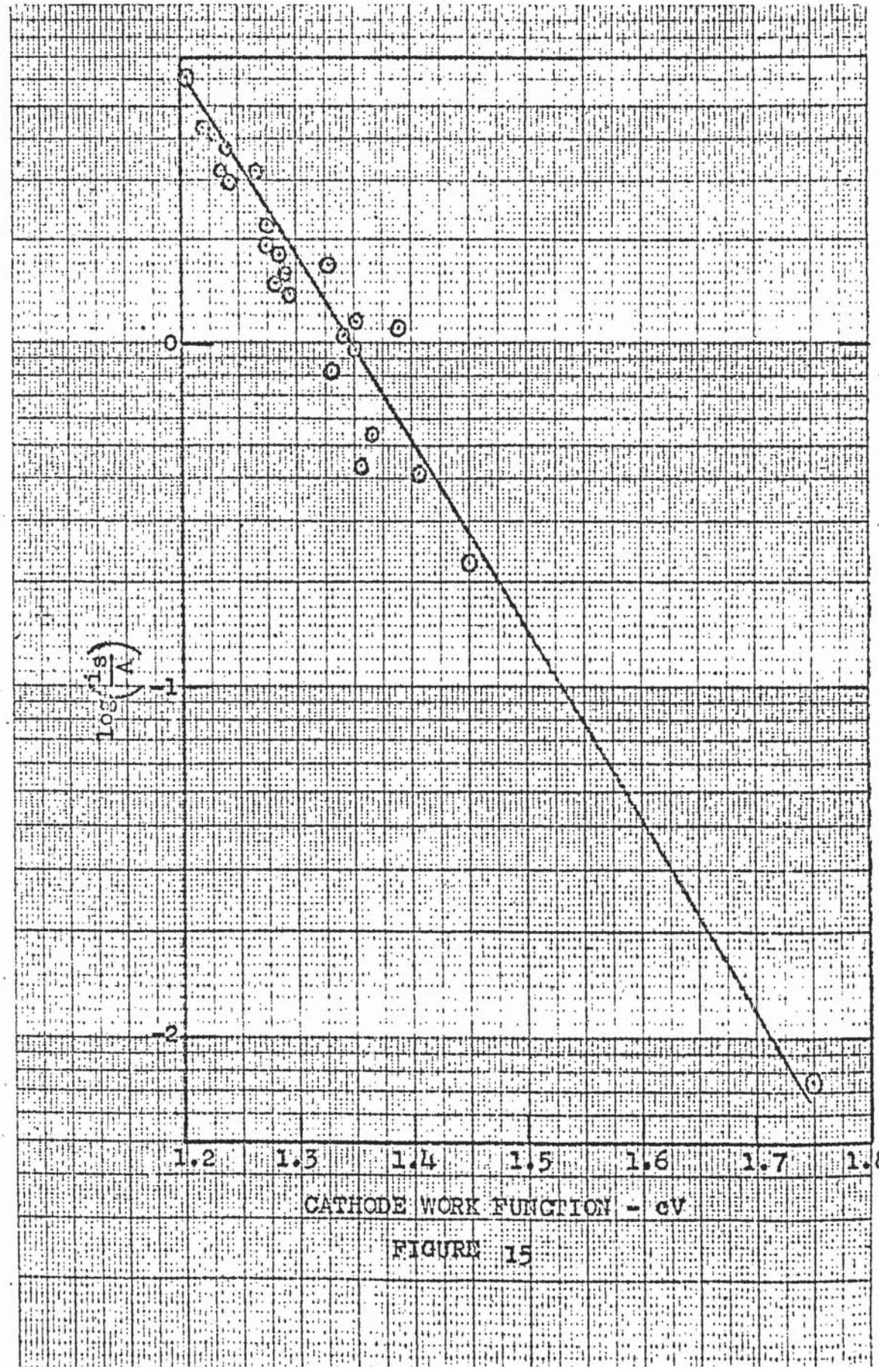
0
-1
-2
$\log\left(\frac{i_s}{A}\right)$
1.2
1.3
1.4
1.5
1.6
1.7
1.8
CATHODE WORK FUNCTION - eV

FIGURE 15

Better agreement could hardly be expected since it is well known that large errors can arise in determining A* by this method. These considerations of the effect of A* are in fair agreement with the work of Stanier and Mee[61], who demonstrated a linear relationship between A* and ϕ_R for oxide cathodes.

The consequences of figures (14) and (15) justify criticism of the work of Krousemeyer and Pursley[62], in which they regard total emission values, measured with pulsed techniques, to be a measure of the cathode work function. They had ignored the possibility of any variation of A*. These remarks are substantiated by those of Dobretsov and Matskevitch[63] who says that two cathodes with same Richardson work functions at the same temperature can give current densities differing by a factor as high as 10^6. This seems particularly high but it certainly is true that it is impossible to give recommendations of efficient thermionic emitters on the basis of ϕ_R without due regard to A*.

Figure 16 now shows that when total emission values at $V_f = 6.3v$ are plotted against those at $V_f = 1.5v$, the correlation is poor. This strongly suggests that the low temperature technique employed by Metson and others, is not a particularly good way of evaluating cathodes for normal high temperature operation. This can be seen from these results because of the variation of C.P.D. with temperature and of A* from diode to diode.

Finally it should be noted that when the space charge limited current is measured at some fixed anode voltage, the method will not be quite so satisfactory in judging the emissive capabilities

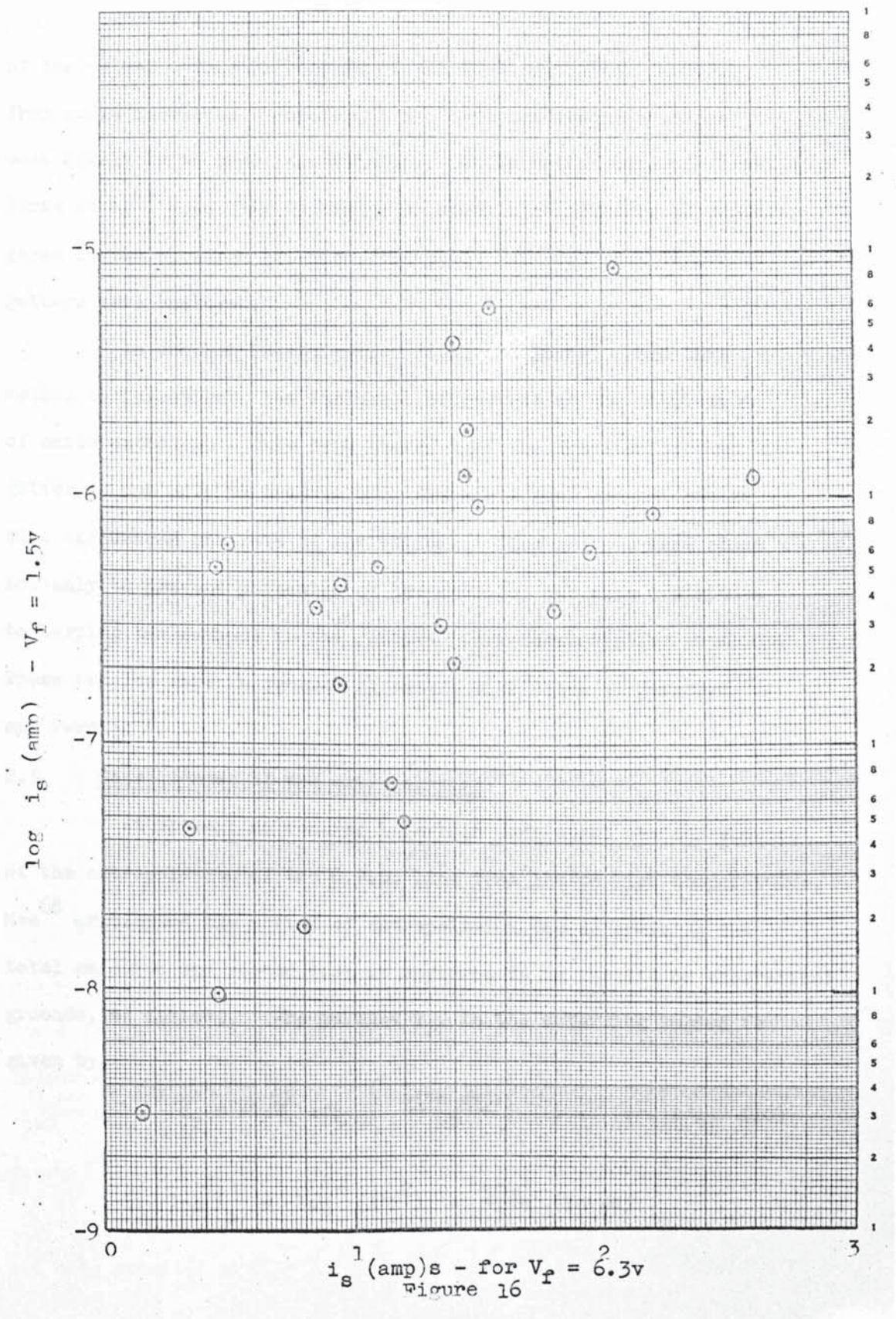

Figure 16

of the valve. This is because of the small variation in C.P.D. from valve to valve. However it is these conditions that are most likely to be used industrially. It is worth noting that della Porta et al[64] used this technique to study the influence of residual gases on the electron emission from oxide cathodes when different getters were employed.

In another investigation Fitch and Young[65] used this method to investigate the influence of getters on the activation of oxide cathodes. This work showed that the function of the getter is not only to produce and maintain a good vacuum, but it also influences the rate of activation. Thus getters were shown not only to prevent poisoning of the cathode, but also contribute to keeping the cathode in the reduced state necessary for emission. These results were in general agreement with those of Nergaard[66] and Perdijk[67].

2.3 Consequences of the extrapolation.

At present no remarks have been made about the consequence of the extrapolation of the C.P.D. line from low to high temperatures. Mee[68] criticised the method of extrapolation for determining the total emission and showed that it appeared to be invalid on theoretical grounds, as follows. The current i_r, in the retarding region is given by,

$$i_r = A^* T^2 \exp \left\{ \frac{e(Va-\phi a)}{kT} \right\} \quad \ldots\ldots\ldots \quad (10)$$

$$\text{ie. } \log i_r = \log (A^* T^2) + \frac{5040}{T} (Va-\phi a)$$

Now from the linear extrapolation on the log i against V_a characteristics we can write,

$$\log i_s = m V_c + C \quad \ldots\ldots\ldots \quad (11)$$

where V_c = C.P.D. and m and C are constants.

Equations (10) and (11) will intersect when $i_r = i_s$ and $V_a = V_c$.

Therefore,

$$mV_c + C = \log (A^* T^2) + \frac{5040}{T} (V_c - \phi_a)$$

giving $$V_c = \frac{5040\,\phi_a - T \log A^* - 2T \log T + CT}{5040 - mT}$$

Now since $V_c = \phi_a - \phi_c$

$$\phi_c = \frac{T(2 \log T + \log A^* - c - m\phi_a)}{5040 - mT}$$

This equation shows that ϕ_c tends to zero as T tends to $0^\circ K$, if ϕ_a is assumed to be constant. This apparently unrealistic behaviour of ϕ_c implied that the extrapolation from the lower to the higher cathode temperatures was invalid. However it should be pointed out that on the log-linear scale, extrapolation down to $0^\circ K$ involves a very much greater change of anode current since the total emission should decrease very rapidly with temperature.

Later work[52] showed that even when the measured current had been extended down to about 10^{-14} amp and the cathode temperature

to about 400°K, the C.P.D. still remained on a straight line. Now, because the temperature measurements were more accurate as measured from the retarding slopes, the earlier curved Richardson plots, which Mee had said were due to the results of the extrapolation, were found to be virtually straight.

This later work therefore not only gave confidence in the method used, but appeared to support Mee's analysis and his conclusion that ϕ_c went to zero as T went to 0°K. This unexpected result still seemed very troublesome, but at about this time Hathaway[69] was conducting work on photo multipliers which proved to be of direct interest.

Using a photo multiplier type 9524S, he measured the dark current at room temperature, 295°K, solid carbon dioxide in acetone, 195°K, and liquid nitrogen, 77°K. He used a pulse height analyser to measure the total number of electrons emitted in fixed intervals of time. The distribution of pulse heights enabled electrons from different sources in the tube to be sorted out and allowance made for them. After such allowance had been made for high energy counts due to fluorescence in the glass and contributions due to thermionic emission from the first dynode and beyond, he assumed the remaining counts were due to thermionic emission from the cathode. The results he obtained were similar to those reported elsewhere, eg. Engstrom[70], Braddick[71]. He found the ratio of the counts (N) over the three temperature intervals as,

$$\frac{N_{295}}{N_{195}} = 5.7 \quad , \quad \frac{N_{195}}{N_{77}} = 13 \quad \text{and} \quad \frac{N_{295}}{N_{77}} = 74$$

He then considered the Richardson equation in the form

$$N_{T_1} = f(T_1) \exp\left\{ -\frac{\phi_{T_1}}{kT_1} \right\}$$

for the number of thermionic electrons emitted per second from the photo cathode of work function ϕ_{T_1}.

Therefore considering a similar expression at T_2, we get,

$$\frac{N_{T_1}}{N_{T_2}} = \frac{f(T_1)}{f(T_2)} \exp\left\{ \frac{1}{k} \left(\frac{\phi_{T2}}{T2} - \frac{\phi_{T1}}{T1} \right) \right\}$$

$$\therefore \quad \frac{\phi_{T_2}}{T_2} - \frac{\phi_{T_1}}{T_1} = k \log_e \left\{ \frac{N_{T_1}}{N_{T_2}} \cdot \frac{f(T_2)}{f(T_1)} \right\}$$

$$= 10^{-4} \times 2.3 \log_{10} \left\{ \frac{N_{T_1}}{N_{T_2}} \cdot \frac{f(T_2)}{f(T_1)} \right\}$$

as $k \sim 10^{-4}$ eV per $^{\circ}K$.

For $T_2 < T_1$, by a range of less than 10 to 1, and from the experimental results for N, over the range $295^{\circ}K$ to $195^{\circ}K$

$$\frac{\phi_{T_2}}{T_2} - \frac{\phi_{T_1}}{T_1} < 10^{-4} \times 2.3 \times \log_{10} 5$$

$$< 1.6 \times 10^{-4}$$

$\therefore$ $\frac{\phi}{T}$ is constant to better than about 0.02%

Similarly over the range 295°K to 77°K

$$\frac{\phi_{T_2}}{T_2} - \frac{\phi_{T_1}}{T_1} < 4.3 \times 10^{-4}$$

So again $\frac{\phi}{T}$ is constant to better than 0.04%.

Thus if we accept Hathaway's analysis that the counts under his experimental conditions are due to thermionic electrons from the photomultiplier cathode, then again we come to the same somewhat surprising conclusion, as for oxide coated cathode diodes, that ϕ tends to zero at 0°K.

It should however be noted that the analysis used by Hathaway becomes less valuable and decisive at higher temperatures, because as T increases to more than 1000°K the magnitude of $\frac{\phi}{T}$ becomes more and more comparable in magnitude to the right hand side of the equation.

Finally it is interesting to note that at the same time Bull[12] had developed a new approach to our considerations of the electron and the electric field. In fact, unknown to Bull, Dirac[72] had also proposed an almost identical model of the electric field. Both were concerned with the problem of why electric charges are observed in multiples of the elementary unit, e, the electron charge. Dirac said that a possible approach to this problem could be in terms of quantised Faraday's lines of force, with a charge +e at one end and -e at the other. The lines of force could form closed loops corresponding to electro-magnetic waves,

and when the line of force is broken this would correspond to the production of an electron-positron pair. Further if the line of force is pictured as a "string", then the string is the cause of the coulomb force between two electron charges. A bare electron means an electron without the coulomb force around it, and this is inconceivable with this picture, just as it is inconceivable to think of the end of a piece of string without thinking of the string itself.

However whilst Dirac states that the model looks very reasonable, he had not been able to develop it further. On the other hand Bull, using his "field lines" has developed the idea considerably further and has brought into its ambit many physical phenomena, including particle physics and gravitation. Some of this work has been published [12], but some has only been privately circulated and not yet published.

One particular aspect of direct interest in our present investigation is the use of quantised electric fields to calculate the work function. The resulting expressions have been published by Bull[12].

This calculation depends upon the idea that the work function is due to a space charge of electrons which diffuse thermally a small distance outside the emitting surface and so produce an electric field opposing the loss of electrons. It is therefore not surprising that the model shows the work function to be field and temperature dependent. The details of this theory will be given in the next chapter. The most interesting and surprising

result is that the work function, calculated from the expression obtained, is zero at $0^{\circ}K$. This is in accordance with the conclusion reached by Mee[68] and Hathaway[69] from the experimental results.

In conclusion of this chapter, it can be seen that experimental and theoretical work in this laboratory predicts hitherto unexpected behaviour of the work function at $0^{\circ}K$. However it is only natural that the experimental work quoted up to this point would be regarded as being inadequate since the measurements were made on complex cathodes. Suggestions that the behaviour is due to surface contamination, impurity levels in the emitter etc., are difficult to counter.

It was therefore decided to attempt to measure the photo-electric work function of a clean metal under as good and rigourously controlled vacuum conditions as could be obtained in this laboratory and over a range of temperatures down to that of liquid helium. Inspection of the literature indicated that few reliable measurements had been made at liquid nitrogen temperature and, at that time, none were found to have been performed at helium temperature.

However before proceeding to the experimental work in chapter 4, the next chapter is devoted to a discussion of the existing and new theories of the work function and its dependence on temperature. A review of the relevant published experimental work is also included.

Chapter 3

Temperature dependence of the Work Function

3.1. Theoretical considerations

It has already been shown in section 1.2 that use of a Richardson plot to infer the temperature dependence of the work function is very uncertain. However the manner in which the work function might be expected to vary with temperature, from theoretical considerations, has been discussed in detail by Herring and Nichols[18] and will be briefly dealt with in this section.

They define the true work function, ϕ, for a uniform surface on the difference between the electrochemical potential, $\bar{\mu}$, of electrons just inside the conductor and the electrostatic potential energy, $-e\Phi_o$, of an electron in the vacuum just outside the surface so that;

$$\phi = -\Phi_o - \frac{\bar{\mu}}{e}$$

where, $\bar{\mu} = \left(\frac{\partial F}{\partial n}\right)_{T,v}$

F = Helmholtz free energy

n = number of electrons in single isolated body

v = volume

T = absolute temperature

The chemical potential , μ , is then defined as,

$$\mu = \bar{\mu} + e\Phi$$

Then if Φ_i is the electrostatic potential inside the conductor,

$$\phi = (\Phi_i - \Phi_o) - \frac{\mu}{e} \quad \ldots\ldots (12)$$

The term $(\Phi_i - \Phi_o)$ represents the difference of potential between the inside and outside of the conductor, and is due to the unsymmetrical charge distribution around the surface ions. This will depend upon the condition of the surface as well as the interior structure. A change, Δ , in the dipole moment per unit area of surface will change $(\Phi_i - \Phi_o)$ by $4\pi\Delta$ Since Δ may be expected to vary for different crystal faces, the work function will also vary for each face. On the other hand the chemical potential is a volume property, independent of the surface structure.

ϕ is in general a function of temperature and the only restriction put forward from thermodynamic principles arises from Nerst's theorem - ie. as T tends to zero, the entropy, S, approaches a limiting value.

Since

$$S = -\frac{\partial F}{\partial T}$$

then

$$\left(\frac{\partial S}{\partial n}\right) = - \frac{\partial^2 F}{\partial n \, \partial T} = - \frac{\partial \bar{\mu}}{\partial T}$$

which tends to zero as T goes to $0^{\circ}K$.

Therefore $\frac{\partial \phi}{\partial T} \rightarrow 0$ as $T \rightarrow 0$

However this thermodynamic argument can be criticised in the case of thermionic emission because if a current is drawn equilibrium does not exist. It would be difficult to specify how far it is effectively off equilibrium.

It is now possible to consider any physical effects which may cause ϕ to vary with T and to look at the magnitude of these effects. If Φ_o is assumed to be the zero of potential, then from equation (12),

$$e\left(\frac{d\phi}{dT}\right) = e\left(\frac{d\Phi}{dT}\right) - \frac{d\mu}{dT} \quad \ldots\ldots (13)$$

Three terms can be distinguished as contributing to $\frac{d\mu}{dT}$, eg.

$$\mu(v,T) = \mu(v,o) + \Delta\mu_T + \Delta\mu_\theta \quad \ldots\ldots (14)$$

Here $\Delta\mu_T$ represents small changes which would occur in μ if the temperature were raised from O to T, while keeping the volume constant and the metal atoms fixed in their equilibrium positions. The last term $\Delta\mu_\theta$ represents the change resulting from the thermal vibration of the atoms.

The term $\left(\frac{d\Phi}{dT} \right)$ can also be subdivided in a similar manner, such that,

$$\Phi(v,T) = \Phi_o(v) + \Delta\Phi + D \quad \ldots\ldots (15)$$

Here $\Phi_o(v) + \Delta\Phi(v,T)$ is the value which the inner potential would have at a temperature T if the mean charge distribution around the surface atoms were the same as that around atoms in the interior. The quantity D represents the amount the inner potential is altered by differences between mean charge distribution in the surface atoms and in those of the interior, and representsan electric dipole moment.

A number of terms result when equations (14) and (15) are inserted into equation (13) with the relation.

$$\frac{d}{dT} = \left(\frac{\partial}{\partial T}\right)_v + \alpha v \left(\frac{\partial}{\partial v}\right)_T$$

where α is the volume coefficient of expansion.

It will be seen that various effects may cancel each other out, but Herring and Nichols[18] state that this is purely fortuitous. These effects are considered separately.

3.1.1. The principal expansion effect

$$\alpha\, v \frac{d}{dv} \left(e\Phi_o - \mu(v,o) \right)$$

has received most attention in the literature and Richardson pointed it out in his early work on thermionic emission. Several attempts (eg. Riemann[74], Seeley[75]) have been made to calculate

the magnitude of the effect. One such case uses the Sommerfeld free electron model, in which the maximum kinetic energy of the occupied state is proportional to $v^{-2/3}$, so that expansion with increasing temperature should increase the work function. Other methods support this result and find that $e\left(\frac{d\phi}{dT}\right)$ is of the order of several k, and is positive. This is most likely for metals such as Ta, W and Mo, but it may be larger for metals like Fe which have a larger value of α.

3.1.2 The effect of atomic vibrations in the interior is such that

$$\left(e\,\Delta\Phi \quad - \Delta_{\mu\theta}\right)$$

measures the amount by which the work function would change if the thermal vibrations could be eliminated by holding all the atoms fixed in their equilibrium positions, without altering the volume, electron temperature or charge distribution at the surface. For the first part, the thermal vibrations of atoms in the interior alter the mean electrostatic potential and $e\left(\frac{\partial\Delta\Phi}{\partial T}\right)$ has been shown to be probably negative and of the order of k. In the second part the vibrations affect the energies of the various levels which the different electrons of the metal occupy. The average energy of each electronic level changes with increasing amplitude of vibration and changes the height of the Fermi level. In this way it has been shown that $\frac{\partial}{\partial T}\left(\Delta\mu_\theta\right)$ can be either negative or positive and is only a fraction of k in magnitude.

3.1.3 The temperature variation of the surface double layer might be expected to contribute an appreciable amount to changes

in ϕ , by changes in relative position of the atoms. By considering a simple picture of the atoms being compressed together or pulled apart a negative value of

$$\alpha ve\left(\frac{dD}{dv}\right)$$

results which is only a fraction of k. It may however be larger on account of the expansion at the surface layers being not identical with the volume expansion. In this particular context another affect is considered by Herring and Nichols[18] and is the increase in the extension of the electron cloud outside the metal's surface due to the thermal energies of the electrons. However they consider this effect to be small and negligible. They do not give any reasons for this but it is interesting to note that the idea of the electron cloud resembles the electron space charge proposed by Bull[12] which is discussed later.

3.1.4 The term $\frac{\partial}{\partial T}\ (^{\Delta}\mu_{T})$ represents the effect of the free electron contribution to the electronic specific heat. This has been found to be normally small and could be either positive or negative. However it may be larger in the case of the transition metals, where the Fermi level lies very close to the top or bottom of the band.

This discussion has shown that the main cause of the variation of ϕ with T, is the principal thermal expansion effect, and that,

$$e\left(\frac{d\phi}{dT}\right) \sim \text{few} \times k$$

$$\therefore \frac{d\phi}{dT} \sim \text{few} \times \frac{k}{e} \triangleq +10^{-4}\ eV/^{\circ}K$$

However as there are other effects which are both positive and negative, it is possible that for most metals $\frac{d\phi}{dT}$ will be less than this value. This expected change of ϕ with T is small and could not account for the speculations put forward in the last chapter that ϕ tends to zero as T approaches $0^{\circ}K$. However these conclusions were drawn from experimental results from complex cathode surfaces.

Before comparing these theoretical predictions with published experimental values, in the next section we shall outline the recent theoretical approach due to Bull[12] which was referred to briefly in the last chapter.

3.2. A new theory of the work function

Although a reasonable estimate of the work function can be made from the image theory, it has already been shown in section 1.5 that it is unsatisfactory. Bull[12] argues that this arises essentially from continuous electrostatic ideas. On this view it is expected that the work function will be virtually independent of temperature. Furthermore the work function is usually only of interest when there is a relatively large emission of electrons whereas the image theory deals with only a single electron. Bull considers that you cannot liberate an electron from an isolated piece of material as you must always take into account the effect of the collecting electrode. He proposed that such an electron will always be joined to the material by a field line. Therefore, on this basis, an electron can only be taken to another electrode if the field line is cut. This can only be the case if there is

a positive collecting electrode from which field lines terminate on the cathode, and are in opposite sense from those joining electrons emitted from this cathode, to the cathode.

Bull's[12] view of the work function is that it is due to a space charge of electrons which diffuse a small distance outside the emitter and thereby produce an electric field. This section summarises the method by which he attempts to calculate the properties of this space charge. Two main assumptions are made. Firstly he neglects the small variation with temperature of the chemical potential and secondly he assumes that electrons near the surface have the same range of energies as those in the interior. This last assumption only alters the magnitude and the details, but not the general nature of the result.

The surface of a metal is capable of emitting electrons according to the Fermi distribution of energies. As T increases it is likely that only electrons above the Fermi level are caused to leave the emitter permanently. The Fermi level is taken as the datum from which electric potential energies can be calculated. In addition it is convenient to define the origin as a plane near the surface at which the potential is sufficient to stop electrons emitted with a kinetic energy corresponding to the Fermi level. The emerging electrons therefore set up an electric field against which further emerging electrons must do work.

Then if an emitted electron has energy, ϵ , higher than the Fermi energy, μ , it can move to a position at which the

potential, U , is

$$eU = \epsilon - \mu \qquad \ldots\ldots\ldots \quad (16)$$

and therefore the field, E, is given by,

$$E(U, x) = - \frac{\partial U}{\partial x} \qquad \ldots\ldots \quad (17)$$

The equations (16) and (17) define the potential and field just outside the emitter surface. They are fluctuating quantities and therefore refer only to average values. Now where the two electric fields due to the emitter and collector have equal and opposite values, the potential, ϕ, is a maximum. In this model, ϕ represents the work function and relates to the emitter. This is so because in thermionic emission the number of field lines from the anode is normally very small compared with the number involved in calculating the space charge. It is now possible to determine the probability distribution for electrons to be able to reach a region in the space having a potential U . From the Fermi-Dirac distribution we have,

$$n \cdot C \int_{\epsilon=0}^{\infty} \frac{1}{\exp\left(\frac{\epsilon - \mu}{kT}\right) + 1} \, d\left(\frac{\epsilon}{kT}\right) = n$$

where n = number of electrons per unit area and

C = normalisation factor.

This gives,

$$C \cdot \ln \frac{1}{1 + \exp\left(\frac{\mu}{kT}\right)} = 1$$

Normally, however, $\mu \gg kT$

Therefore $C \simeq \frac{kT}{\mu}$

Now the probability that an electron will have energy in the range ϵ to $(\epsilon + d\epsilon)$ will therefore be,

$$\frac{kT}{\mu} \cdot \frac{1}{\exp\left(\frac{\epsilon-\mu}{kT}\right) + 1} \cdot d\epsilon \quad \ldots (18)$$

Therefore using equations (16) and (18), the probability distribution for the emitted electrons to reach regions in the space charge in the range of potential U to $(U + dU)$, and then come to rest, is

$$P\left(\frac{eU}{kT}\right) d\left(\frac{eU}{kT}\right) = \frac{kT}{\mu} \cdot \frac{1}{\exp\left(\frac{eU}{kT}\right) + 1} \cdot d\left(\frac{eU}{kT}\right) \ldots (19)$$

The electric field in this region is due to the electrons which reach it and those which pass right through it.

Thus the electric field where the potential is U, is,

$$E(U, x) = \frac{ne}{\epsilon_o} \int_{\frac{eu}{kT}}^{\infty} P\left(\frac{eU}{kT}\right) d\left(\frac{eU}{kT}\right)$$

Therefore using equation (19) we get,

$$E(U, x) = \frac{ne}{\epsilon_o} \cdot \frac{kT}{\mu} \ln\left\{1 + \exp\left(\frac{-eU}{kT}\right)\right\} \ldots (20)$$

Thus the electric field at the surface of an emitter when U = 0, for typical value of $n = 10^{19}/m^2$, kT = 0.1v and μ = 1.0eV is,

$$E(o, o) = 10^8 \text{ v/cm}$$

This is an extremely large field and can only really be achieved in practice when the emitter and collector are in, or almost in, contact. Thus under normal conditions it is unlikely that all the electrons with energies greater than the Fermi energy can reach the collector.

Rearranging equation (20) and putting U = ϕ, the work function, we get,

$$1 + \exp\left(\frac{-e\phi}{kT}\right) = \exp\left\{E(U,x)\ \frac{\epsilon_o \mu}{nekT}\right\}$$

For typical values of n, T and μ, the right hand side of this equation is small and therefore can be written to a good approximation as,

$$\exp\left(-\frac{e\phi}{kT}\right) = \frac{E(U, x)\ \epsilon_o \mu}{nekT}$$

or in the form,

$$\text{Work function} = \phi = \frac{kT}{e} \cdot \ln\left\{\frac{nekT}{E(U,x)\epsilon_o \mu}\right\} \quad \ldots\ldots (21)$$

If we substitute values previously given we get a value for ϕ = 1.3eV, which is rather typical of an oxide cathode. However if kT = 0.3v, which corresponds to normal emission for a high melting point metal like tungsten or tantalum, then we get ϕ = 4.0 eV. Both of these values are close to measured work functions using thermionic emission methods.

Now for constant applied field equation (21) can be written as

$$\phi = a_1 T \ln (a_2 T) \quad . \quad . \quad . \quad . \quad . \quad (22)$$

where a_1 and a_2 are constants.

This shows that ϕ varies almost linearly with T and that ϕ = o at T = 0°K, which agrees with the prediction based on the qualitative argument presented earlier.

Furthermore we see that at constant temperature

$$\phi = b_1 \ln \left\{ \frac{b_2}{E(U,x)} \right\} \quad . \quad . \quad . \quad . \quad (23)$$

where b_1 and b_2 are constants, and therefore ϕ is also dependent upon the applied field.

It would therefore appear that the results of sections 3.1 and 3.2 are in almost complete contradiction. This was certainly thought to be so initially, but in the next chapter it will be shown that it is possible to regard them as being complimentary rather than contradictory. However before proceeding to the next chapter it is proposed to review the relevant and most

reliable experimental results that have been published on the variation of work function with temperature.

3.3 Experimental values of the variation of work function with temperature

A large quantity of literature has been published on the experimental and theoretical values of the work function of the elements and their chemical compounds. An attempt has been made by the Russian author, Fomenko[76], to compile the work of about 500 published papers up to 1966. A glance at this book shows that there is often a wide range of values for both the elements and the compounds. Certain cases can presumably be criticised on the grounds that the vacuum conditions were not adequate to produce clean surfaces. However even when this is more satisfactory, say 10^{-10}torr, it cannot be assumed that the values must be accepted. For example, exceedingly careful measurements (Ref. 77, 78, and 79) appeared, until recently, to have established the work function of gold to be between 4.7 and 4.8eV. However Huber[80] measured this using an Ion pumped vacuum system and found the value to be about 5.2 to 5.3eV, considerably different from those previously reported. It was shown that the low values were due to the use of mercury diffusion pumps. The mercury reacted with the gold and lowered its work function by about 0.5eV. This particular example is important because many measurements of C.P.D. (eg. Dillon and Farnsworth[81]) have been made using gold as a standard reference surface and assuming the lower value of work function.

The quantity of published literature on the variation of

work function with temperature is much less and often less reliable. The most reproducible value of work function is for tungsten. Hopkins and Rivière [82] consider that the value of 4.545eV at 300°K for well outgassed polycrystalline tungsten should be accepted, and it is now used as a standard reference surface, (eg. Barry et al [83]). On the other hand the variation in work function for different crystal faces of tungsten is quite considerable. Sultanov [84] gives the value for the (110) plane at 5.3eV and the (116) plane as 4.3eV. For a polycrystalline tungsten surface Potter [85], using the Kelvin method, found that between 300 and 1900°K, $\frac{d\phi}{dT} = 6.5 \times 10^{-5}$ eV/°K. However for different crystal faces Van Oostrom [86], using field emission techniques in the range 78 to 293°K, found $\frac{d\phi}{dT} = 0.6 \times 10^{-5}$eV/°K for the (111) plane and 5.7×10^{-5}eV/°K for the (116) plane. In a similar investigation between 78 and 900°K, Swanson and Crouser[87] obtained the value of -14.3×10^{-5}eV/°K for the (112) plane. However they state that for certain crystal planes - eg (100) and (110) - the Fowler - Nordheim model did not give sensible values for the work function and this method must therefore be used with considerable caution. It is certainly the case that in field emission studies it is necessary to make assumptions about the geometry of the emitting tip and the effect of the field.

Comsa et all [88, 89] used the electron beam method for molybdenum and nickel. They claimed that this method is the most suitable as it is capable of producing errors of less than

10^{-6}eV/°K. They say that with other methods the errors might be as great as the expected variation. The electron beam method actually measures change in C.P.D. In order to measure changes in work function corrections were made for the change in electrochemical potential of the heated target surface, using an assumed value of the Thomson coefficient. For the Mo they found $\frac{d\phi}{dT} = 7.8 \times 10^{-5}$eV/°K between 600 and 1100°K and for Ni, $\frac{d\phi}{dT} = -3.1 \times 10^{-5}$eV/°K.

However despite the extreme confidence of Comsa et al in this method, Hopkins and Smith[90] recently made a comparison between the Kelvin and electron beam methods for measuring C.P.D. They concluded that the electron beam method can produce appreciable errors due mainly to the effect of work function patches. However it is interesting to note that they considered that the discrepancy between the two methods was not due to the temperature variation of the work function of the barium surface employed. They stated that this is unlikely as a coefficient of about 2×10^{-3}eV/°K would be required to explain this difference.

Blevis and Crowell[91] used the Shelton[4] method for copper in the range 20 to 700°C and found $\frac{d\phi}{dT}$ for various crystal faces to be all negative, but varying from -3.4×10^{-4}eV/°K for the (111) plane to -13.8×10^{-4}eV/°K for the (100) plane.

Crowell and Armstrong[92] used a C.P.D. method for silver and a retarding field method for sodium and potassium and obtained values of $\frac{d\phi}{dT} = -13.4 \times 10^{-5}$eV/°K for silver, -51×10^{-5}eV/°K for sodium and -26×10^{-5}eV/°K for potassium. However in the case of silver the C.P.D. between the two silver electrodes was

not zero even when both surfaces were at room temperature.

In contrast Garron and Testard[93] found the variation of photo-electric work function with temperature for potassium to be positive and equal to 4×10^{-4} eV/°K in a similar temperature range of 82 - 300°K.

For Silicon, Allen[94], using thermionic measurements, assuming A = 120 and r = o, found $\frac{d\phi}{dT} = 3.75 \times 10^{-4}$ eV/°K in the range 1400 to 2400°K. However when this was extrapolated to lower temperatures, it did not give the value of ϕ at room temperature found by both field emission and C.P.D. measurements. He said that this implied that the sign $\frac{d\phi}{dT}$ must change as the temperature is lowered. This remark appears to be quite unjustified due to his initially dubious assumptions that A = 120 and r = 0. It is therefore surprising that Bachman et al[95], using a molybdenum reference electrode in the Kelvin method, found a similar value for silicon of $\sim 10^{-4}$ eV/°K between 300 and 800°K.

Crowell[96] employed the Fowler technique for the photoelectric work function of iron, and observed that the work function first decreased and then increased as the temperature was increased. This was attributed to a change from the α(b.c.c.) to the γ(f.c.c.) form. Thus the change in photoelectric sensitivity was more associated with the number density of free electrons than the actual change in work function. This conclusion was made as a result of the observed vertical shift on the Fowler plots. However Crowell recognised that the vacuum conditions, less than 10^{-8} torr, were not really adequate.

In two recent papers by Wilson[97,98] he describes measurements of the thermionic work function of a number of metals. In order to define a small emitting area he employed an aperture collector in conjunction with an axial magnetic field. He found only small variations, both positive and negative, in work function with temperature - eg $\frac{d\phi}{dT} = -8 \times 10^{-4}$ eV/°K for titanium and $\frac{d\phi}{dT} = +4.2 \times 10^{-4} \times$ eV/°K for platinum. However these measurements were effective work functions taking A = 120 and r = 0 for all materials and temperatures. This method has already been shown in chapter (1) to be only of interest in approximate studies of thermionic emitters.

The writer is only aware of one publication on the measurement of work functions at liquid helium temperature. Beddard and White[99] investigated the long wavelength limit of photoelectric emission from a pure sample of tin at room, liquid nitrogen and liquid helium temperatures. In order to obtain high sensitivity he used a 14 - stage electron multiplier. A beam deflecting capacitor was used to direct the emitted electrons at right angles to the incident radiation onto the first dynode of the multiplier. The pulses from the multiplier were amplified, passed through an integral descriminator to reduce the noise counts, and then counted for a 10 second interval. In this way they reported that it was possible to reduce the spectral bandwidth of the incident radiation to as little as 1A°. They claim that there is considerable variation in room temperature and liquid nitrogen curves near the threshold wavelength, whereas none appear at liquid helium temperature. However inspection of their published curves near

the threshold do not seem to support these remarks. On the contrary they indicate an extension of the long wavelength tail at helium temperature. It should also be said that although the system was claimed to be capable of ultra high vacuum conditions, the reported measurements were performed in a vacuum of 5×10^{-7} torr.

It should be clear from the discussion in this section that for metals the coefficient of variation of work function with temperature appears to be small in magnitude and either positive or negative in sign. Furthermore the magnitude of the measured variations seems to be in reasonable agreement with the theoretical predictions outlined in section 3.1. It is, however, difficult to say which experimental results are reliable because in some cases they differ in sign for the same material in a similar temperature interval. The use of different experimental methods, and the interpretation of the results, may well account for some of these discrepancies.

In general for compounds, such as metallic oxides, the variation has been found to be larger- eg. $\frac{d\phi}{dT}$ is about 7×10^{-4} ev/°K for the oxides of barium, calcium and strontium (Beinar and Nikonov[100]) but it is likely that the results for complicated cathode surfaces are even less reliable.

Most of the measurements of $\frac{d\phi}{dT}$ for all types of surfaces have been made at and above room temperature. A few measurements have been reported at liquid nitrogen temperature and during the course of this present work reference has been found to only the one measurement at liquid helium temperature.

In view of this and the tentative conclusions reached as a result of the experimental work described in chapter (2) and the new theoretical ideas of Bull[12], it was considered necessary and desirable to attempt to measure the work function of clean metals between room temperature and liquid helium temperature. The experimental techniques and the results of this work are discussed in the next chapter. The results of similar measurements on oxide coated cathodes are given in chapter 5.

Chapter 4.

Photoelectric work functions of clean metals

4.1. Introduction

The only feasible method for measuring the work function of a surface as a function of temperature, and down to liquid helium temperature, is the photoelectric method. Any method involving C.P.D., such as the Kelvin method, would be difficult as this would require cooling one electrode only and maintaining the other at a constant temperature. Other methods employing a thermal source of electrons, such as the electron beam method, would be extremely difficult at very low temperatures.

It is clear that to make reliable measurements of the work function, measurement techniques for very small photoelectric currents are required under ultra-high vacuum conditions. The way in which an attempt was made to bring together the three conditions of very low temperatures, very small currents and ultra-high vacuum will now be discussed. It should however be stated that it was realised that this approach, using sealed-off experimental tubes, was not necessarily the most desirable, but this method was determined upon on account of the availability of equipment, in particular the liquid helium cryostat.

4.2. Liquid helium cryostat

The helium cryostat was designed in conjunction with, and made by, The Oxford Instrument Company. A schematic diagram is shown in figure (17) and the actual cryostat is included in the photograph in figure (18). The complete cryostat was supported on an angle iron frame, in order that the quartz window at the lower end was above bench height, and therefore level with the output slit of the monochromator. The cryostat was supported in the frame from the top plate and was demountable in this position. The complete outer vessel was joined to the top plate by an 'O' ring seal and the lower section, containing the experimental tube, was also demountable and sealed in a similar manner. All the electrical lead-throughs were made with vacuum sealed connectors in the top plate, which used P.T.F.E. as an electrical insulator.

The cryostat is an all metal one, made mainly of copper and stainless steel. The diagram shows that there is a common vacuum space to the nitrogen and helium sections. The helium section is entirely surrounded by the copper radiation shield which is at liquid nitrogen temperature. The vacuum inside the cryostat was produced by a conventional rotary pump and oil diffusion pump system capable of evacuating it to a pressure of about 10^{-5} torr, recorded on a Penning gauge. When the cryostat had been left at atmospheric pressure for sometime, the pump down was rather slow and it was usually necessary to warm the outer vessel with heater tapes at about 70°C. The temperature could not be taken higher than this on account of a "Wood's" metal joint at the bottom of the liquid

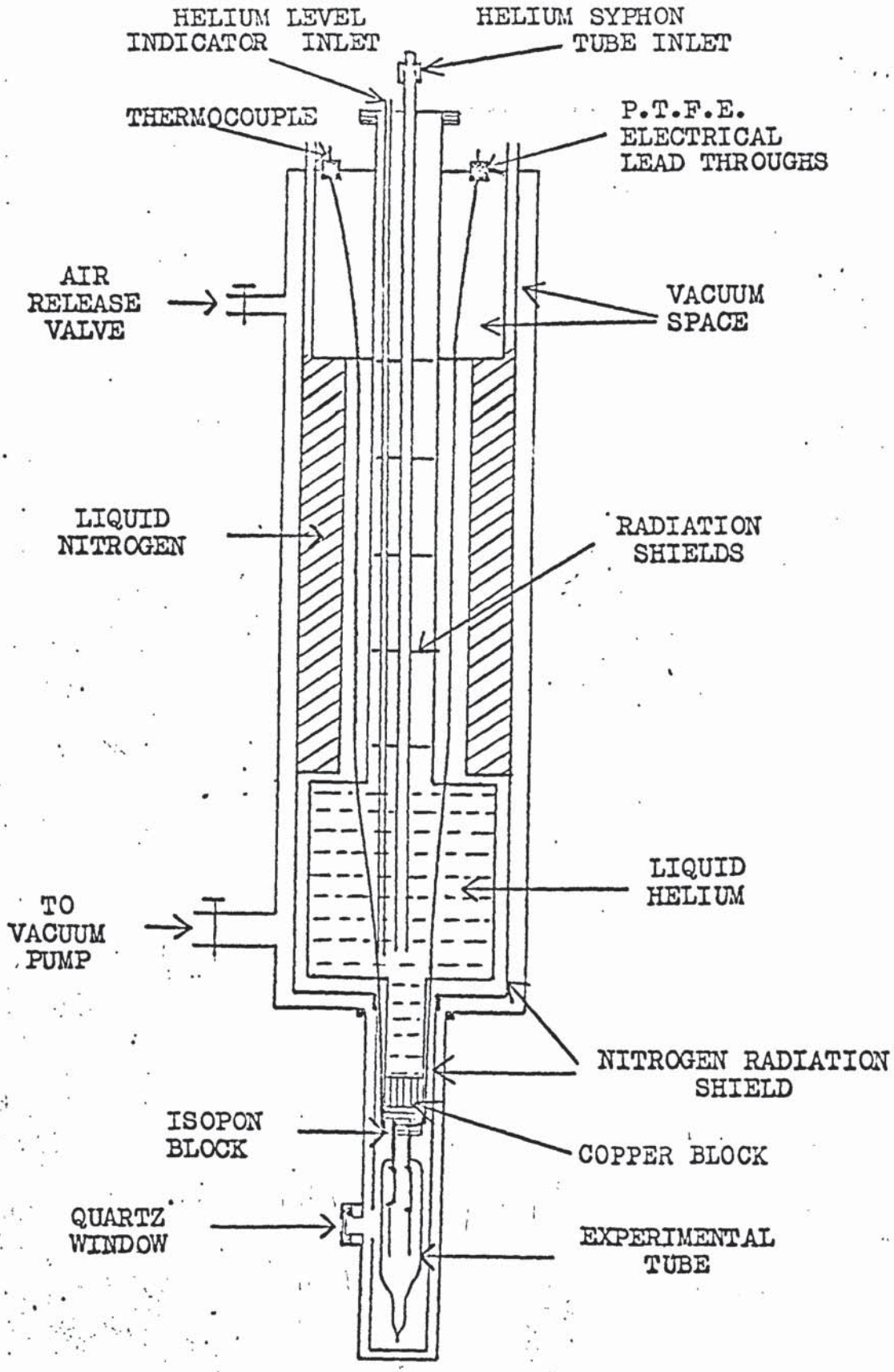
HELIUM LEVEL INDICATOR INLET
HELIUM SYPHON TUBE INLET
THERMOCOUPLE
P.T.F.E. ELECTRICAL LEAD THROUGHS
AIR RELEASE VALVE
VACUUM SPACE
LIQUID NITROGEN
RADIATION SHIELDS
LIQUID HELIUM
TO VACUUM PUMP
NITROGEN RADIATION SHIELD
ISOPON BLOCK
COPPER BLOCK
QUARTZ WINDOW
EXPERIMENTAL TUBE
6"
HELIUM CRYOSTAT

FIGURE 17

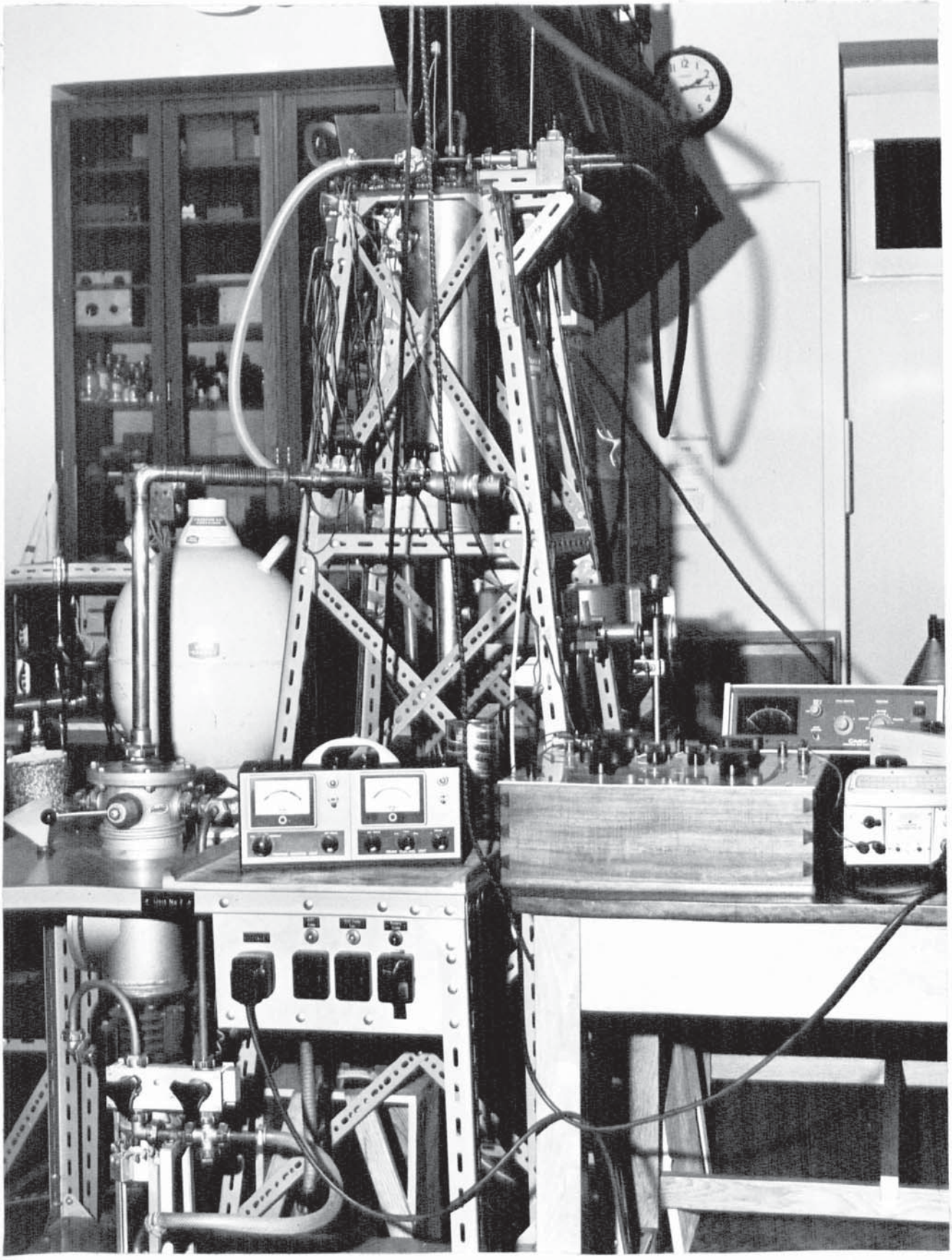

Figure 18

helium section.

The liquid nitrogen capacity was 3 litres and the liquid helium capacity 2 litres. The normal boil-off of the liquid nitrogen was about 0.25 litre/hour so that it was not necessary to fill up the cryostat during any one experimental run. Once the cryostat was filled and cooled, the helium boil-off was also quite small. The liquid nitrogen level was measured with a small apezion oil mannometer, and the helium level was measured with a small 280 Ω carbon resistor which could be inserted into the helium on the end of a thin wall stainless steel tube. When the resistor was inserted into the liquid helium, ($4.2^{\circ}K$), its resistance increased to about 26 K Ω.

The experimental tube was cooled by radiation and by conduction through the tungsten leads. These leads made thermal contact to the copper block through copper supports sealed into "Isopon" embedded in the lower section of the block. The Isopon is a polyester resin and was very satisfactory, not only in providing adequate electrical insulation between the leads, but also in maintaining sufficient thermal conductivity at all temperatures. For example with 45v applied across the copper leads in the Isopon, under vacuum conditions, this gave a resistance of about $5 \times 10^{15}\Omega$ at room temperature.

The procedure for cooling the cryostat was somewhat complicated but relatively straightforward once the initial problems had been overcome. These were mainly concerned with leaks between the helium and vacuum sections. They were particularly troublesome

to overcome as they were "cold leaks" occuring only at either nitrogen or helium temperatures. The cryostat was pumped down to about 10^{-5} torr and then cooled down with liquid nitrogen. Before introducing liquid helium, the whole cryostat was allowed to cool down to about 80°K. This whole operation took about two days because the cooling was almost entirely by radiation. This is the main disadvantage of this design of cryostat which has one common vacuum space. When the copper block was between 80 and 90°K the liquid helium was admitted, after isolating the cryostat from the vacuum system. This was necessary to avoid cryo-pumping of the vacuum system. Transfer of the liquid helium from the main helium storage vessel was made through a vacuum syphon. The syphon and helium sections were evacuated and then filled with helium gas. A small excess pressure was built up above the liquid helium level in the main vessel by squeezing a rubber ball connected to the main vessel. The helium boil-off then maintained this excess pressure sufficient for helium transfer to take place. During the cooling period, about two litres of liquid helium boiled off and the gas was collected in one of two small storage bags (about 30 cubic feet capacity) suspended above the cryostat. When these were full the gas was pumped to a main storage and recovery unit in an adjacent laboratory. With no experimental tube present the lowest block temperature was found to be at about 5°K.

4.3. Thermocouples

Four thermocouples were used for monitoring temperatures. Three were kept at fixed points, namely ice, liquid nitrogen and

liquid helium temperatures. The other was attached to the copper block and its temperature could be measured against one of the fixed points. The thermocouples were constructed from Chromel wire and gold wire containing 0.03% of iron. The sensitivity was in the region of 20 $\mu/^{\circ}K$ and the thermoelectric e.m.f's were measured on a type 4025 Tinsley potentiometer, which, with a Pye galvanometer, gave a lower sensitivity of about $\pm 1 \mu V$.

In order to make the thermocouple junction, the chromel wire was first tinned with silver solder. The gold wire was then joined to this with "Woods metal" using coraline flux which was kindly provided by Dr. K.E. Grew of the University of Exeter. Electrical insulation between the wires was maintained in the cryostat using small ceramic insulators.

The thermocouples were calibrated at four fixed points, ice, solid carbon dioxide 195°K, liquid nitrogen 78.8°K and liquid helium, 4.2°K. The whole temperature range was then interpolated using these fixed points by comparison with a complete calibration, for different wire samples, which was kindly supplied by Dr. R. Berman of the Clarendon laboratory, Oxford. Calibration curves in the range of temperatures 80 to 280°K and 4.2 to 80°K are shown in figures 19(a) and 19(b).

Very good agreement was found between the e.m.f's of pairs of thermocouples. However two precautions were found to be necessary as the thermocouples were all terminated on a junction board near the top of the cryostat. First, rubber tubes were fitted to the liquid nitrogen boil-off points to stop cold air flowing

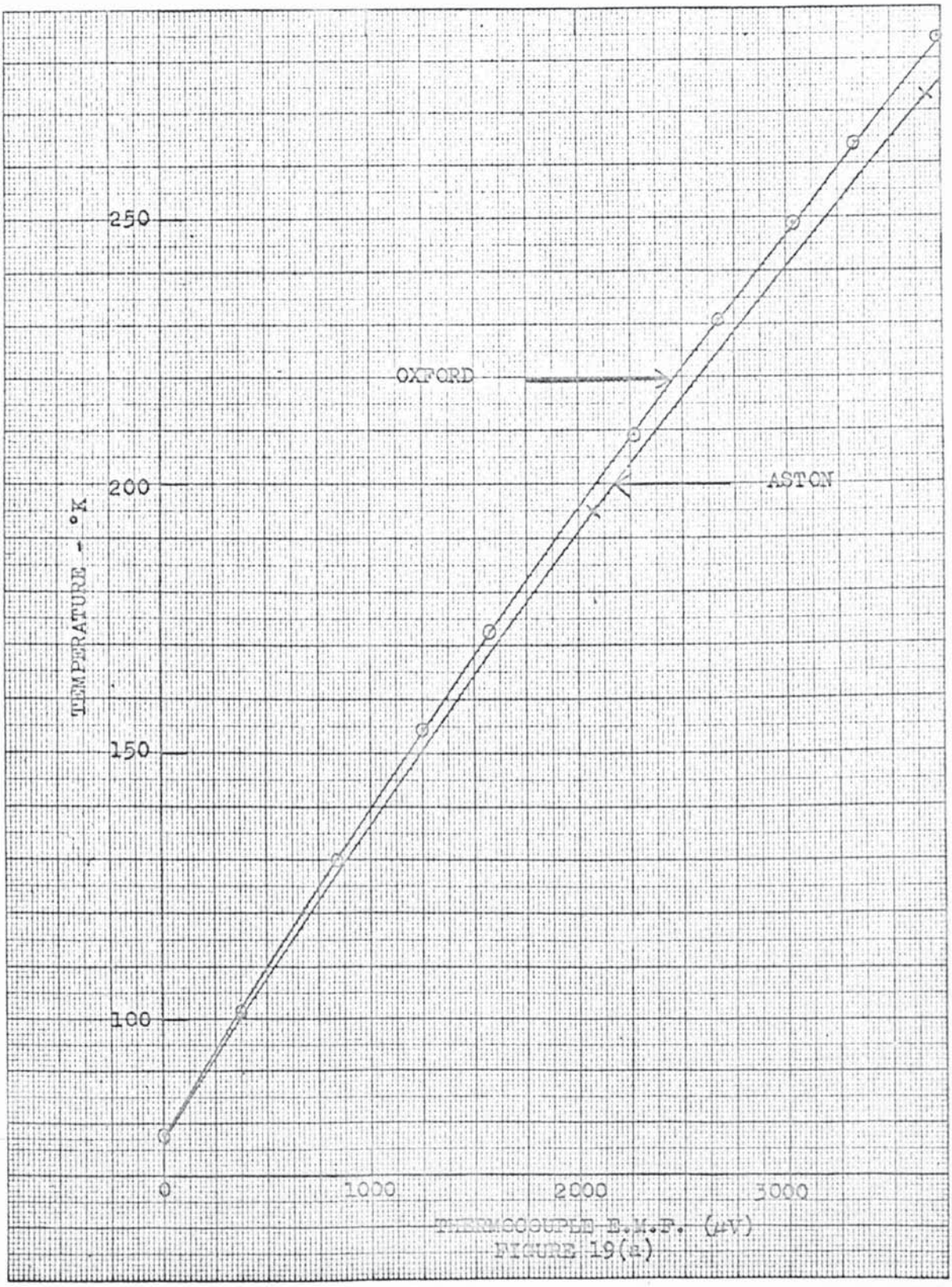
250
200
150
100
0
1000
2000
3000
OXFORD
ASTON
TEMPERATURE - °K
THERMOCOUPLE E.M.F. (μV)

FIGURE 19(a.)

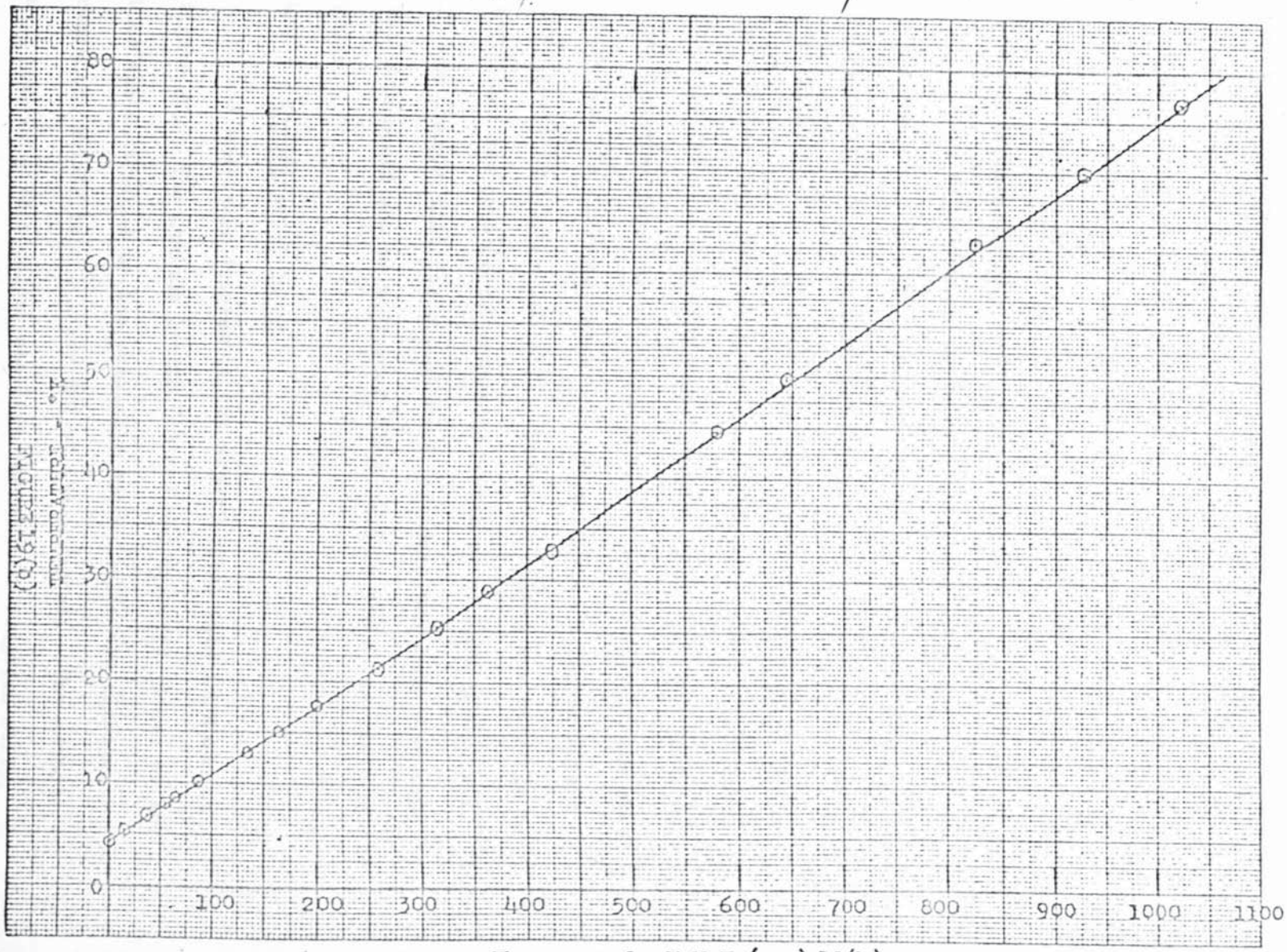
Temperature °C (Thermocouple 19(a))
0
10
20
30
40
50
60
70
80
100
200
300
400
500
600
700
800
900
1000
1100
Thermocouple E.M.F.(μv) 19(b)

over the junctions. Second, since immediately after introducing liquid helium the region around the junctions frosted over, it was only after about 30 minutes, when the junctions had returned to room temperature, that it was possible to get meaningful and reproducible readings.

4.4 Vacuum system

The experimental tubes were evacuated on an oil free stainless steel system. This consisted of a liquid nitrogen zeolite sorption pump, a 15 litre/sec Vac-Ion pump and a 300 litre/sec automatically controlled and water cooled sublimation pump. The initial pump down with the sorption pump, down to 10^{-3} torr, was measured with a thermocouple gauge. This pump and gauge were then isolated from the main system with a bakeable stainless steel valve and the ultimate vacuum was measured with a Bayard-Alpert type gauge (Mullard - IOG 12). The whole system was bakeable to 450°C and was capable of producing pressures of less than 2×10^{-10} torr. It was thought that the actual total pressure was less than this, but this could not be indicated since this is the X-ray limit of the gauge.

4.5 Experimental tubes

A schematic diagram of the experimental tube is shown in figure 20. The maximum length (15 cm) and diameter (3 cm) of the tube was determined by the available space inside the nitrogen radiation shield in the lower end of the cryostat. The cathode was made of either polycrystalline tantalum or tungsten strip, 30m.m. x 5m.m., and was spot welded to a 1.5m.m. diameter tungsten rod.

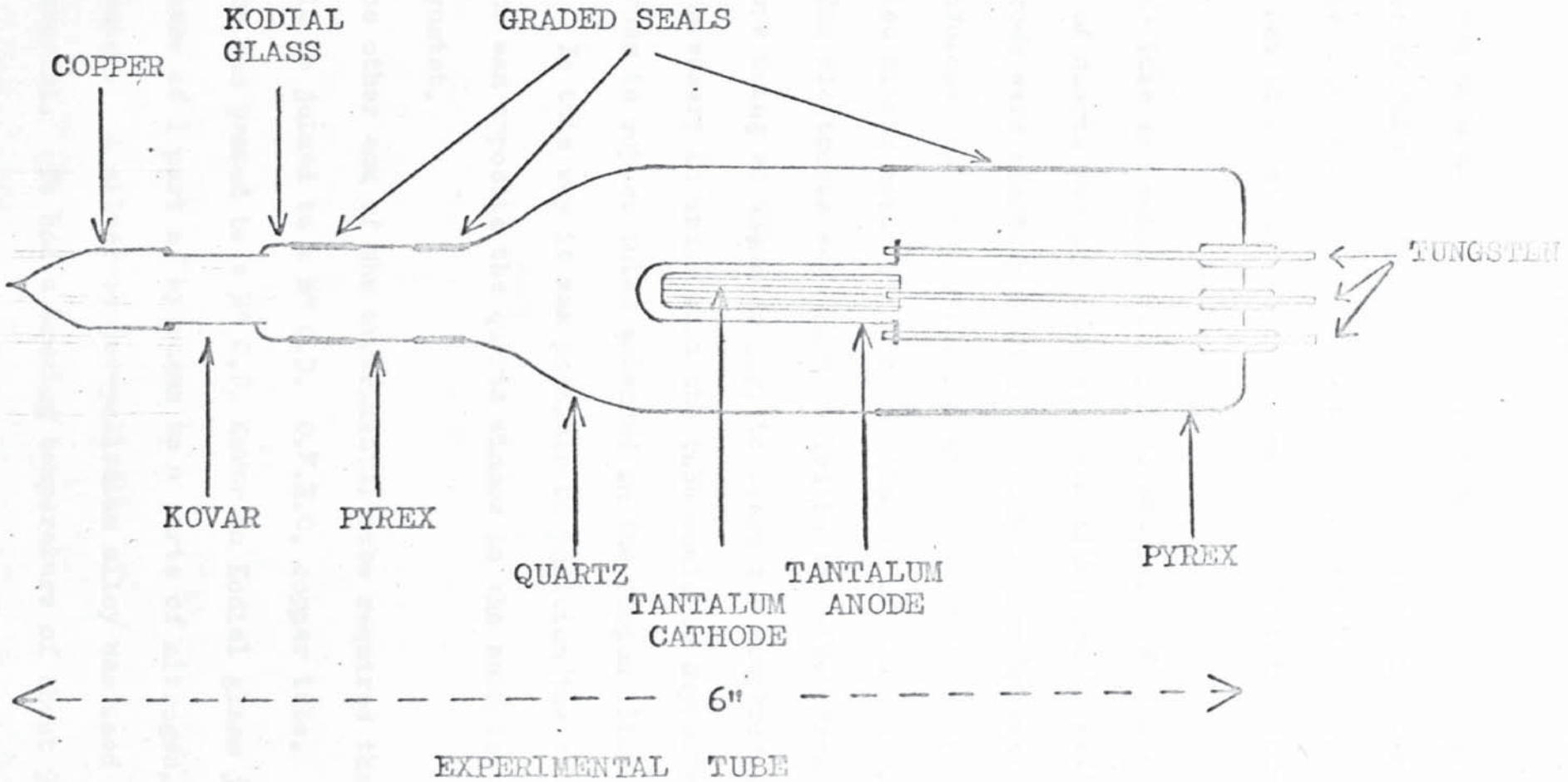

FIGURE 20

EXPERIMENTAL TUBE

The anode was made as a 'U' shaped filament from 0.25mm diameter tungsten or tantalum wire, which was welded to two similar tungsten rods. The anode was made in this way in order that it could be used as a hot filament for electron bombardment of the other electrode.

The tube was constructed in two stages. The main envelope was made of quartz and pyrex with intermediate graded seals. The tungsten rods were electropolished in a 10% sodium hydroxide solution and the envelope was cleaned first with a detergent and then in concentrated nitric acid before being finally rinsed in distilled water. The electrodes were then sealed in the wide pyrex end of the envelope using an asbestos jig, to space the electrodes accurately. This was necessary in order that the tube could be supported by the tungsten rods in copper tubes embedded in the Isopon block in the cryostat. In this way it was possible to position the tube so that the cathode was opposite the quartz window in the cold lower chamber of the cryostat.

The other end of the experimental tube required that the pyrex could be joined to a ⅜" O.D. O.F.H.C. copper tube. The copper tube was brazed to a ¼" O.D. Kovar to Kodial glass joint in an atmosphere of 1 part of hydrogen to 4 parts of nitrogen, using an R.F. heater. A silver-copper-palladium alloy was used for the brazing material. It had a brazing temperature of about 905°C which was just below the M.P. of the copper. The purpose of the palladium is that it discourages diffusion of the silver into the Kovar. The copper, Kovar to Kodial tube was then joined onto the

main tube envelope using a third graded seal.

The tube was then leak tested on a helium mass spectrometer and was then joined to the vacuum system via a Varian compression port. This consists of a collet on the outside of the copper tubing which impresses the tubing on the inner stainless steel seat. Using the specified sealing torque of 10ft - lbs, this was found always to produce a reliable vacuum seal.

4.6. Tube processing

Processing the tube to the highest degree of cleanliness we could obtain took one or two weeks on this vacuum system.

The vacuum system and experimental tube were evacuated first by the sorption pump and then by the Ion pump until the vacuum was less than 10^{-6} torr. The whole system was then baked under a thermostatically controlled oven until the temperature had reached 350°C. It was then maintained at this temperature for a further 24 hours. During this time the ionisation gauge was outgassed and the titanium sublimation filaments were also outgassed at a current of 30 amps.

With the oven cold the tube filament was outgassed using a variac and a step-down transformer. The strip electrode was gradually heated by electron bombardment using an E.H.T. supply. Finally the electrodes were heated to about 2000°K - this being measured with a disappearing filament pyrometer. To achieve this temperature it required an emission of about 30 m/a with 5Kv applied to the anode. It may have been desirable, but it was not possible, to heat the electrode to a higher temperature,

as on attempting this it was found to cause excessive heating of the tungsten-glass seals and bending of the electrodes. The tube was then baked at 250°C for a further 24 hours whilst still maintaining the electrodes as hot as possible. When the system was cool the sublimation pump was put into operation and the time and frequency of the sublimation was adjusted as the pressure decreased. It was finally possible to maintain the electrodes at the maximum temperature without giving any noticeable pressure rise at 2×10^{-10} torr. This was the criterion used that the electrodes were as clean and gas free as was possible with this experimental arrangement.

The operation of sealing off the tube from the vacuum system was performed in two stages. The copper tube was first flattened at a convenient point using a flattener tool made from conventional bolt cutters. The final pinch-off was made with a Varian pinch-off tool having tungsten carbide rollers and which operated very reliably. This operation cold welded the soft copper walls whilst simultaneously severing the metal. Furthermore during pinch-off the ionisation gauge showed no rise in pressure at its limit of 2×10^{-10} torr. It is therefore reasonable to assume that the gas released at seal-off was exceedingly small. Earlier tubes using glass seal-off techniques showed that the pinch off method was very much superior in this respect.

4.7 Electrical measuring equipment

With earlier experiments, the small photo currents, 10^{-14} to 10^{-11} amp, were measured with an E.I.L. 33c Vibron

Electrometer, but the later measurements were made with a Cary 401 electrometer. Both instruments use the vibrating reed principle and measure current as a result of the voltage developed across an input resistor, usually $10^{10}\Omega$, placed across the input impedance of the electrometer, for which the latter was greater than $10^{16}\Omega$. However the Cary instrument was fully transistorised and its overall stability, sensitivity and performance was much better than the E.I.L. instrument. Furtheremore it was more convenient to use since the input resistors of 10^{8}, 10^{10} and $10^{12}\Omega$ were mechanically switched in and out of circuit instead of having to be interchanged by dismantling part of the input circuit.

The accelerating field for the photocurrents was provided by dry batteries which were conveniently switched in 1.5v steps from 0 to 45v. Additional higher voltages from 90 to 630v were also available.

The eventual, and most successful, circuit arrangement used is shown diagramatically in figure 21, with the anode at earth potential and connected directly to the electrometer input, switched in the negative position. The variable voltage source was then used with negative output so that the cathode was biased negatively with respect to the earthed anode. The battery box and tube were both screened and all interconnections were made with non-microphonic low noise cable.

Preliminary measurements on the earlier tubes were made with the sealed-off tube in a screened box but the final measurements were all made with the tube in the cryostat, which also acted as

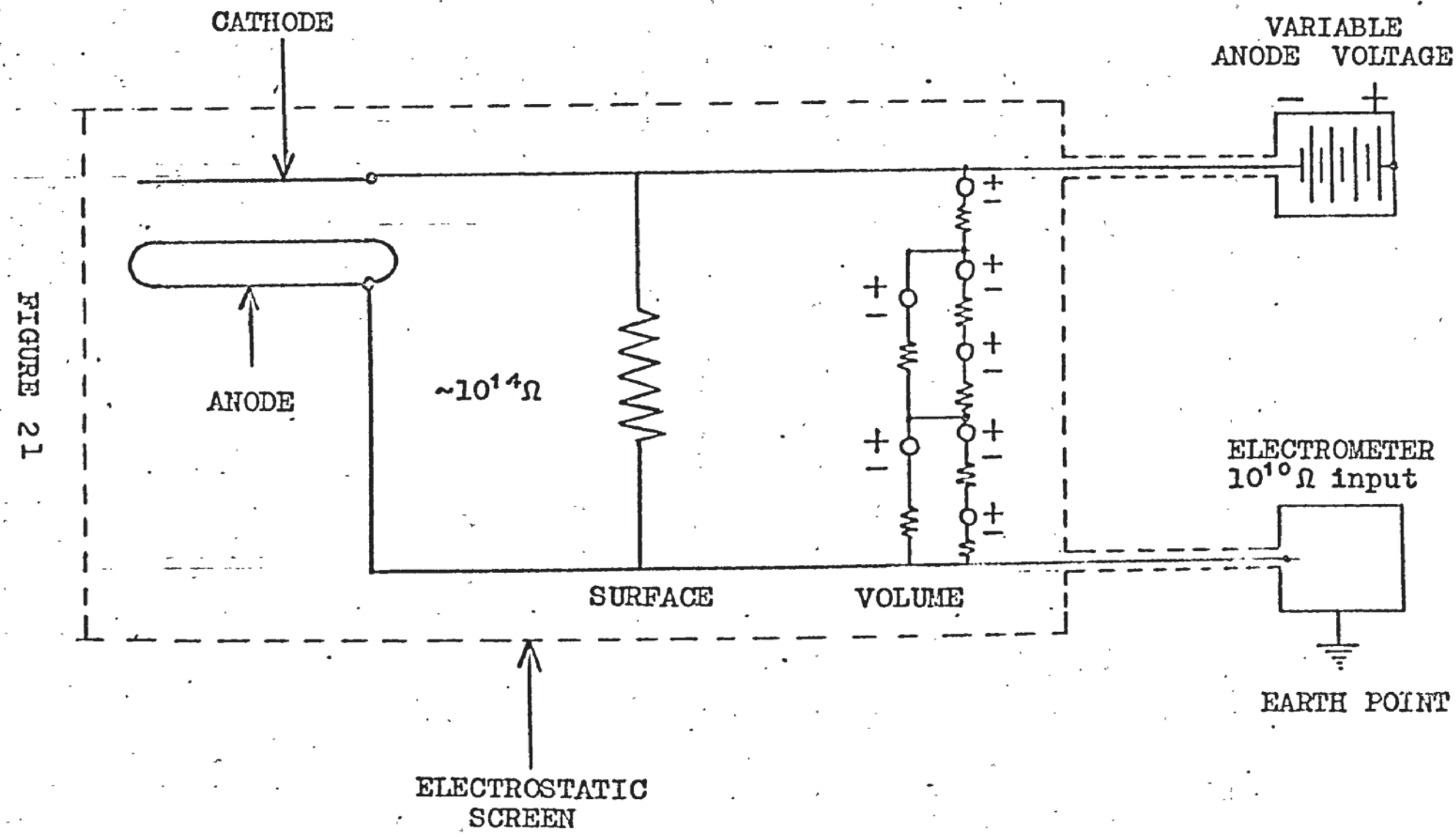
CATHODE
VARIABLE
ANODE VOLTAGE
ANODE
~10¹⁴Ω
SURFACE
VOLUME
ELECTROMETER
10¹⁰Ω input
EARTH POINT
ELECTROSTATIC
SCREEN

FIGURE 21

an electrostatic screen. Connections were made from the P.T.F.E. connectors to the leads on the Isopon block via copper wire insulated with P.T.F.E. sleeving and passing through the helium section.

4.8 Ultra violet source

The source of ultra violet radiation was a Deuterium lamp (Hilger and Watts - FL39) with its associated stabilised power supply - FA140. This lamp gives a continuous spectrum from about 2000°A into the visible region. The selected band of wavelengths were then produced by means of a Hilger and Watts constant deviation monochromator (type D323) which employed front silvered reflecting mirrors in conjunction with a vitreous silica prism. When the entrance and exit slits were fully open these gave a maximum bandwidth of about 325°A at 3000A°.

The output from the monochromator was calibrated using a photomultiplier tube (EMI 9256B). This had been calibrated and very kindly loaned by Dr. Mee of the Physics Department, University of Southampton. The yield (electrons/photon) as a function of incident wavelength, for a working voltage of 1 Kv on the tube, is shown in figure 22. This was done using a bolometer in conjunction with a tungsten filament lamp with glass envelope and a tungsten filament quartz iodine lamp.

With the U.V. lamp against the entrance slit of the monochromator and the photomultiplier 2" from the exit slit, the photomultiplier current was recorded for various slit widths between 1950 and 6000A°. This was done in a dark room and considerable effort was made to shield the photomultiplier from any stray light.

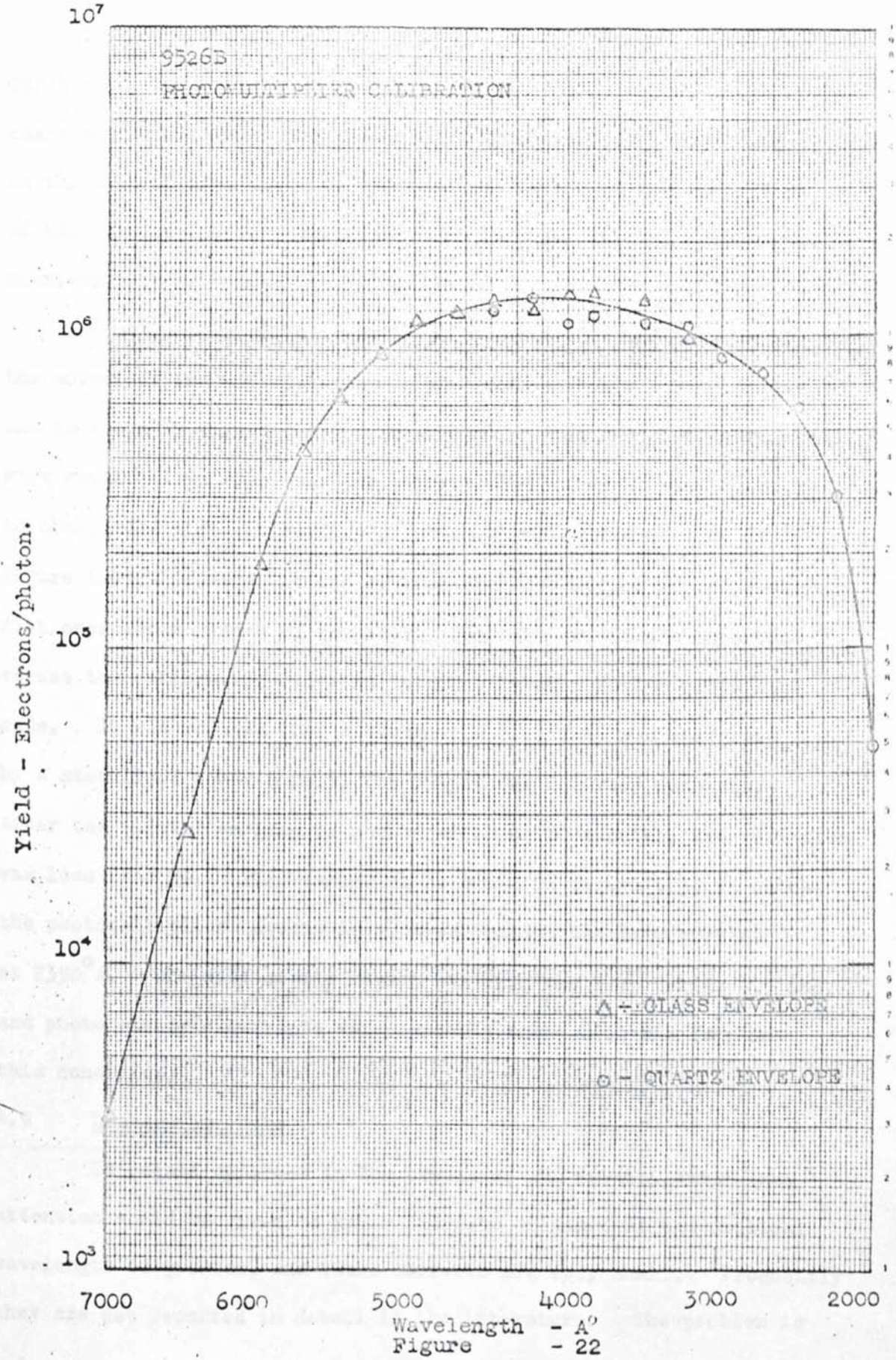
9526B
PHOTOMULTIPLIER CALIBRATION
10^7
10^6
10^5
10^4
10^3
Yield - Electrons/photon.
△ - GLASS ENVELOPE
○ - QUARTZ ENVELOPE
7000
6000
5000
4000
3000
2000
Wavelength - A°

Figure - 22

Three such characteristics are shown in figure 23. The characteristics shown were obtained using a piece of quartz used in the experimental tubes to simulate the effect of the absorption of the tube envelope. This was about 10 - 15% for all wavelengths measured.

Combination of the results of figures (22) and (23) gave the output of the monochromator in photons/sec for all wavelengths and is shown in figure (24). Consequently when any photo currents were recorded, in amps, for the experimental tubes it was possible to obtain the yield in electrons/photon by using the results of figure (24). However it can be seen that the output is reasonably flat over large ranges of the energy spectrum and it was important to use the calibration curve in detail only when Fowler plots were made. It was noticed that although the U.V. lamp was energised by a stabalised power supply, the output was not very constant. After the initial warming up period of about 10 minutes, the variation was less than 6%. This variation is shown in figure (25) in which the photomultiplier current is plotted against the lamp current at 2350°A. The most stable region was with the lamp taking 0.5 amp, and photo electric currents were normally taken with the lamp in this condition.

4.9 Leakage currents

It became apparent in the course of the investigation that attention would be given to photo currents obtained at the critical wavelength or greater, and these currents are very small. Frequently they are not reported in detail in the literature. The problem is

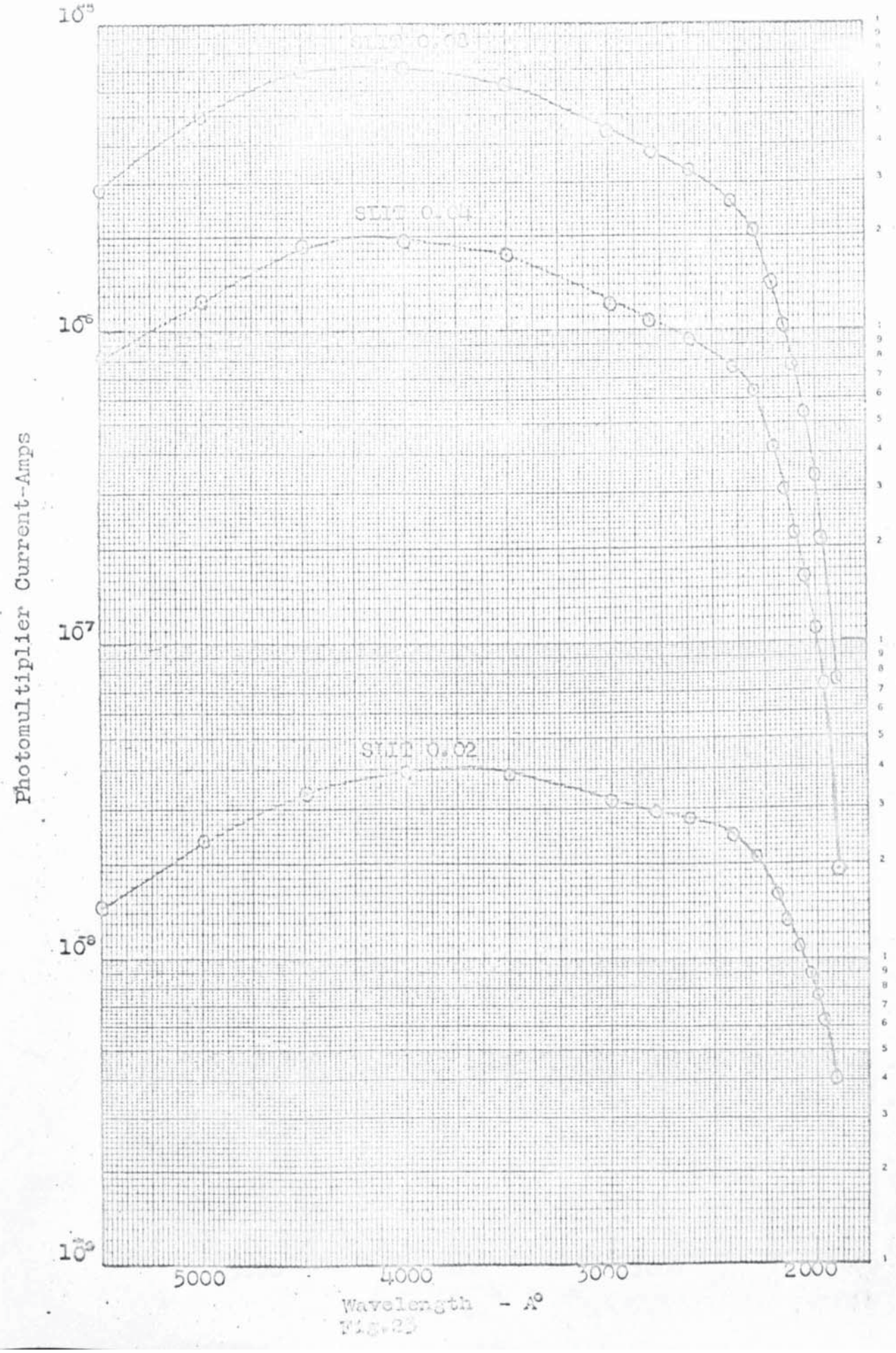
Photomultiplier Current-Amps
10^{-5}
10^{-6}
10^{-7}
10^{-8}
10^{-9}
SLIT 0.08
SLIT 0.04
SLIT 0.02
5000
4000
3000
2000
Wavelength - A°

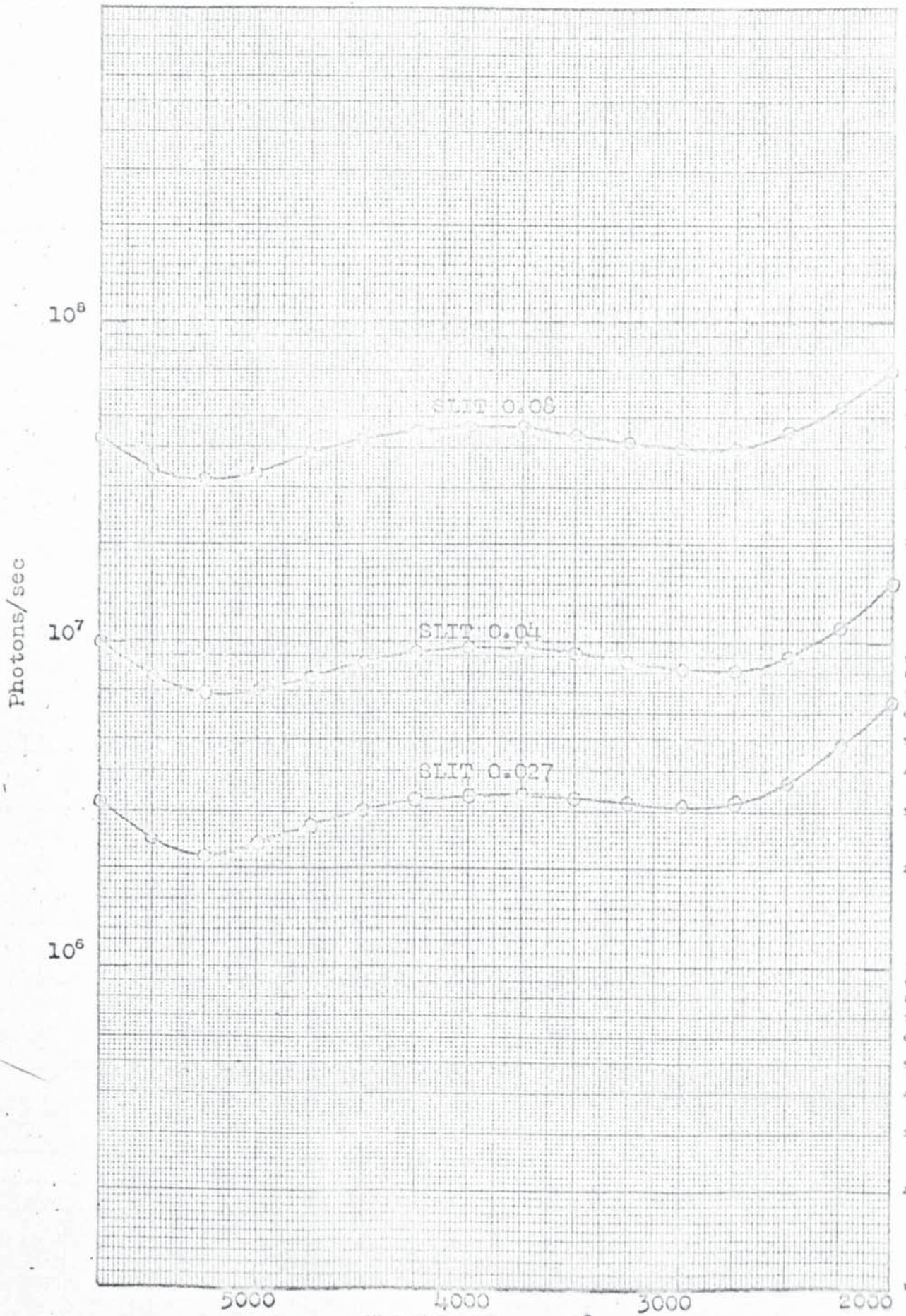
Photons/sec
10^8
10^7
10^6
SLIT 0.06
SLIT 0.04
SLIT 0.027
5000
4000
3000
2000
Wavelength - A°

Figure 24

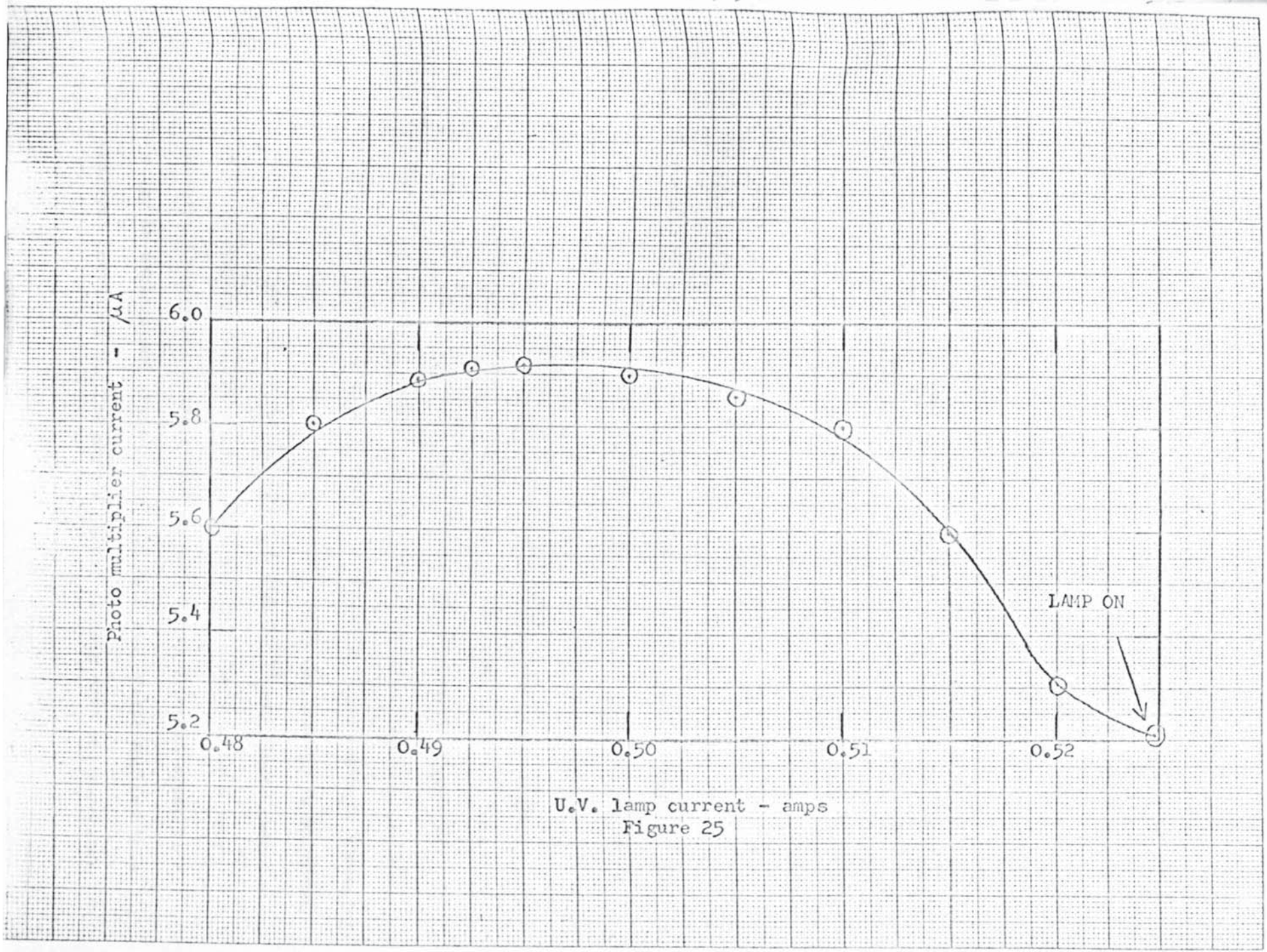
Photo multiplier current - μA
6.0
5.8
5.6
5.4
5.2
0.48
0.49
0.50
0.51
0.52
LAMP ON
U.V. lamp current - amps

Figure 25

avoided by the use of Fowler plots on account of the difficulty in determining the thermionic tail in the presence of leakage currents. It is also partly for this reason that in these experiments the Deuterium lamp, giving a continuous emission spectrum, was used rather than an intense mercury arc source which gives characteristic lines at a much greater intensity.

However currents near the threshold are necessarily small and the limit of detection is determined by the sensitivity of the measuring instrument and, perhaps more so, by any standing or leakage currents present. In this work considerable trouble was experienced with the last two phenomena. It was expected that with the experimental tube to be used, and allowing for the fact that the outside of the tube would also be under vacuum in the cryostat, the resistance between the tungsten leads across the glass would be sufficiently large - ie. $> 10^{14}\Omega$. This would give leakage currents of $< 10^{-13}$ amp for an accelerating voltage of 10v. To ensure this the glass was cleaned on the outside of the tube between the tungsten leads with iso-propyl alcohol to remove any finger marks etc. However it was found that after sealing off the tubes and putting them in position in either an electrostatic screening and light tight box, or in the cryostat, with the circuit arrangement shown in figure 21, a current greater than 10^{-13} amp flowed even with an applied voltage zero. This current proved to be a very erratic feature and a great deal of effort and time was spent in order to explain and avoid its effects. With zero volts applied this current continued to flow over a period of many days and sometimes

a few weeks, although this was not monitored continuously. During this time the magnitude fell and it eventually became very small and steady. It was suggested that this may have been due to charging up of the glass envelope and its subsequent slow discharge. However although the value of the tube capacitance and resistance were not known, a reasonable estimate would be that C ~ 200pF and R ~ $10^{14}\Omega$, which gives a time constant for this arrangement of only several hours. This could not therefore explain the large decay times experienced, although it may have been a contributory factor. Furtheremore when the insulating glass was coated on the inside with conducting films of platinum or gold, it produced little or no effect on this standing current. However it was not possible to coat all the envelope because a clear window had to be left to admit the U.V. radiation.

The effect of an applied voltage was then investigated and can be seen for example in figure (26) for tube (5) which had no conducting layer on the glass. Three graphs are shown taken at 1 day, 6 days and 11 days after sealing off the tube. All these graphs have a similar slope but cut the voltage axis for zero current at about -45, -29 and -16v respectively. These large retarding voltages therefore removed any possibility of this effect being due to thermal energies or contact potential differences. All these measurements were made with a vibrating reed electrometer, but the same effects were found with an Avo D.C. amplifier. Furthermore after many tests on possible circuit faults the tube was replaced by a resistor of $10^{13}\Omega$ and this arrangement gave exactly the

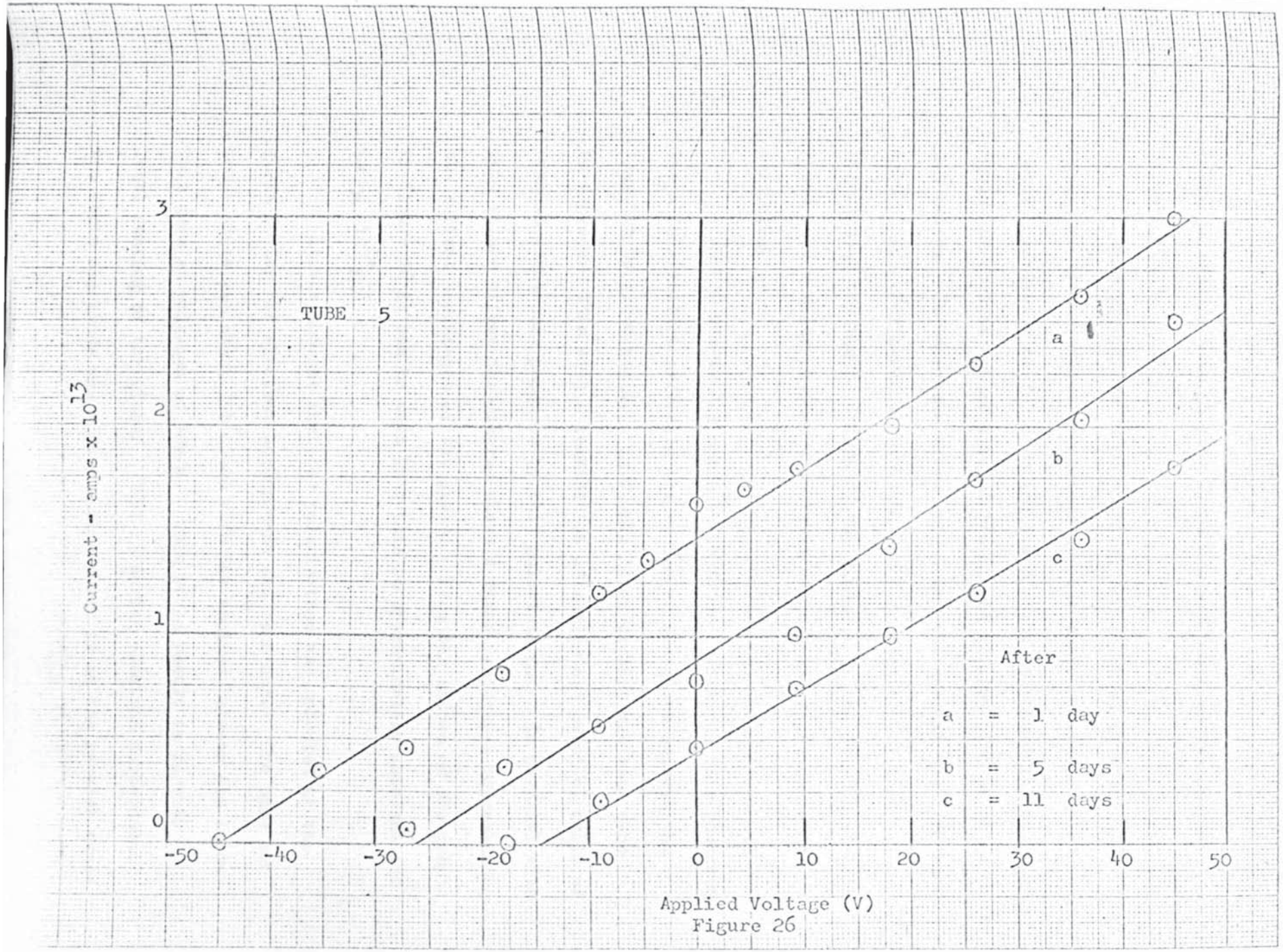
TUBE 5
Current - amps x 10^{13}
3
2
1
0
-50
-40
-30
-20
-10
0
10
20
30
40
50
a
b
c
After
a = 1 day
b = 5 days
c = 11 days
Applied Voltage (V)
Figure 26

expected results - ie obeying Ohm's law with zero current at zero applied volts.

This effect was found with all other tubes, although the magnitude of the effect was not always the same. Figure (27) shows a similar plot for tube (6) taken about 35 days after seal-off. Again the current is not zero at V = 0, but becomes zero at about 1.5 volts. In this tube after only 1 day the current was zero at about 10V. Furthermore this tube had a conducting layer of platinum on the inner surface of the glass. On the other hand both tubes were similar in that a tantalum cathode and tungsten anode were used.

It was eventually proposed that the reason for this phenomena was a polarisation effect in the volume of the glass between the tungsten to glass seals. In figure 21 an attempt has been made to represent this with a combination of series and parallel cells of unknown resistance produced by this polarisation. In parallel with this volume effect the diagram shows a fixed resistance representing the surface resistance of the glass. From the slopes of the graphs in figure 26 it can be seen that this is approximately constant and is $\geq 10^{14}\Omega$.

It was thought that the polarisation was embedded in the glass during the electron bombardment and bake out. The bake out temperature was about 350°C and with 5Kv applied between the leads this gave an emission of 30m/a. This would result in further local heating of the glass. That is during electron bombardment the strip electrode was made positive which is in the reverse sense

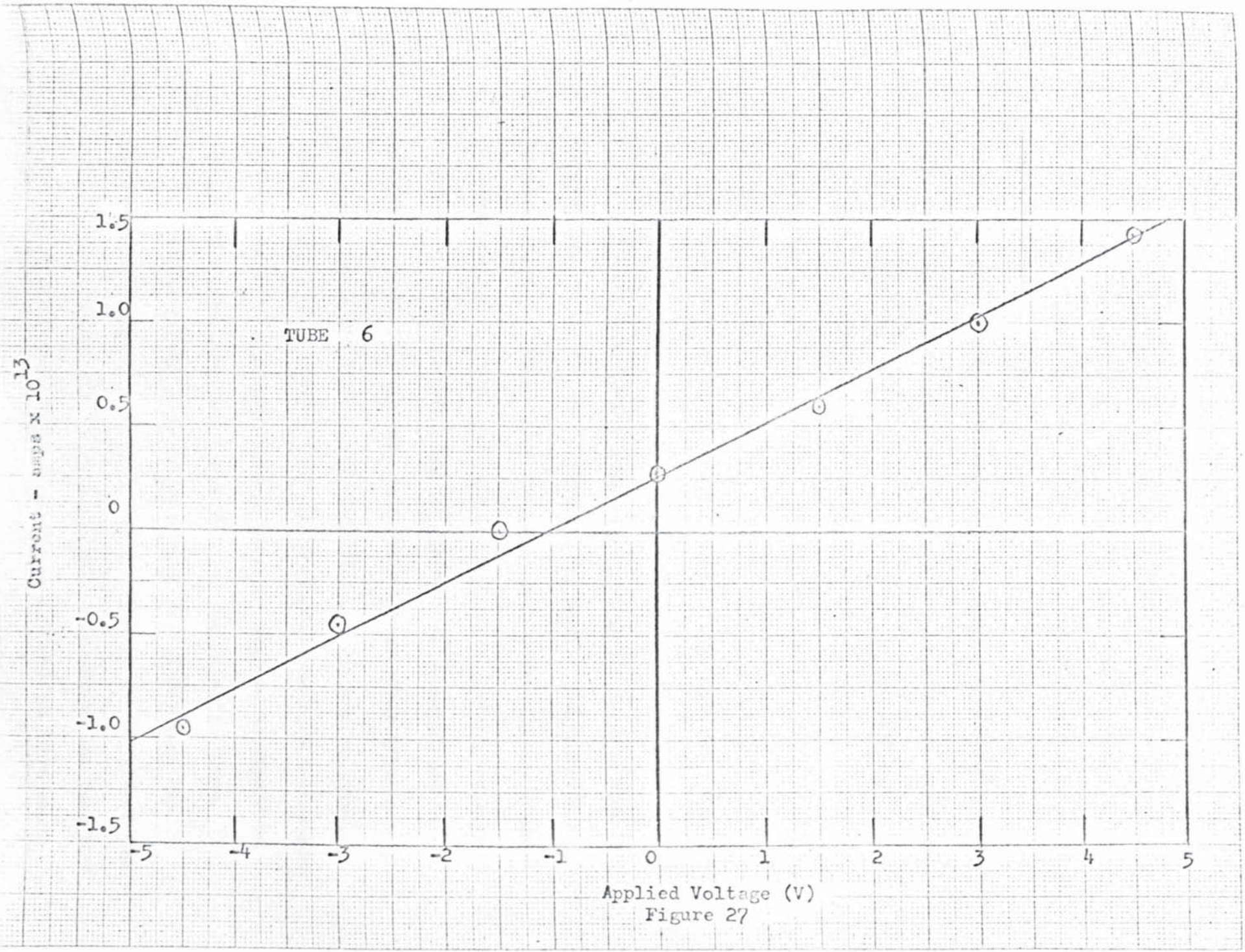
TUBE 6
Current - amps x 10^{13}
1.5
1.0
0.5
0
-0.5
-1.0
-1.5
-5
-4
-3
-2
-1
0
1
2
3
4
5
Applied Voltage (V)
Figure 27

for normal subsequent use during photo electric measurements. Thus under measuring conditions this could explain the direction of current flow found experimentally which was equivalent to an electron current from the cathode to the anode.

In order to substantiate this argument a tube base including the tungsten leads was made and inserted in the cryostat under vacuum conditions. No effect was observed and a normal D.C. resistance of about $4 \times 10^{14} \Omega$ was measured. In addition with a complete and evacuated tube but with no electrodes, baking or E.H.T. bombardment, a similar absence of reverse current was observed. In both instances there was no effect when U.V. light from the Deuterium lamp was allowed to fall directly onto the glass.

These arguments are well supported by the remarks made by Stookey and Maurer[101], who says that at ordinary temperatures and voltages surface conductivity of glass is most important whereas at elevated temperatures and voltages volume resistivity is more important. Furtheremore, because glass is an electrolyte, at high temperature D.C. current flows through the glass between metallic electrodes producing electrolysis. However at normal lower temperatures and voltages the electrode reactions are so slow that space charge or polarisation occurs. This would appear to explain the slow discharge found with the experimental tubes.

Additional evidence in favour of this explanation was found in later experiments using oxide cathodes, as the effect was almost entirely absent. This could have been due to the fact that only relatively low voltages were used to bombard the wire anode

using the oxide coated electrode as an emitter. The effect of polarisation was not observed in the first tube. In the second such tube a small effect was observed but was in the opposite direction to that observed in the tubes having tantalum and tungsten electrodes. This could be expected as the cathode was made negative in this case during the bombardment process.

The trouble caused by these currents could not be removed, but once they were understood, they did not prevent progress, but merely slowed down and made the observations difficult and less accurate than would have been liked. In fact because their source, the glass, has a very high impedance, and provided they were constant during the course of a particular set of measurements, it was sufficient to regard them as a fixed standing current. In noother way did they interfere with the photoelectric currents from the cathode. However effects of this type could have interfered very seriously with contact potential measurements. Without this qualitative understanding and proposed model for this mechanism, it would not have been possible to study the very small photo currents near the threshold. Nevertheless it would have been desirable to have made the experimental tubes larger and with the electrode leads further apart. This may have reduced the effect entirely but it was not possible in this design of cryostat.

4.10 Photoelectric measurements using the monochromator

Tubes (1) and (2)

4.10.1 Tungsten was chosen as the first metal to be investigated as it has been shown to be capable of giving the most reliable and

reproducible values of work function at room and higher temperatures. In the first instance tungsten coil electrodes were used as they could be easily outgassed by A.C. heating. The anode was made with about 5 turns and the cathode with about 20 turns of electropolished tungsten wire. With this arrangement the U.V. could be directed through the anode coil onto the more closely wound cathode coil. Various modifications of this were tried in tubes (1) and (2) but this method was eventually abandoned because of the distortion of the coils produced during heating and the inefficient interception of U.V. at the cathode. All subsequent experimental tubes were made according to the details outlined in section 4.5 and the sheet metal cathode was cleaned by electron bombardment.

4.10.2 Tube 3

Tube 3 was constructed with a tungsten cathode and a tungsten anode. The photo currents were so small, $\sim 10^{-14}$ amp, that it was necessary to mount it in a screened box in which the tube could be moved by external controls in all directions in order to align the cathode with the output beam of the monochromator. With these small currents it was necessary to use the input resistor to the electrometer of $10^{11}\Omega$ and this produced further difficulties due to the large time constants. An attempt was made to increase these currents by using the U.V. source more efficiently with the aid of a 4 cm focal length quartz lens. However whether used either at the entrance or exit slit of the monochromator it produced no real gain and was discontinued.

However a plot of incident wavelength against current is shown in figure 28 using the slits fully open. It is possible

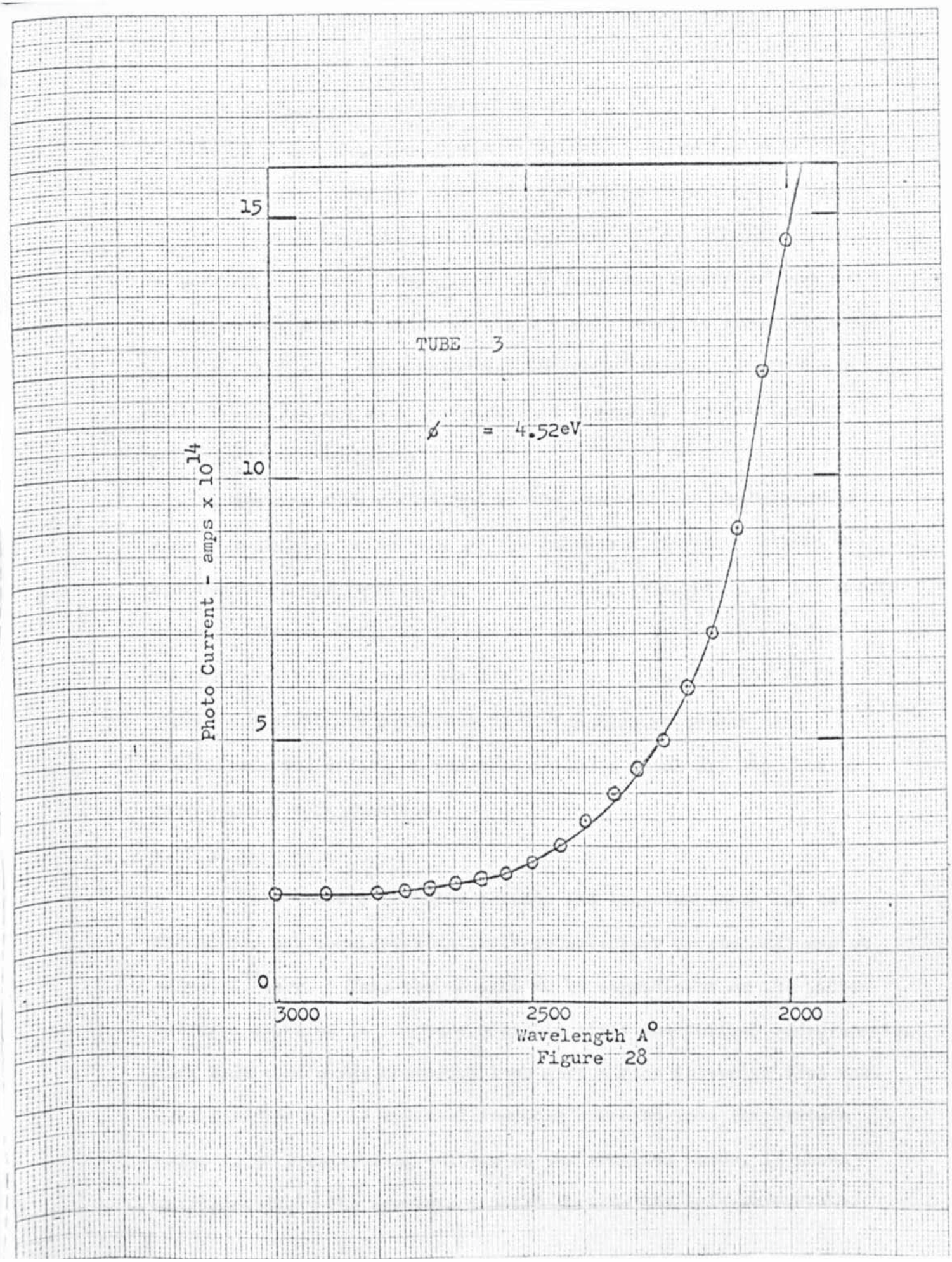
TUBE 3
ϕ = 4.52eV
Photo Current - amps x 10^{14}
15
10
5
0
3000
2500
2000
Wavelength A°
Figure 28

to judge the threshold wavelength as 2750°A ± 100°A, which gives a value of ϕ for tungsten as 4.52 ± 0.15eV. Using the same results a Fowler plot was made and is shown in figure 29. This is not a particularly good plot as it is over only a limited range of current. However comparison with the standard Fowler plot shown in Figure 30, shows a shift of the x - axis equal to about 182 which gives ϕ = 4.55eV. Both these values are in reasonable agreement with themselves and with the published figure of 4.545eV[82] for polycrystalline tungsten.

However when positioned in the cryostat the photocurrents were even smaller on account of the increased distance between the monochromator and cathode and the additional absorption of the quartz window. Consequently as it was not possible to obtain a higher intensity continuous spectrum U.V. source, it was decided at this stage to discontinue measurements on tungsten specimens and concentrate the effort on tantalum cathodes which are expected to have a lower work function.

4.10.3 Tube 4

Tube 4 has a tantalum cathode and tungsten anode but the vacuum was not considered entirely satisfactory as seal-off was at only $<10^{-8}$ torr. This was thought to be significant as the photocurrents appeared to decrease a little after the initial measurements. With this tube a new deuterium lamp gave a higher intensity than that used for tube 3. A spectral response curve at room temperature using 22.5V accelerating voltage on the tungsten anode, is shown in figure 31. The currents plotted include the leakage currents

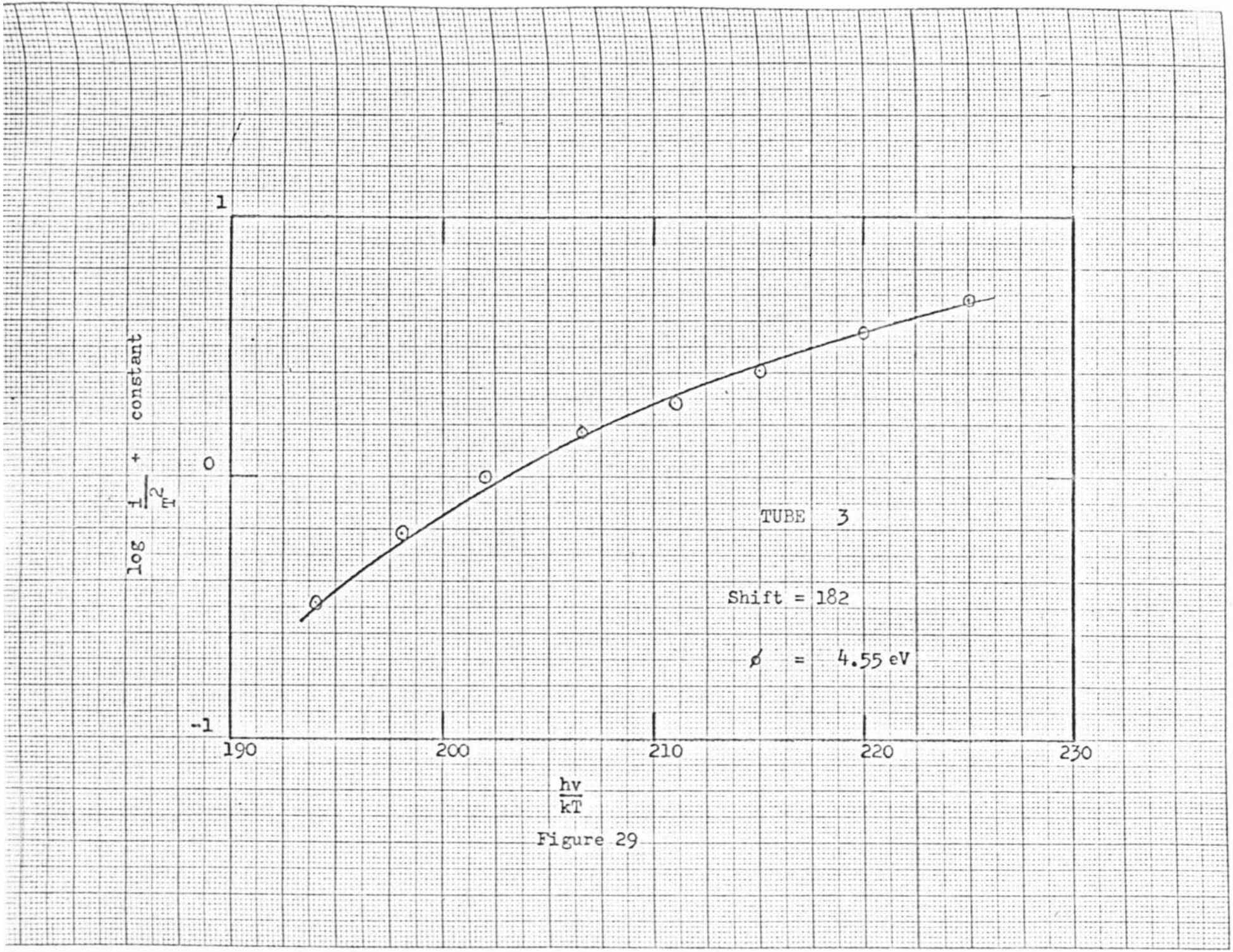
1
0
-1
log $\frac{I}{T^2}$ + constant
190
200
210
220
230
$\frac{h\nu}{kT}$
TUBE 3
Shift = 182
ϕ = 4.55 eV

Figure 29

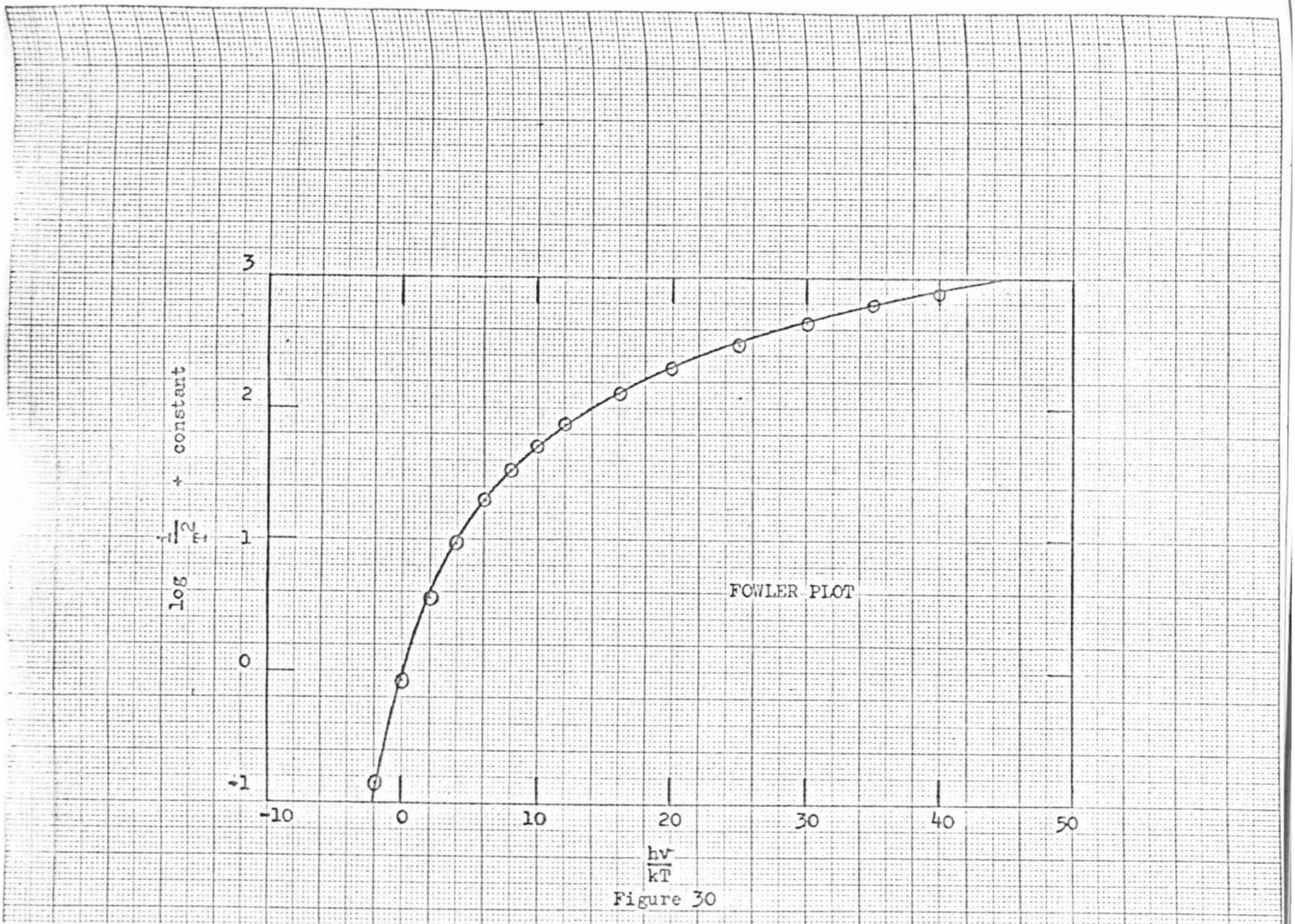
FOWLER PLOT
log $\frac{i}{T^2}$ + constant
3
2
1
0
-1
-10
0
10
20
30
40
50
$\frac{h\nu}{kT}$

Figure 30

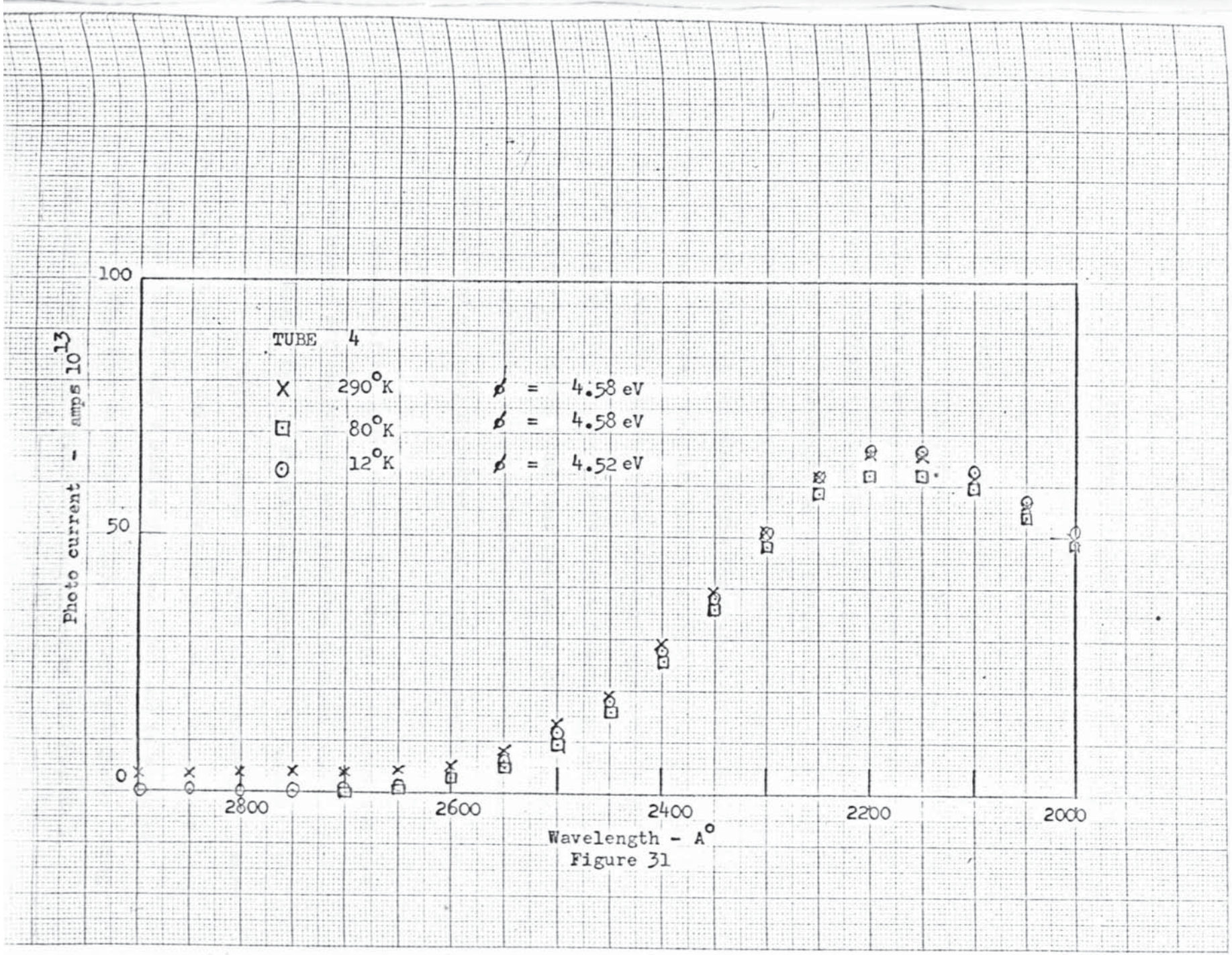
TUBE 4
× 290°K ϕ = 4.58 eV
⊡ 80°K ϕ = 4.58 eV
⊙ 12°K ϕ = 4.52 eV
Photo current - amps 10^-13
100
50
0
2800
2600
2400
2200
2000
Wavelength - A°
Figure 31

and when this is taken into account the threshold wavelength of 2700°A gives the work function of tantalum as 4.58eV. Although this value was considered too high, similar measurements were taken at 80°K using only liquid nitrogen, and also with liquid helium when the block temperature was recorded as 12°K. It can be seen that there is very little difference in these curves. However it is not possible to draw any conclusions from the magnitude of the currents at different wavelengths due to possible changes in source intensity, and small movements of the deuterium lamp or monochromator between each set of measurements. In addition the leakage currents were always found to decrease as the temperature of the block and tube was lowered. However from the results of figure 31 it was possible to detect a shift in the threshold wavelength from 2700 at 290°K to 2750°A at 12°K which corresponds to a work function change from 4.58 to 4.52eV. It was found that the use of different slit widths had very little effect on the resolution of the threshold wavelength and was only effective in altering the magnitude of the photocurrent.

Because of the high value of work function although the tube was now sealed off the cathode was re-heated to about 2000°K, this being 100°K higher than in the initial treatment. A response curve at room temperature is shown in figure 32 which now gave a work function of 4.36eV. Using these values and taking the leakage current as 2×10^{-13} amp, a Fowler plot was drawn and is shown in figure 33. This gave an x-shift of 175, giving $\phi = 4.35$eV. Owing to the fact that the work function was reduced by this treatment,

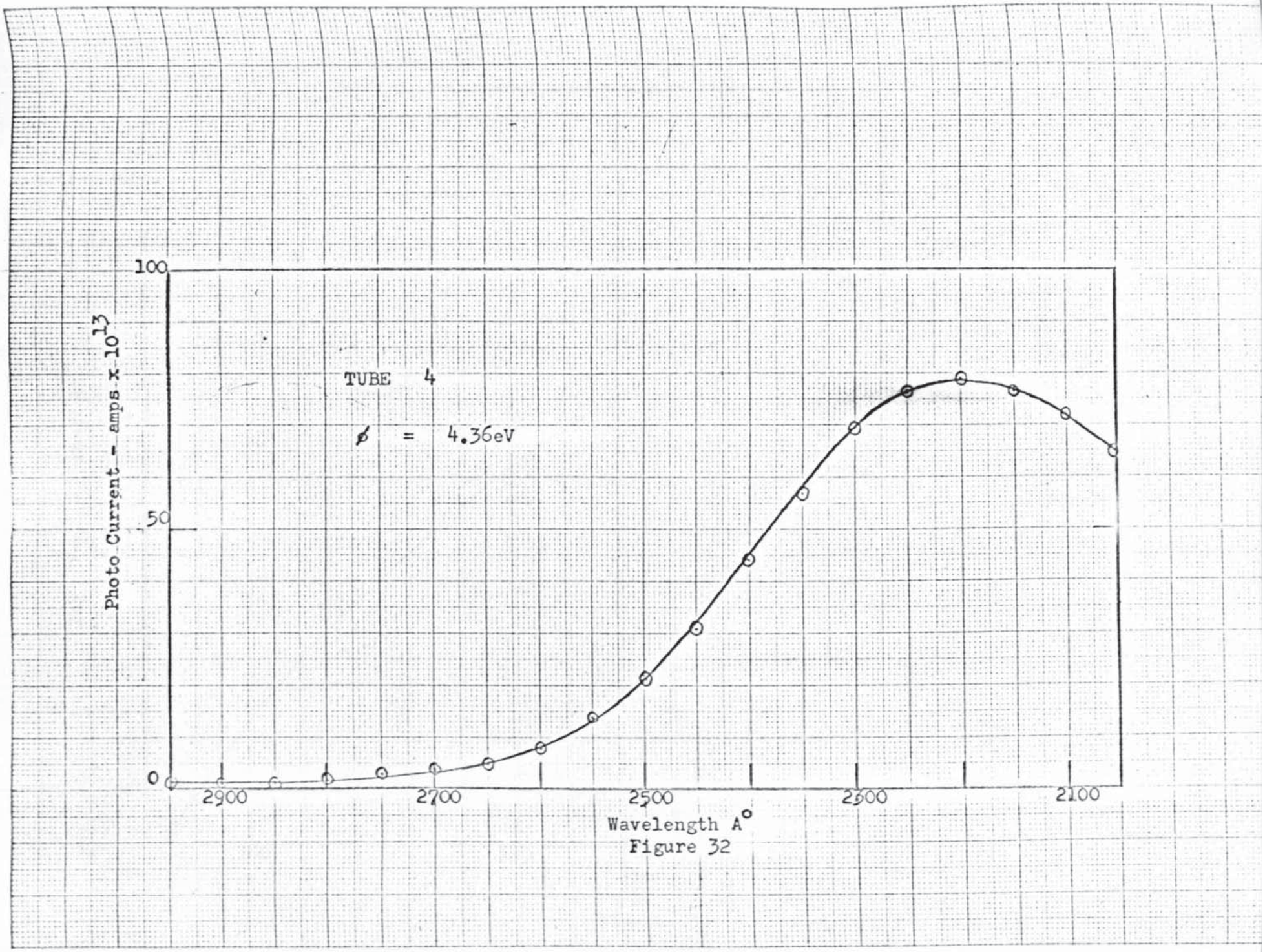
TUBE 4
ϕ = 4.36eV
Photo Current - amps x 10^{13}
100
50
0
2900
2700
2500
2300
2100
Wavelength A°
Figure 32

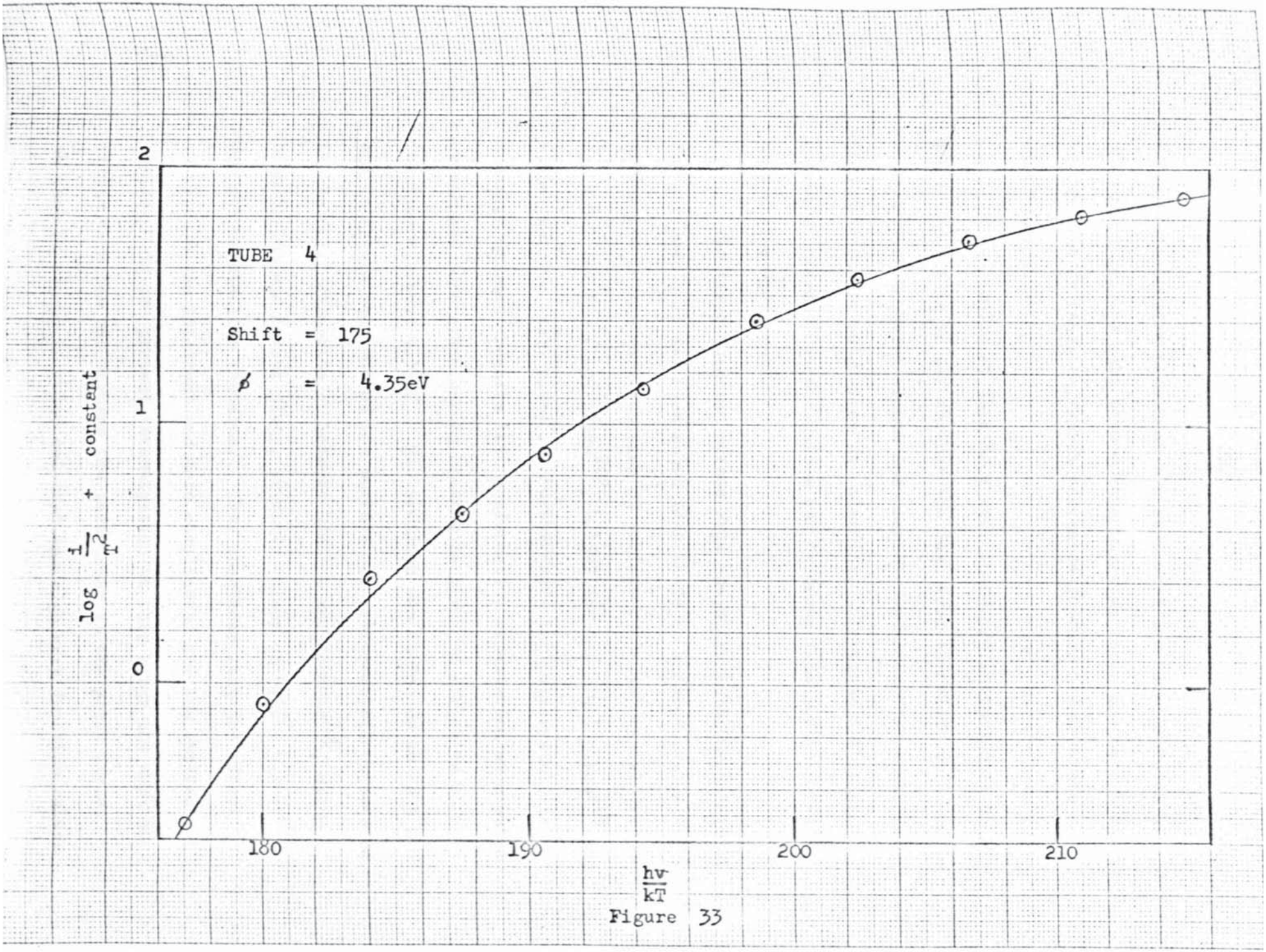
TUBE 4
Shift = 175
ϕ = 4.35eV
log i/i² + constant
2
1
0
180
190
200
210
hν/kT

Figure 33

a further extensive treatment was attempted but this produced a high electrical leakage path between the tungsten leads due to evaporation of tantalum or tungsten, which prevented further measurements on this tube.

The results of this tube were therefore inconclusive as it was not possible to say whether the high work functions were due to the somewhat doubtful vacuum and possibly on account of insufficient high temperature outgassing and cleaning. In these and other respects interesting conclusions can be drawn from published work on tantalum speciments.

The first question arises from the polycrystalline nature of the surface. It has been shown that there is a considerable difference in the work function of various tantalum crystal faces - eg. 4.8eV for the (110) plane[102], 4.15eV for the (100) plane[103] and 4.35eV for the (211) plane[4]. Furtheremore for polycrystalline tantalum Wilson[98] reports that preferential orientation of crystal growth can take place during heating to given an effective work function of about 4.35eV. His specimen was heated up to 2375°K and he showed that 70% of its surface was preferentially orientated in the (211) direction. However Gummick and Juenker[104], using high fields and Fowler plots, obtained values of 4.16 - 4.24eV for polycrystalline tantalum. They concluded that the effect of patches was important and more complicated for low applied fields. In the present investigation at this stage the applied fields were low and perhaps the same order as the patch field, so that it cannot be ruled out that the high work function values

obtained were not due to patchiness of the surface.

The second question arises from the degree of heat treatment of the tantalum.

In a very early paper by Cardwell[105], in which presumably the vacuum conditions were not adequate, he concluded that tantalum could only be completely outgassed by raising the temperature to 2300°K for more than a 1000 hours. He obtained a photoelectric work function of 4.18eV after this treatment but it is difficult to draw any conclusions from this work as there is some confusion in the paper between °K and °C. More recently Klein and Leder[106] report the effect of the solubility of carbon dissolved in tantalum. They found that once dissolved it was not possible to remove it by high temperature treatment even at 2700°K. On the other hand it is possible to remove carbon from tungsten by this method. They further showed that the effect of carbon was to increase the tantalum work function.

The history of the tantalum specimens used in this present investigation was not known, but this might explain the high values of work function found in these earlier tubes. The design of the tube did not however allow the temperature to be raised much above 2000°K.

Finally it can be said that with this tube, even if the surface was not pure clean tantalum, it showed very little change in work function from 290 to 12°K. The measurements indicated a value of $\frac{d\phi}{dT}$ of about 2×10^{-4} eV/ °K.

4.10.4 Tube 5

Tube 5 was of similar construction to tube 4 with no conducting coating on the glass. It was at this stage in the work that some opinions had been formed but not thoroughly tested on the problem of the leakage currents experienced in earlier tubes. Consequently most of the measurements on this tube were made keeping this aspect of the measurements in view. The most significant and conclusive results have already been discussed in Section 4.9. However many other small tests and experiments were made with this tube to bring to light any flaws in the electrical measuring circuit which could be likely to interfere with the measurement of very small D.C. currents. The only likely remaining effect was that due to wall charges. The next tube was made with a conductive coating of liquid bright platinum on the glass.

The photoelectric response in the U.V. for tube 5 was similar to tube 4 giving a threshold of about 2800°A corresponding to a work function of 4.43eV. Because of this similar high value, measurements were not made on this tube at low temperatures in the cryostat. However it should be noted that the sealed-off vacuum in this tube was $< 5 \times 10^{-10}$ torr, so that this seemed to indicate that the high work function values in tubes 4 and 5 were possibly due to the carbon, as mentioned above. The value of 4.43eV for this tube remained stable during the period of investigation.

4.10.5 Tube 6

Tube 6 also had tantalum and tungsten electrodes but small glass discs were incorporated on the tungsten-glass seals to ensure

that no leakage problems occured due to evaporation of tantalum or tungsten. In addition a small moveable glass plate was put into the tube to maintain a clear window for the U.V. if any evaporation took place from the electrodes. The main part of the inside of the envelope was coated with liquid bright platinum which was at anode (earth) potential.

The tantalum strip was bombarded to as high a temperature as possible ($>2000^{\circ}K$) and the limit was finally set by the electrodes bending under their weight. At seal-off ($<3 \times 10^{-10}$torr) the cathode was separated from the anode at its closest point by about 2 m.m.

In this experiment an extra copper radiation shield, maintained at liquid helium temperature, was fitted into the cryostat in order to try and get lower block and tube temperatures. However this was found to be only marginally effective - few $^{\circ}K$ - and considering the difficulties it was not considered worthwhile.

Despite the use of the conducting platinum coating on the glass, it was found that a current still flowed with OV on the anode. This seemed to support the idea of electrolysis in the glass, but once this was understood, even if in only a qualitative way it did not prevent progress. However it did mean that it was not possible to take very steady readings and consequently very good graphs were not obtained.

A photoelectric response curve for this tube is shown in figure 34. It was taken before the tube was mounted in the cryostat, with 22.5v applied to the anode. The currents were

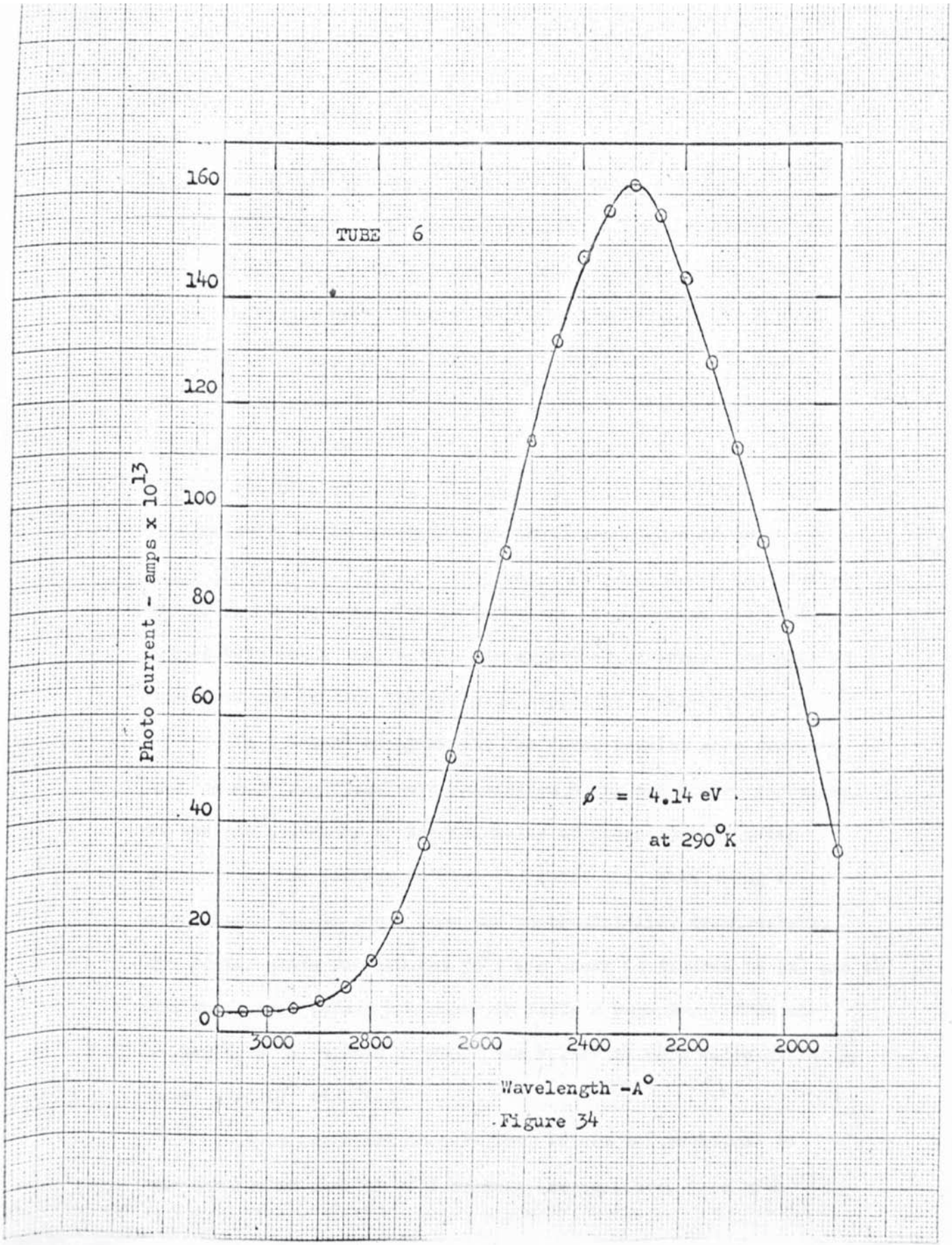
TUBE 6
160
140
120
100
80
60
40
20
0
Photo current - amps x 10^{13}
ϕ = 4.14 eV
at 290°K
3000
2800
2600
2400
2200
2000
Wavelength -A°

Figure 34

somewhat larger than in the previous tube and the work function determined from the threshold wavelength of 3000A° was 4.14eV. This is in better agreement with other published figures,[76,104].

With the tube in the cryostat three response curves were drawn at 290, 90 and 12°K., and are shown in figure 35. The threshold values were taken to be that when the current fell by only 1×10^{-14} amp for an increase in wavelength of the light of 50A°. This reduction was taken relative to the leakage currents which fell to virtually zero at 12°K. These values are equivalent to work function of 4.14, 4.11 and 4.08 eV at 290, 90 and 12°K respectively, which gives a temperature dependence of about $+ 2 \times 10^{-4}$ eV/ °K. It is, of course, not possible to say whether $\frac{d\phi}{dT}$ is linear or not. It is important to note that the room temperature value was, within the experimental error, the same as that produced outside the cryostat soon after seal-off.

In a second experimental run these results were repeated and the work functions were calculated using the Fowler technique. It was now necessary to use the value of photo current after subtracting the leakage current and correcting them using a normalising factor found from the photomultiplier measurements. The Fowler plots for 290 and 90°K are shown in figures 36 (a) and (b) and the actual values are shown in Table 2 page 94. From the x- shift, ϕ = 4.18eV at 290°K and 4.14eV at 90°K which gives $\frac{d\phi}{dT}$ equal 2×10^{-4} eV/ °K.

It is important to note that it was not practical to use the Fowler plot at 12°K because, as expected, this both

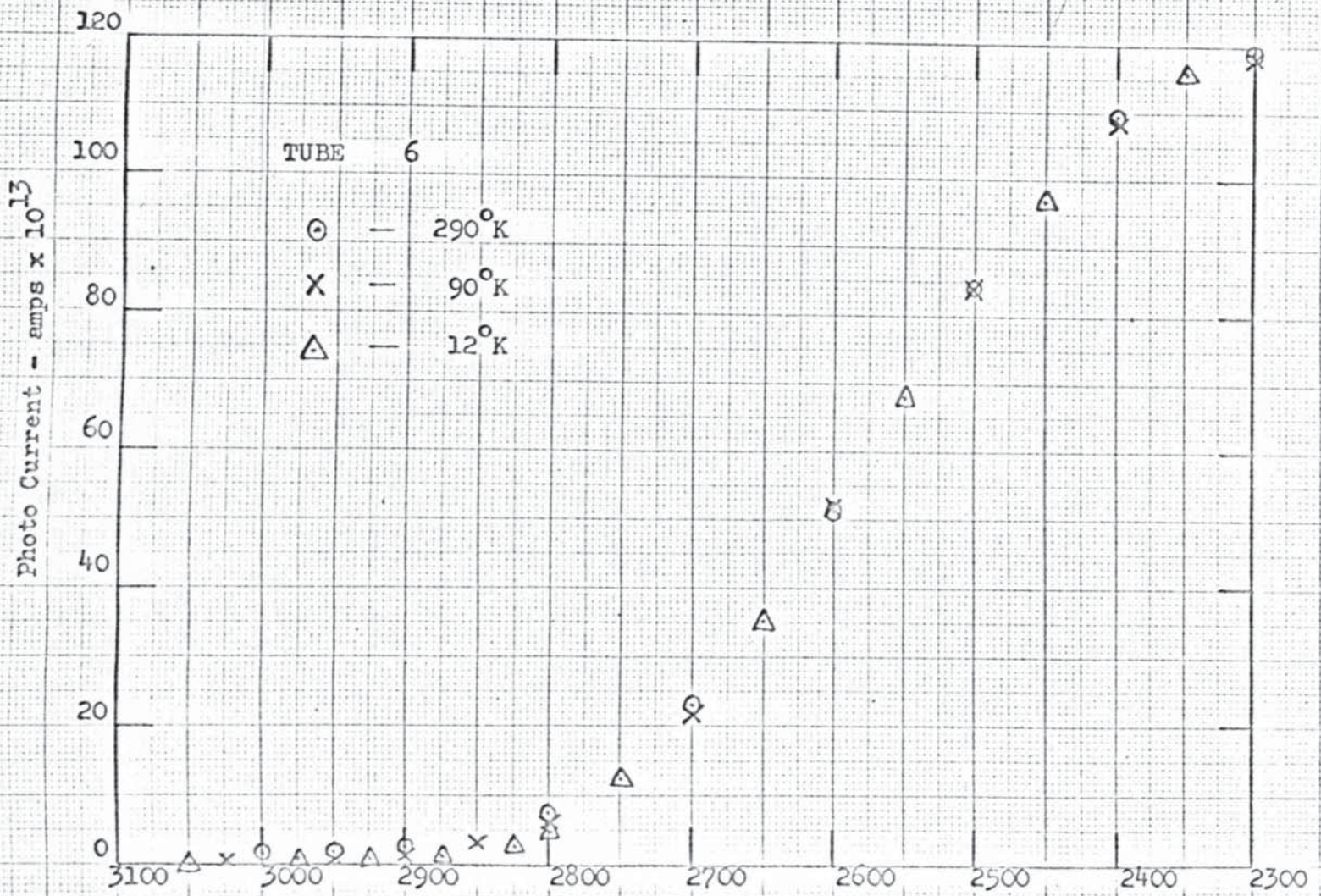
TUBE 6
⊙ — 290°K
X — 90°K
△ — 12°K
Photo Current - amps x 10^{13}
120
100
80
60
40
20
0
3100
3000
2900
2800
2700
2600
2500
2400
2300
Wavelength A°

Figure 35

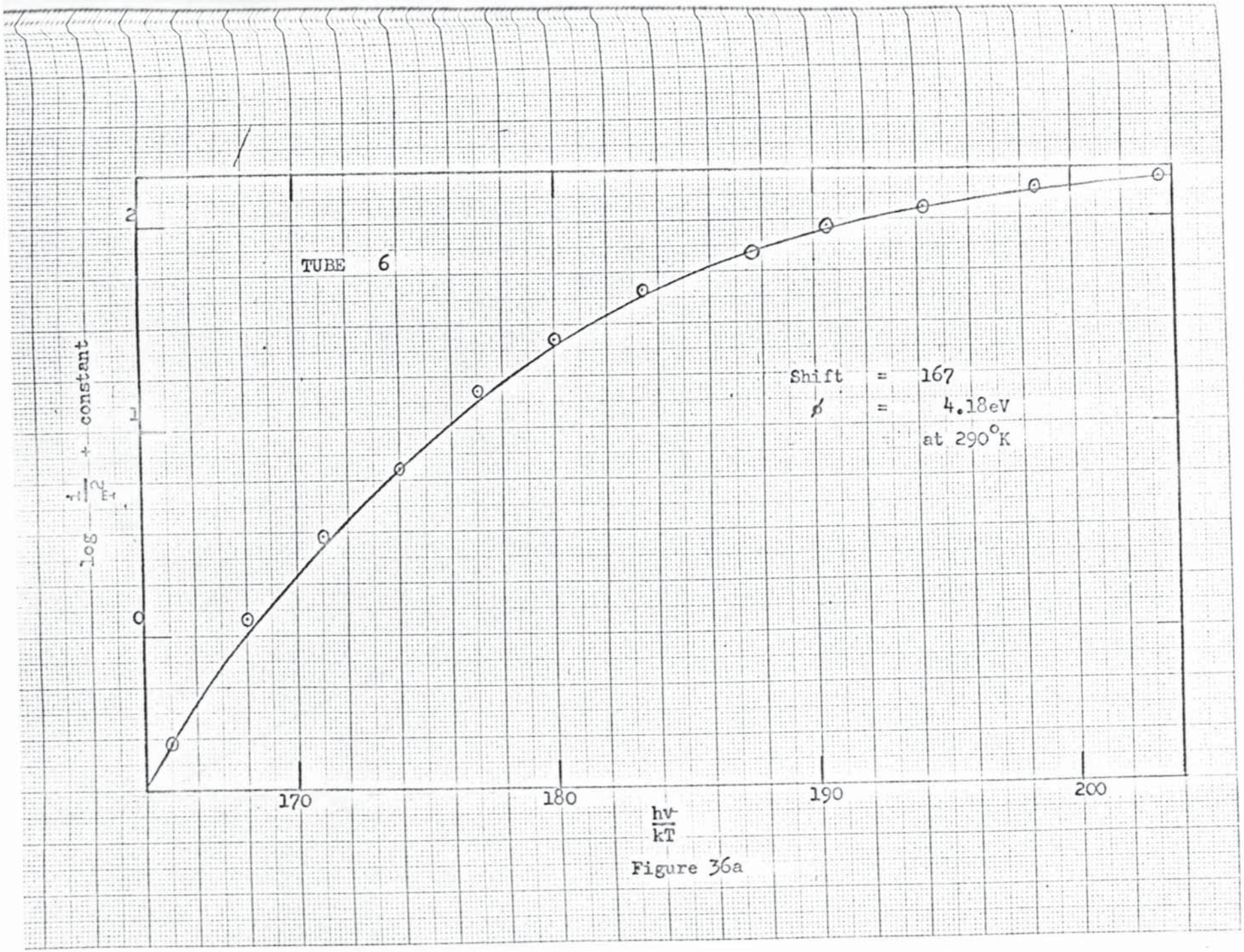
TUBE 6
Shift = 167
ϕ = 4.18eV
at 290°K
log (1/2 + constant)
2
1
0
170
180
190
200
hν/kT

Figure 36a

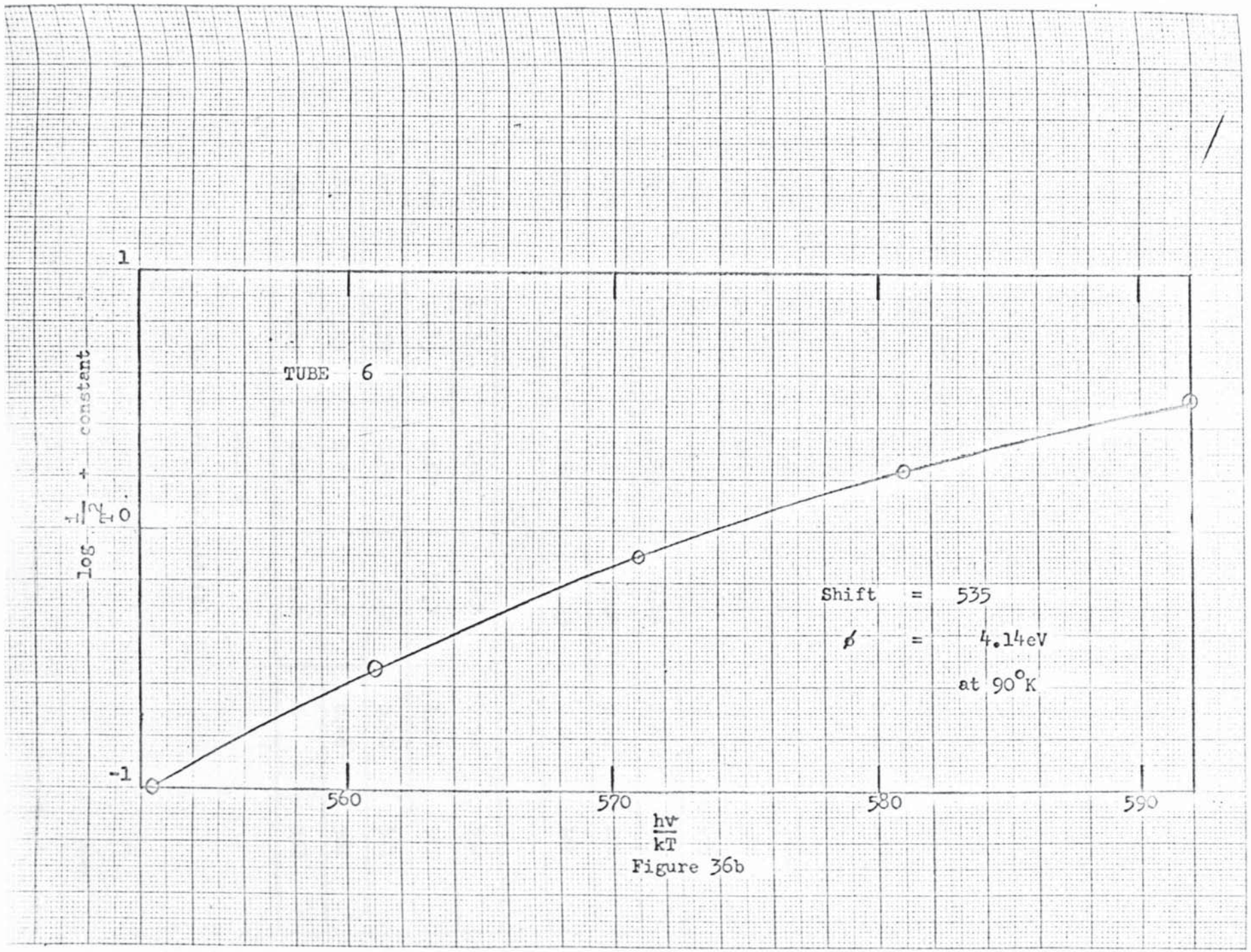
1
0
-1
log $\frac{i}{i_0}$ + constant
TUBE 6
Shift = 535
ϕ = 4.14eV
at 90°K
560
570
580
590
$\frac{h\nu}{kT}$

Figure 36b

Wavelength Å°	Current x 10^{13} amp	Normalising Factor	Corrected Current x 10^{13} amp	log i + CONST.	$\frac{h\nu}{kT}$
			290°K		
2450	127.5	0.79	161.5	2.21	202.5
2500	108.5	0.76	143	2.16	198.3
2550	87.5	0.74	118.2	2.07	194.2
2600	67.5	0.72	93.7	1.97	190.5
2650	48.5	0.70	69.3	1.84	187.5
2700	31.5	0.68	46.3	1.67	183.5
2750	17.5	0.67	26.1	1.42	180
2800	10.0	0.66	15.2	1.18	177
2850	4.2	0.65	6.46	0.81	174
2900	2.0	0.65	3.08	0.49	171
2950	0.8	0.65	1.23	0.09	168
			90°K		
2700	22.3	0.68	32.8	1.52	592
2750	11.85	0.67	17.7	1.25	581
2800	5.15	0.66	7.95	0.90	571
2850	1.95	0.65	3.0	0.48	561
2900	0.65	0.65	1.0	0	552

TABLE 2

for figures 36(a) and (b)

enlarged the scale on the $\frac{h\nu}{kT}$ axis ($\frac{h\nu}{kT}$ is 4000 to 5000) and moved the curve into the less steep region of the standard Fowler curve. It therefore becomes increasingly difficult to determine the shift on the $\frac{h\nu}{kT}$ axis as the temperature is reduced unless accurate knowledge of the absolute magnitude of the currents are known, in order to determine the vertical shift as well. In this investigation this was not possible as the monochromator was not calibrated at the higher intensities used in these experiments. However the accuracy at room temperature is quite satisfactory because the curves can be fitted at the knee. For temperatures greater than 300°K this is even more satisfactory. It is presumably for this reason that the author is unaware of much published work using Fowler plots below room temperature.

It was therefore decided to complete a third run on this tube between room temperature and about 150°K, in which the Fowler plot would be rather more accurate than at 90°K. These two plots are shown in figures37(a) and (b) with the results tabulated in Table 3 page 97 . The shifts give ϕ = 4.18eV at 290°K and ϕ = 4.15eV at 145°K and therefore $\frac{d\phi}{dT}$ = + 2 x 10^{-4} eV/ °K.

The values of $\frac{d\phi}{dT}$ for this tube from both threshold measurements and Fowler plots are in reasonable agreement but the actual values of ϕ differ by about 0.04eV at the same temperature. This is not unreasonable as the threshold measurements are more uncertain in absolute values due to the difficulty of judging the actual threshold value.

The results on this tube and on the earlier tubes

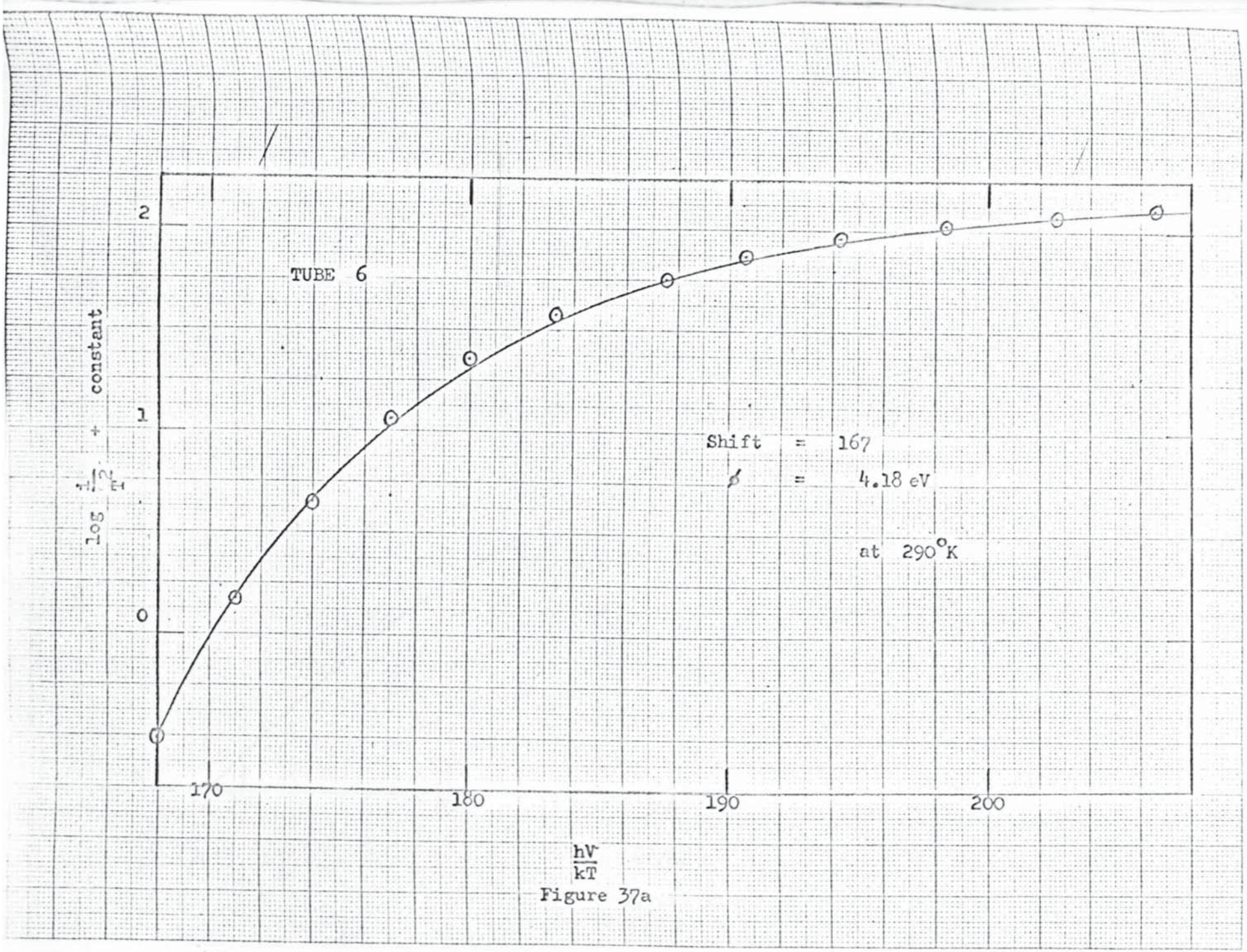
TUBE 6
Shift = 167
ϕ = 4.18 eV
at 290°K
log (i/i+) + constant
2
1
0
170
180
190
200
hν/kT

Figure 37a

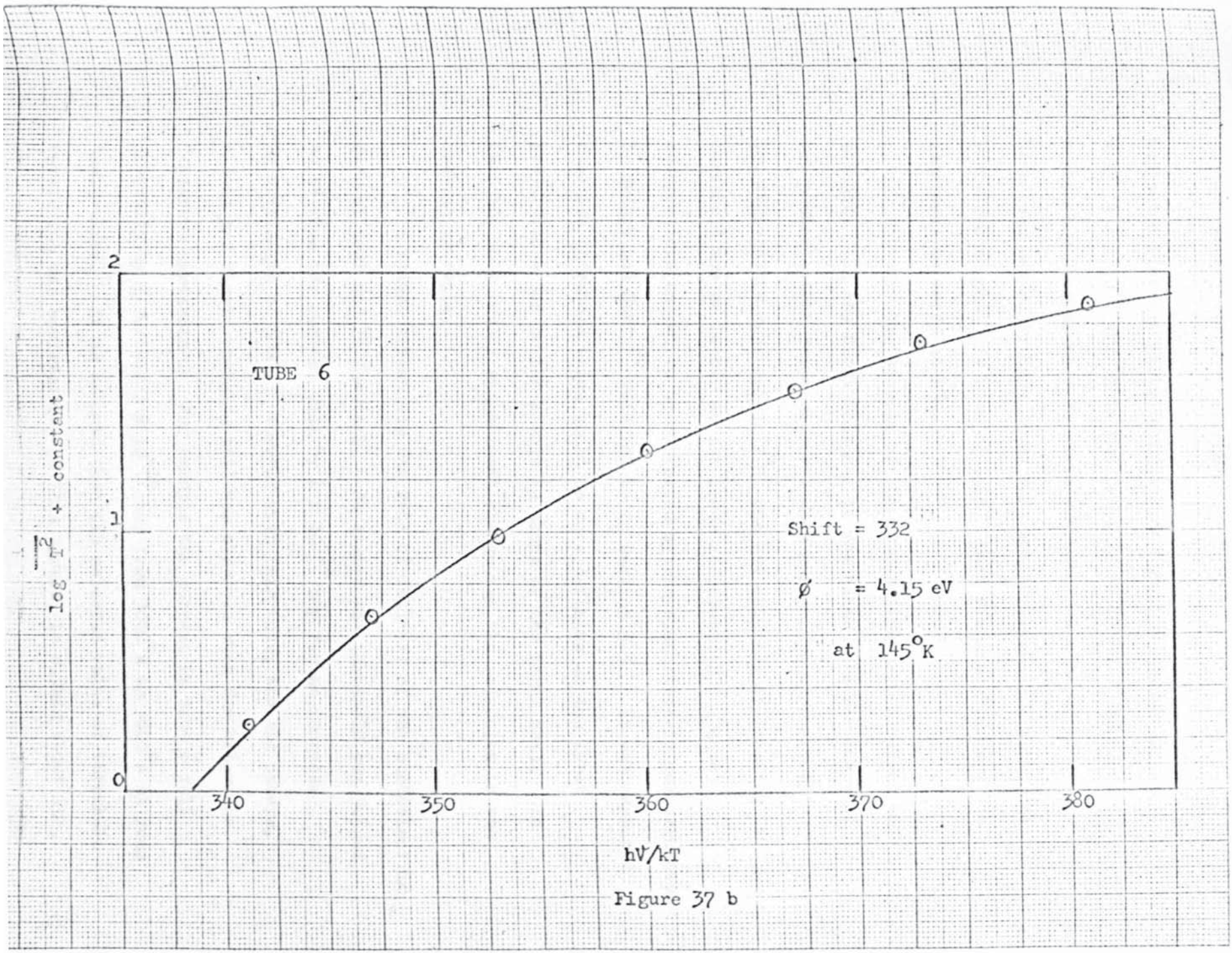
TUBE 6
Shift = 332
ø = 4.15 eV
at 145°K
log (I/I₂ + constant)
2
1
0
340
350
360
370
380
hν/kT

Figure 37 b

indicated that the photoelectric work function changed by about only $+ 2 \times 10^{-4}$ eV/ $^{\circ}$K in the range 12 to 290°K. This is reasonably consistent with other published measurements, which have been generally made above room temperature. This did not therefore support the view of Bull[12] that the work function decreases to zero at 0°K.

However two aspects of the measurements still caused some concern. In the first instance it was clear that the shape of the photoelectric response curve does not change appreciably as the temperature approached 12°K, and the accuracy of locating the threshold was no better at the lower temperatures. These observations appear to be supported by the photoelectric measurements by Bedard and Harte[99] referred to in section 3.3. It was expected that the threshold value would be more definite at the lower temperatures due to the change in shape of the Fermi tail. In fact the only really significant change was the reduction in the leakage currents.

A second aspect was the rate of fall-off of the photoelectric current near and in the tail. As stated the threshold was judged to be when the current fell by 1×10^{-14} amp for an increase in wavelength of 50A$^{\circ}$. However with this tube, and all others, a long and slowly changing tail was observed even far below the "apparent threshold". For example the current in tube 6 fell gradually by a further 3×10^{-14} amp from 3000°A to 3800°A at room temperature. It is assumed that the selected value of threshold wavelength was satisfactory as this agreed, to within about 1%,

Wavelength A°	Current $\times 10^{13}$ amp	Normalising Factor	Corrected Current $\times 10^{13}$ amp	log i + const.	$\frac{h\nu}{kT}$
		$290^{\circ}K$			
2400	105	0.82	128.2	2.11	206.5
2450	95	0.79	120.2	2.08	202.5
2500	84	0.76	110.5	2.04	198.3
2550	70	0.74	94.7	1.98	194.2
2600	54	0.72	75.0	1.88	190.5
2650	39	0.70	55.7	1.75	187.5
2700	25.5	0.68	37.5	1.57	183.5
2750	15.4	0.67	23	1.36	180
2800	7.7	0.66	11.7	1.07	177
2850	2.9	0.65	4.47	0.65	174
2900	1.0	0.65	1.54	0.19	171
2950	0.2	0.65	0.31	$\bar{1}.49$	168
		$145\ ^{\circ}K$			
2600	53	0.72	73.7	1.87	381
2650	38	0.70	54.3	1.73	373
2700	24.5	0.68	35.5	1.55	367
2750	14.5	0.67	21.1	1.32	360
2800	6.45	0.66	9.78	0.99	353
2850	2.85	0.65	4.38	0.64	347
2900	1.15	0.65	1.77	0.25	341

TABLE 3

for figures 37 (a) and (b)

of the value of the work function found using the Fowler technique. These effects were difficult to investigate as the background current was not completely stable but it apparently occurred, but to a lesser extent, even at the lower temperatures. It was therefore decided to investigate this variation of the long tail with wavelength in more detail and the efforts to do this are described in the following section.

4.11 Photoelectric measurements using visible source

4.11.1 Tube 6

It was shown that the long wavelength tail beyond the nominal threshold was not due to scattered U.V. in the monochromator by inserting a glass plate in the emerging light beam. Illuminating the tantalum with an ordinary 60w lamp gave no clear effect, but a slight indication of some photoemission. As a result an optical bench was set up using a 6v, 36w car head lamp bulb, overun at 9v, in conjunction with a good 2½" diameter photographic lens. This optical system enabled a small (2 m.m diameter) bright spot to be projected through the quartz window on the tantalum electrode. With this arrangement a small (1.5×10^{-13} amp) photo current was recorded with 22.5v on the anode. Moving the spot towards and past the edge of the tantalum showed that this effect was due to this light on the electrode and not to the glass. Although the magnitude of this current is similar to that recorded with the monochromator at say 2900°A, it must be realised that with the white light source this intensity is very much higher and the pass band much greater.

A coil carrying 3 amps was then placed around the tail of the cryostat producing a magnetic field of about 0.2 Wb/m^2. The effect of this magnetic field was to reduce the photo current almost to zero, whereas it had no effect on the standing leakage current. This established that the recorded current was in fact electron emission from the tantalum cathode. Furthermore when a dummy tube containing no anode and cathode was illuminated in the above manner, this gave no current. It was also found that with the use of optical filters in the white light beam, a red filter reduced the emission more than a blue one.

All of these measurements were made at room temperature. The photo emission due to visible light was next investigated as a function of temperature. The results of several sets of measurements are shown in figure 38. This shows that as the temperature is increased above room temperature (290°K) to about 325°K (850μV), using heater tapes round the cryostat, the photo current increases. On subsequent cooling the current decreases to a very small value, $< 1 \times 10^{-14}$ amp, before 90°K. No current was measurable as the temperature was reduced even further to about 15°K. Now it is apparent that for this tube an acceptable value of the work function for tantalum has been found using either threshold or Fowler plots, and this value is nearly independent of temperature. The results shown in figure 38 show however a small photo effect which is clearly dependent on the emitter temperature and which occurs at wavelengths noticeably longer than the ordinary or Fowler threshold value.

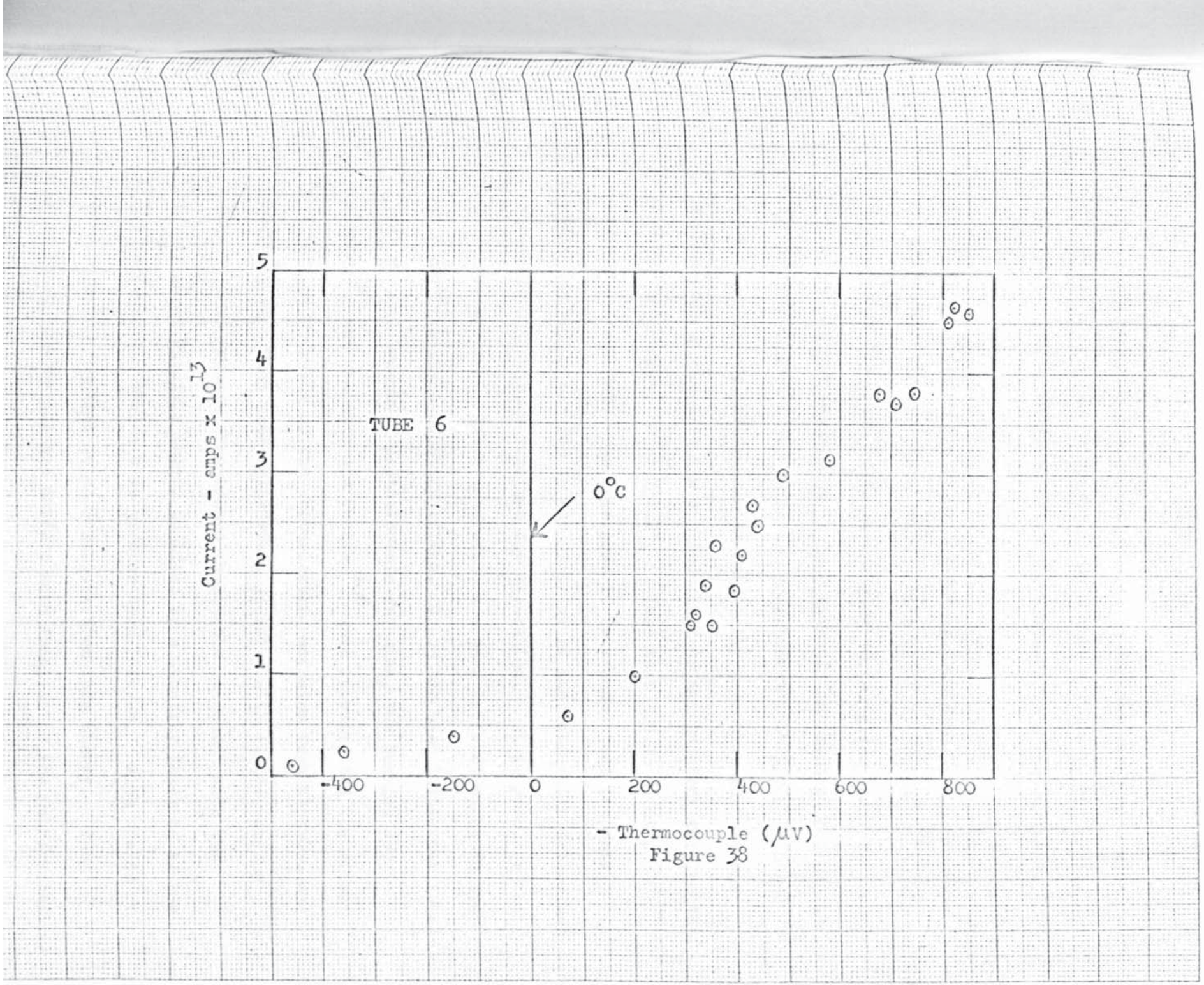
TUBE 6
Current - amps x 10^{-13}
5
4
3
2
1
0
0°C
-400
-200
0
200
400
600
800
- Thermocouple (μV)

Figure 38

All the measurements discussed so far have been made with fixed anode voltages of 22.5V. The effect of varying the applied field was then investigated with the source of visible radiation, figure 39 shows that the photo current increases from about 1×10^{-13} amp to 2.5×10^{-13} amp as the anode voltage is increased from 9 to 360V. On the other hand the photo current with the U.V. source was hardly dependent on the anode voltage. Figure 40 (a) gives the variation between 0 and 40V with the U.V. lamp directly in front of the quartz window and figure 40 (b) using the monochromator at 2300, 2750 and 2900 A°. In the latter case it is clearly seen that the current varies very little with the applied field at all incident wavelengths. However the change, 5% at 2300A°, is less than 20% at 2900A°, between 4.5 and 36V. In this case it is assumed that the main effect is simply one due to the geometry of the tube which determines the necessary voltage required for saturation. It is possible that the small increase, after saturation has been achieved, might be due to a photo electric Schottky effect. There has been little published work on this aspect of photoelectric emission, but Gummick and Juenker[104] and Jaklevic and Juenker[107] have investigated the effect of very high fields on the photoelectric emission from tantalum and molybdenum. They used cylindrical geometry with fields varying from 0 to 90 Kv/cm. They found reasonable agreement with the Fowler photo electric theory modified by a Schottky lowering of the barrier when the fields were greater than 16Kv/cm. With fields less than 16Kv/cm they found departure from this theory. They attributed this to the non uniform work function of the polycrystalline

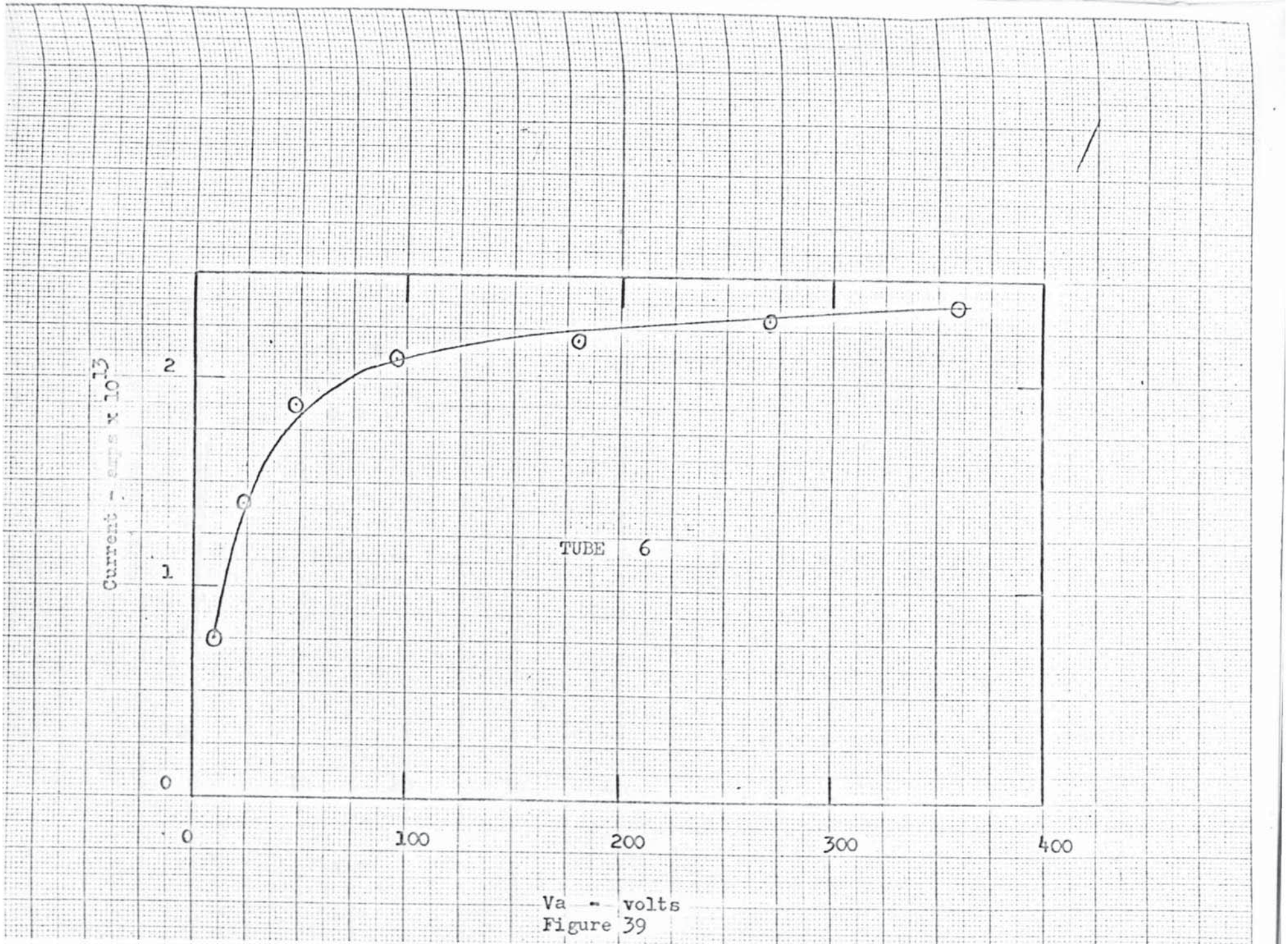

Figure 39

Figure 40a

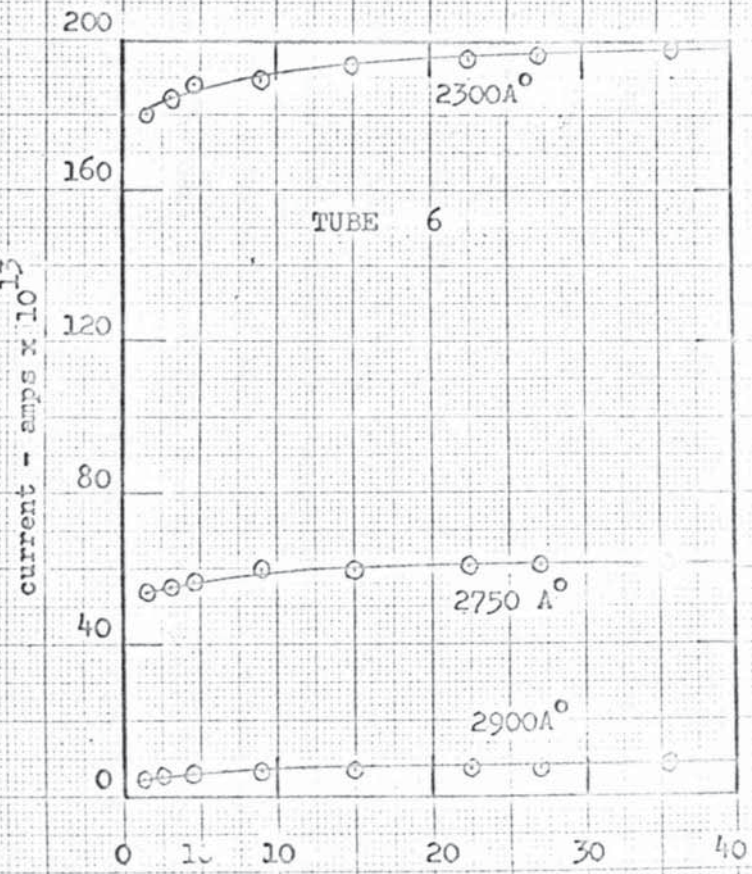

Figure 40b

surfaces. However it is interesting to note that they found no evidence for periodic deviations of the Schottky effect referred to in the thermionic cases in section 1.4.

At this stage in the work it was realised that, although the results showing the effect of field and temperature on the long wavelength tail were very interesting, they could be possibly criticised on the grounds of contamination of the tantalum specimens. Thus further discussion of these results will be left until a later section. The next two sections describe the efforts that have been made to produce further confidence in the results already presented.

4.11.2 Tube 7

Tube 7 had a V-cross section tantalum cathode in order to attempt to reduce the bending produced during heating. However, during processing, the glass insulating tube on the tungsten rod cracked and made it impossible to take photoelectric measurements. The only interesting result from this tube was the fact that the same effect, of the very slowly decaying current at zero anode volts, was found as with previous tubes. This was also despite the use of a conducting platinum coating on the inside of the envelope.

4.11.3 Tube 8

Tube 8 was made with an evaporated gold conducting layer on the inside of the envelope and the vacuum system was modified in order that the tube could be mounted vertically. This eliminated the problem of the bending of the electrodes during

bombardment. However even with this arrangement the electrodes were pulled together by the electrostatic force due to the applied E.H.T. With this tube no current was observed at zero volts after the tube had been baked at 250°C, but before the electrodes were bombarded. This appeared to confirm that the E.H.T. bombardment process was mainly instrumental in producing the electrolysis effect referred to earlier. In order to maintain a clear window for the U.V. an iron slug in glass was used which could be held in position by a magnet during the bombardment.

After sealing off the tube at about 2.5×10^{-10} torr and putting it into the cryostat, the visible light gave a small photo-emission of about 1×10^{-13} amp with Va = 22.5V. During this time the leakage current was falling as expected and it was difficult to take accurate readings. However it was shown that the current increased to about 1.5×10^{-13} amp with the applied voltage increased to 45V.

However during the next few hours this photo current decreased to zero. It was also observed that the photo emission, with the Deuterium lamp placed in front of the tube, also had decreased by a significant amount in this period.

It was therefore suspected that this might be on account of the gradual formation of a layer of adsorbed gas on the tantalum. No definite reasons can be given for this but it may have been caused by a very slow evolution of gas from the glass-sealed iron slug or gold coating.

It was therefore decided to bombard the tantalum at about

1200°K for 15 minutes, which should remove this adsorbed gas, in an attempt to support this conclusion. After heating, the photo current was quite measurable - few x 10^{-13} amp - using the visible light source, even with 22.5V on the anode. However this again decreased in a period of several hours. Further heating enabled the effect to be confirmed, although the magnitude of the currents varied. This could be expected on account of the varying leakage currents. In all cases it was possible to demonstrate that this was electron emission from the cathode. Firstly the current could be cut off by a magnetic field and secondly it also decreased as the light spot was moved away from the electrode. During these clean-up experiments it was also found that the photo-emission from the visible light increased as the applied voltage was increased from 22.5 to 360V. This appeared to increase in a manner similar to that found for tube 6, but it was not possible to take any accurate measurements. On the other hand the emission with the Deuterium lamp saturated at a very low anode voltage of about 6V.

It is reasonable to argue that if the reduction in the emission is due to gas contamination then it is likely that measurements made on the tube soon after clean-up are made when the surface is least contaminated. It is difficult to imagine the reverse to be the case.

The tube was then reheated, but in this case with the copper seal-off tube immersed in liquid nitrogen. The photoemission with the visible light now seemed to decay away rather more slowly. Again this could be expected as the desorped gas from the electrodes

would be expected to adsorb very much more readily on the cooled tip. Therefore readsorption on the tantalum electrode might be expected to be slower.

A final attempt was made to heat the electrodes in position in the cryostat, and using a copper gauge surrounding the complete tube to act as an electrostatic screen. It was hoped therefore to be able to take measurements almost immediately after clean-up. Unfortunately the tube was slightly displaced which cracked one of the tungsten-glass seals.

It can be seen that this particular tube was not very successful, in that the effects produced were unreliable on account of what is now believed to be an inadequate vacuum. However with the measurements that were possible it did show that photo emission observed beyond the normal threshold was field dependent. On account of the uncertainty of these results it was considered necessary to modify the electrical equipment so that measurements could be undertaken on the next tube immediately after clean up with the tube still on the vacuum system at about 2×10^{-10} torr.

4.11.4 Tube 9

It was decided to make this tube without the complication of an internal conducting coating and a glass enclosed iron slug. It has been shown that these modifications did not give any great benefits and may have produced undesirable outgassing effects. The photo cathode was again made from Tantalum sheet but the anode was constructed from 0.25 m.m. tantalum wire. This was done in order to eliminate any possibility of tungsten evaporating

-onto-the-tantalum cathode. The tube was mounted in a vertical position on the vacuum system and the tantalum strip was heated to about 2000°K. This limit was again set by the bending of the electrodes, caused by the electrostatic force at large values of applied E.H.T. In this experiment an electrostatic screen box was built around the tube so that measurements could be made on the vacuum system itself. After the bake-out and cleaning up procedure the optical bench incorporating the tungsten filament lamp and lens was set in position so that the light beam could be focussed on the tantalum cathode through a narrow slot in the screening box. It was usually possible to set up this arrangement within about 10 minutes after switching off the E.H.T. At the recorded pressure of 2×10^{-10} torr the degree of contamination in this time would be negligible.

On account of the leakage current falling continuously after the bombardment, it was not possible to take accurate readings but a photo current was observed and was found to be dependent on the applied field. Two plots taken after successive clean-up operations are shown in figure 41. The shape of the photo current - voltage characteristics are very similar, although the magnitude of the current at a given voltage is not the same. This could be expected as it was virtually impossible to set up the optical arrangement in exactly the same position on each occasion. The photo current could be cut off with a suitable magnetic field.

In addition, the photo current was found to vary as the light spot was moved along the tantalum cathode, and was greatest at the end of the electrode. It is possible that this was due

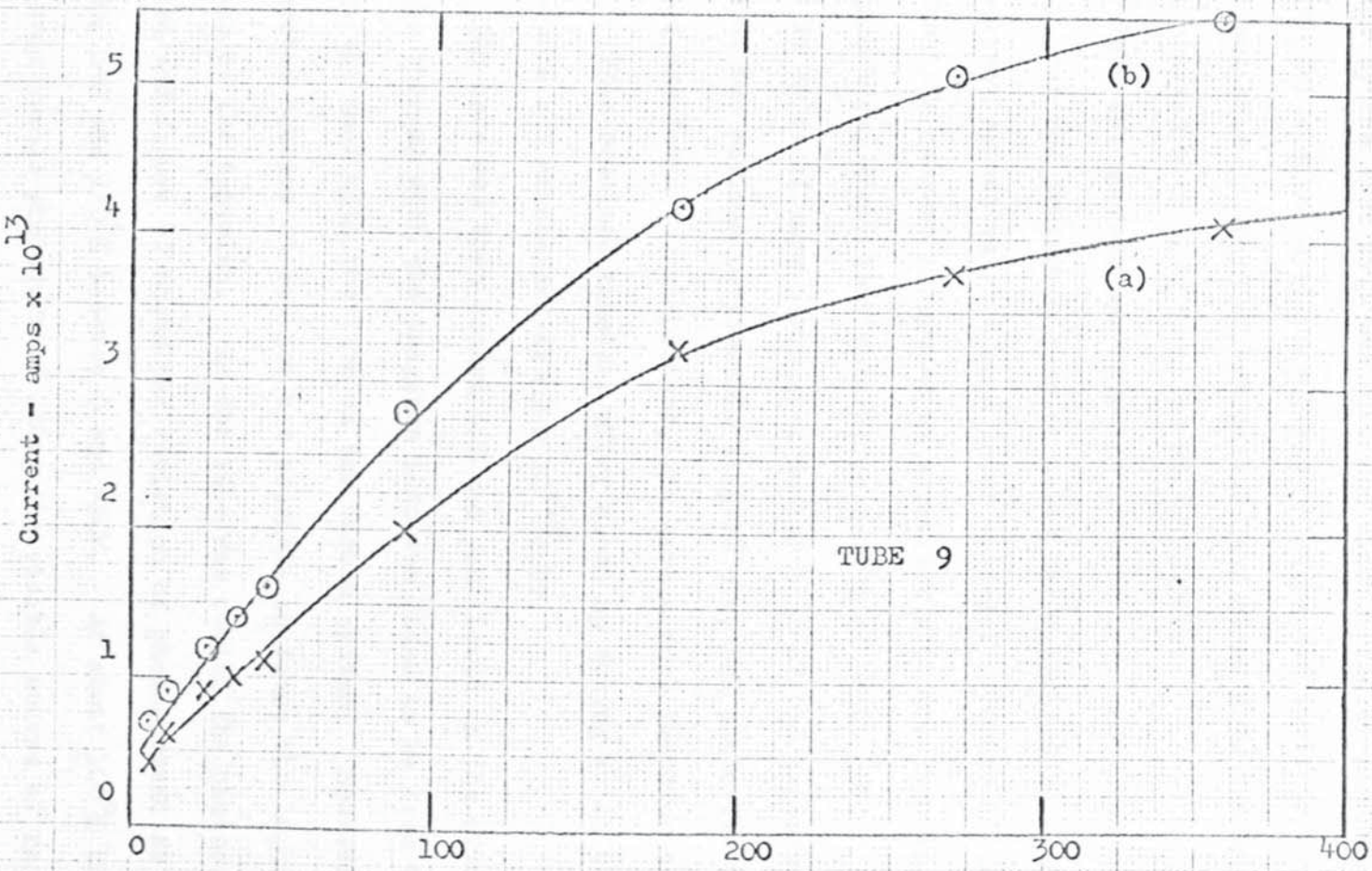

Figure 41

to the patchy nature of the emitting surface. However it could be explained by the fact that the electric field would be higher at the edges for a given applied voltage. It is difficult to be certain but this "patchy" effect seemed less clear when the surface was illuminated with U.V. from the monochromator.

When the surface was illuminated with U.V. radiation either directly from the deuterium lamp or using the monochromator, the photo current saturated at a much lower voltage. Figure 42 (a) shows that the current saturated at about 10V with the lamp direct, and figure 42(b) shows that saturation occurs at about 20V.

In spite of long periods of bombardment of the tantalum cathode at the maximum permissable temperature, the photoelectric threshold was found to be constant, and gave a work function of 4.34eV. This remained constant after clean up during which time the pressure was maintained at $< 2 \times 10^{-10}$ torr.

The tube was then sealed off and positioned in the cryostat. The photo current with the tungsten lamp was found to be less than had been the case with the tube on the vacuum system. However this was expected because it was now not possible to focus the light on all areas of the tantalum. As the tube was cooled the photocurrent decreased and figure 43 shows the variation of photocurrent at 290, 220, 140 and 110°K between 0 and 720V. At about 100°K there was no measureable photocurrent using the visible source of radiation. It is also interesting to see in figure 43 that as the current decreased with falling temperature, there is some indication that the current is saturating at a lower anode voltage. For example

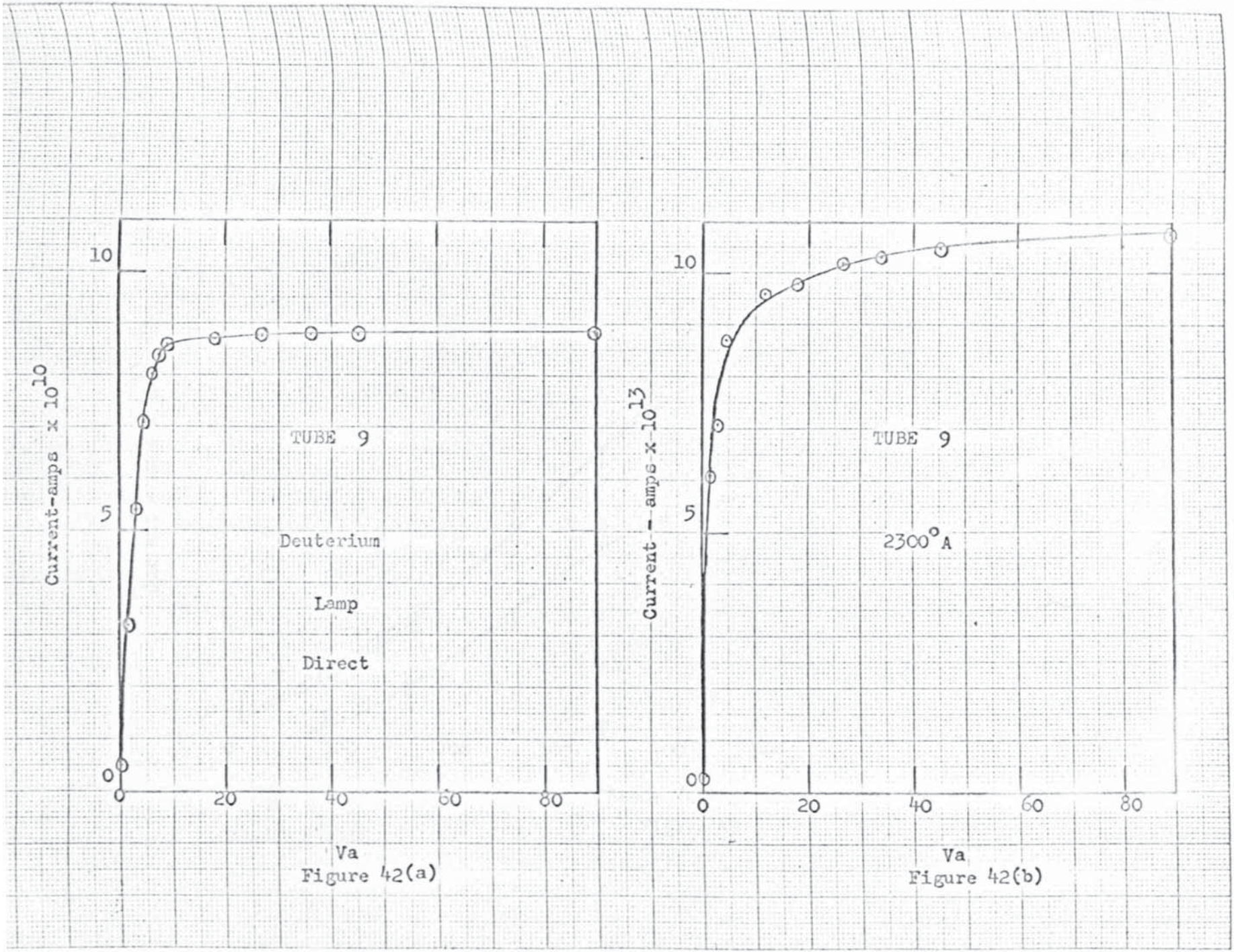

Figure 42(a)

Figure 42(b)

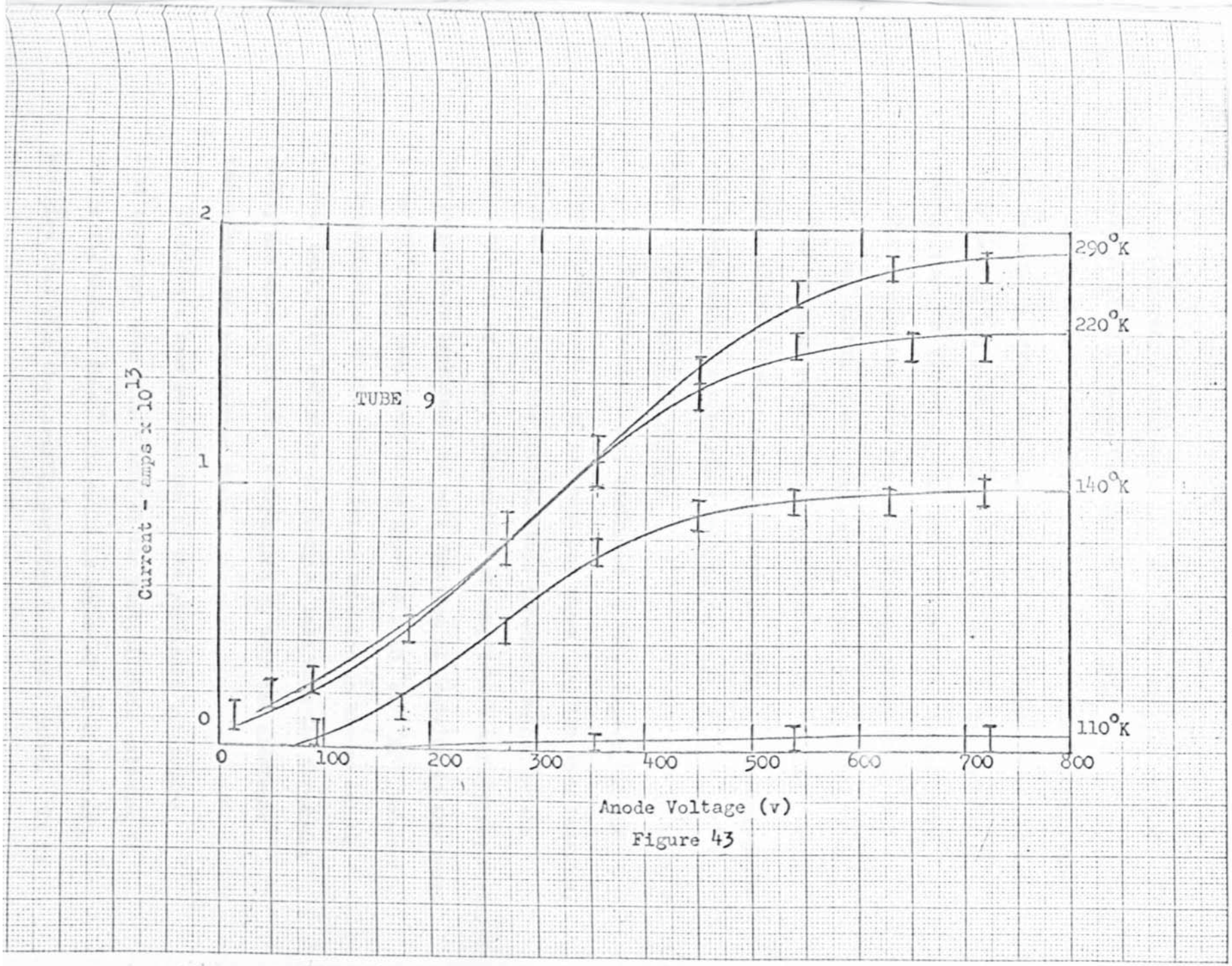
TUBE 9
Current - amps x 10^{13}
2
1
0
0
100
200
300
400
500
600
700
800
290°K
220°K
140°K
110°K
Anode Voltage (v)

Figure 43

at room temperature saturation does not occur until about 750V whereas at 140°K it seems to occur at about 550V.

During these measurements it was found that the photocurrent was reasonably stable over a period of 1 to 2 hours and it did not decay away as had been the case with tube 8. It was therefore assumed that the vacuum in this tube had remained satisfactory.

Furthermore the work function, although rather high, was found to be, within experimental error, unchanged from the value of 4.34eV measured on the vacuum system at 2×10^{-10} torr. This remained constant from room temperature to 100°K. No measurements were taken with this tube below this temperature.

4.12 Discussion of results

Experimental work, described in this chapter, of the photoelectric emission of tantalum has shown that the work function, determined by either the photoelectric threshold method or the Fowler method, is almost independent of temperature and applied field. The temperature dependence of work function of tantalum in the range 12 to 290°K has been found to be about $+2 \times 10^{-4}$ eV/ °K. However an investigation of the photoelectric emission in the so called thermal tail, with radiation of energies less than the threshold value, has shown that this is dependent on both the electrode temperature and the applied field.

It appears from examination of the published literature that there has been little work on the photoelectric emission in the region where a Fermi tail would be expected and at photon energies less than the normally accepted threshold value. It is

possible that in some experiments, the Fermi tail was indistinguishable from leakage currents. However recently there has been an increasing interest in multiphoton photoelectric emission. The two photon-photoelectric effect was predicted theoretically by Smith[108], and he considered this to be possible using optical lasers. This was later shown experimentally by Teich et al[109] for sodium (ϕ = 1.95eV) using a Ga As laser which emitted radiation at 1.48eV. They plotted log (photon current) against log (peak incident power) and observed a curve which had two distinct slopes. At the lower intensities the slope = 1 and was supposed due to the normal single photon effect in the Fermi tail. At higher intensities the slope = 2 and was thought to represent double photon effect. Other 2 photon effects have been reported - e.g. Sonnerberg et al[110] observed it for Cs_3Sb and Imamura et al [111] for alkali antimonides.

In addition Logothetis and Hartman[112] observed what they considered to be a 3 photon photoelectric effect in Gold using a Q - switched ruby laser (photon energy = 1.78eV). However the gold surface was probably contaminated with mercury because its work function was low (ϕ = 4.8eV) (Huber [80]).

With all these experiments it was found that at high intensities the signal was strongly dependent on the laser intensity, which was said to be due to thermionic emission as the laser heated the surface. In this respect it is interesting to note that Ready[113], using a Ruby laser with different surfaces - eg. tungsten - found no evidence for a 2 - photon effect and believed that all the observed emission was thermal in origin. Verber and Adelman[114]

have also shown that a laser can induce thermionic emission from tantalum. They found that with a laser beam of 10^5 W/cm^2 peak power density, this can produce a temperature rise of about 200°K. Furthermore Farkas et al[114] were unable to decide whether the non-linear emission from silver was due to a multiphoton process, thermal emission or a field emission like mechanism, in which the component of the field of the incident radiation for a laser is about 10^7V/cm.

Therefore there is still some doubt as to the existence of a multiphoton photoelectric process. It would be interesting to see if the emission varied as the temperature of the emitting surface was changed in a controlled manner. This might help to distinguish between genuine multiphoton processes and thermal effects.

However although a multiphoton process may take place when a laser is used as the source of radiation, it seems most unlikely that this could occur with the sources of radiation used in this present work, which are of incomparably smaller intensity.

The effects of applied fields on the photoelectric emission from metals has already been referred to in section 4.11.1 but all of this work was with very high fields. Crowe and Gumnick[116] have reported enhancement of the photoelectric quantum efficiency in the near I.R for $CsNa_2KSb_4$ cathodes, using applied fields of about 10^4V/cm. They believe the enhancement arises primarily from a lowering of the potential barrier found at the vacuum interface of the photocathode. The gain in emission with the higher fields produced a maximum in the I.R. and they explained this as being due to emission from impurity levels in the forbidden region, since

these electrons will have higher average energy at the vacuum surface than electrons from the valence band. Comparison between results from such a complex cathode with those obtained from a clean metal would be of dubious significance.

Recently Hussain and Walsh[117] reported a photo-field effect in which the field emission from a CdS single crystal was enhanced when illuminated with an Argon ion laser. This combination of high fields and high illuminating intensities is very different from the relatively very low fields and intensities used in the present work.

Thus explanations of the observed phenomena with tantalum cannot be accounted for by the results of the foregoing discussion. On the other hand some explanation can be put forward if we consider again the model of the work function described by Bull[12]. It is necessary to recall that this model is based on the idea that the work function is due to the potential barrier set up at the surface by the thermal diffusion of electrons. This effect was given by Herring and Nichols[18] but they considered it to be negligible. It is now clear that Bull was more concerned with the work function from a thermionic point of view and with the effect of the emitter temperature and applied field. He did not consider the photoelectric work function as such.

From the results of this investigation it now seems probable that the work function must be considered in two parts. Firstly the bulk or volume work function in which the non-isotropic state near the surface is neglected. In this case it is expected that the work function of a metal will be almost independent of the applied field

as the field is unable to penetrate the metal to any significant extent. However this may be more important with complex emitters such as oxide cathodes. Similarly the effect of temperature should be small as the Fermi level is also almost independent of changes in temperature. Hence the temperature variation of the bulk work function, as observed in this present work with tantalum, will vary probably as a consequence of the principal thermal expansion effect discussed earlier in section 3.1. These results with clean tantalum have shown that $\frac{d\phi}{dT}$ is about $+2 \times 10^{-4}$ eV/ ^{o}K and that the effect of increasing the applied field to about 1000 V/cm has only a small influence on the photoelectric current.

The second part of the work function is associated, not with the volume, but with the surface. Now this seems more appropriate to the theory of Bull[12] in which he shows that the surface work function, arising from the potential barrier due to the space charge of thermal emitted electrons, varies with both the field and temperature. These ideas of a volume and surface work function have been previously reported in the literature - eg. Sommer and Spicer[118] - but the surface effect has not been considered in the same manner as that of Bull.

The work with the clean tantalum in which the surface was illuminated with visible light at energies less than the measured threshold value does, in fact, show that the photoelectric emission depends on both the emitter temperature and the applied field. That is, as the field increases, the potential barrier, which emerging electrons must overcome, is reduced. On the other hand as the

temperature is reduced there are less electrons which have thermally diffused to the surface, so that the photocurrent also decreases. Now we cannot think of this work function in the normal sense, but only of the photocurrent itself. In fact no attempt has yet been made to calculate the variation in magnitude of this photocurrent. In this respect Bull's assumption that the electrons moving near the surface have the same range of available energies as those in the interior is inaccurate and inadequate, since new integrals are required to work it out. This would not, however, change the nature of the result, and Bull's present theory gives something of the form of the variation. It can now be seen that his original hypothesis , that the work function goes to zero at $0^{\circ}K$ is not incorrect, if we think of the surface work function in this way. However it does mean that the energy required to liberate an electron at these temperatures is very small, but because the number of available electrons for emission is also small, the probability of such emission is also small. At $0^{\circ}K$ there will be none available for emission.

It is appreciated that in the present work the actual bulk work functions were something higher than expected. It is thought that this was due to the inability to remove the dissolved carbon. However the work function remained stable during measurements on each tube - except tube 8 - over the range of temperature investigated, and it is not thought that this affected the results in any other way.

Chapter 5.

Photoelectric emission from oxide coated cathodes

5.1 Introduction

The earlier work on total emission measurements described in Chapter 2 was with oxide coated cathodes. It was partly as a result of this work that the result was inferred that the work function would be zero at $0^{\circ}K$. It was therefore thought necessary to make measurements of the photoelectric work function of oxide coated cathodes over a similar temperature range and using the same experimental techniques as have been described in Chapter 4 for tantalum. It was realised that the interpretation of the results from such a composite cathode would be much more difficult, but it was hoped that it would give some additional insight into the problem.

The experimental tubes were very similar in construction to those using tantalum cathodes. The oxide cathode, of the type used in PL81 valves, and kindly supplied by Mullards Ltd., was made from mixed alkaline earth carbonates, which had been sprayed onto a nickel box-shaped base. The cathode was heated indirectly by an insulated heater supported inside the nickel box, and one end of the heater was connected to the cathode itself.

The carbonates were converted into the oxides, and the cathode activated, by gradually raising the filament temperature and anode voltage over a period of several days. Eventually with 30v on the filament, 0.36amp filament current and 400v on the anode, this gave an emission of about 8m/a. During this time the anode was outgassed by electron bombardment from the cathode. This condition was finally achieved whilst the whole system was being baked at 250°C. After the oven was removed, but with the cathode and anode still hot, the pressure was recorded as about 2×10^{-10}torr.

5.2 Tube 10

The voltage - current characteristics of the diode were as expected. However the retarding, saturated and space charge regions were not well defined as was the case with the EB91's, because the anode-cathode spacing was very much larger. It was therefore not possible to estimate any total emission values by the extrapolation method described in Chapter 2. Furthermore it was found that with this tube no measureable current flowed at Ov. This supported the view that electrolysis in the glass observed in the tubes already described was mainly caused by the E.H.T. bombardment process.

The initial photoelectric measurements were done with the tube on the vacuum system. However it was necessary to take extreme precautions to shield the cathode from any stray illumination, because the cathode was, as expected, sensitive to visible light.

A spectral response curve, taken at room temperature at a pressure of 2×10^{-10}torr and with Va = 45v, between 4000 and

10,000A° is given in figure 44. The photocurrents are the actual measured currents after subtraction of the leakage current. The currents cannot be regarded as being proportional to the quantum efficiencies at all wavelengths because the source and monochromator was not calibrated at the longer wavelengths. However the curve shows a long wavelength tail between 8000 and 10,000A°. No measurements could be taken above 10,000A° because the monochromator drum was not calibrated above this value. However a current was just detectable with the monochromator drum set at an estimated 12,000A°. If the value of 10,000A° can be regarded as a threshold value this is equivalent to an energy of 1.25eV which is typical of the value for the thermionic work function of an oxide cathode. Fowler plots are sometimes quoted for complex cathodes but it is unlikely that such a plot has much significance except when used for pure metals. The figure also shows three peaks at 7300, 6500, 5830 and 4830A° which are equivalent to 1.7, 1.91, 2.13 and 2.57eV respectively. Comments on these will be made in the discussion in section 5.4

Figure 45 shows the photocurrents at 4000 and 8000A° plotted as a function of the applied anode voltage between 0 and 45v. This does show that the current at the longer wavelength is more field dependent. However this effect is probably less significant than with a metallic emitter as it is expected that the field will penetrate the oxide cathode.

The temperature of the oxide cathode was then raised slightly, using a Solatron stabilised power supply for the cathode

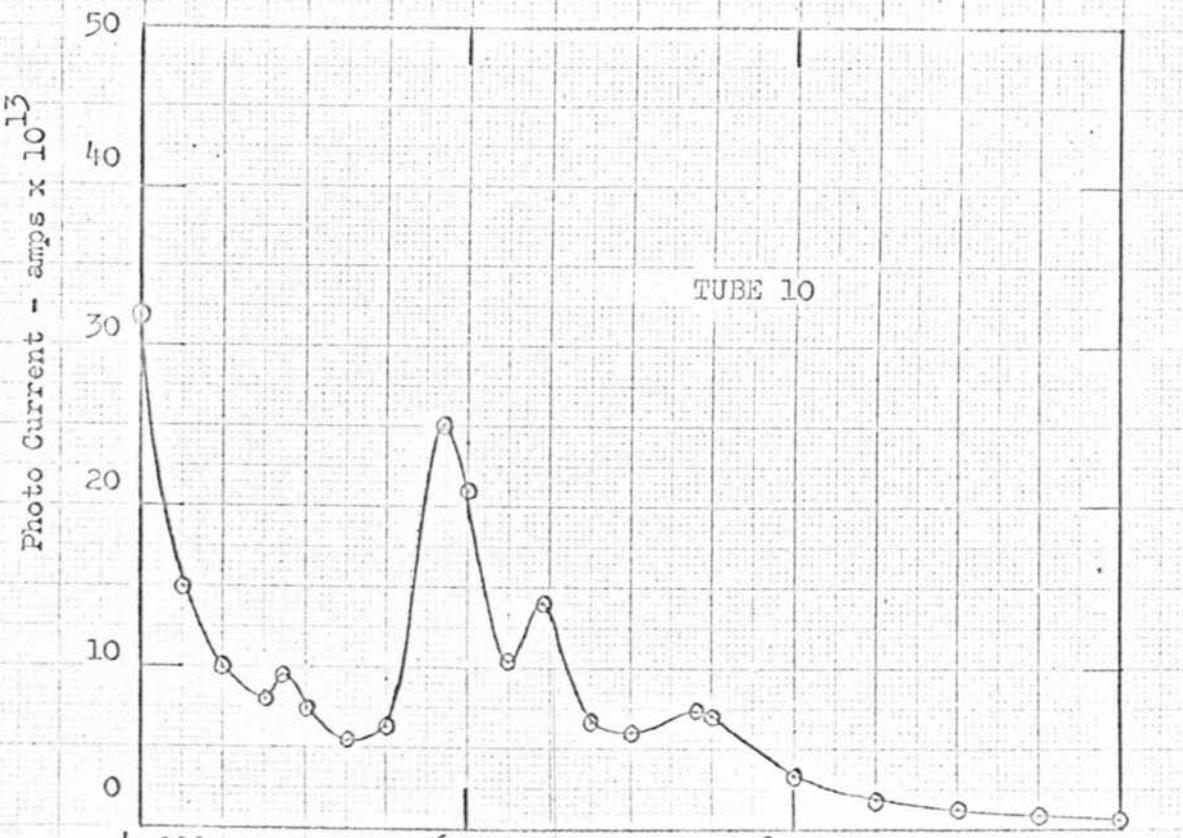
50
40
30
20
10
0
Photo Current - amps x 10^{13}
TUBE 10
4,000
6,000
8,000
10,000
Wavelength A°

Figure 44

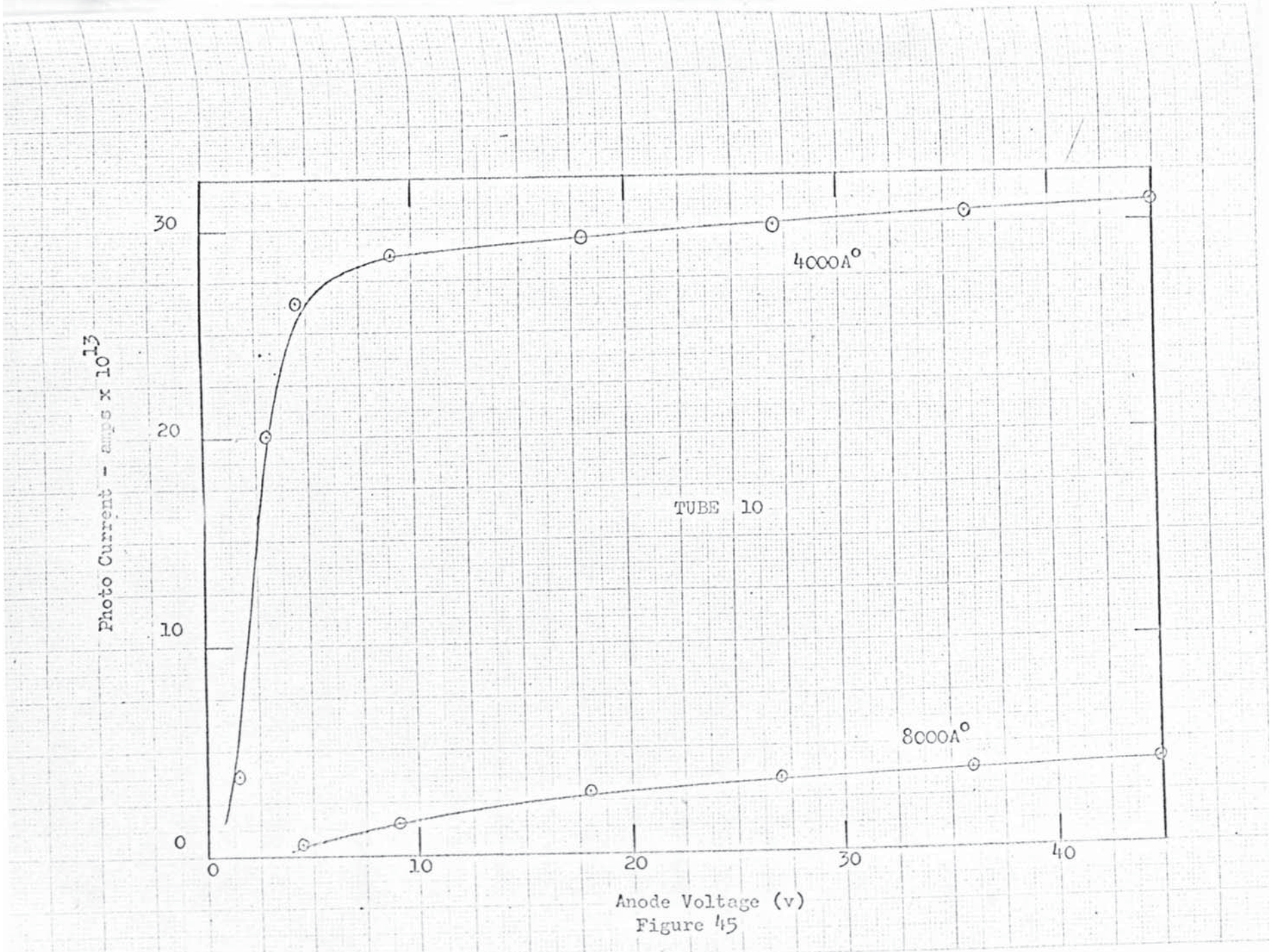
Photo Current - amps x 10^{13}
30
20
10
0
4000A°
8000A°
TUBE 10
0
10
20
30
40
Anode Voltage (v)

Figure 45

heater. With no illumination on the cathode and Va = 45v, the heater was gradually increased until the leakage current increased by about 5×10^{-14} amp. It is thought this increase in current was mainly thermionic emission, although the true leakage current may have also increased due to a change in the conductivity of the glass. The actual cathode temperature could not be measured but as the normal operating filament voltage for this cathode is 20v, it is expected that the cathode temperature was probably less than 50°C above room temperature. The photoelectric response of the cathode for the filament at 0, 0.9, 1.1, 1.3, and 1.5v was recorded and in each case allowance was made for the leakage current. These results are shown in Table 4. The most interesting regions are in the long and short wavelength regions. The effect of the change of cathode temperature in the intermediate region between 4500 and 7000A° was very little. The photocurrents at the short and long wavelength region are shown in figure 46. It can be seen that the currents between 7000 and 10,000A° increase as the filament temperature increases, whereas they decrease between 3500 and 4500A°. The experimental tube was then sealed off from the vacuum system and photoelectric measurements were made in the cryostat. The photoelectric response was very similar to that observed in the vacuum system. Exact comparison should not be expected due to the change in illuminating intensity and the particular area of cathode illuminated - Stanier and Mee[119] have shown that the photoelectric work function of a barium oxide cathode may vary by about 0.15eV across its surface. However when the cryostat was cooled the photocurrents between 7000 and 10,000A°

Wavelength -A°-	Photocurrent - amps x 10^{13}				
	Filament Voltage - V_f				
	0	0.9	1.1	1.3	1.5
3500	84.8	81.0	77.2	75.3	73
4000	33.8	32.2	32	31	29
4500	10.8	11	11.2	11	11
4850	9.8	9.5	9.8	10	10
5000	7.8	7.7	8	8.4	8
5500	6.8	7	7.2	7.4	7
5850	25.8	26	26.2	26	26
6000	21.8	22	22.2	22	22
6450	14.8	15	15.6	15.3	15
7000	6.3	6.7	7	7	7
7450	7.8	8	8.6	8.6	8.7
8000	3.9	4.2	4.4	4.8	5
9000	1.8	2	2.4	2.6	3
10000	0.7	0.8	1.2	1.3	1.4

TABLE 4
Reference to Figure 46

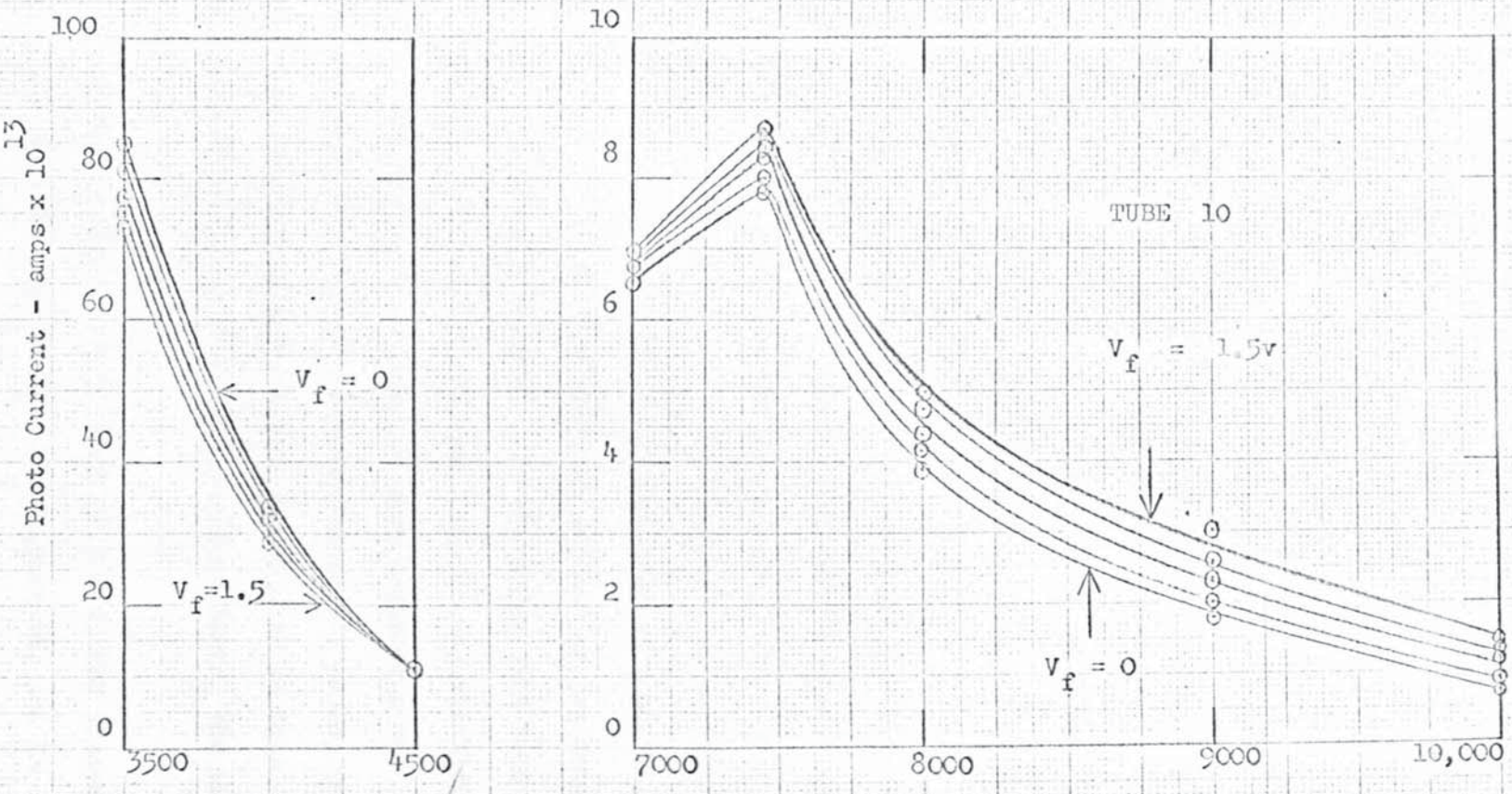
100
80
60
40
20
0
Photo Current - amps x 10^{13}
V_f = 0
V_f=1.5
3500
4500
10
8
6
4
2
0
TUBE 10
V_f = 1.5v
V_f = 0
7000
8000
9000
10,000
Wavelength A°

Figure 46

gradually fell and at about 100°K there was no measurable current at 10,000A°. With a much higher anode voltage of 360v, a small detectable current was observed. Figure 47 shows the change of photocurrent between 7000 and 10,000A° for four cathode temperatures of 290, 240, 180 and 95°K. There was some change in the current between 3500 and 4500A° but this was much less noticeable.

Over the whole temperature range investigated from above room temperature to 80°K, the positions of the peaks appeared, within the experimental error of ± 25A°, to be constant.

The results of the photoelectric measurements with this tube were very reproducible but it was considered necessary to repeat these measurements on a second experimental tube.

5.3 Tube 11

This tube was constructed and processed in a similar manner to Tube 10, but it was noticeable that the surface of the oxide coating appeared to be considerably rougher. Furthermore, with this tube a small "polarisation effect" was observed, but the current flowing with Va = 0v was in the opposite direction to that found with the tantalum tubes. If this was also due to polarisation in the glass, then this direction of current flow was to be expected as in this case the photoelectric cathode had been made negative during the bombardment process.

A spectral response curve taken on the vacuum system at room temperature with Va = 45v is given in figure 48, and is similar to that found for Tube 10. However the long wavelength tail decreases rather more quickly and only one clearly defined peak, again at 5830A°,

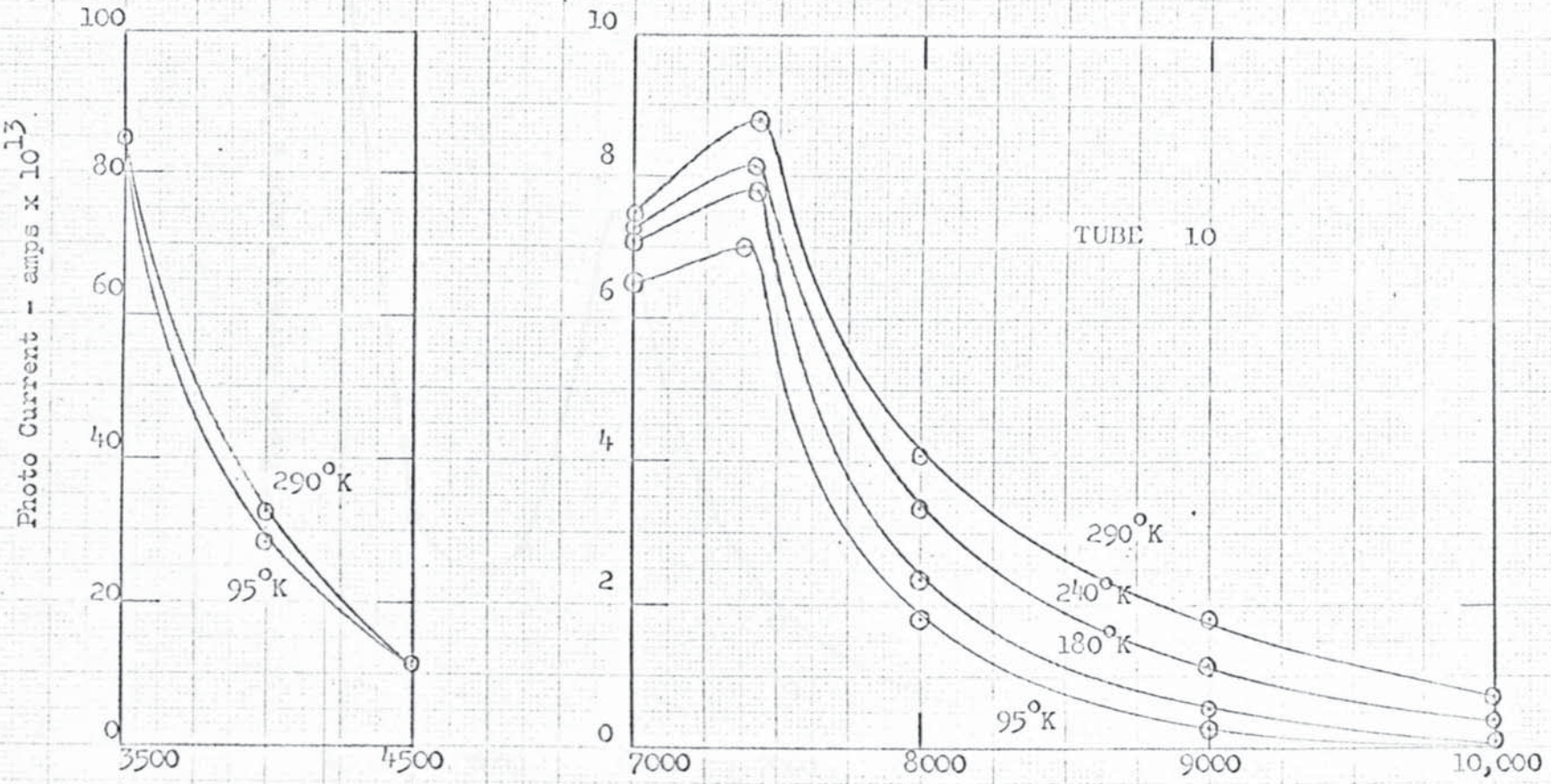

Wavelength A°

Figure 47

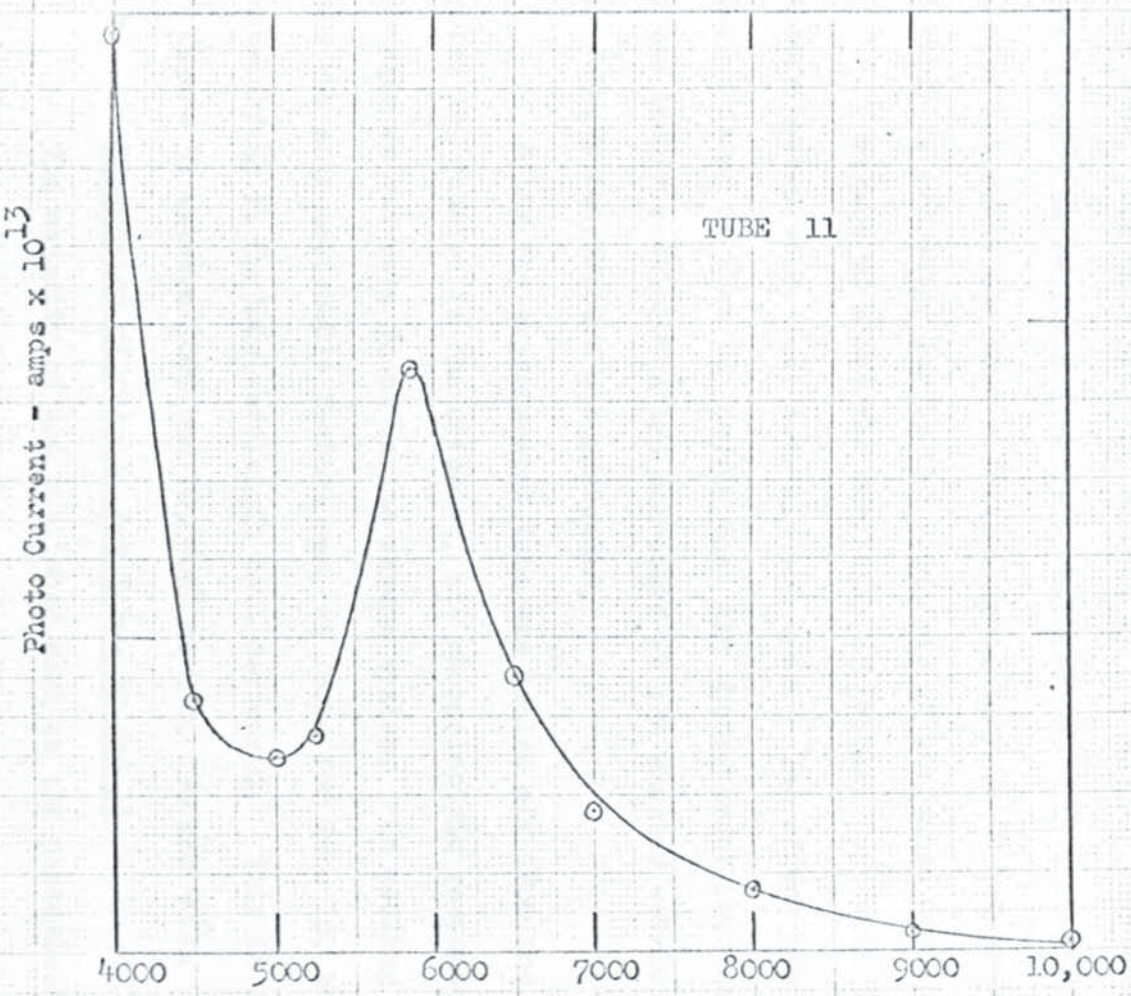
TUBE 11
Photo Current - amps x 10^{13}
4000
5000
6000
7000
8000
9000
10,000
Wavelength A°

Figure 48

can be seen. A second, but not very pronounced, peak at 7200A° was also observed. Figure 49 shows the photocurrent at 4000 and 8000A° plotted as a function of the applied anode voltage between 0 and 630v. In this case the current at the shorter wavelength also appears to be field dependent, but less so than that at 8000A°. This is not quite the same effect as found in Tube 10 but could possibly be accounted for by the roughness of the oxide coating.

Figure 50 shows the variation of photocurrent with the cathode heater at 0, 1.2, 1.4, 1.5 and 1.6v. The effect was the same as found in Tube 10, namely that the photocurrent increased at the longer wavelengths and decreased at the shorter wavelengths as the cathode temperature was increased.

After the experimental tube was sealed off from the vacuum system and mounted in the cryostat, the photoelectric response was the same as had been found on the vacuum system. On cooling the tube the most noticeable feature was, as found for Tube 10, that the photocurrent in the long wavelength tail decreased. This is shown in figure 51 between 8000 and 10,000A° at 290, 130 and 90°K.

5.4 Discussion of results for Tubes 10 and 11

The majority of the published work on the photoelectric emission from the alkali earth oxides has been on barium, calcium or strontium oxide rather than the more commonly used mixed oxide thermionic emitter.

One particularly interesting result found by McNarry[120] with BaO and Jones and Mee[121] with SrO is the enhancement of the photoemission after irradiation with U.V. It has been suggested

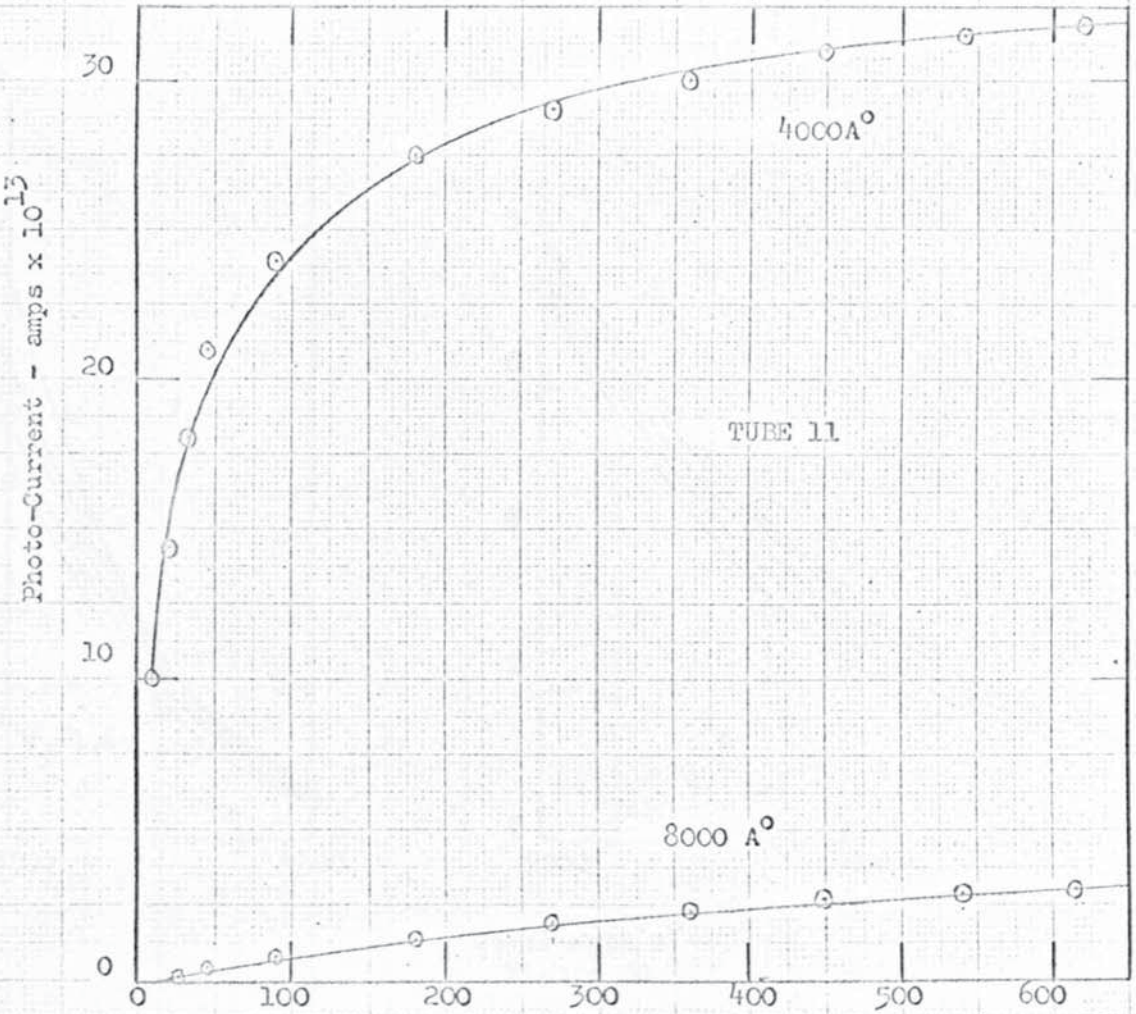
Photo-Current - amps x 10^{-13}
30
20
10
0
4000A°
TUBE 11
8000 A°
0
100
200
300
400
500
600
Anode Voltage (v)

Figure 49

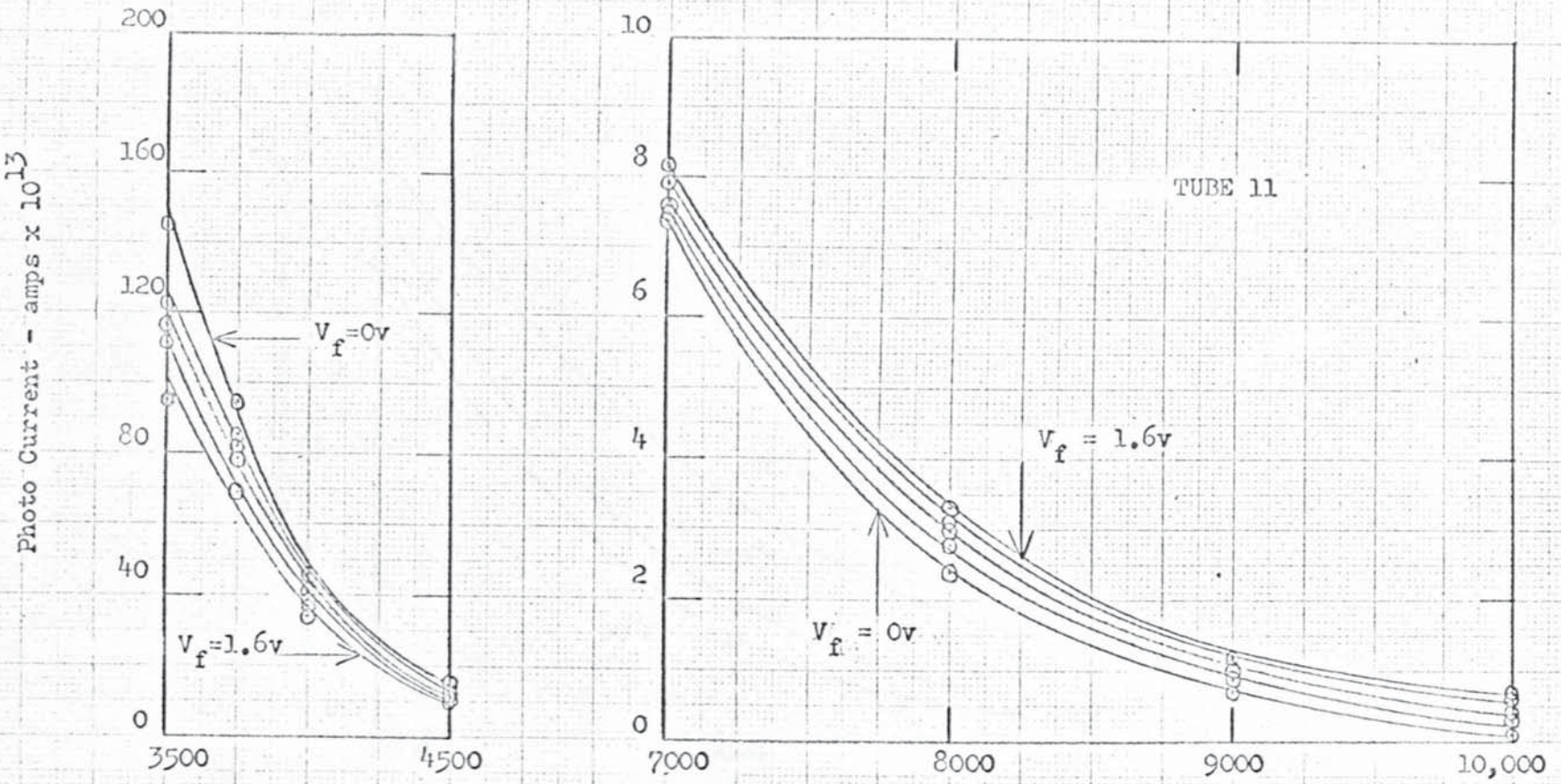
TUBE 11
Photo Current - amps x 10^{13}
200
160
120
80
40
0
3500
4500
V_f=0v
V_f=1.6v
10
8
6
4
2
0
7000
8000
9000
10,000
V_f = 1.6v
V_f = 0v
Wavelength A°

Figure 50

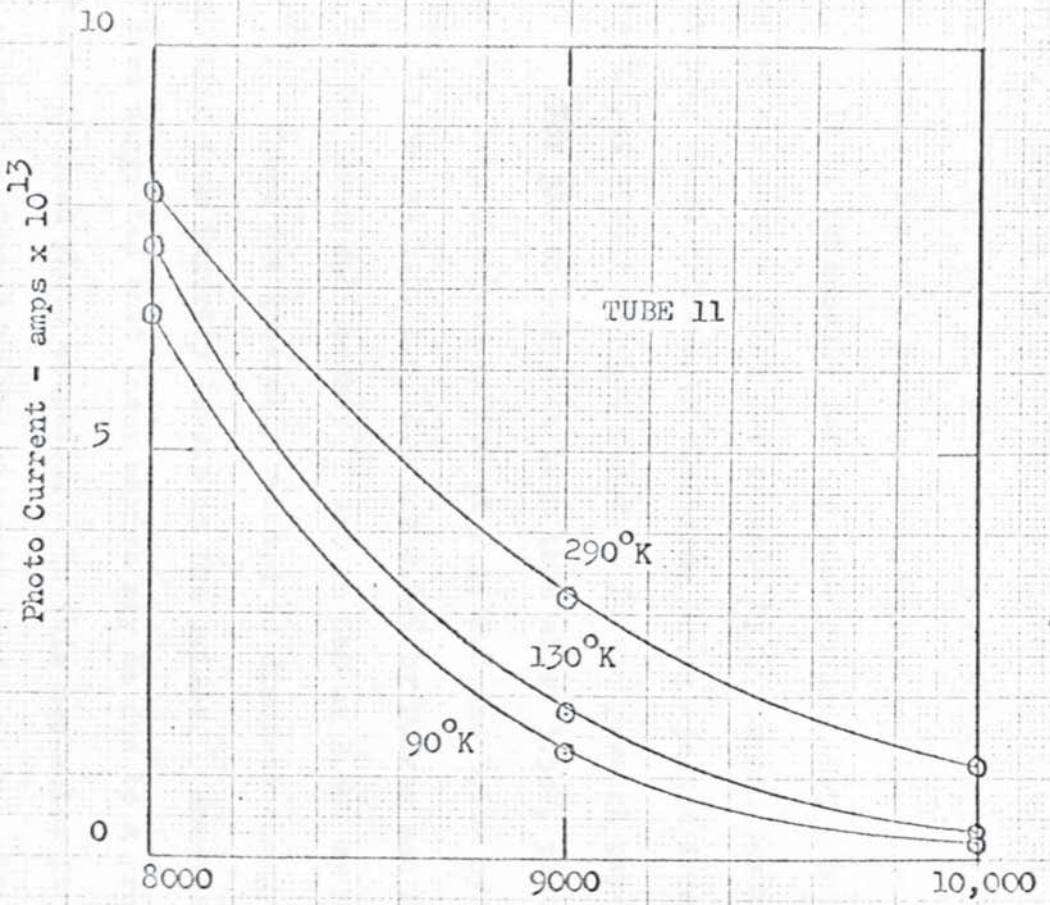
10
5
0
Photo Current - amps x 10^{13}
TUBE 11
290°K
130°K
90°K
8000
9000
10,000

Figure 51

that the enhancement may be due to a photon-induced population of a broad band of meta-stable donor levels at about 2 to 3.5eV below the vacuum level. In the present work the photoelectric emission curves were quite reproducible when measurements were started at either the low or high photon energies, and no such enhancement was observed. However the cathodes were never illuminated with energies greater than 3.5eV and the enhancements reported were found mainly after illumination with photons of energies greater than about 4eV.

It is presumably for the same reason that a strong photoelectric peak - found for example by Devore and Dewdney[122] for BaO at 5eV, which represents electrons being ejected from the top of the filled band - was not observed in the present experiments.

For photon energies less than about 3.5eV, photoelectric peaks have been observed in SrO at 2.1, 2.8 and 3.1eV by Jones and Mee[121], in BaO at 1.0, 1.4, 2.0 and 2.6eV by Ducker and Hensley[123], at 2.5eV by Devore and Dewdney[122] and in CaO at 2.6eV by Mee and Vick[124]. These are generally related to discrete energy levels originating from impurity levels in the oxides. However it has also been suggested that these maxima may be due to a process of exciton - induced photo emission. In this mechanism it is supposed that an exciton, formed by the absorption of a photon with an energy of about 4eV, gives up its energy to an electron in a donor level so that the electron is emitted into the vacuum.

In the present work with the mixed oxide cathode it seems likely that the most significant peak found at 2.13eV results from an impurity level in the SrO, whereas the other minor peaks

may arise from impurity levels in the BaO or CaO.

Phillip [125] investigated the photoelectric emission from BaO and found that, for photon energies between 1.2 and 1.9eV, the photoemission increased as the temperature was raised from 300 to 500°K, whereas at about 3.2eV the photoemission decreased with increasing temperature. In the intermediate region between 2 and 3eV no temperature dependence was observed. These results are in very good agreement with the present work. However the present work has shown further that the photoelectric emission in the long wavelength tail decreases as the temperature is reduced to about 90°K. This latter effect from room temperature to liquid nitrogen temperature in the long wavelength tail has also been observed by Hora et al[126] for mixed alkali cathodes.

Mee and Vick[124] found that with CaO the structure peak at 2.6eV was insensitive to changes in the thermionic work function, ϕ_R, and was therefore not associated with thermionic emission. However they found that cathodes with low values of ϕ_R had extended tails in spectral sensitivity towards low photon energies, and the photoemission increased as the cathode temperature was increased. The arbitary threshold values were also found to agree approximately with the values of ϕ_R, although they point out that such agreement depends on the sensitivity of the current measuring device and the source intensity.

It should be clear from this discussion that the results of the photoelectric measurements taken in the range of photon energies, 1.25 to 3.5eV, are in good agreement with published work with the

alkali oxides. The positions of the characteristic photoelectric peaks are insensitive to changes of temperature and are therefore presumably not associated with the thermionic activity of the cathode. On the other hand the photoelectric emission in the long wavelength tail decreases rapidly as the cathode temperature is reduced. Furthermore other published work eg. Mee and Vick[124], has shown that this long wavelength tail is extended for cathodes with low thermionic (Richardson) work functions.

It would thus appear that there is close association between the photoelectric emission in this low photon energy range and the thermionic capabilities of the cathode. However the author agrees with the remarks of Mee and Vick[124], that agreement between the value of the photoelectric threshold and the Richardson work function, cannot be used in strong support of this argument, on account of the difficulty in judging the threshold value.

It has been shown that the photoelectric emission from the mixed oxide cathodes in the long wavelength tail behaves in a similar way to those found for the tantalum cathodes using the white light source of radiation. In both cases the emission decreased as the temperature was reduced. In addition this photoemission has been shown to be much more dependent on the applied field than in the short wavelength regions. However it is likely that this field effect with oxide cathodes are less significant than in the case of clean metals on account of the roughness of the oxide and the ability of the electric field to penetrate into the bulk of the oxide itself. In the published work referred to earlier on the photoelectric

measurements on oxide cathodes, no reference has been seen on the effect of varying the applied field. Measurements were all taken at a fixed anode voltage - typically 20 to 50v.

It appears possible to explain the results, of this section using Bull's[12] model that the 'work function' - in this case thermionic - is associated with the surface in which there is an electron space charge arising from the thermal diffusion of electrons. This model can explain why the photoelectric emission in the long wavelength tail decreases as the temperature is reduced, because the number of electrons available for emission also decreases. To a less certain extent, the behaviour is also consistent with the model that the emission is strongly dependent on the applied field.

We can again reach the same conclusion that at the very low temperatures the work function - as defined by Bull - decreases rapidly as the temperature approaches $0^{\circ}K$. However it must be stressed that on this view we cannot think of a work function in the more commonly accepted way, because although the work function - that is the barrier to the photoemission from the surface layers - decreases, the number of electrons available for emission also decreases. Nevertheless this new model does offer some explanation of the experimental results found for both the metal and oxide cathodes.

The final short Chapter in this thesis includes the results of some additional measurements, made on the commercial diodes employed in the total emission work described in Chapter 2, in which the effect of applied field was investigated.

Chapter 6

The influence of the field on thermionic currents

It has already been pointed out in section 1.5 that the use of Schottky plots for composite emitters is of dubious value. Many reports have been made of deviations from the Schottky theory and both Hensley[2] and Beck[23] state that the simplest, and most commonly used plots of log i against Va, with extrapolation back to Va = o, is the best empirical approach.

However, despite this, some workers still apply Schottky plots in an attempt to obtain the zero field emission. For example, this approach was used recently by Kiselev and Nikonov[127] for alkaline earth oxide cathodes. Agreement with Schottky theory was only found for applied voltages greater than about 400v and, for electrode spacing used, this is equivalent to an applied field of about 10^4V/cm. Frequently it is desirable to use only very small anode voltages and then the Schottky plots are quite impracticable, because the C.P.D., which may be not much less than the applied anode voltage, is unknown. This, in turn, means that the effective anode voltage is also unknown.

As an illustration of this, figure 52 shows Schottky plots of log i against $V^{\frac{1}{2}}$ for diode M16/1, referred to in Chapter 2,

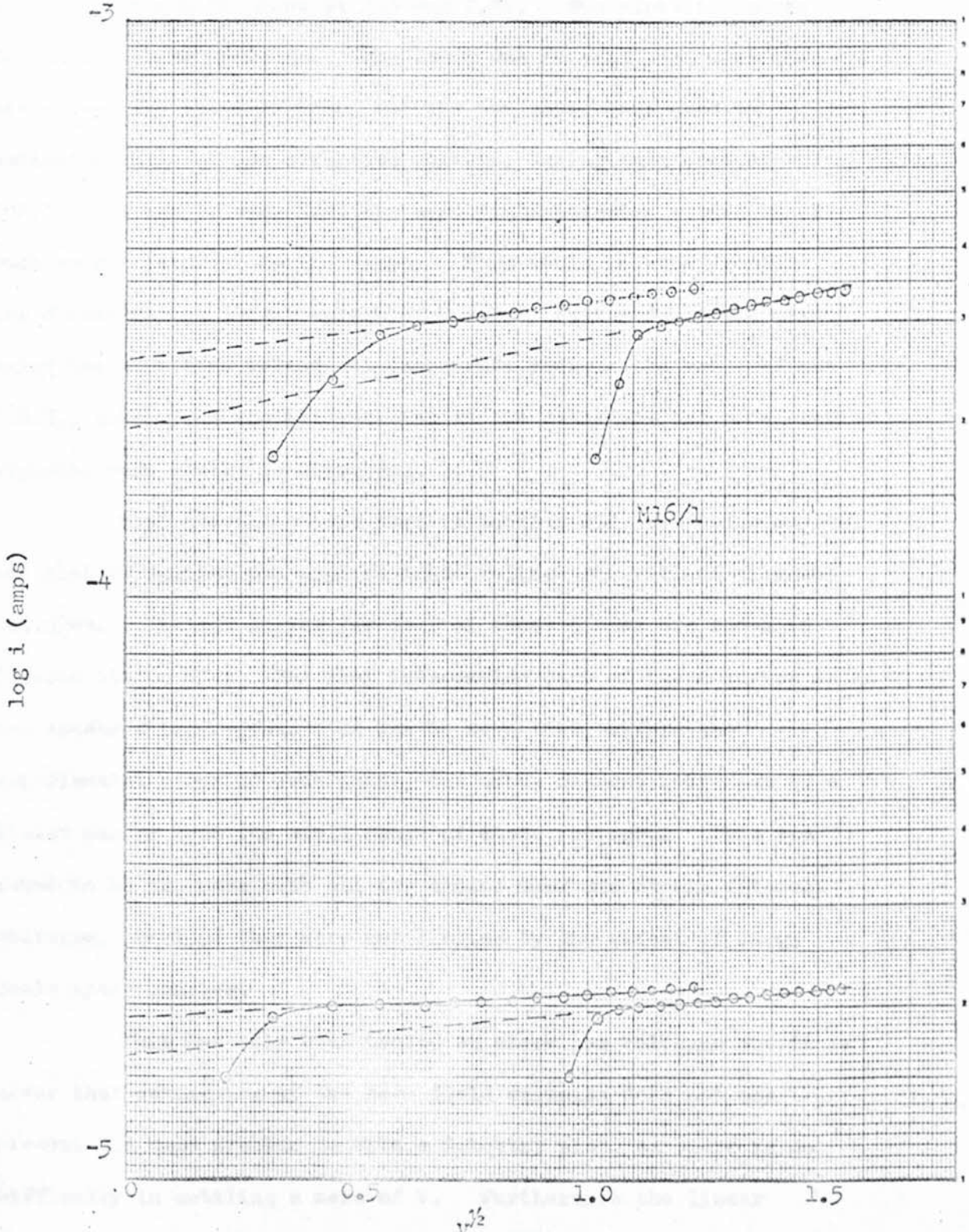

Figure 52

with the cathode filament at 2.0 and 2.5v. Two plots are shown for each filament voltage. The lower one in each case uses the actual applied anode voltage, whereas the upper ones used an estimated value of the effective voltage, taking into account the C.P.D. It can be seen that the zero field emission varies by as much as 25% between the two cases. This would be even greater for diodes having larger values of C.P.D. Furtheremore the method using the effective voltage is inaccurate because the value of the C.P.D., taken from the intersection of the retarding and accelerating regions, must itself be uncertain.

With all the diodes used in section 2.2, the anode current was plotted against the applied anode voltage for various filament voltages. Typical curves for four of these diodes are shown in figures 53a to 53d. The most interesting part of these curves is in the accelerating region. It can be seen that, within the experimental error of each point, the anode current increases in a linear manner over the small range of anode voltages. This was found to be the case with all the diodes used and at all filament voltages, provided they were not limited by the effect of large scale space charges.

This has only been tested at these low voltages but it is clear that estimation of the zero field emission does not now present the same problem as with a Schottky plot, as there is no difficulty in settling a zero of V. Furthermore the linear section of the Schottky plots, with this small range of anode voltage, cannot be regarded as being very significant because it is

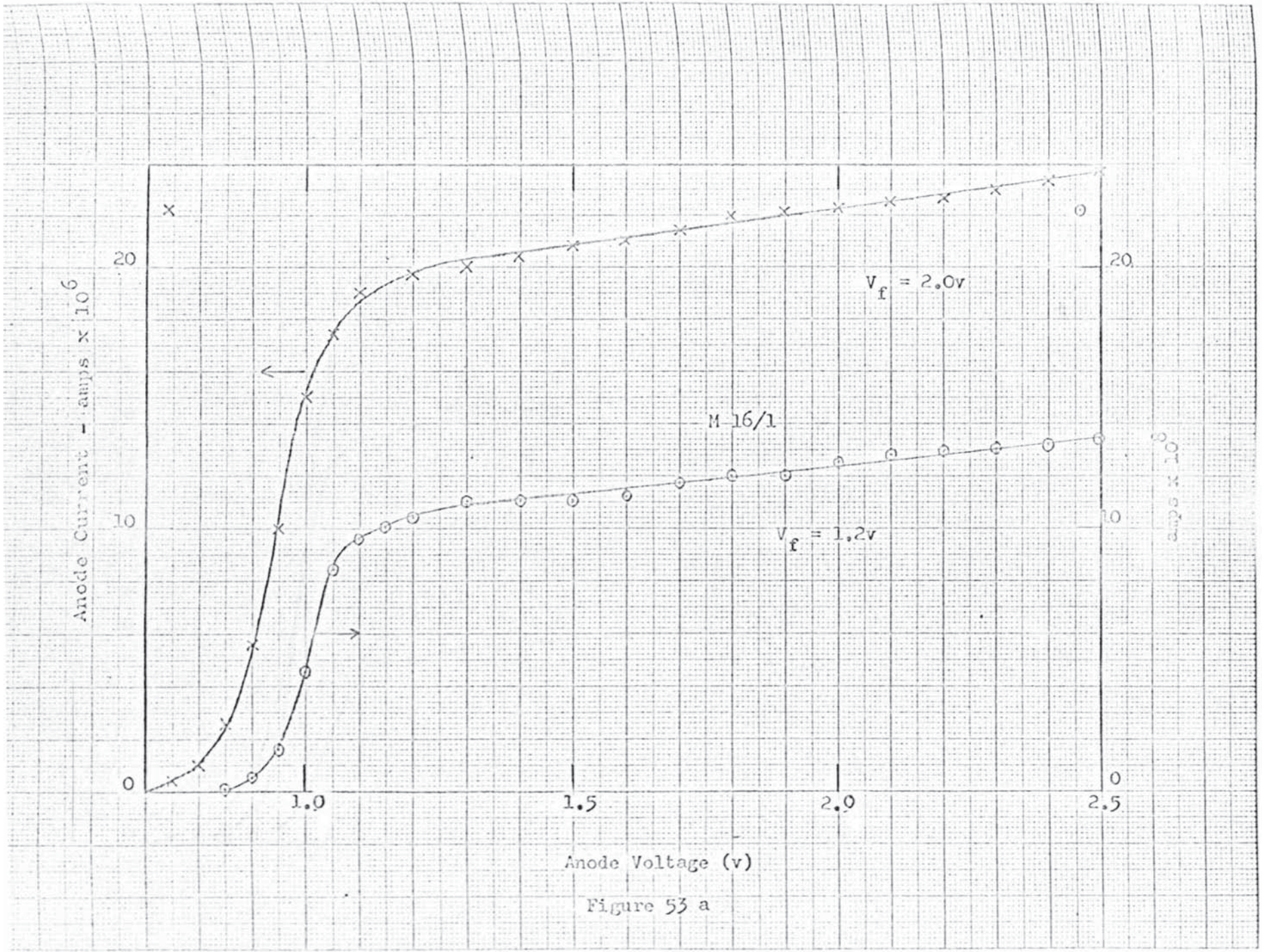
Anode Current - amps x 10^6
20
10
0
1.0
1.5
2.0
2.5
Anode Voltage (v)
V_f = 2.0v
V_f = 1.2v
M 16/1

Figure 53 a

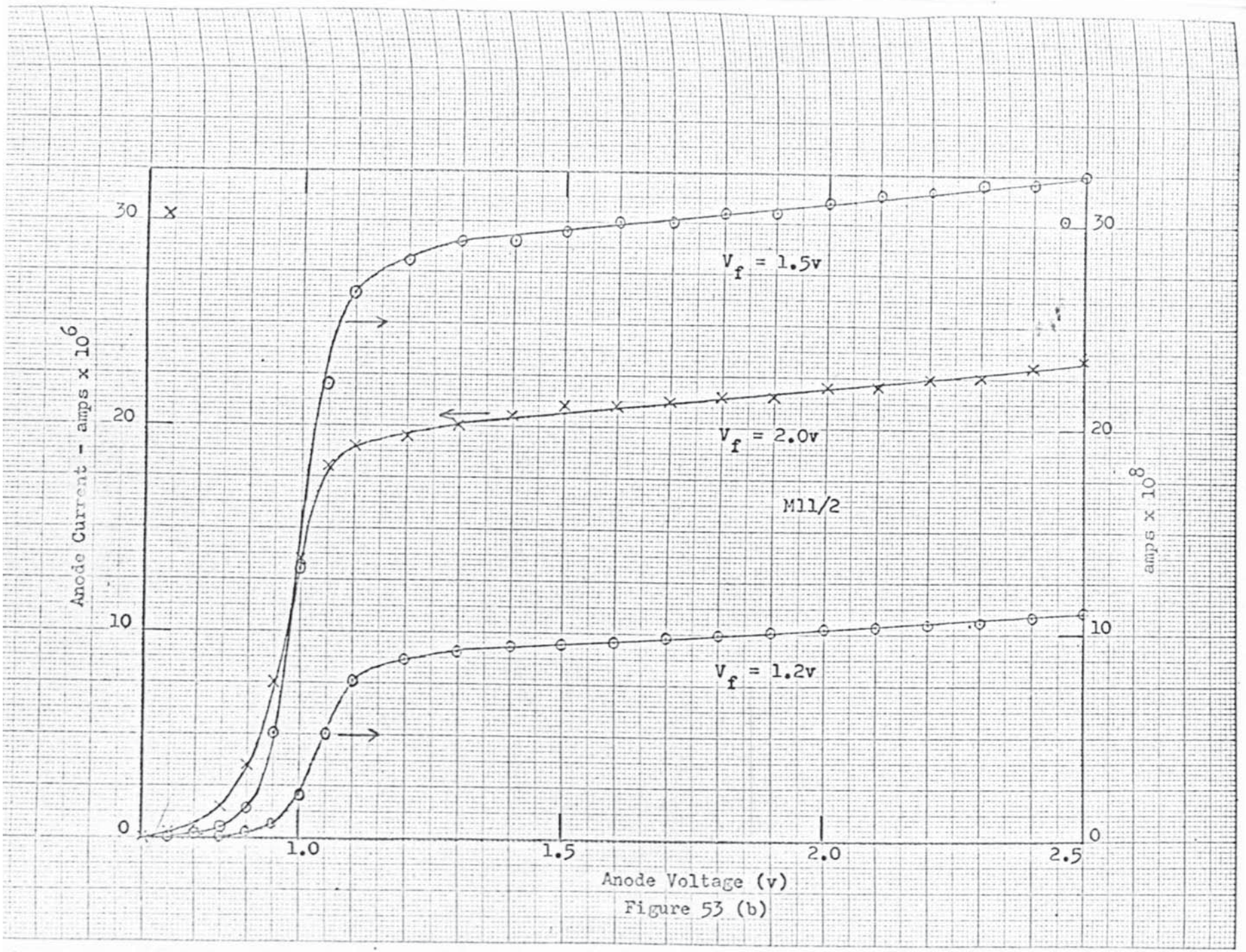
Anode Current - amps x 10^6
30
20
10
0
V_f = 1.5v
V_f = 2.0v
V_f = 1.2v
M11/2
amps x 10^8
30
20
10
0
1.0
1.5
2.0
2.5
Anode Voltage (v)

Figure 53 (b)

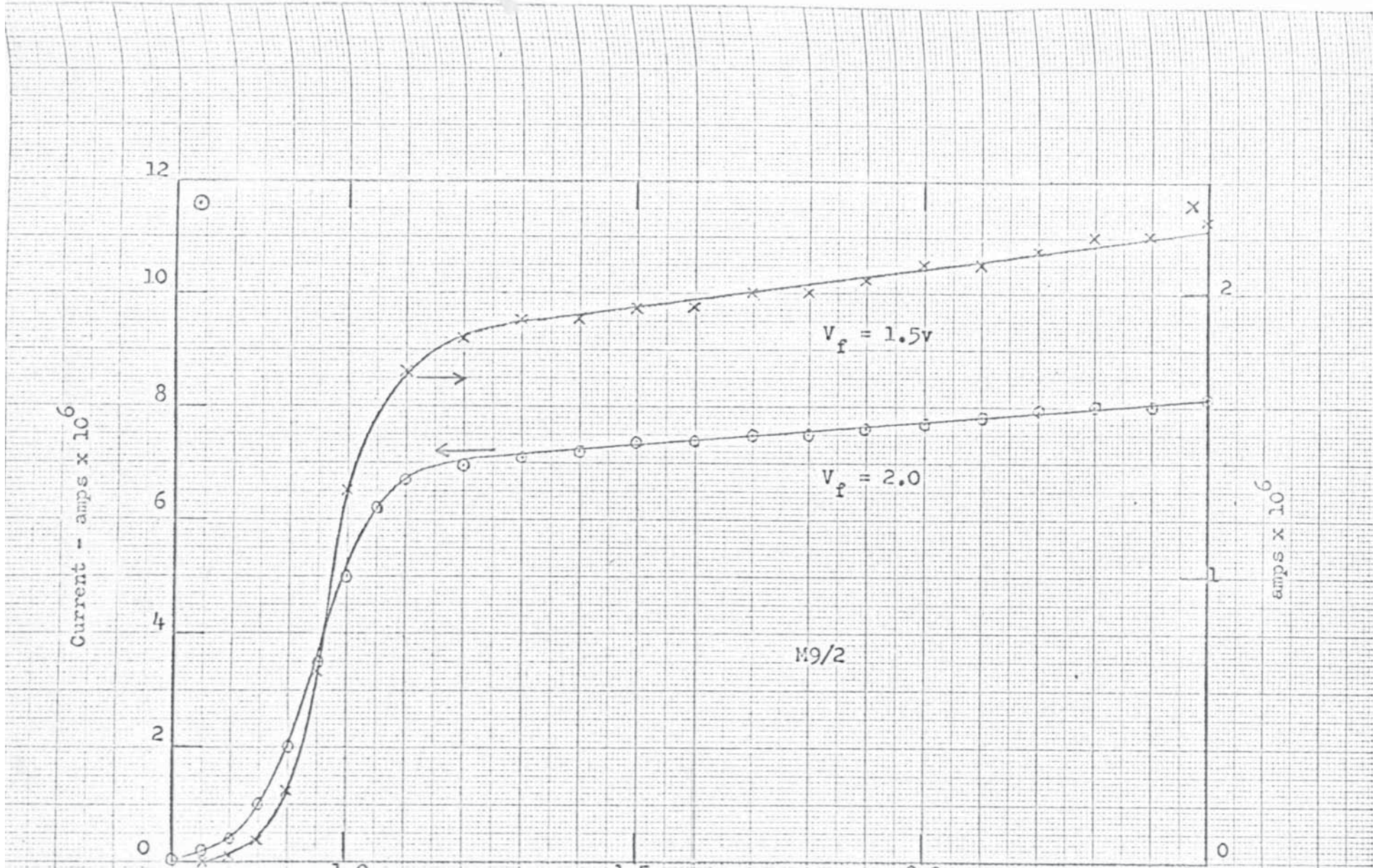
12
10
8
6
4
2
0
Current - amps x 10^6
1.0
1.5
2.0
2.5
Anode Voltage (v)
V_f = 1.5v
V_f = 2.0
M9/2
2
1
0
amps x 10^6

Figure 53 c

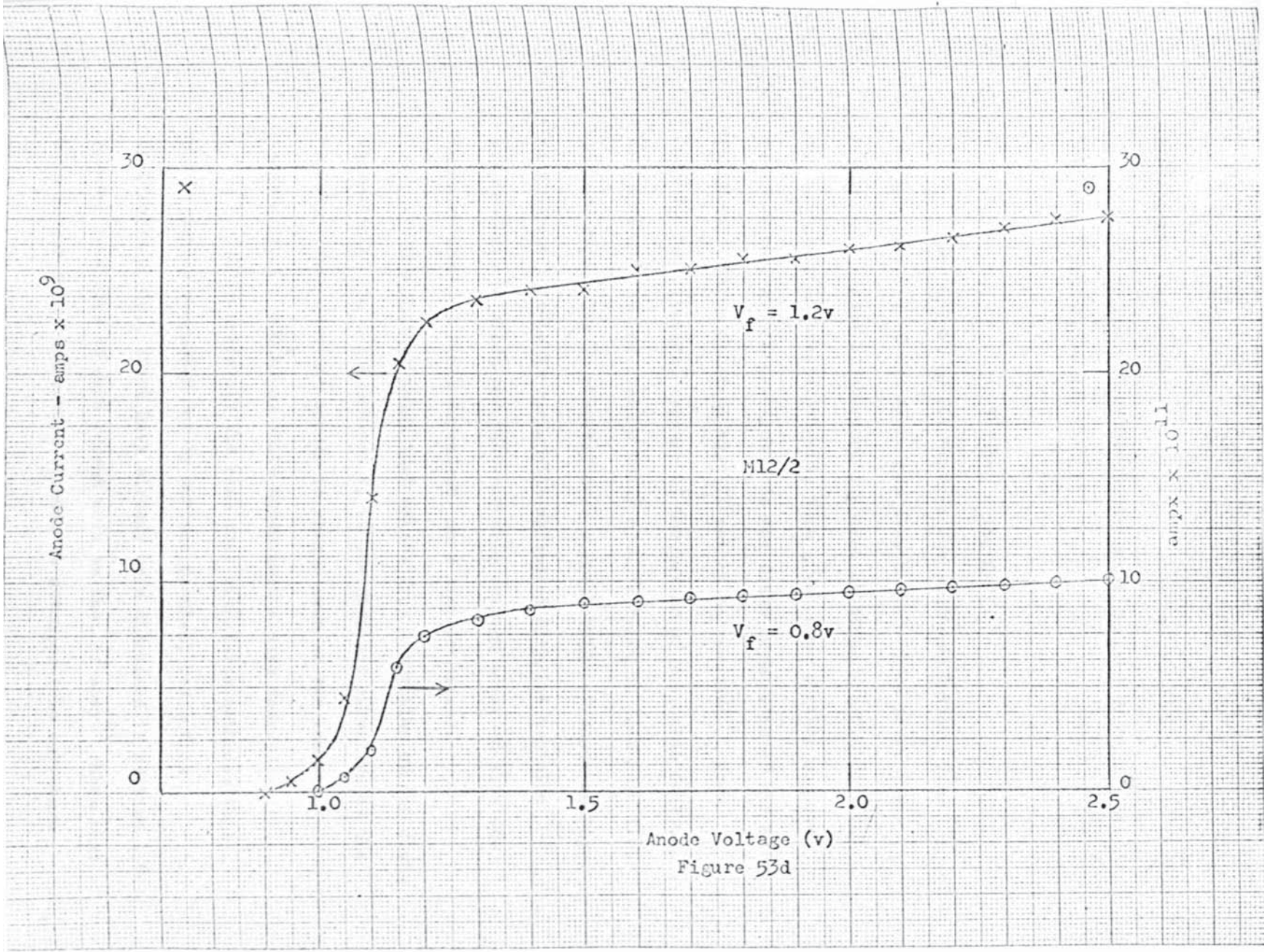
30
20
10
0
Anode Current - amps x 10^9
V_f = 1.2v
M12/2
V_f = 0.8v
1.0
1.5
2.0
2.5
Anode Voltage (v)
amps x 10 11
Figure 53d

plotted on a log-linear scale.

If we now reconsider equation 21 derived by Bull[12] for the work function, we see that,

$$\therefore \quad \phi \propto -\log E$$

So that if we put this in the Boltzmann factor, then the current, $i \propto E$ and therefore also to V. Thus if we again regard Bull's idea of the work function as being associated with the thermally emitted electrons, this gives some further support to the theory and in particular to the field dependence of the work function. It is realised that it cannot be regarded as any complete verification, because of the nature of the oxide surface. Nevertheless its low average value of work function does mean that such an effect can be observed over a small range of anode voltage. Furthermore this is in reasonable agreement with the tantalum measurements in which the photoelectric current observed with the tungsten lamp was field dependent in a similar manner.

One further point that arises from inspection of the diode characteristics, log i against V, is the distinct curvature of the "knee". This does not appear to change even at the lowest temperature ($\sim 400^{\circ}K$) at which measurements were made.

It is certainly the case that with these cathodes this can be partly accounted for by surface patches, reflection coefficients etc., which have already been discussed in section 1.6. However reference to such recent work as that of Abey[31] shows that this is not fully understood because he obtained this curvature

using single crystals under very controlled conditions.

In Bull's[12] account of the emission of electrons from one electrode to another he says that when the applied field changes from an accelerating one to a retarding one, or vice versa, we cannot expect a discontinuous change in the electric field. The potential barrier at the surface, which represents the work function, is not constant but is a fluctuating quantity and depends upon the probability of collision between "field lines". Even without the concept of "field lines", this point of view has also been supported by Breeze in this laboratory, and referred to by Bull[12], who found during noise studies on valves that the fluctuation of the characteristics was greatest in the intermediate region between the accelerating and retarding fields. If this experimental evidence is accepted, an abrupt change from the retarding to the accelerating region should not be expected. Thus there is some evidence from both the experimental work reported in this thesis, and other published work, that the curvature of the "knee" may be partly due to a process of this nature.

Chapter 7

Conclusions and suggestions for further work

The first part of this investigation has shown that the total emission can be satisfactorily measured by the extrapolation method. Furtheremore evidence has been presented that the results obtained are more satisfactory than those produced by other methods. In one particular application this was applied to a number of commercial oxide cathode valves to demonstrate that the space charge limited current is dependent on the value of the total emission. However when the consequences of the extrapolation were investigated in more detail this brought to light unexpected behaviour of the work function at low temperatures.

It was partly for this reason that an attempt has been made to measure the photoelectric work function of clean metals down to liquid helium temperatures. This has led to the belief that the work function as normally understood is associated with the bulk properties of the material. In this case the value of $\frac{d\phi}{dT}$ for tantalum between 290 and 12°K was found to be small ($\sim +2\times10^{-4}$ eV/ °K). In addition the work function was not very dependent on the applied field.

In contrast the photoemission in the long wavelength tail,

from both tantalum and oxide cathodes, has been observed to be very much more temperature and field dependent, and it is thought to be a surface effect.

This effect appears to be closely associated with the theoretical ideas of Bull[12]. However the present work has shown that his view of the work function was too simplified as he had not considered these bulk properties. Furthermore if these experimental results and their interpretation are accepted, it must be understood that Bull was not referring to a work function in the normally accepted way. With the surface effect the current decreases as the temperature decreases on account of the decrease in the number of electrons available for emission. As yet no attempt has been made to calculate this variation of current with temperature.

The experimental work has established, with some degree of success, the rather difficult techniques for measurement of photoelectric and thermionic emission over a large range of temperature and under ultra-high vacuum conditions. However it is realised that a number of criticisms can be made of the methods employed.

It would be beneficial to repeat the photoelectric measurements in the low temperature region with other metals and preferably with known crystallographic orientations. Experience has shown that this could be done more satisfactorily with a larger cryostat. With this additional facility larger experimental tubes could be used and hence the electrical lead-throughs made further apart and so reduce the possibility of "polarisation" in the glass.

Alternatively some method using ohmic heating for both electrodes could be beneficial in this respect.

Other improvements are possible in the design of the experimental tubes. It is likely that the use of a Channel Multiplier, incorporated in the tube itself, might be advantageous for the measurement of these small D.C. currents. In order to be more certain of the vacuum conditions the tube could be sealed off from the main vacuum system together with a small ion pump. Both could then be mounted in the cryostat and the ion pump operated during measurements. The vacuum could also, with advantage, incorporate a mass spectrometry facility to record the partial pressure of residual gases.

It would also be of considerable interest to perform thermionic measurements on metal single crystals at various temperatures without the complexity of additional electrodes and magnetic fields. One suggested way in which this could be done is by heating the cathode by electron bombardment from a pulsed supply and measuring the emission on only every half cycle at very small anode voltages. This should not only give information about the variation of C.P.D. with temperature, but should also help to resolve the problem concerned with the "knee" of the characteristics and the influence of small fields on the total emission.

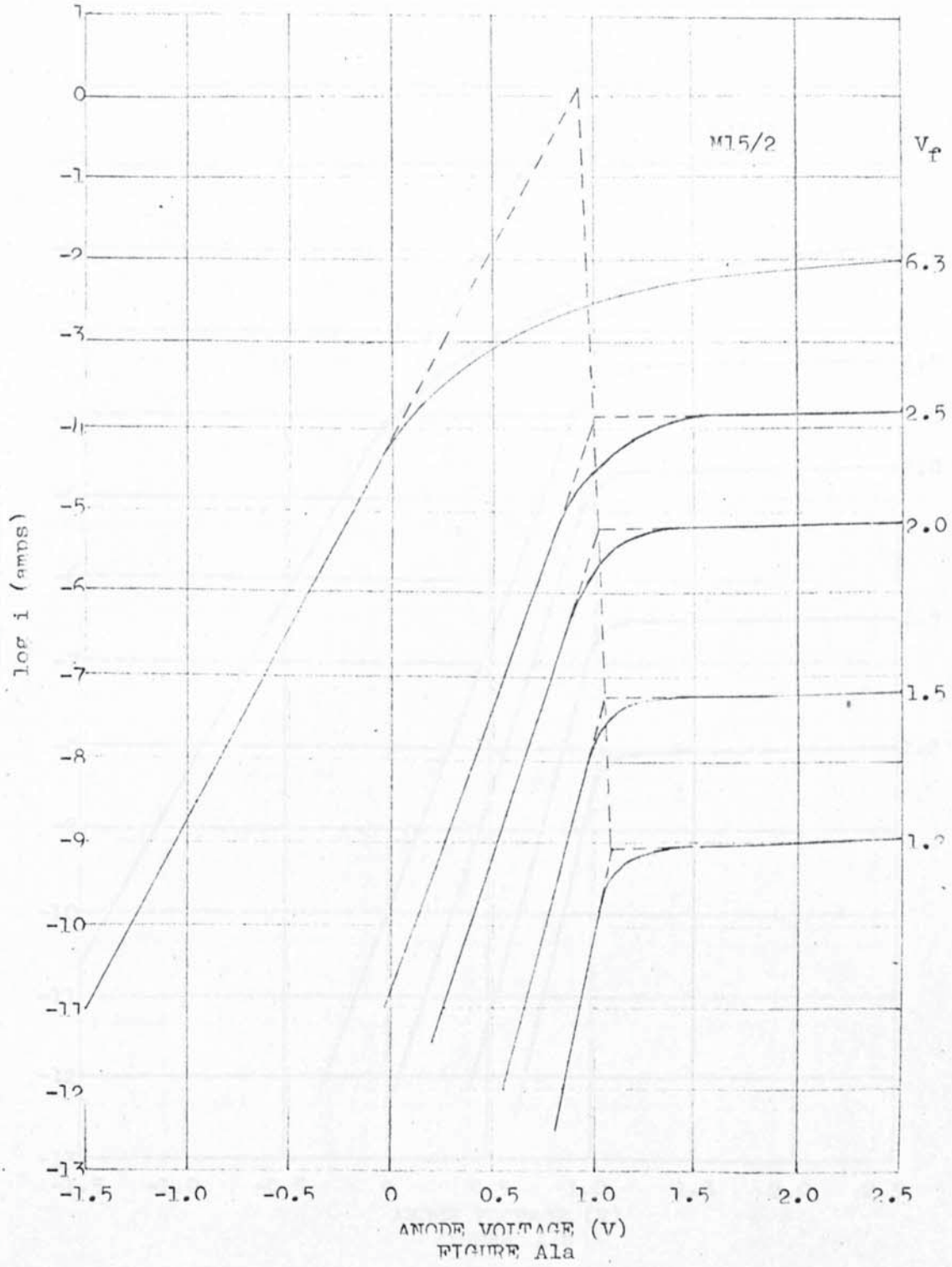
M15/2
V_f
6.3
2.5
2.0
1.5
log i (amps)
1
0
-1
-2
-3
-4
-5
-6
-7
-8
-9
-10
-11
-12
-13
-1.5
-1.0
-0.5
0
0.5
1.0
1.5
2.0
2.5
ANODE VOLTAGE (V)

FIGURE A1a

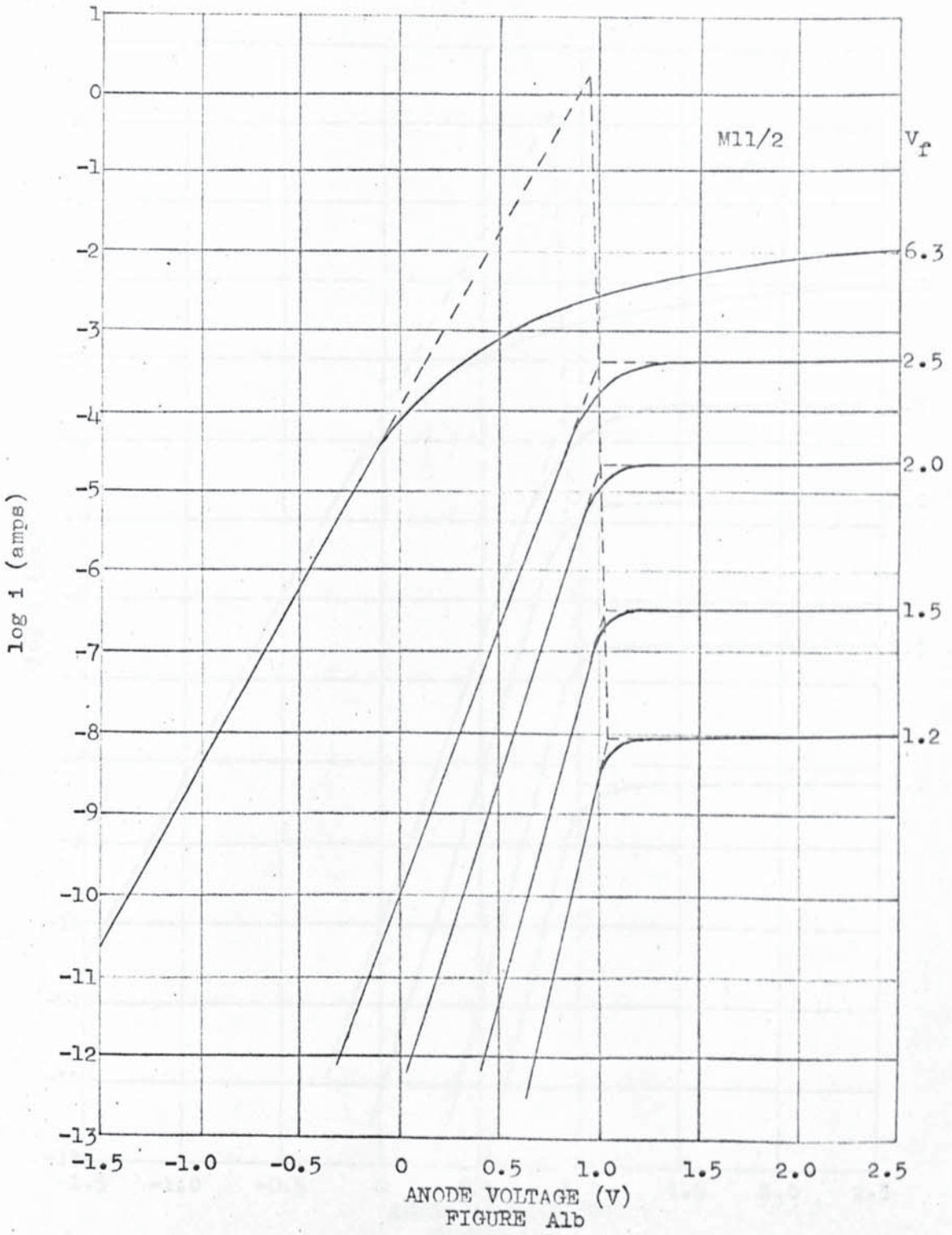
M11/2
V_f
6.3
2.5
2.0
1.5
1.2
log i (amps)
1
0
-1
-2
-3
-4
-5
-6
-7
-8
-9
-10
-11
-12
-13
-1.5
-1.0
-0.5
0
0.5
1.0
1.5
2.0
2.5
ANODE VOLTAGE (V)

FIGURE A1b

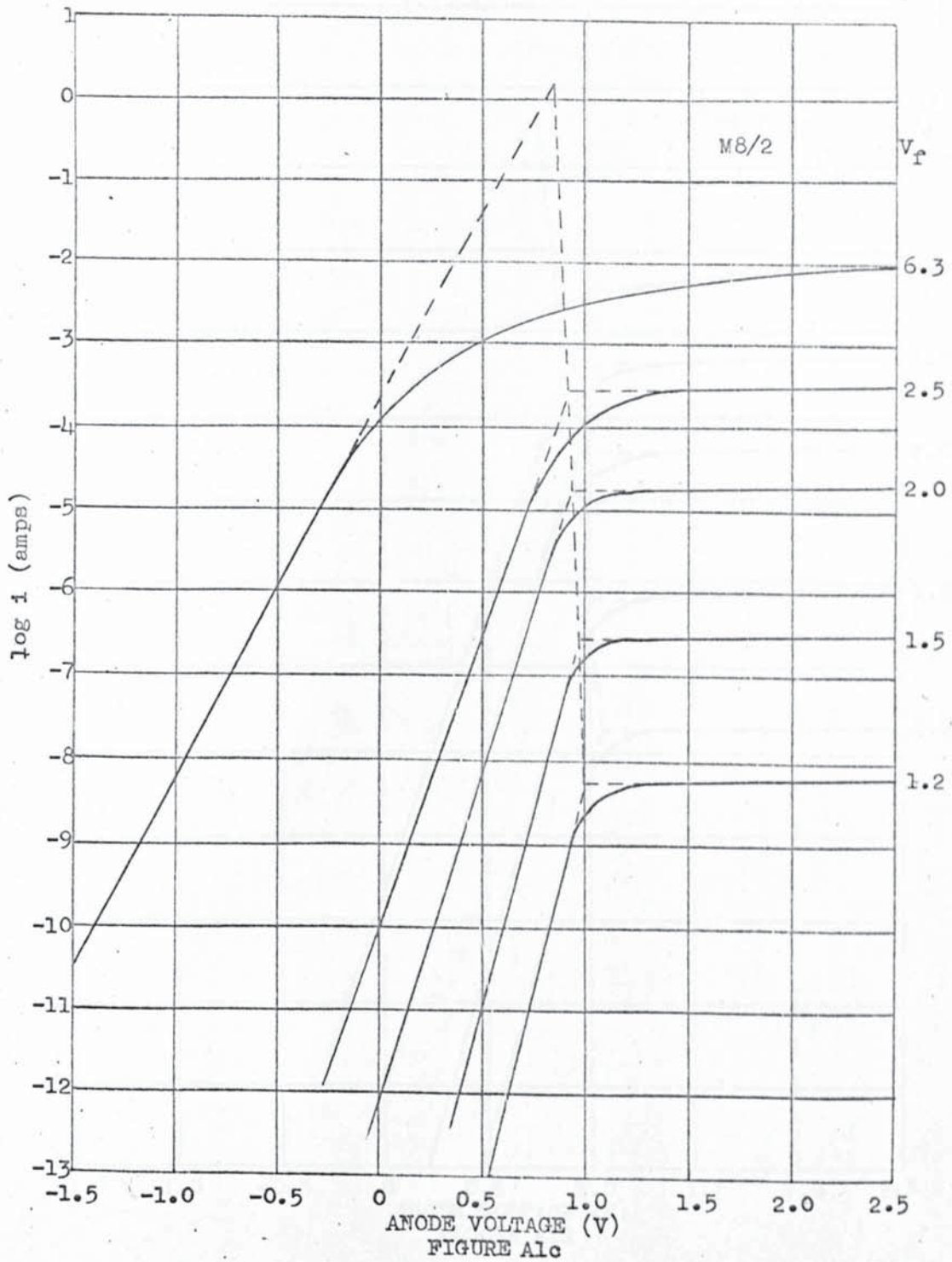
M8/2
V_f
6.3
2.5
2.0
1.5
1.2
log i (amps)
1
0
-1
-2
-3
-4
-5
-6
-7
-8
-9
-10
-11
-12
-13
-1.5
-1.0
-0.5
0
0.5
1.0
1.5
2.0
2.5
ANODE VOLTAGE (V)

FIGURE A1c

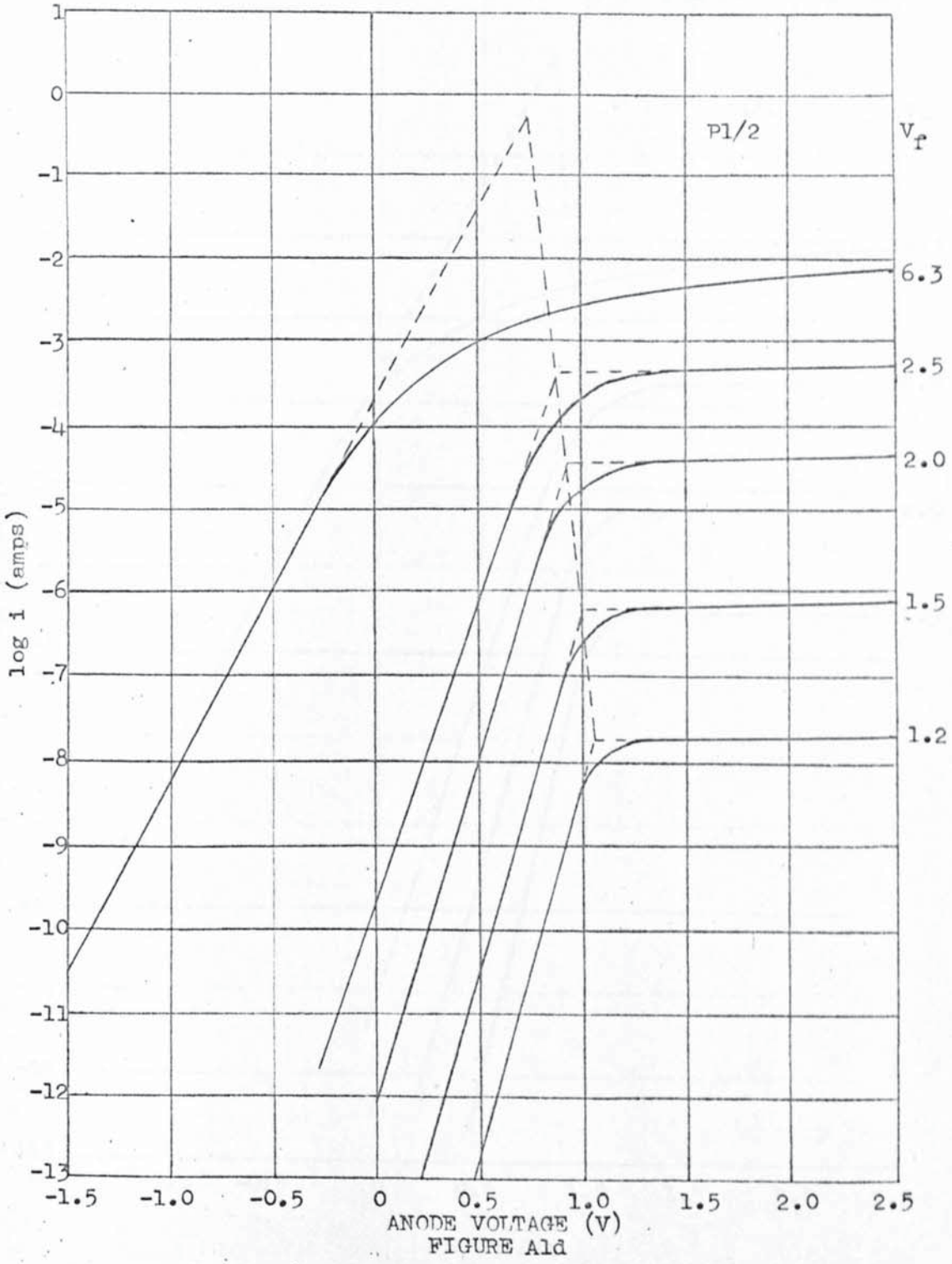
P1/2
V_f
6.3
2.5
2.0
1.5
1.2
log i (amps)
1
0
-1
-2
-3
-4
-5
-6
-7
-8
-9
-10
-11
-12
-13
-1.5
-1.0
-0.5
0
0.5
1.0
1.5
2.0
2.5
ANODE VOLTAGE (V)

FIGURE A1d

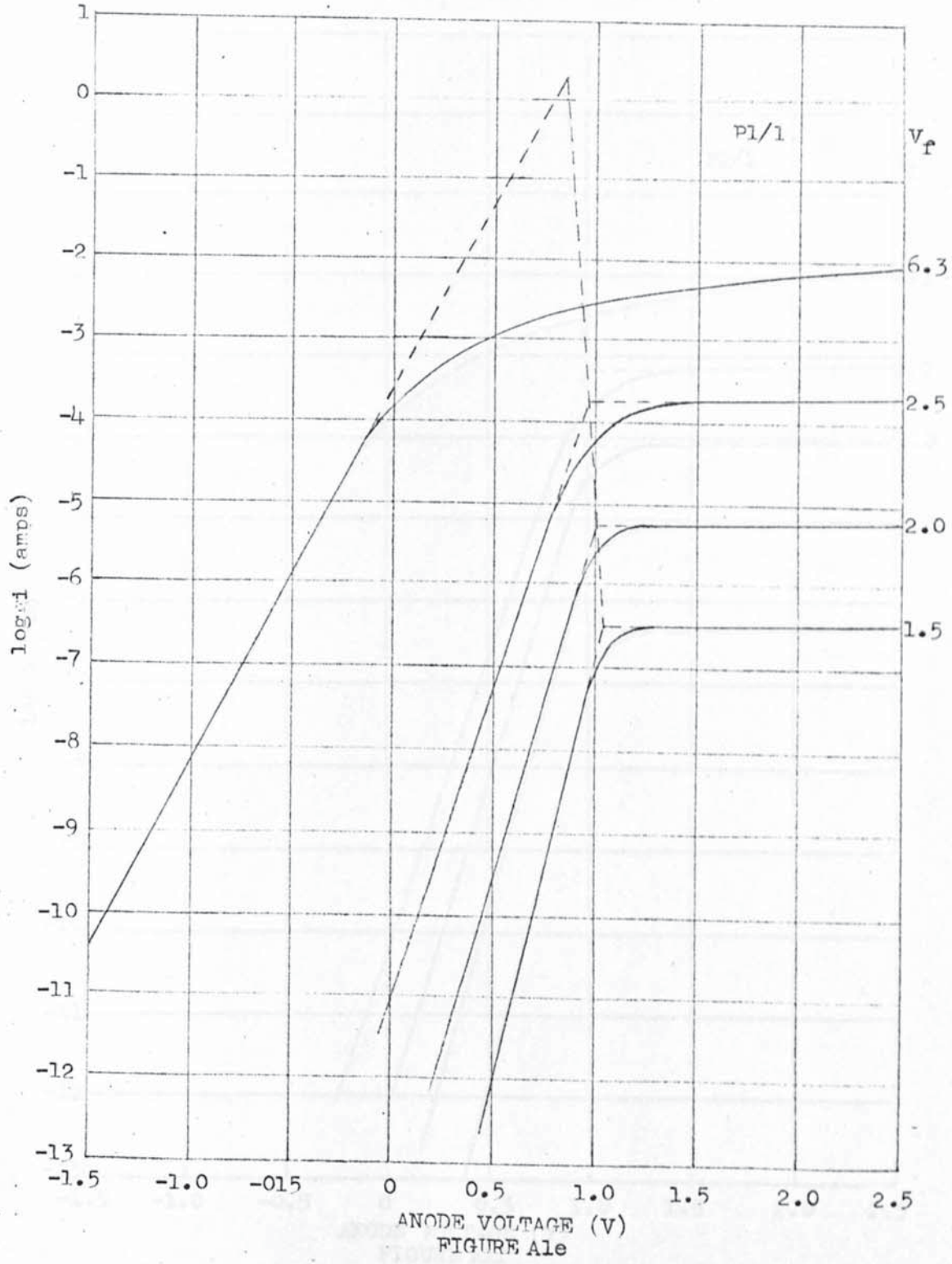
1
0
-1
-2
-3
-4
-5
-6
-7
-8
-9
-10
-11
-12
-13
log i (amps)
-1.5
-1.0
-015
0
0.5
1.0
1.5
2.0
2.5
ANODE VOLTAGE (V)
P1/1
V_f
6.3
2.5
2.0
1.5
FIGURE A1e

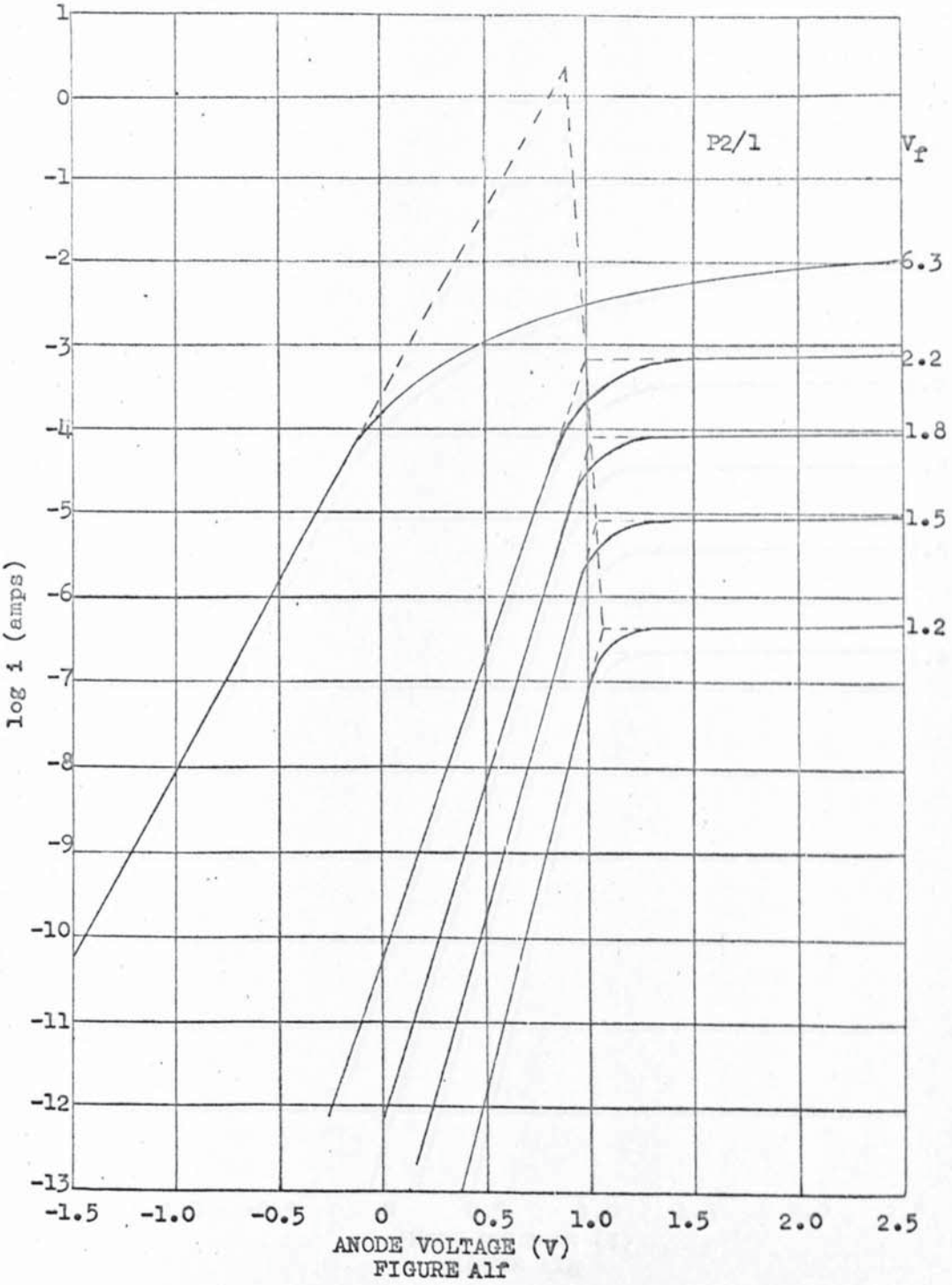
P2/1
V_f
6.3
2.2
1.8
1.5
1.2
log i (amps)
1
0
-1
-2
-3
-4
-5
-6
-7
-8
-9
-10
-11
-12
-13
-1.5
-1.0
-0.5
0
0.5
1.0
1.5
2.0
2.5
ANODE VOLTAGE (V)

FIGURE A1f

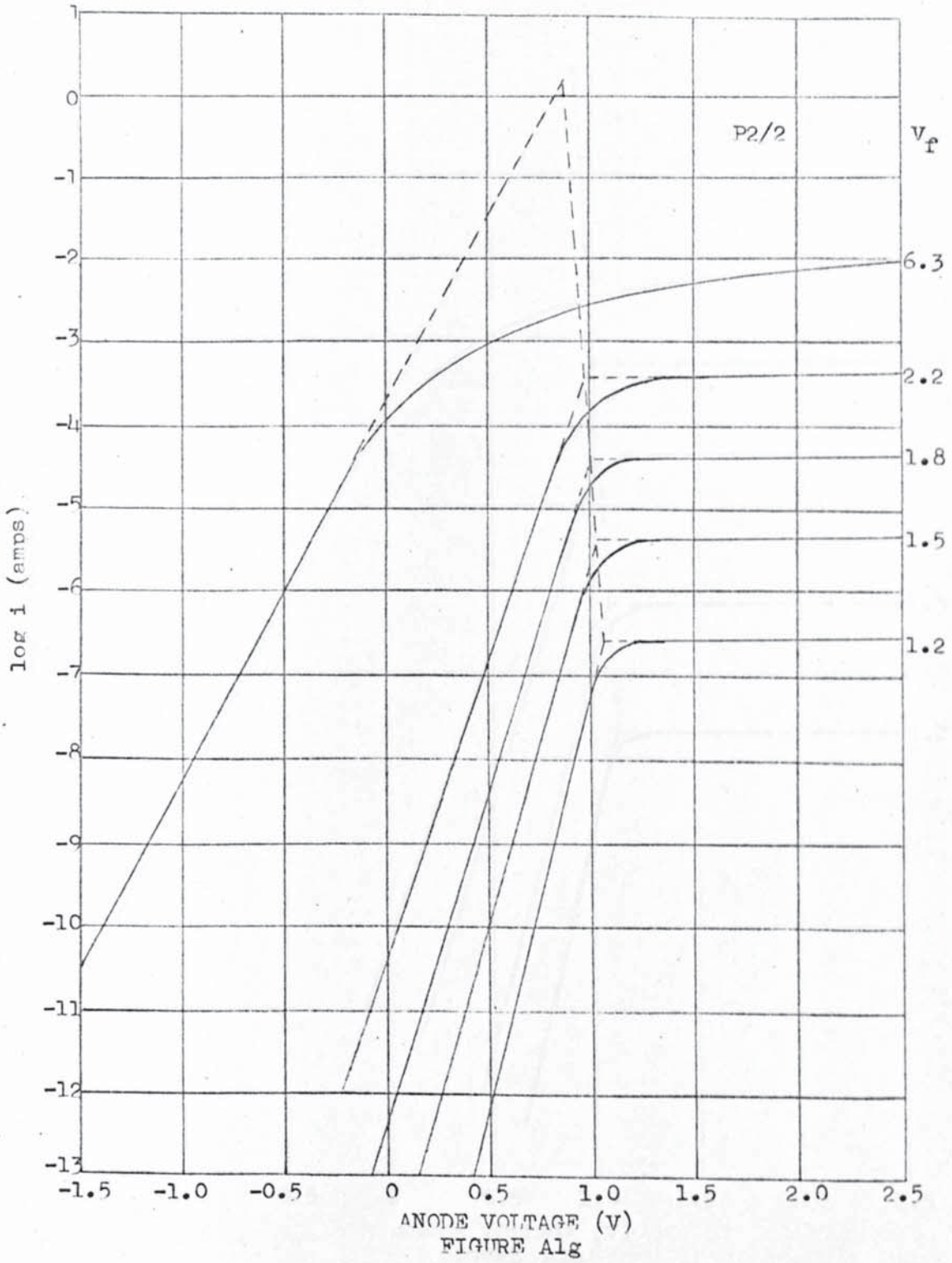
P2/2
V_f
6.3
2.2
1.8
1.5
1.2
log i (amps)
1
0
-1
-2
-3
-4
-5
-6
-7
-8
-9
-10
-11
-12
-13
-1.5
-1.0
-0.5
0
0.5
1.0
1.5
2.0
2.5
ANODE VOLTAGE (V)

FIGURE A1g

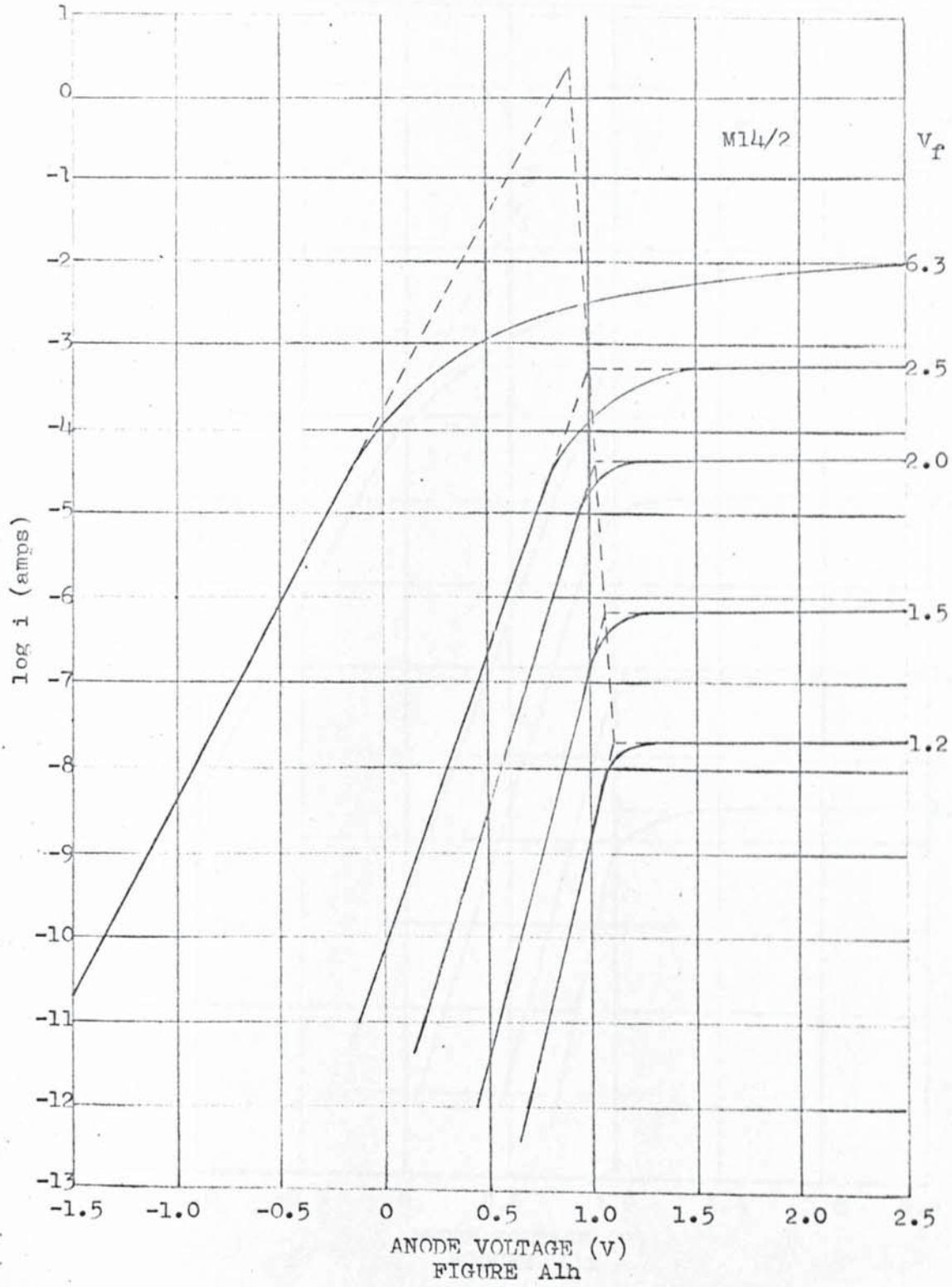
M14/2
V_f
6.3
2.5
2.0
1.5
1.2
log i (amps)
1
0
-1
-2
-3
-4
-5
-6
-7
-8
-9
-10
-11
-12
-13
-1.5
-1.0
-0.5
0
0.5
1.0
1.5
2.0
2.5
ANODE VOLTAGE (V)

FIGURE A1h

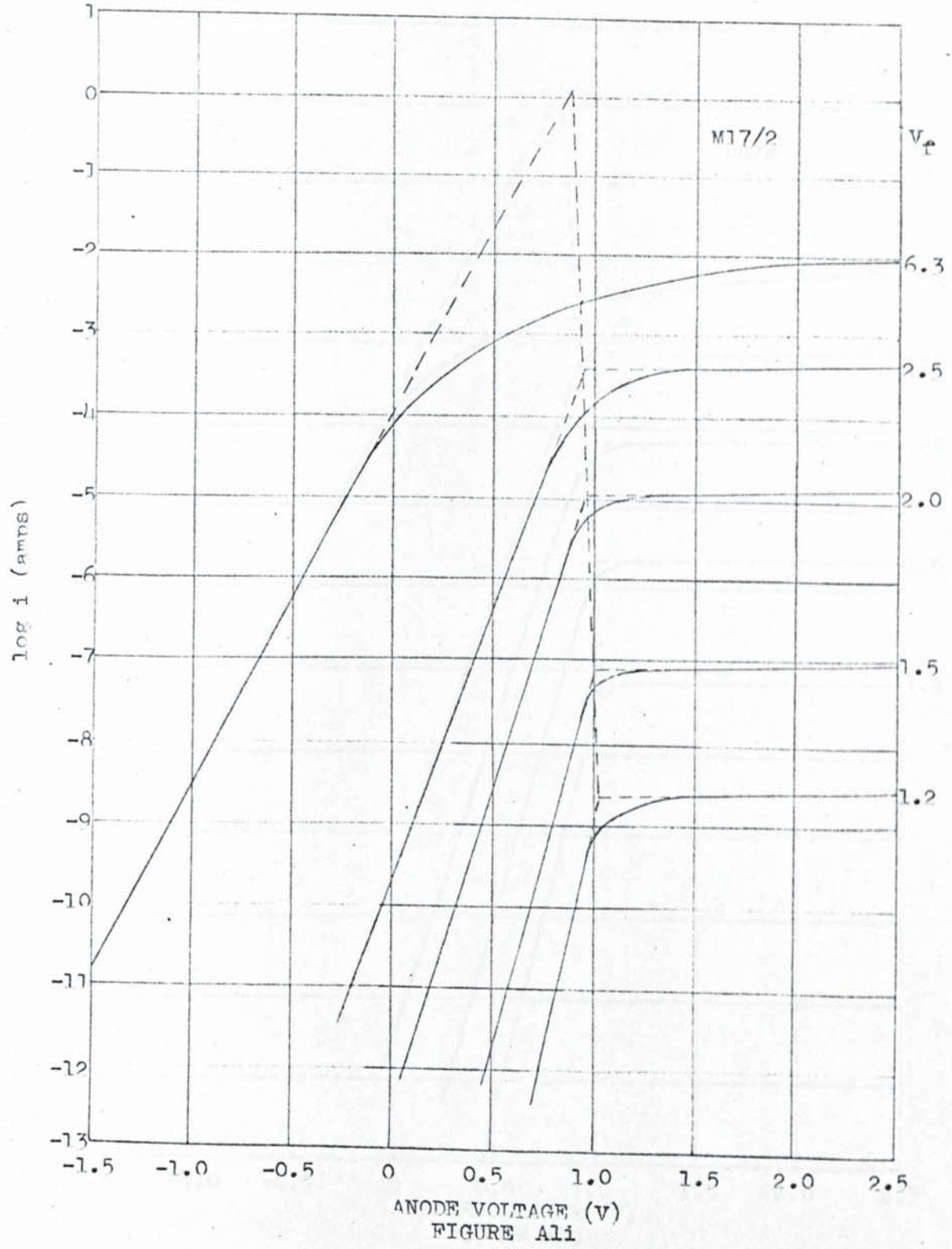
M17/2
V_f
6.3
2.5
2.0
1.5
1.2
log i (amps)
1
0
-1
-2
-3
-4
-5
-6
-7
-8
-9
-10
-11
-12
-13
-1.5
-1.0
-0.5
0
0.5
1.0
1.5
2.0
2.5
ANODE VOLTAGE (V)

FIGURE A1i

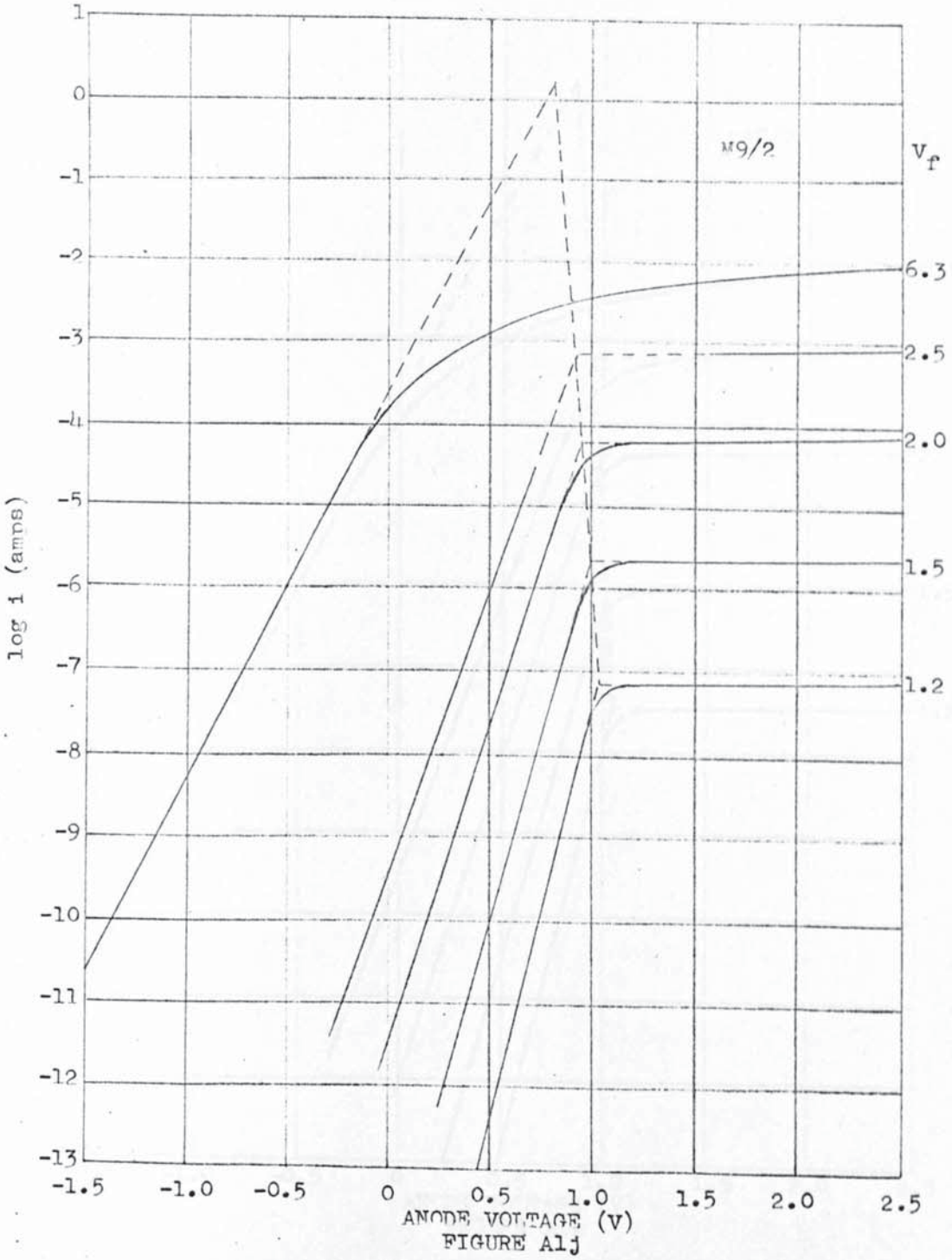
M9/2
V_f
6.3
2.5
2.0
1.5
1.2
log i (amps)
1
0
-1
-2
-3
-4
-5
-6
-7
-8
-9
-10
-11
-12
-13
-1.5
-1.0
-0.5
0
0.5
1.0
1.5
2.0
2.5
ANODE VOLTAGE (V)

FIGURE A1j

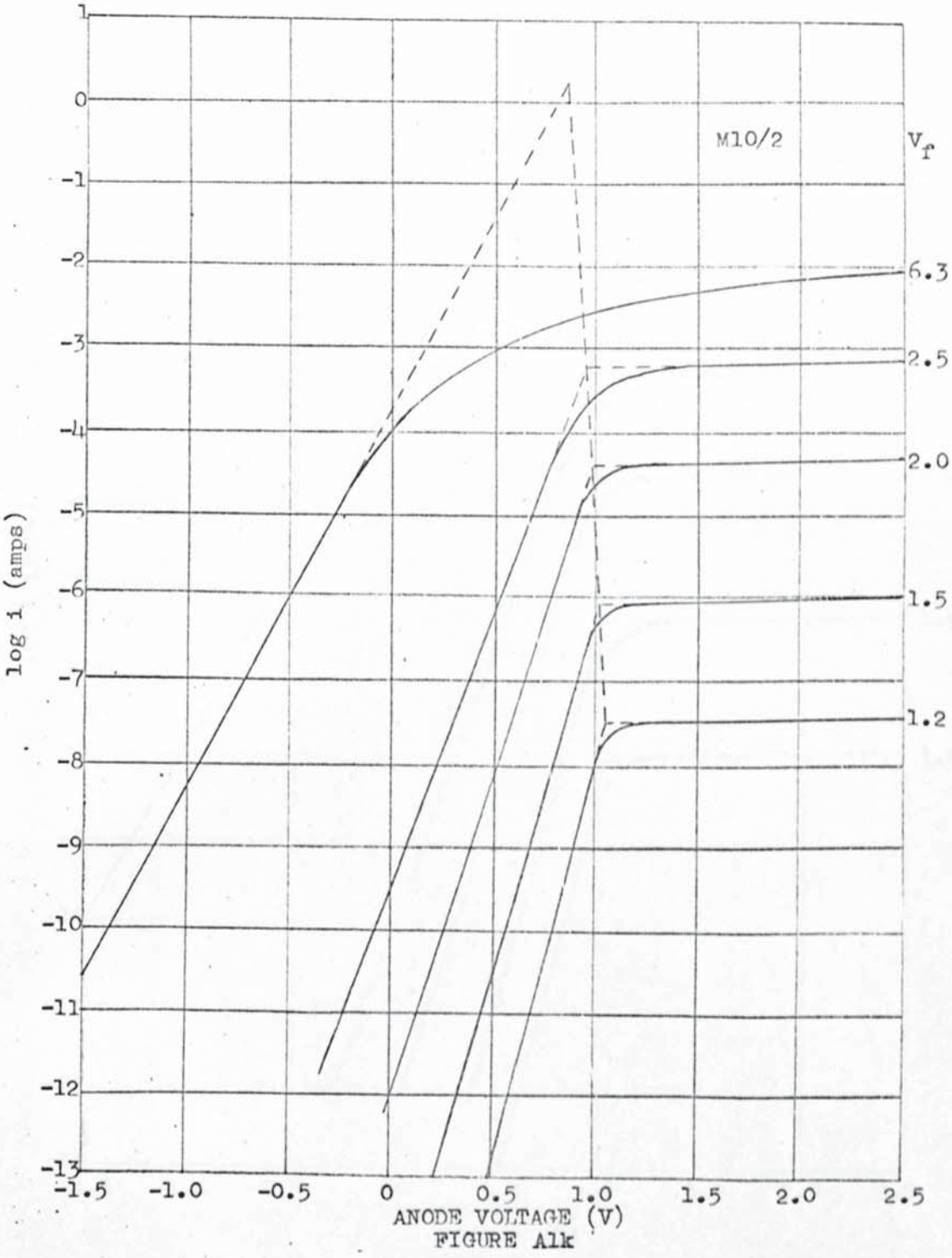
M10/2
V_f
6.3
2.5
2.0
1.5
1.2
log i (amps)
1
0
-1
-2
-3
-4
-5
-6
-7
-8
-9
-10
-11
-12
-13
-1.5
-1.0
-0.5
0
0.5
1.0
1.5
2.0
2.5
ANODE VOLTAGE (V)

FIGURE A1k

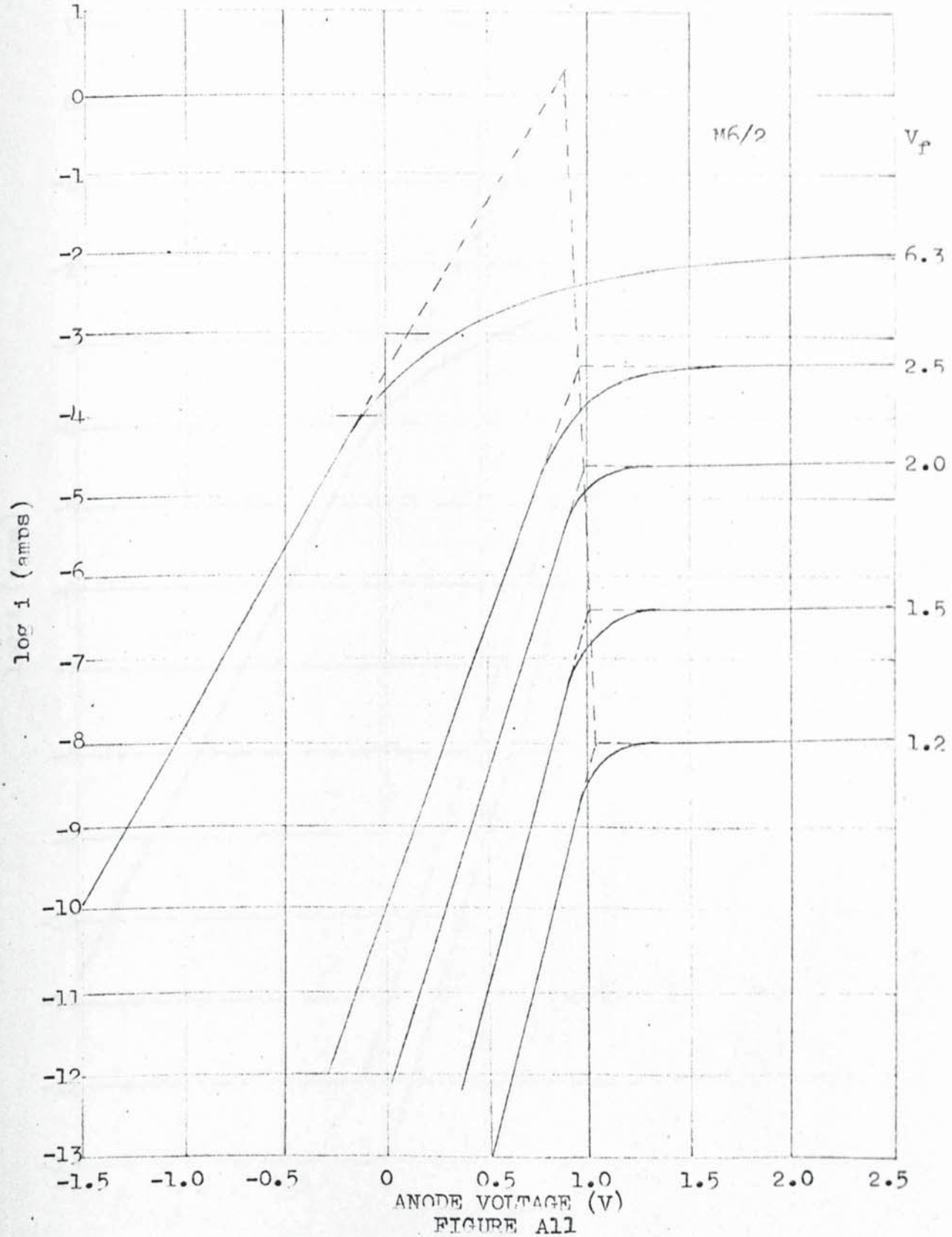
M6/2
V_f
6.3
2.5
2.0
1.5
1.2
log i (amps)
1
0
-1
-2
-3
-4
-5
-6
-7
-8
-9
-10
-11
-12
-13
-1.5
-1.0
-0.5
0
0.5
1.0
1.5
2.0
2.5
ANODE VOLTAGE (V)

FIGURE A11

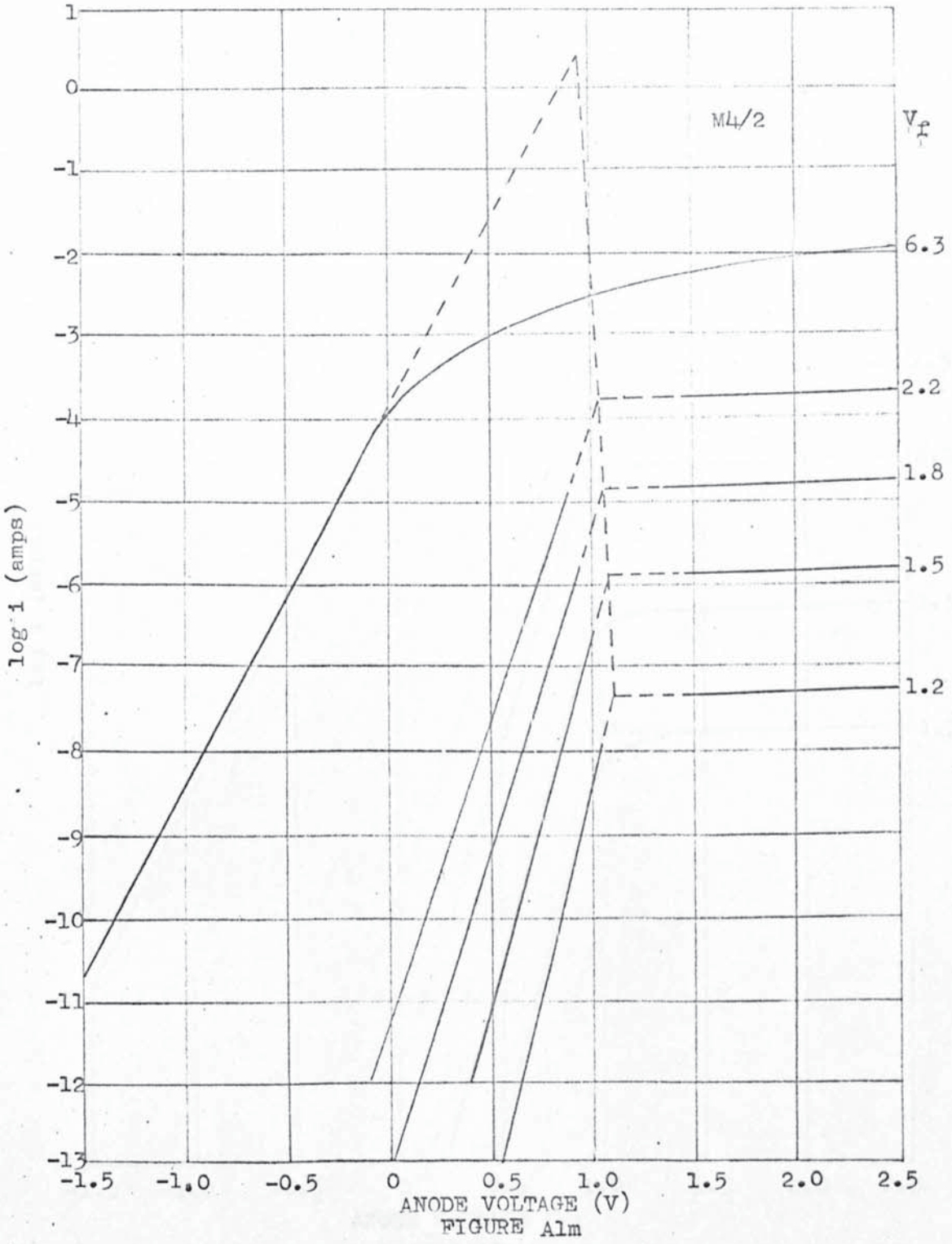
M4/2
V_f
6.3
2.2
1.8
1.5
1.2
log i (amps)
1
0
-1
-2
-3
-4
-5
-6
-7
-8
-9
-10
-11
-12
-13
-1.5
-1.0
-0.5
0
0.5
1.0
1.5
2.0
2.5
ANODE VOLTAGE (V)

FIGURE A1m

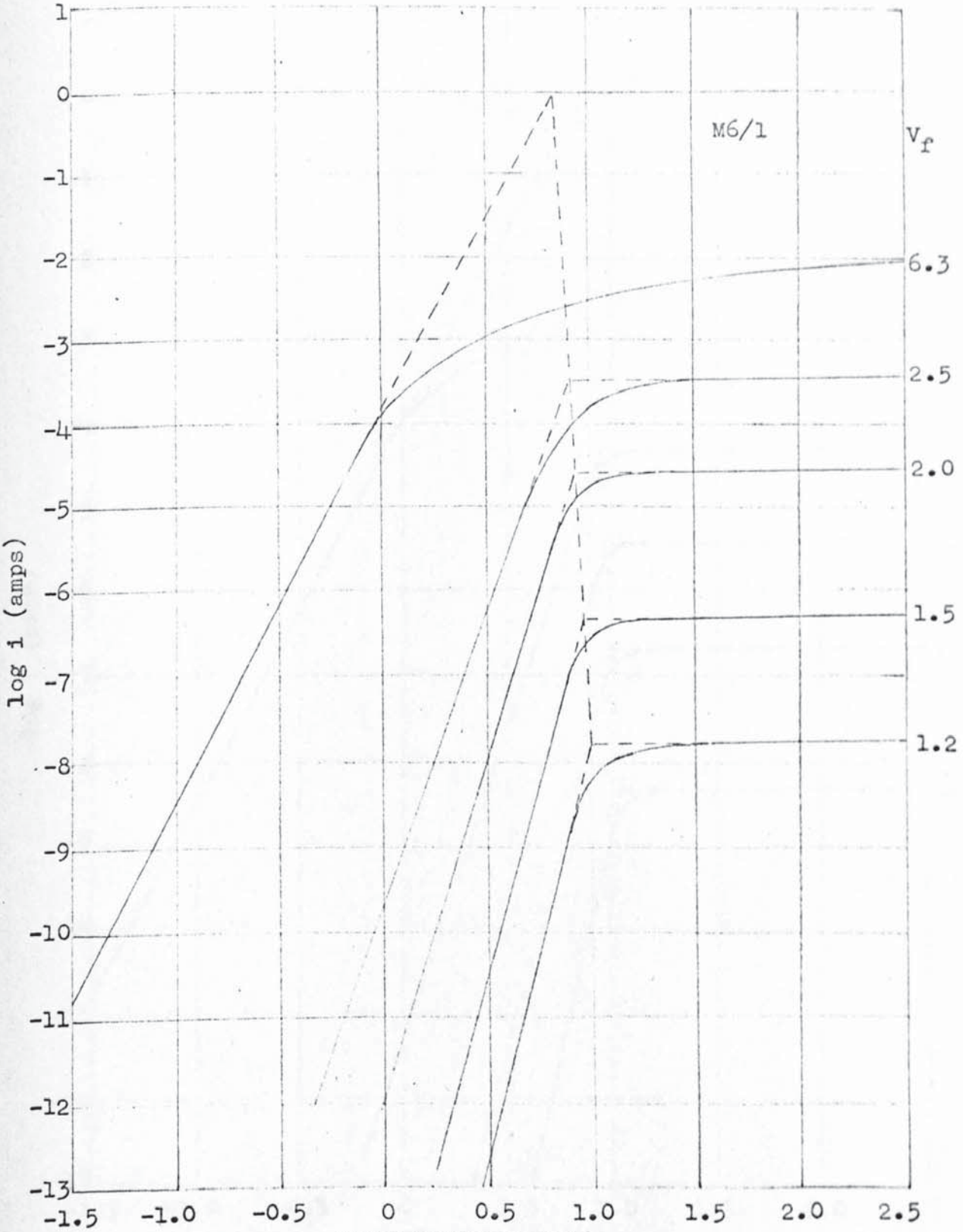
M6/1
V_f
6.3
2.5
2.0
1.5
1.2
log i (amps)
1
0
-1
-2
-3
-4
-5
-6
-7
-8
-9
-10
-11
-12
-13
-1.5
-1.0
-0.5
0
0.5
1.0
1.5
2.0
2.5
ANODE VOLTAGE (V)

FIGURE A1n

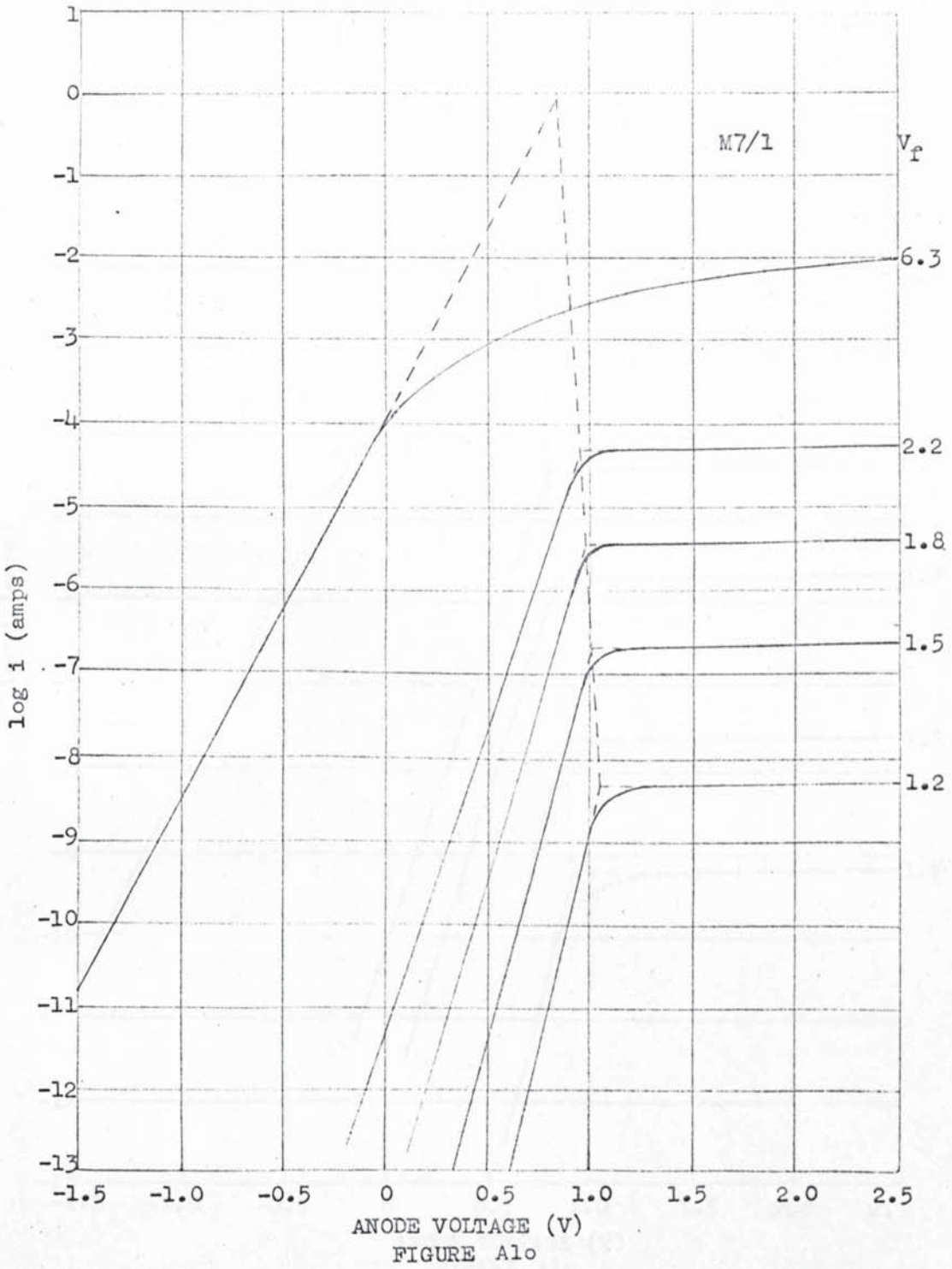
M7/1
V_f
6.3
2.2
1.8
1.5
1.2
log i (amps)
1
0
-1
-2
-3
-4
-5
-6
-7
-8
-9
-10
-11
-12
-13
-1.5
-1.0
-0.5
0
0.5
1.0
1.5
2.0
2.5
ANODE VOLTAGE (V)

FIGURE A1o

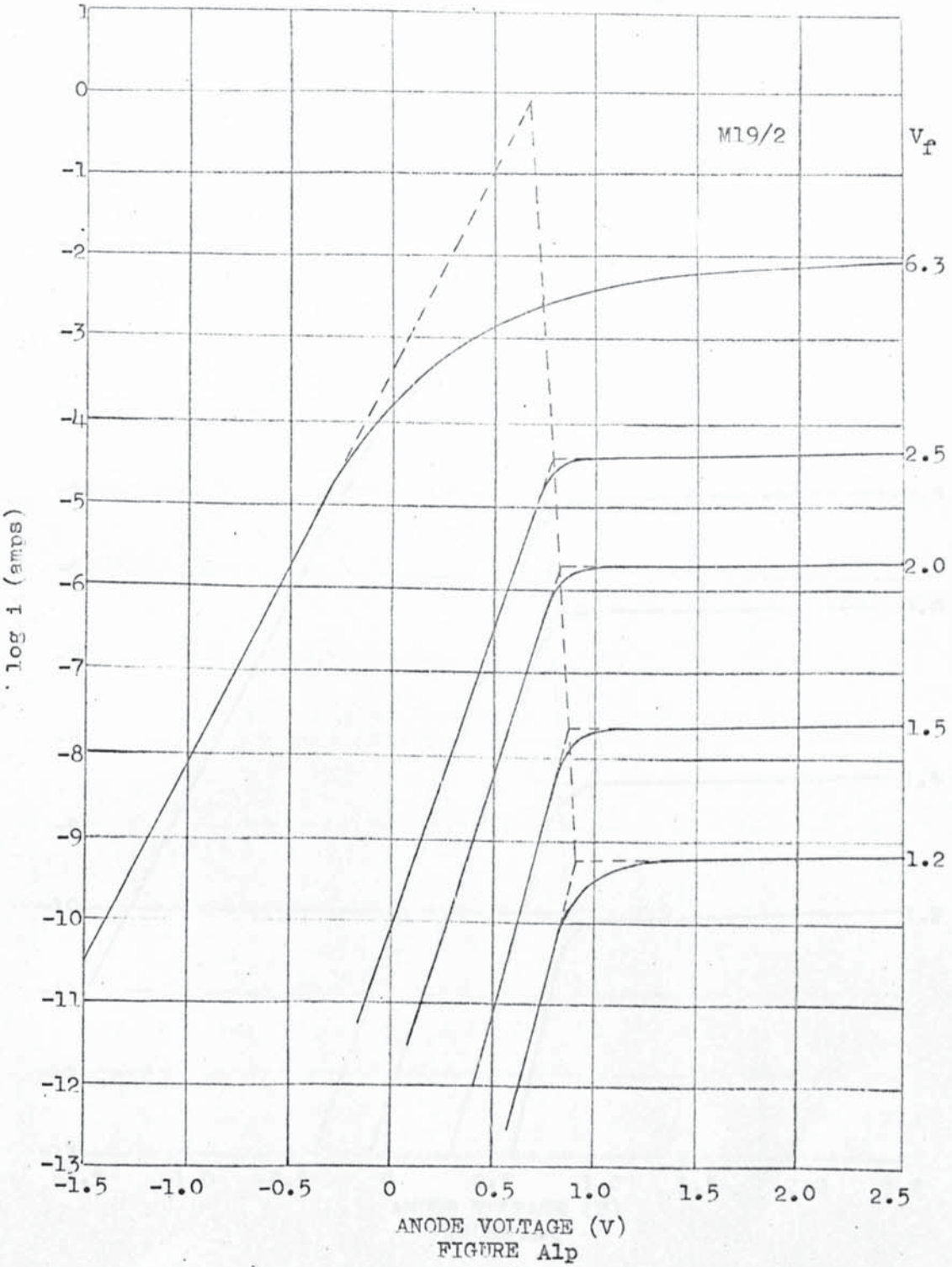
M19/2
V_f
6.3
2.5
2.0
1.5
1.2
log i (amps)
1
0
-1
-2
-3
-4
-5
-6
-7
-8
-9
-10
-11
-12
-13
-1.5
-1.0
-0.5
0
0.5
1.0
1.5
2.0
2.5
ANODE VOLTAGE (V)

FIGURE A1p

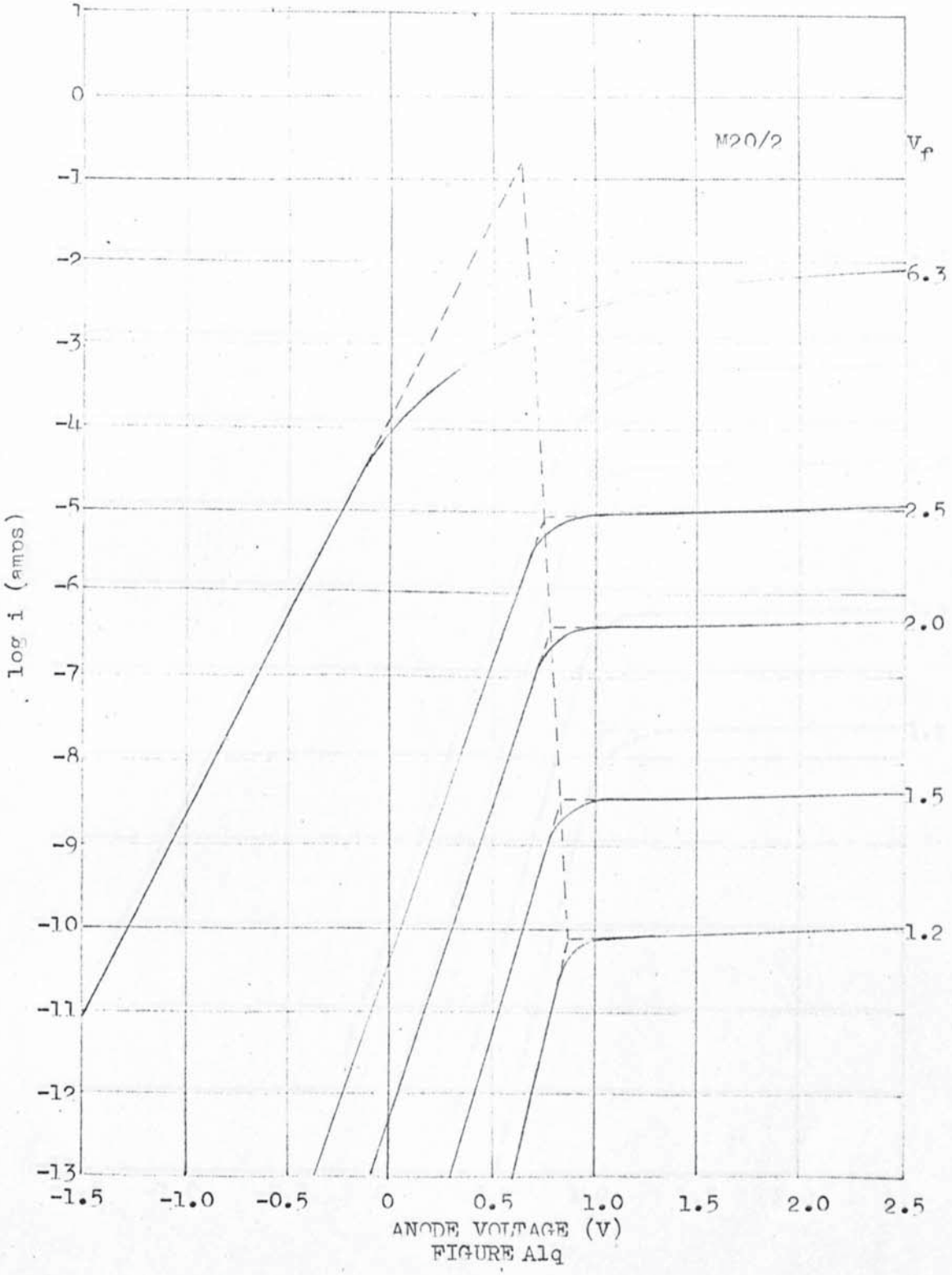
M20/2
V_f
6.3
2.5
2.0
1.5
1.2
log i (amps)
1
0
-1
-2
-3
-4
-5
-6
-7
-8
-9
-10
-11
-12
-13
-1.5
-1.0
-0.5
0
0.5
1.0
1.5
2.0
2.5
ANODE VOLTAGE (V)

FIGURE A1q

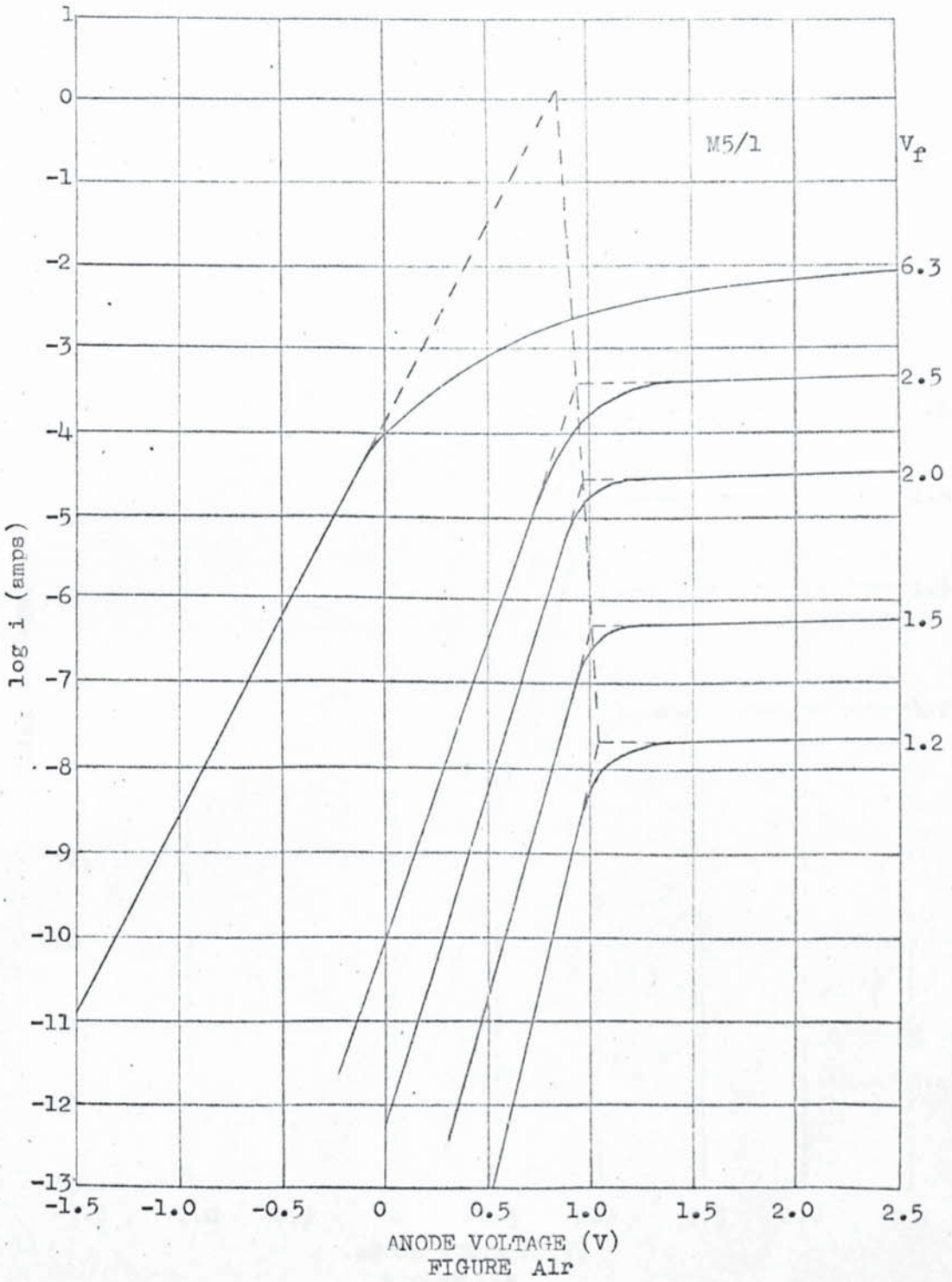
M5/1
V_f
6.3
2.5
2.0
1.5
1.2
log i (amps)
1
0
-1
-2
-3
-4
-5
-6
-7
-8
-9
-10
-11
-12
-13
-1.5
-1.0
-0.5
0
0.5
1.0
1.5
2.0
2.5
ANODE VOLTAGE (V)

FIGURE A1r

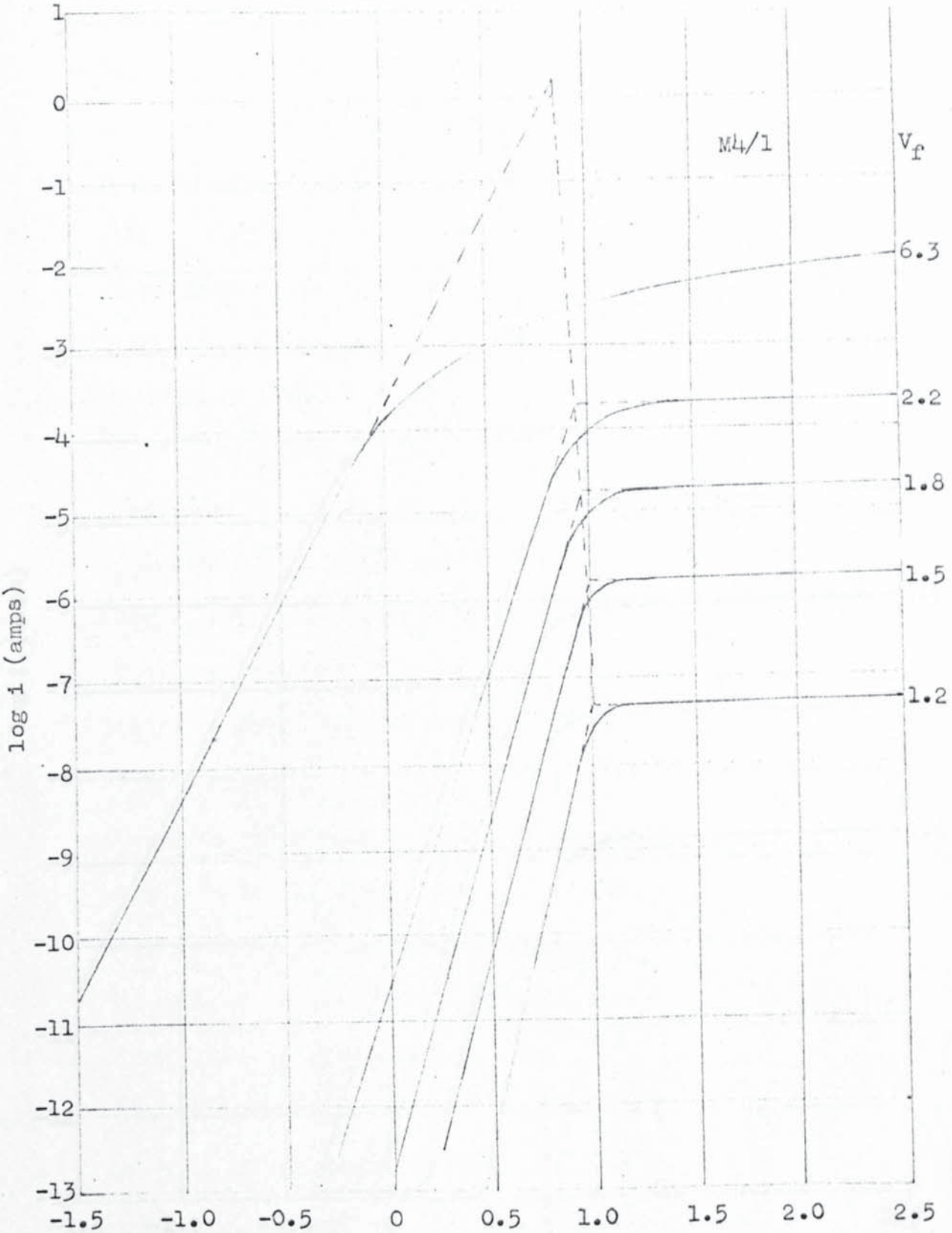
M4/1
V_f
6.3
2.2
1.8
1.5
1.2
log i (amps)
1
0
-1
-2
-3
-4
-5
-6
-7
-8
-9
-10
-11
-12
-13
-1.5
-1.0
-0.5
0
0.5
1.0
1.5
2.0
2.5
ANODE VOLTAGE (V)

FIGURE A1s

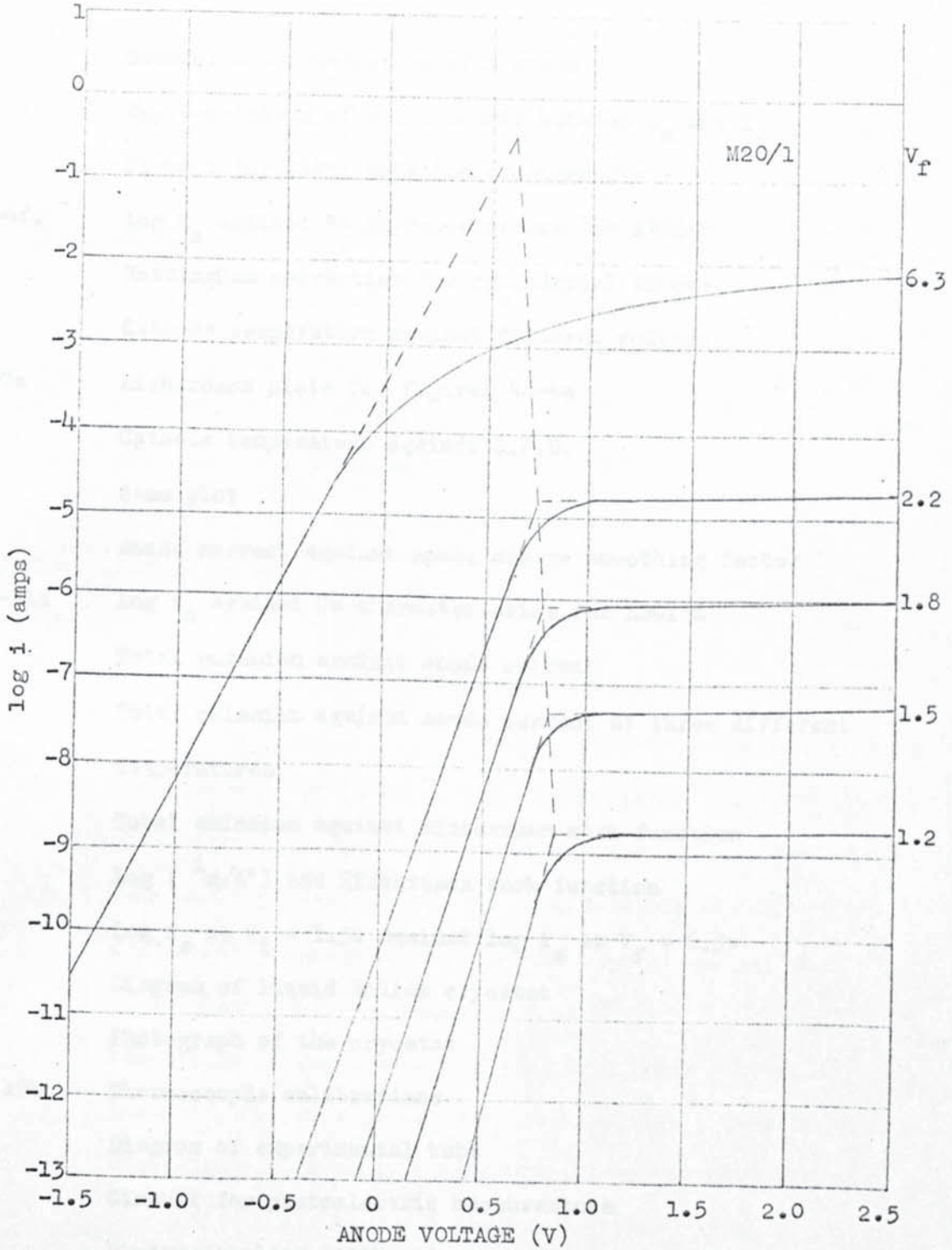
M20/1
V_f
6.3
2.2
1.8
1.5
1.2
log i (amps)
1
0
-1
-2
-3
-4
-5
-6
-7
-8
-9
-10
-11
-12
-13
-1.5
-1.0
-0.5
0
0.5
1.0
1.5
2.0
2.5
ANODE VOLTAGE (V)

FIGURE A1t

List of Figures

25. Photomultiplier current against Deuterium lamp current

26. Current against anode voltage - Tube 5

27. " " " " - Tube 6

28. Photoelectric response curve - Tube 3

29. Fowler plot - Tube 3

30. Standard Fowler plot

31. Photoelectric response curves - Tube 4

32. " " curve - Tube 4

33. Fowler plot - Tube 4

34. Photoelectric response curve - Tube 6

35. " " curves - Tube 6

36a, 36b. Fowler plots - Tube 6

37a, 37b " " - Tube 6

38. Photocurrent (tungsten lamp) against temperature - Tube 6

39. " " " " anode voltage - Tube 6

40a, 40b Photocurrent (deuterium lamp) against anode voltage - Tube 6

41. Photocurrent (tungsten lamp) against anode voltage - Tube 9

42a, 42b Photocurrent (deuterium lamp) against anode voltage - Tube 9

43. Photocurrent (tungsten lamp) against anode voltage and as a function of temperature - Tube 9

44. Photoelectric response curve - oxide cathode - Tube 10.

45. Photoelectric current against anode voltage - Tube 10.

46. Photoelectric response at different temperatures - Tube 10

47. " " " low temperatures - Tube 10

48. " " curve - Tube 11

49. " current against anode voltage - Tube 11

50.	Photoelectric response at different temperatures
51.	" " " low temperatures
52.	Schottky plots - EB91
53a-53d	Anode current - voltage curves at various filament voltages for 4 EB91's
Ala-Alt	Diode characteristics for EB91's

List of main symbols

A	=	Richardson constant
A^*	=	$(1 - r)$
a	=	Cathode to anode ratio
d,x	=	Anode - cathode spacing
D	=	Electric dipole moment
e	=	Charge on the electron
E	=	Electric field
F	=	Helmholtz free energy
g_m	=	Conductance
g_x	=	Motional conductance
h	=	Planck's constant
i_a,i	=	Anode current
i_d	=	Noise diode current
i_s	=	Total emission
i_r	=	Retarding field current
k	=	Boltzman's constant
m	=	Mass of the electron
p	=	Momentum
r	=	Reflection coefficient for electrons
S	=	Entropy
T	=	Temperature
U	=	Potential
Va,V	=	Anode voltage
v	=	Volume
V_c	=	Contact potential difference, C.P.D.

V_E = Effective anode voltage

V_f = Filament voltage

V_m = Potential minimum

α = Volume coefficient of expansion

ϵ = Energy

ϵ_o = Permittivity of free space

ϕ = Work function

ϕ_a = Anode work function

ϕ_c = Cathode work function

ϕ_E = Effective work function

ϕ_R = Richardson work function

Φ = Work factor

Φ_i = Electrostatic potential energy

λ = Wavelength

μ = Chemical potential

$\bar{\mu}$ = Electrochemical potential

ν = Frequency

References

1)	Nottingham W.B.	"Thermionic Emission", Encyclodepia of Physics, Vol 21, Ed - S. Flugge (Berlin - Springer Verlag)1956
2)	Hensley E.B.	J. App. Phys. 32, 301, 1961
3)	Sano S.	E.T.J. Tokyo 5, 78, 1941
4)	Shelton H.	Phys. Rev. 107, 1553, 1957
5)	Kisliuk P.	Phys. Rev. 122, 405, 1961
6)	Love H.M. and Dyer G.L.	Canad J. Phys. 40, 1837,1962
7)	Ferris W.R.	R.C.A. Review 10, 134, 1949
8)	Boot A.H. and Randall J.T.	J. Inst. Elec Engs. 93, 928, 1946
9)	Hermann and Wagener	"The oxide coated cathode" Chapman and Hall, Vols 1 and 2 1951
10)	Gysae B.& Wagener S.	E. tech Physik 19, 264, 1938
11)	Crowell C.R.	J. App. Phys. 27, 93, 1956
12)	Bull C.S.	"Fluctuations of Stationary and Non-Stationary Currents" - Butterworths - 1966
13)	Bull C.S.	J.I.E.E. 97, 159, 1950
14)	Bull C.S.	Ph.D. Thesis - Univ of London 1940
15)	Schottky W.	Ann der Physik 44, 1011, 1914
16)	Hass G.A. and Coomes E.A.	Phys. Rev. 93, 1421, 1954
17)	Padovani F.A.	Solid State Electronics 11, 193, 1968.
18)	Herring C. and Nichols M.H.	Rev. Mod Phys. 21, 185, 1949
19)	Venema A. Jansen C.G.J. and Weekers T.H.	J. App. Phys. 37, 2234, 1966.

20)	Hung C.S.	J. App Phys. 21, 37, 1950
21)	Shibata C.	J. Phys. Soc. Japan 16, 51, 1961
22)	Hass G.A. and Thomas R.E.	J. App Phys. 38, 3969, 1967
23)	Beck A.H.W.	Thermionic Valves" 1953 Cambridge Univ Press
24)	Good R.H.	J. App. Phys. 28, 1405, 1957
25)	Christov S.G.	Phys. Stat. Sol. 17, 11, 1966
26)	Nottingham W.B.	Phys. Rev. 57, 935, 1940
27)	Hutson A.R.	Phys. Rev. 98, 889, 1955
28)	Love H.M. and Wilson J.R.	Canad. J. Phys. 45, 225, 1967.
29)	Heil H. and Holloway T.	Phys. Rev. 164, 881, 1967
30)	Heil H.	Phys. Rev. 164, 887, 1967
31)	Abey A.E.	J. App. Phys. 39, 120, 1968
32)	Hinsh W.	Z - techn Phys. 12, 528, 1931
33)	Roethe H.	Z. Physik. 36, 737, 1926
34)	Almer F.H.R., Fransen J.B., and Santing H.	Supplemento al Nuovo Cimento 1, 860, 1963
35)	McCormack R.L.	Proc. Inst. Radio Engs. 37, 683, 1949
36)	Dominquez R., Doolittle H.D., and Varadi P.F.	Paper presented at 24th Annual Conf on Physical Electronics, M.I.T. 1964
37)	Metson G.H.	Proc. I.E.E. 102(B), 657,1955
38)	Lawson R.W.	Supplemento al Nuovo Cimento 1, 727, 1963
39)	Holmes M.F.	Proc. I.E.E. Monograph 214, 1956
40)	Yazawa K.M.	Supplemento al Nuovo Cimento 1, 770, 1963

41) Sproul R.J. Phys. Rev. 166, 67, 1945

42) Coomes E.A. J. App. Phys. 17, 647, 1946

43) Beck A.H. and Maloney C.E. B.J.A.P. 18, 848, 1967

44) Eisenstein A. J. App. Phys. 17, 439, 1946

45) Wright D.A. Proc. Roy Soc 190 (A), 394, 1947

46) Metson G.H., Wagener S., Holmes M.F., and Child M.R. Proc. I.E.E. 99, 69, 1952

47) Hopkins B.J. and Vick F.A. B.J.A.P. 9, 257, 1958

48) Nagy L.Z. Proc. of Symposium on Vacuum Electronics Budapest 229, 1963

49) Nergaard L.S. R.C.A. Review 13, 464, 1952

50) Nottingham W.B. M.I.T. Report Jan, 1963

51) Bull C.S. and Fitch R.K. B.J.A.P. 12, 566, 1961

52) Fitch R.K. and Coutts P.W. B.J.A.P. 14, 605, 1963

53) Higginson G.S. B.J.A.P. 9, 106, 1958

54) Dewsburry R. B.J.A.P. 15, 71, 1964

55) Arizumi T. J. Phys. Soc. Japan 3, 143, 1948

56) Krasin'Kova M.V. Moyzhes B.Y and Shklyar A.G. Radio Engs and Elec Phys 11, 1457, 1960

57) Hopkins B.J. B.J.A.P. 11, 124, 1960

58) Hopkins B.J. and Ross K.J. B.J.A.P. 15, 393, 1964

59) Richards C.B. M.Sc. Thesis Univ. of Wales 1955

60) Fitch R.K. and Coutts P.W. B.J.A.P. 15, 1327, 1964

61) Stanier B.J. and Mee C.H.B. J. Elec. Control 16, 545,1964.

62) Krusemeyer H.J. and Pursley M.W. J. App. Phys. 27, 1537, 1956

63) Dobretsov L.N. and Matskevich T.L. Soviety Phys - Tech Phys 11, 108, 1967

64)	della Porta P., Giorgi T., and Michan L.	Supplemento al Nuovo Cimento 1, 458, 1963
65)	Fitch R.K. and Young M.A.	Supplemento al Nuovo Cimento 1, 825, 1963
66)	Nergaard L.S.	R.C.A. Review 20, 191, 1959
67)	Perdijk H.J.R.	Supplemento al Nuovo Cimento 5, 73, 1967
68)	Mee C.H.B.	B.J.A.P. 13, 182, 1962
69)	Hathaway D.J.	Unpublished, private communication Phys. Dept., Univ. of Aston in Birmingham 1965
70)	Engstrom R.W.	Optical Soc. of America 37, 420, 1947
71)	Braddick H.J.	Reports on Progress in Phys. 23, 154, 1960
72)	Dirac P.A.M.	Scientific American May 1963
73)	Moyzhes B.Y., Nilov O.M. Sorokin O.V. and Chudnovskiy F.A.	Radio Eng. Elec. Phys. 12, 453, 1967
74)	Reimann R.L.	Nature 133, 83, 1934
75)	Seely S.	Phys. Rev. 59, 75, 1941
76)	Fomenko V.S.	Handbook of Thermionic Properties Ed. G.V. Samsonov., Plenum Press 1966
77)	Rivière J.C.	Proc. Phys. Soc. B.70, 676, 1957
78)	Anderson P.A.	Phys. Rev. 115, 553, 1959
79)	Hopkins B.J., Mee C.H.B., and Parker D.	B.J.A.P., 15, 865, 1964
80)	Huber E.E. (Jr)	App. Phys. Letters 8, 169, 1966
81)	Dillon J.A. and Farnsworth H.	J. App. Phys. 28, 174, 1957
82)	Hopkins B.J. and Rivière J.C.	Proc. Phys. Soc. 81, 590, 1963

83)	Barry D.E., Hopkins B.J. and Sargood A.J.	Surface Science 7, 365, 1967
84)	Sultanov V.M.	Radio Eng. Elec Phys. 9, 252, 1964
85)	Potter J.G.	Phys. Rev. 58, 623, 1940
86)	Van Oostrom A.	Phys. Letters (Netherlands) 4, 314, 1963
87)	Swanson L.W. and Crouser L.C.	Phys. Rev. 163, 622, 1967
88)	Gel'berg A., Iosifesku B. Comsa G. and Mussa G.	Radiotekhnika i elektronika 3, 1000, 1958
89)	Comsa G., Gel'berg. A. and Iosifesku B.	Phys. Rev. 122, 1091, 1961
90)	Hopkins B.J. and Smith B.J.	J. App. Phys. 39, 213, 1968
91)	Blevis E.H. and Crowell C.R.	Phys. Rev. 133, A580, 1964
92)	Crowell C.R. and Armstrong R.A.	Phys. Rev. 114, 1500, 1959
93)	Garron R. and Testard D.	C.R. Acad Sci. (France) 253, 1770, 1961
94)	Allen F.G.	J. Phys. Chem. Solids 8, 119, 1959
95)	Bachman R., Busch C., and Schumacher R.	Helv. Phys. Acta (Switz) 39, 593, 1966
96)	Crowell C.R.	Phys. Rev. 92, 554, 1953
97)	Wilson R.G.	J. App. Phys. 37, 2261, 1966
98)	Wilson R.G.	J. App. Phys. 37, 3170, 1966
99)	Bedard F.D. and Harte W.E.	Proc. of Int. Colloq. Paris 342, 1965
100)	Beinar, K.S.,Nikonov V.P.	Radiotekhn i Electron 10, 476, 1965
101)	Handbook of Physics	Stookey S.D. and Maurer R.D., Eds. E.U. Condon and H. Odishaw McGraw-Hill Part 8, Chap.7, 1967
102)	Fehrs D.L. and Stickney R.E.	Surface Science 8, 207, 1967

103)	Protopopov O.D., Mikheeva E.V. Shreinberg B.N., and Shuppe G.N.	Sov.Phys.Solid State (U.S.A.) 8, 909, 1966
104)	Gumnick J.L., and Juenker D.W.	J. App.Phys. 31, 102, 1960
105)	Cardwell A.B.	Phys.Rev. 38, 2041, 1931
106)	Klein R., and Leder L.B.	J. Chem Phys (U.S.A.) 38, 1863, 1963
107)	Jaklevic R.C., and Juenker D.W.	J.App.Phys. 33, 562, 1962
108)	Smith R.L.	Phys.Rev. 128, 225, 1962
109)	Teich M.C., Schroeer J.M. and Wolga G.J.	Phys. Rev.Letters 13, 611, 1964
110)	Sonnerberg H., Heffner H., and Spicer W.	App. Phys. Letters 5, 95, 1964
111)	Imamura. S., Shiga F., Kimoshita K., and Suzuki T.	Phys. Rev. 332, 166, 1968
112)	Logothetis E.M., and Hartman P.L.	Phys.Rev.Letters 18,581,1967
113)	Ready J.F.	Phys.Rev. 137, A620, 1965
114)	Verber C.M., and Adelman H.H.	J.App.Phys. 36, 1522, 1965
115)	Farkas G., Kertész I. Naray Z., and Varga P.	Phys. Letters (Netherlands) 24A, 475, 1967
116)	Crowe K.R., and Gummick J.L.	App.Phys.Letters 11, 249, 1967
117)	Husain S.A., and Walsh D.	Electronic Letters 3, 121, 1967
118)	Sommer A.H., and Spicer W.E.	Photoelectric materials and devices, Editor - S, Larach. Chap 4, 1965
119)	Stanier B.J., and Mee C.H.B.	Int.J. of Elec. 18, 401, 1965
120)	McNarry D.M.	Phys.Rev. 81, 631, 1951
121)	Jones M.D., and Mee C.H.B.	B.J.A.P. (J. Phys. D.) 1, 467, 1968
122)	Devore H.B., and Dewdney J.W.	Phys. Rev. 83, 805, 1951
123)	Ducker J.E. and Hensley E.B.	Phys.Rev. 136, A190, 1964
124)	Mee C.H.B., and Vick F.A.	B.J.A.P. 12, 698, 1961

125) Phillip H.R. Phys.Rev. 107, 687, 1957

126) Hora H., Kantlehner R. Riehl H., and Thoma P. Z. Naturforsch 21a, 324, 1966

127) Kiselev A.B., and Nikonov B.P. Trans.Radio Eng. and Elec Phys. 12, 812, 1967